The role of inflammsasome signalling in the pathology of depression

Wickens, Robin

Award date:
2017

Awarding institution:
University of Bath

The role of inflammasome signalling in the pathology of depression

Robin Alfred Wickens

A thesis submitted for the degree of Doctor of Philosophy

University of Bath

Department of Pharmacy and Pharmacology

November 2016

Table of Contents

List of Figures

List of Tables

Acknowledgements

This work was funded by a CASE studentship with the Medical Research Council and Janssen Pharmaceutica, with experiments conducted at the University of Bath, UK and at Janssen Pharmaceutica, Beerse, Belgium. I would like to thank my supervisors, Dr Amanda Mackenzie and Dr Sarah Bailey, for their excellent guidance and support over the past 4 years, and for giving me this opportunity in the first place. Thanks to Dr Luc Ver Donck for his help and supervision during my fantastic time in Belgium. Also, I would like to thank the staff in the animal units in Bath and Janssen: Jean, Lesley, Jane, Martin, Patrick, Michel and Roland.

Thanks goes to all the people in the PhD office over the years that have made my time in Bath so enjoyable and have helped me in the lab, particularly Alex, Annelisa, James, Benny, Jo, Jenny, Marina, Malika, Laura, Helen, and Dearbhla. But a special appreciation is for the lunatics that are Matt and Emma, who have maintained an impressive level of insanity over the years and have kept me thoroughly entertained.

A huge thanks goes to my friends and family in Southampton. To my parents, Frankie and Rob, for their unconditional support throughout the last 4 years, and the 23 years prior to that. Also, to Simon for your support, and to my brother, to my sister, and to my friends who provided a welcome relief from work.

Finally, I have enormous gratitude for Katrina, who I was lucky enough to meet during my time in Belgium and spent the last 3 years adventuring with. Thank you for your love and support.

Abstract

Neuroinflammation is considered to be an important underlying process in the pathology of major depressive disorder (MDD) within a subpopulation of patients. MDD is associated with increased levels of proinflammatory cytokines in the blood, and cytokine-based treatments can induce depression. In mice, the induction of systemic inflammation with lipopolysaccharide (LPS) can induce depressive-like behaviours that are associated with symptoms of MDD. Microglia mediate the neuroinflammatory response within the brain and have a critical role in inflammation-induced depressive-like behaviours. Microglia within the brain exist in low O_2 conditions (~5 %), though experimentation *in vitro* is typically carried out in high O_2 conditions (20 %). The NLRP3 inflammasome is a molecular complex central to the production of the proinflammatory cytokine IL-1β and the propagation of the inflammatory response. NLRP3 inflammasome activity has been implicated in chronic stress and inflammation-based models of depressive-like behaviours in mice.

The aims of this thesis were to study LPS-induced depressive-like behaviour in C57BL/6J mice, the role of NLRP3 in the behavioural output and the influence of oxygen (O_2) availability on NLRP3 inflammasome activity in microglia cell cultures. Acute LPS induced depressive-like behaviours were observed in hedonia-based tasks but not in the forced swim test (FST). However, acute LPS induces a brief period of inflammation that does not address the sustained nature of depression. A FST depressive-like behaviour was observed in a novel 3-day increasing dose LPS model of sustained inflammation, whilst circumventing the development of LPS tolerance. The LPS-induced sickness was partially dependent upon NLRP3, though the resulting depressive-like behaviour was not. NLRP3 inflammasome signalling in microglia was studied in 5 % O_2 conditions to replicate the hypoxic environment within the brain. Primary microglia isolated from mixed glial cultures by mild trypsinisation exhibited functional NLRP3 inflammasome expression and activity. When exposed to 5 % O_2 (24 hours), NLRP3 inflammasome activity and adenosine triphosphate (ATP)-induced cell death was attenuated, whilst the production of other proinflammatory cytokines were unaffected. These data demonstrate the O_2 sensitivity of NLRP3 inflammasome signalling in microglia.

This thesis demonstrates a novel model of sustained inflammation and that inhibiting NLRP3 signalling may provide a target for attenuating neuroinflammation and the resulting behavioural changes. The importance of understanding the influence of O_2 in microglia function and neuroinflammation was highlighted by the sensitivity of NLRP3 inflammasome activity to low O_2.

List of abbreviations

ACTH	adrenocorticotropic hormone
AD	Alzheimer's disease
AIM2	absent in melanoma 2
AMPA	α-amino-3-hydroxy-5-methyl-4-isoxazolepropionic acid
ANOVA	analysis of variance
ASC	apoptosis speck-like protein containing a CARD
ATP	adenosine triphosphate
Aβ	amyloid-β
BBB	blood-brain barrier
BDNF	brain-derived neurotrophic factor
BMDM	bone marrow-derived macrophage
CARD	caspase activation and recruitment domain
CD	constant dose
CNS	central nervous system
COX-2	cyclooxygenase-2
CRF	corticotropin-releasing factor
CRP	C-reactive protien
CSF	cerebrospinal fluid
DAMP	danger-associated molecular patterns
DCFDA	2',7' –dichlorofluorescin diacetate
FST	forced swim test
FUST	female urine sniffing test
GR	glucocorticoid receptor
GSDMD	gasdermin D
h	hours
H_2O_2	hydrogen peroxide
HIF-1α	hypoxia-inducible factor 1α
HPA	hypothalamic-pituitary-adrenal
i.c.v.	intracerebroventricular
i.p.	intraperitoneal
ID	increasing dose
IDO	indoleamine-2,3-dioxygenase
IFN-α	interferon-α
IL-10	interleukin-10
IL-1R	interleukin-1 receptor
IL-1β	interleukin-1β
IL-6	interleukin-6

LDH	lactate dehydrogenase
LPS	lipopolysaccharide
LRR	leucine-rich repeat
MAOI	monoamine oxidase inhibitor
MAPK	mitogen-activated protein kinase
MDD	major depressive disorder
mRNA	messenger ribonucleic acid
MyD88	myeloid differentiation primary response 88
NBD	nucleotide binding domain
NF-κB	Nuclear factor-κB
NLR	NOD-like receptor
NLRP3	NOD-, LRR- and pyrin domain-containing 3
NMDA	N-methyl-D-aspartate receptor
NO	nitric oxide
NOS	nitric oxide synthase
NOX	NADPH oxidase
NSAID	non-steroidal anti-inflammatory drug
O_2^-•	superoxide radical
OFT	open field test
OH•	hydroxyl radical
PAMP	pathogen-associated molecular pattern
PGE2	prostaglandin E2
PHD	prolyl hydroxylases
PI3K	phosphoinositide 3-kinase
poly(I:C)	polyinosinic:polycytidylic acid
ROS	reactive oxygen species
s.c.	subcutaneous
SEM	standard error of the mean
SNRI	serotonin-noradrenaline reuptake inhibitor
SOD	superoxide dismutase
SPT	sucrose preference test
SSRI	selective serotonin reuptake inhibitor
TRX	thioredoxin
TCA	tricyclic antidepressant
TLR4	toll-like receptor 4
TNF-α	tumour necrosis factor-α
TST	tail suspension test
TXNIP	thioredoxin-interacting protein

Chapter 1: Introduction

1.1 An overview of major depressive disorder (MDD)

1.1.1 Symptoms of depression

Major depressive disorder (MDD) is a mental illness that has been documented in people as early as Ancient Greece, with Hippocrates description of “melancholic affection” (Nestler et al., 2002). The current Diagnostic and Statistical Manual of Mental Disorders (DSM-5) criteria for MDD requires the presence of at least 5 of 9 listed symptoms, including persistent low mood, a reduced sensation of pleasure or interest, suicidal thoughts, feelings of low self-worth, loss of energy, reduced ability to concentrate and changes in sleep, weight or activity (American Psychiatric Association, 2013). Whilst a diagnosis of depression does not require all symptoms to be present, patients must have experienced symptoms everyday for at least two weeks. The disorder is not only detrimental to the well-being of the affected individual and people close to the individual, but depression as a whole also has a negative effect on society and the economy due to the resulting reduction in productivity and increased healthcare costs.

1.1.2 Prevalence and economic burden of depression

Depression reportedly affects 350 million people worldwide and over the course of a lifetime, the prevalence of depression is considered to lie between 10-20 % (Kessler et al., 2003a; Lépine and Briley, 2011). Women are almost twice as likely to be diagnosed with depression than men, with depression affecting 5 % of males and 9 % of females in a given 12-month period in the United States (Kessler et al., 2003b; Kessler et al., 2005; Lohoff, 2010). Furthermore, as age increases, the prevalence of depression increases (Blazer, 2003). In 2010, the economic cost of depression was estimated to be €19.2 billion in the UK and $210.5 billion United States (Fineberg et al., 2013; Greenberg et al., 2015). These figures incorporate the direct medical costs incurred as well as indirect costs, such as lost productivity in the workplace, which accounted for almost 50 %. In 2010, depression accounted for 2.5 % of worldwide disability adjusted life years (DALYs), which represent the average number of years of life an individual will lose due to an illness, and 8.2 % of years spent living with disability (Ferrari et al., 2013). The World Health Organization predicts depression will become the second biggest cause of DALYs (5.7 % of the worldwide total) by the year 2030 (Mathers and Loncar, 2006). Furthermore, depression is a risk factor for a number of other disorders, such as acute coronary syndrome (Litchman et al., 2014).

The consensus is that depression is a growing global health problem that requires effective intervention to reduce its individual and economic burden on the global population (Moussavi et al., 2007; Ferrari et al., 2013; Lopez et al., 2006; Murray and Lopez, 1997).

1.1.3 Pathophysiology and treatment of depression

The treatment of depression changed in the mid-20th century with the development of a number of antidepressant drugs targeting the neurotransmission of monoamines. These monoamines include serotonin, noradrenaline and dopamine (Delgado, 2000). The new drugs were primarily tricyclic antidepressants (TCAs), which inhibit the reuptake of monoamines, and monoamine oxidase inhibitors (MAOIs), which inhibit the metabolism of monoamines. By inhibiting the metabolism or uptake of monoamines from the synaptic cleft, higher levels of synaptic neurotransmitter are available to stimulate their post-synaptic receptors (Delgado, 2000). However, TCAs and MAOIs have a number of adverse effects. Along with sedation, dry mouth and constipation, TCAs can also cause cardiac abnormalities, and MAOIs, which are very rarely used today, can have potentially dangerous interactions with tyramine rich foods (Gray and Stahl, 2012; Harrigan and Brady, 1999). The presence of these side effects prompted the development of more selective drugs. As a result, selective monoamine reuptake inhibitors were developed for serotonin (SSRIs), noradrenaline (NRIs) and/or dopamine (DRIs). There are also drugs that inhibit the uptake of multiple monoamines, such as serotonin-noradrenaline reuptake inhibitors (SNRIs). The ability of these drugs to treat depression led to the most prominent theory of depression, based upon the concept of reduced monoamine neurotransmission (Heninger et al. 1996). Today, the first line treatment for MDD are SSRIs, with sertraline and citalopram considered the safest option due to low interaction potentials (National Collaborating Centre for Mental Health UK, 2010).

Whilst generally well-tolerated, current mainstream antidepressants still exhibit some adverse effects, such as include sexual dysfunction (Gregorian et al., 2002) and nausea (Beasley et al., 2000). The antidepressant activity of these drugs has a delayed onset of several weeks, during which the rate of suicidal behaviours can increase (Vázquez et al., 2015; Rosen et al., 1999; Jick et al., 2004). Furthermore, the rate of remission for antidepressant intervention is between 35 – 50 % (Cleare et al., 2015). For example, the SSRI citalopram is reported to have a remission rate of only one third (Trivedi et al., 2006). This low rate of success leads to patients having to often change

their course of antidepressants in order to find a tolerable and effective treatment. Subsequent treatment courses have an even lower success rates (Rush et al., 2006a). The cumulative remission rate following a maximum of four treatment courses was 67 %, and patients that did not respond to initial treatment were more likely to relapse (Rush et al., 2006a). Treatment-resistant depression is a term applied to cases in which multiple courses of treatment fail to improve the symptoms of MDD and is seen in up to 50 % of depressed patients (Fava, 2013). Treatments that enhance monoamine signalling do not treat the underlying cause of depression but simply attempt to treat a physiological symptom of depression. Understanding the various mechanisms by which depression develops in different subpopulations of depression can help elucidate and address the underlying causes.

Alternatives to the monoamine hypothesis for depression are being explored, such as glutamate signalling and the hypothalamic-pituitary-adrenal (HPA) axis. Ketamine is a non-competitive antagonist for the N-methyl-D-aspartate (NMDA) receptor for glutamate and has been shown to exhibit antidepressant activity in humans and in animal models (Berman et al., 2000; Fond et al., 2014; Browne et al., 2013). The effects of ketamine on mood are rapid, with a reduction in depressive symptoms reported 2 h after administration, and can last at least one week, even in treatment-resistant depression (Zarate et al., 2006). Such findings have led to intranasal administration of ketamine as an alternative treatment for depression, which can significantly improve depressive symptoms after 24 h (Lapidus et al., 2014). The primary role of the HPA axis is to respond to stress and induce the production of glucocorticoids. Depressed patients often exhibit high levels of cortisol in their blood (Butler and Besser, 1968). The increase in cortisol is thought to be a result of a faulty inhibitory feedback loop via the glucocorticoid receptor (GR) that regulates HPA axis activity. Impaired GR function results in the high levels of cortisol observed in depressed patients and can contribute to the physiological and behavioural changes in depression (Pariante and Lightman, 2008). Whilst a range of CRF antagonists have been tested in clinical trials in humans, none have been successful in phase III trials (Zorilla and Koob, 2010; Koob and Zorilla, 2012). Other potential targets for intervention include adult hippocampal neurogenesis (Sahay et al., 2007), which is enhanced following antidepressant intervention (Malberg et al., 2000; Perera et al., 2007), and kappa opioid receptor antagonism (Lutz et al., 2013), which can induce antidepressant-like behaviours in rodents (Mague et al., 2003).

Though some of the components underlying the pathophysiology of depression have been elucidated, the etiology of the disorder is still unclear. The roles of psychological stress, genetics, hormones, neurogenesis, neuroplasticity and

inflammation have each been shown to influence distinct cellular processes implicated in the development of depression and depressive symptoms, and are thought to feed into each other (Hasler, 2010; Pittenger and Duman, 2008).

1.2 Linking depression and inflammation

Over recent decades, our understanding of the interactions between the immune system, the brain and behaviour has grown and the role of inflammation in depression has become a popular topic of research. The concept of the immune system contributing to depression in a subpopulation of patients is supported by pre-clinical and clinical evidence.

1.2.1 Elevation of cytokine levels in depression

Cytokines are signalling proteins that are produced and released by immune cells in response to stimulation, whether by an exogenous or endogenous signal. Their function is critical in the innate immune system and act by either propagating or inhibiting the inflammatory response. Proinflammatory cytokines, including interleukin (IL)-6, IL-1β and tumour necrosis factor (TNF)-α, have a wide range of functions and play a key role in regulating both innate and adaptive immunity, with functions such as attracting and activating other immune cells, stimulating differentiation and inhibiting or inducing apoptosis (Hopkins, 2003; Scheller et al., 2011; Bradley, 2008).

The elevation of circulating proinflammatory cytokines in the blood in depressed, but otherwise healthy, individuals is a marker of inflammation (Dowlati et al., 2010). This phenomenon has been repeatedly observed and systematically reviewed in a number of meta-analyses (Table 1.1.). These studies had slightly different inclusion criteria and target proteins but all reported elevations in certain inflammatory cytokines. Three meta-analyses included studies assessing people with an MDD diagnosis (Dowlati et al., 2010; Howren et al., 2009; Liu et al., 2012), one assessed depressive symptoms (Hiles et al., 2012a), and one studied suicidal patients (Black and Miller, 2015), all compared to healthy controls. All five meta-analyses reported a significant positive association of circulating IL-6 with depression, whilst positive associations were also reported for TNF-α, IL-1β, C-reactive protein (CRP), IL-1 receptor antagonist (IL-1ra), soluble IL-2 receptor (sIL-2R), as well as the anti-inflammatory cytokine IL-10. CRP is an acute phase protein produced by the liver in

response to inflammation. The elevation in IL-1ra is associated with elevations in IL-1β as an endogenous negative regulator. sIL-2R is the soluble receptor for IL-2, which is necessary for its inflammatory actions. In addition to blood samples, one meta-analysis also examined post-mortem brain tissue of suicide victims and reported a significant increase in IL-6 and IL-1β compared to healthy controls (Black and Miller, 2015). In depressed patients, circulating monocytes in the blood have been shown to exhibit an enhanced proinflammatory phenotype following stimulation that is positively associated with the severity of depressive symptoms (Suarez et al., 2004).

IL-6 is the only cytokine to be consistently reported to associate with depression, and this association is supported in animal studies that will be discussed later. IL-6 expression can be induced via the transcription factor nuclear factor (NF)-κB and can exert proinflammatory effects through the activation of Janus kinase/signal transducer and activator of transcription (JAK/STAT) and the mitogen activated protein kinase (MAPK) signalling, both culminating in transcription and the production of cytokines (Hodes et al., 2016).

Two further meta-analyses have been carried out reviewing the effect of antidepressant treatment on cytokine levels in the blood (Hannestrad et al., 2011; Hiles et al., 2012b). The first review assessed serum levels of IL-6, IL-1β and TNF-α before and after antidepressant treatment (Hannestad et al., 2011). It was found that overall antidepressant treatment reduced depressive symptoms as well as serum levels of IL-6 and IL-1β, whilst SSRI treatment in particular reduced serum levels of IL-6 and TNF-α. The second review assessed serum IL-6, CRP and IL-10 levels before and after treatment and found that pharmacological intervention significantly reduced IL-6 and CRP levels, and did not affect the anti-inflammatory cytokine IL-10 (Hiles et al., 2012b). The findings of these two reviews support the theory that abnormalities in cytokine levels are linked to depressive behaviour, though variability exists amongst treatment groups. Classes of antidepressants other than SSRIs did not significantly reduce cytokine levels whilst still reducing depressive symptoms (Hannestad et al., 2011). Although this finding indicates not all antidepressant treatments result in reduced cytokine levels, it could still be argued that antidepressants attenuate the negative effects of cytokines on the brain without addressing cytokine irregularity.

	Howren et al., 2009	Dowlati et al., 2010	Hiles et al., 2012a	Liu et al., 2012	Black & Miller, 2015
IL-6	↑	↑	↑	↑	↑
IL-1β	↑	-		-	↑
IL-10		-	-	-	↑
TNF-α		↑		↑	-
IL-4		-		-	
IL-2		-		-	
IFN-y		-		-	
IL-8		-		-	
CRP	↑				↑
IL-1ra	↑				
sIL-2R				↑	

Table 1-1. A summary of meta-analysis findings linking serum cytokine levels with depression.

Significant positive associations (↑) or no significant associations (-) are shown for inflammatory markers that were assessed.

1.2.2 Cytokine-induced depression

To understand the direct effect of cytokines on mood, cytokine-based treatments and depressive symptoms can be monitored. This can be done with patients receiving interferon (IFN)-α treatments for diseases including hepatitis C and some cancers. IFN-α is proinflammatory cytokine that has anti-viral properties as well as efficacy against tumours (Capuron and Miller, 2004). IFN-α has the capacity to induce the expression of other cytokines and has been shown to significantly increase the levels of IL-6 and monocyte chemoattractant protein-1 (MCP-1) in the cerebrospinal fluid (CSF) of hepatitis C patients (Raison et al., 2009). The development of depressive symptoms occurs in up to 50 % of hepatitis C and cancer patients receiving IFN-α treatment and often results in the withdrawal from treatment (Musselman et al., 2001; Capuron et al., 2002; Capuron et al., 2003). Following termination of treatment, depressive behaviours return to baseline, indicating the effects of IFN-α are transient and reversible (Huckans et al., 2015). One of the studies detailing increased depressive symptoms following IFN-α and IL-2 treatment showed that the severity of symptoms correlated with a decrease in serum levels of the essential amino acid tryptophan, the precursor to serotonin (Capuron et al., 2002). These findings show that cytokine-induced depression interacts with the monoamine system and can alter serotonergic synthesis and neurotransmission. It was also reported that IFN-α-induced depressive symptoms correlated with an increase in

adrenocorticotrophic hormone (ACTH) and cortisol, indicating the activation of the HPA axis (Capuron et al., 2003). Furthermore, pre-treatment with the SSRI paroxetine before IFN-α treatment in malignant melanoma patients provided significant protection from the development of depression, with only 11 % of patients reporting depressive symptoms compared to 45 % of placebo-treated patients (Musselman et al., 2001). Similarly, one study showed that paroxetine treatment during IFN-α-induced depression resulted in significant reduction in depressive symptoms and allowed 11 out of 14 hepatitis C patients that had developed depression to complete their course of treatment (Kraus et al., 2002). These findings indicate the administration of IFN-α can induce depression that is pathologically similar to idiopathic depression and responds to existing pharmacological interventions. Taken together with the raised levels of cytokines seen in depressed patients, it is likely that the elevation in cytokines is, at least in part, contributing to the development of depression.

1.2.3 Anti-inflammatory drugs in depression

The effect of anti-inflammatory drugs on depression and depressive symptoms has been studied and reviewed in a recent meta-analysis (Köhler et al., 2014). It was found that anti-inflammatory intervention with both non-steroidal anti-inflammatory drugs (NSAIDs), such as celecoxib, and cytokine inhibitors (primarily TNF-α inhibitors such as infliximab and etanercept) reduce depressive symptoms when compared with a placebo. Furthermore, treatment with cytokine inhibitors or NSAIDs did not result in increases in infections or increases in adverse gastrointestinal or cardiovascular effects, demonstrating a low risk of serious adverse effects. Anti-inflammatory treatment has also been shown to enhance the antidepressant activity of SSRIs (Mendlewicz et al., 2006; Akhondzadeh et al., 2009).

Cyclooxygenase (COX) is an enzyme that contributes to the inflammatory process via the synthesis of prostaglandins (PGs), including PGE_2 (Sugimoto and Narumiya, 2006). PGE_2 elevations have been reported in depressed patients and can induce the expression of cytokines such as IL-6 (Ohishi et al., 1988; Hinson et al., 1996). COX-2 is expressed within the brain and cerebral blood vessels and has been shown to be induced by inflammatory insults and cytokines, indicating it can propagate the inflammatory process within the brain (Madrigal et al., 2003; Skelly et al., 2013). In clinical trials, the inhibition of COX-2 with NSAIDs, such as celecoxib and acetylsalicylic acid, alongside SSRI treatments have been shown to improve depressive symptoms greater than antidepressant treatment alone (Akhondzadeh et

al., 2009; Müller et al., 2006; Mendlewicz et al., 2006). In addition, these findings have been supported in preclinical experiments that show reduced depressive-like behaviour in mice treated with anti-inflammatory drugs such as celecoxib and minocycline (Brunello et al., 2006; Henry et al., 2008; Guo et al., 2009). Similarly, cytokine inhibitors, such as TNF-α antagonist infliximab, have been shown to significantly improve depressive symptoms in MDD patients exhibiting elevated levels of TNF-α (Raison et al., 2013). This finding is supported by preclinical experiments that show TNF-α inhibition reverses TNF-α-induced depressive behaviour in mice (Kaster et al., 2012). Together, these findings indicate that inhibiting aspects of inflammation, whether by directly inhibiting cytokines or upstream processes, can benefit depressed patients who are experiencing inflammation-associated depression, without a significant risk of immunological complications.

1.2.4 Depression co-morbidity with inflammatory diseases

Another observation that may support the concept of inflammation-induced depression is the finding that people experiencing chronic inflammatory disorders are more likely to develop MDD. Inflammatory disorders, such as rheumatoid arthritis, lupus, Alzheimer's disease, multiple sclerosis and HIV, have an estimated prevalence of depression greater than the general population (Iwata et al., 2013; Evans et al., 2005). However, this finding should be interpreted with caution, as these reviews that have compiled the rates of depression for various illnesses have not incorporated the impact of reduced quality of life. People with debilitating, painful, stressful and/or chronic disorders may be expected to have a higher incidence of depression when compared to the otherwise healthy general population.

1.2.5 From psychological stressors to inflammation

The mechanisms by which an emotional state could result in endogenous cytokine expression are unclear. NF-κB is a highly conserved transcription factor that is critical in the innate immune response by regulating the expression of proteins involved in inflammation. NF-κB signalling can be induced by upstream detection of stimuli such as pathogens, cytokines or ultraviolet irradiation, and can induce the expression of proinflammatory cytokines (Gilmore, 2006). It has been shown in humans that acute psychological stress, induced by speaking and performing mental tasks in front of an audience (Trier social stress test; TSST), causes an immediate increase in the level of

NF-κB in the peripheral blood mononuclear cells (PBMCs) taken from blood samples (Bierhaus et al., 2003). Furthermore, it has also been shown that depressed patients have a higher baseline level of NF-κB than healthy controls as well as a greater increase in NF-κB following the TSST (Pace et al., 2006). These findings demonstrate a pathway by which psychological stress is conveyed into a physiological change that stimulates inflammation.

In addition, psychological stressors induce HPA activity and the transient production of glucocorticoids, whereby cortisol suppresses the immune system, increases blood glucose levels and contributes to the acute stress response (McEwen et al., 1998). However, people experiencing chronic psychological stress, such as the familial caregivers of brain-cancer patients, is associated GR dysfunction (Miller et al., 2008). This impairment in GR signalling and immunoregulation can lead to an enhanced inflammatory signalling (Cohen et al., 2012).

1.2.6 Genetics of inflammation and depression

With the accumulating evidence of the involvement of inflammation in depression, the genetic variation of proinflammatory proteins may convey some risk or resilience to the influence of inflammation on mood. A genetic polymorphism in the gene encoding IL-6 have been shown to be associated with reduced depressive symptoms following chronic interpersonal stress (Tartter et al., 2015). Furthermore, a polymorphism in the gene encoding IL-1β was associated with higher depressive symptoms in people that exhibited elevated IL-1β following chronic interpersonal stress (Tartter et al., 2015). In addition to genetic variation, there are epigenetic factors that may also influence mood disorders. FK506 binding protein 5 (FKBP5) is a protein that is involved in the regulation of the GR and important in the negative feedback loop of HPA axis activation via its upregulation. Allele-specific demethylation of the FKBP5 gene has been reported to be associated with the development of depression and suicide in people that have experienced trauma or abuse during childhood (Klengel et al., 2013). Such findings demonstrate the risk of particular genetic polymorphisms in conjunction with environmental factors on depressive symptoms

1.3 Central nervous system inflammation

1.3.1 Overview of microglia

First described in 1919 by Pio del Rio-Hortega, microglia are mononuclear phagocytes known as the tissue-resident macrophages and primary immune cells of the central nervous system (CNS) (del Rio-Hortega, 1919). Microglia in mice originate from haematopoietic stem cells in the yolk sac that migrate to the neuroepithelium during early embryonic development at embryonic day (E)9.5, and are in the brain at E10.5, as opposed to neuronal and other non-neuronal cells which are derived from the neuroectoderm (Ginhoux et al., 2013). Microglia comprise between 5 and 20 % of glial cells, alongside astrocytes and oligodendrocytes (Lawson et al., 1990). The primary function of microglia is to support homeostasis and to protect the brain from infection and injury. In addition, microglia play an important role in the development of the brain and neuronal networks via the pruning of synapses (Paolicelli et al., 2011). In the absence of any stimulation, a 'resting' or 'ramified' microglia has a highly branched morphology that enables the surveillance of its local microenvironment, with a vast range of extracellular receptors to detect any pathogen- or danger-associated molecular patterns (PAMPs or DAMPs), as well as neurotransmitters and neuromodulators (Kettenmann et al., 2011). Such receptors include chemokine receptors, cytokines receptors (including TNF-α, INF-α, IL-1β, IL-10, IL-2 and IL-6), Toll-like receptors (such as TLR4 which recognises lipopolysaccharide, LPS), purinergic receptors (such as P2X7 which recognises extracellular ATP) and monoamine receptors (including serotonin, noradrenaline and dopamine), amongst many others.

Upon stimulation, whether by detection of tissue damage or pathogenic material, the morphology and function of microglia transform into what is generally referred to as an 'active' state, though the implication that a ramified microglia is inactive would be misleading (Kettenmann et al., 2011). An activated microglia will retract much of its processes and form a more amoeboid morphology, allowing increased motility to migrate towards the site of stimulation. Microglia can phagocytose cell debris or microbes and produce inflammatory cytokines and chemokines that propagate an inflammatory response via the attraction of other microglia and peripheral immune cells (Napoli and Neumann, 2009; Hanisch and Kettenmann, 2007). In addition, the activation states of microglia are thought to exhibit a range functions that can be proinflammatory and anti-inflammatory, similar to the 'M1' and 'M2' activation states of macrophages (Figure 1.1) (Orihuela et al., 2016). Such states can be induced

by certain cytokines and PAMPs, and can result in different expression profiles, though this theory has not been tested as rigorously in microglia as it has in macrophages (Martinez and Gordon, 2014). Following a period of activation, microglia will seek resolution of acute inflammation through the activity of anti-inflammatory proteins, such as IL-10, and can eventually return to a ramified state (Cherry et al., 2014).

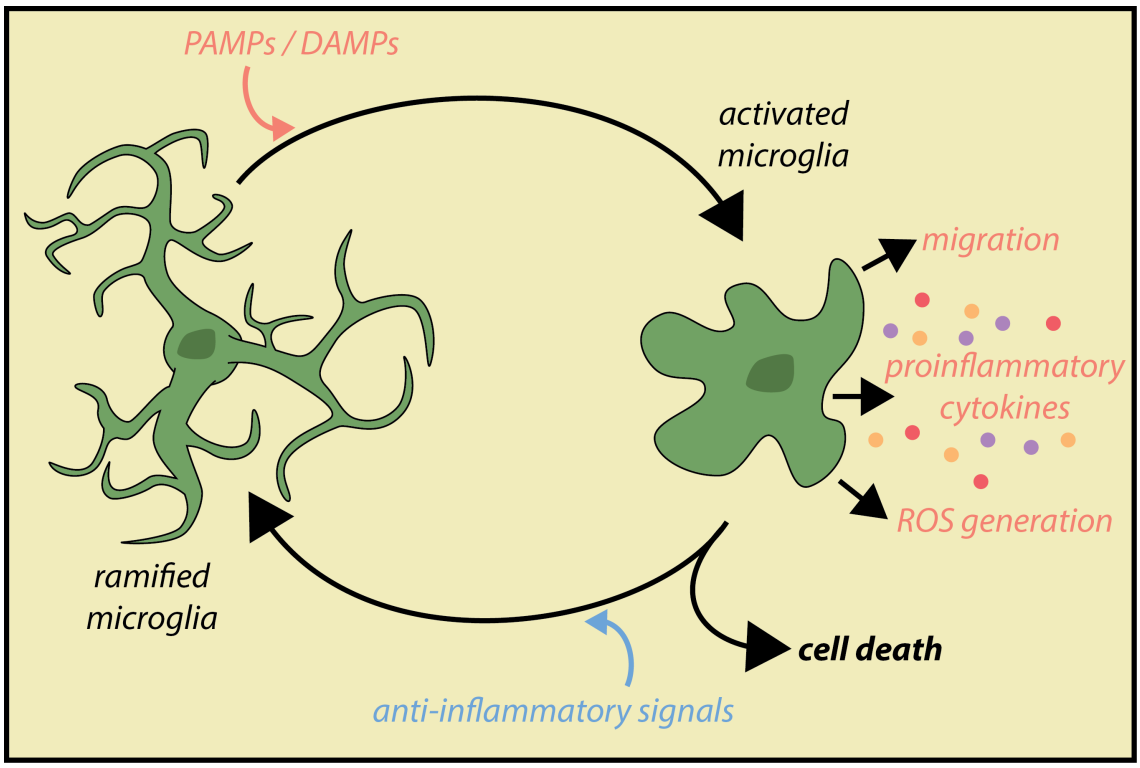

Figure 1.1. Microglia activation.

Ramified microglia is the 'resting' form of microglia that exhibit a branched morphology for environment surveillance. Microglia become activated upon detection of pathogen-associated molecular patterns (PAMPs), such as LPS, or danger-associated molecular patterns (DAMPs), such as proinflammatory cytokines. Activated microglia produce proinflammatory cytokines, generate reactive oxygen species (ROS) and have a more amoeboid morphology to enable migration. Activated microglia can return back to a resting state following stimulation with anti-inflammatory signals, such as IL-10, or can undergo cell death. *Wickens original artwork.*

1.3.2 Microglia in disease

Microglia activation is neurotoxic, and therefore, exaggerated or chronic responses can have negative effects on homeostasis. Diseases associated with activated microglia include neurodegenerative and inflammatory disorders, such as Alzheimer's disease (AD), Parkinson's disease and multiple sclerosis (Saijo and Glass, 2011). For example, in AD, microglia are considered to have both neuroprotective and

neurodegenerative roles. Microglia are activated by amyloid-β (Aβ) and have been shown to aid the degradation of Aβ in mice (Majumdar et al., 2007; Takata et al., 2007). However, the chronic activation of microglia is thought to be detrimental via the effects of inflammatory cytokines that inhibit Aβ degradation (Koenigsknecht-Talboo and Landreth, 2005). The administration of minocycline, an anti-inflammatory agent that can penetrate the brain and inhibit microglia activation, can improve behavioural deficits in a genetic mouse model of AD (Fan et al., 2007).

Post-mortem analyses of brains from depressed suicide victims have indicated enhanced microglia activation, as assessed by expression of a marker of neuroinflammation, HLA-DR (Steiner et al., 2008). Additionally, microglia priming, as assessed by microglia morphology, was increased in depressed suicides as well as the expression of the proinflammatory chemokine MCP-1, which attracts circulating monocytes (Torres-Platas et al., 2014). The authors reported an association between the elevated levels of cytokines in depressed suicides, low-level neuroinflammation and the recruitment of monocytes. However, this finding is not consistent with an earlier study reporting only one of six depressed suicides showing signs of microglia activation (Bayer et al., 1999). *In vivo* assessment of depressed patients by PET scanning using a marker of inflammation (translocator protein) has also shown increased microglia activation (Setiawan et al., 2015).

Microglia activation can be evaluated with far more ease in rodents than in humans and can be correlated with various behaviours associated with depression. Acute stress, chronic stress and inflammatory insults can all induce robust microglia activation (Sugama et al., 2009; Alcocer- Gómez et al., 2015; Hines et al., 2013; Yirmiya et al., 2015). For example, brief restraint stress and water submersion stress in rats causes a significant increase in morphological microglia activation (Sugama et al., 2007). Inescapable shock stressor in rats also induces microglia activation, as well as potentiating the *ex vivo* microglia response to inflammatory insult with LPS (Frank et al., 2007). Chronic unpredictable mild stress has been shown to increase microglia activation, which could be reversed with antidepressant treatment (Pan et al., 2014). Neuroinflammation in rodent models of depression will be discussed in detail in Chapter 3.

1.3.3 Effects of inflammation on the brain

Preclinical data demonstrates that stress and inflammatory insults can induce the production of proinflammatory cytokines, which in turn leads to microglia activation

and inflammatory signalling within the brain. The resulting neuroinflammation leads to pathophysiological and behavioural changes. Here, the effects of cytokines and inflammation in the brain are detailed.

1.3.3.1 Immune signals from the periphery to the brain

Circulating cytokines are a common feature of depression and intravenous administration of cytokines can induce depression in humans (Dowlati et al., 2010; Musselman et al., 2001). Many animal models use systemic inflammatory insults to induce and study neuroinflammation. The method by which peripheral inflammation is transmitted to the brain and induces microglia activation is unclear. The main obstacle of brain-immune communication is the blood brain barrier (BBB). The BBB separates circulating blood and the CNS, tightly controlling the movement of molecules and preventing the entry of pathogens and toxins. The BBB consists of endothelial cells with structural and functional support from astrocytes and pericytes (Ballabh et al., 2004). The endothelial cells of the BBB have intercellular tight junctions that restrict paracellular movement and forces transcellular movement. Transcelluar movement is highly selective via the control of transport proteins and receptor-mediated transcytosis, though some lipophilic molecules can pass through the lipid membrane (Abbott et al., 2006; Obermeier et al., 2013).

The mechanisms by which inflammatory signals overcome the BBB have generally been studied in rodents. The main theories include 1) the stimulation of endothelial cells and the subsequent release of secondary messengers, 2) the active transport of cytokines across the BBB, 3) the passage of cytokines through leaky regions of the BBB, 4) signal transduction via afferent nerves and 5) the infiltration of peripheral immune cells (Figure 1.2) (Quan and Banks, 2007). The administration of LPS in rats caused the activation of endothelial cells in the BBB and the expression of the enzyme COX-2 and its prostaglandin product, PGE_2 (Inoue et al., 2002). The PGE_2 expression correlated with the time-point at which sickness behaviour was observed, indicating that the behavioural response occurred after once inflammatory signals have entered the CNS. In addition, endothelial cells express receptors for various cytokines, including TNF-α, IL-1β and IL-6, which can result also in COX-2 expression (Skelly et al., 2013). TNF-α has also been reported to be transported across the BBB and into the CNS via its receptor (Pan and Kastin, 2002; Gutierrez et al., 1993). Leaky regions of the BBB include circumventricular organs (Ganong, 2000), which are areas of the BBB that are less tightly regulated and allow the passage of certain molecules, such as IL-1 (Breder et al., 1988). The vagal nerve is the most common example of afferent nerve

signal transduction in inflammation. Inflammatory insult causes an upregulation of IL-1β in the vagal nerve as well as increased plasma levels, and the behavioural sickness can be blocked by severance of the vagal nerve (Goehler et al., 1999; Goehler et al., 1997). Finally, although the brain was once considered immune-privileged, *i.e.* being inaccessible to peripheral immune cells, it has since been shown that immune cells, such as monocytes, can infiltrate the CNS in response to TNF-α signalling (D'Mello et al., 2009). Whilst LPS is commonly used as an inflammatory insult, its ability to cross the BBB itself is very limited and its neuroinflammatory effects are considered to be via mechanisms secondary to systemic inflammation (Figure 1.2) or direct stimulation of endothelial cells in the BBB (Banks and Robinson, 2010).

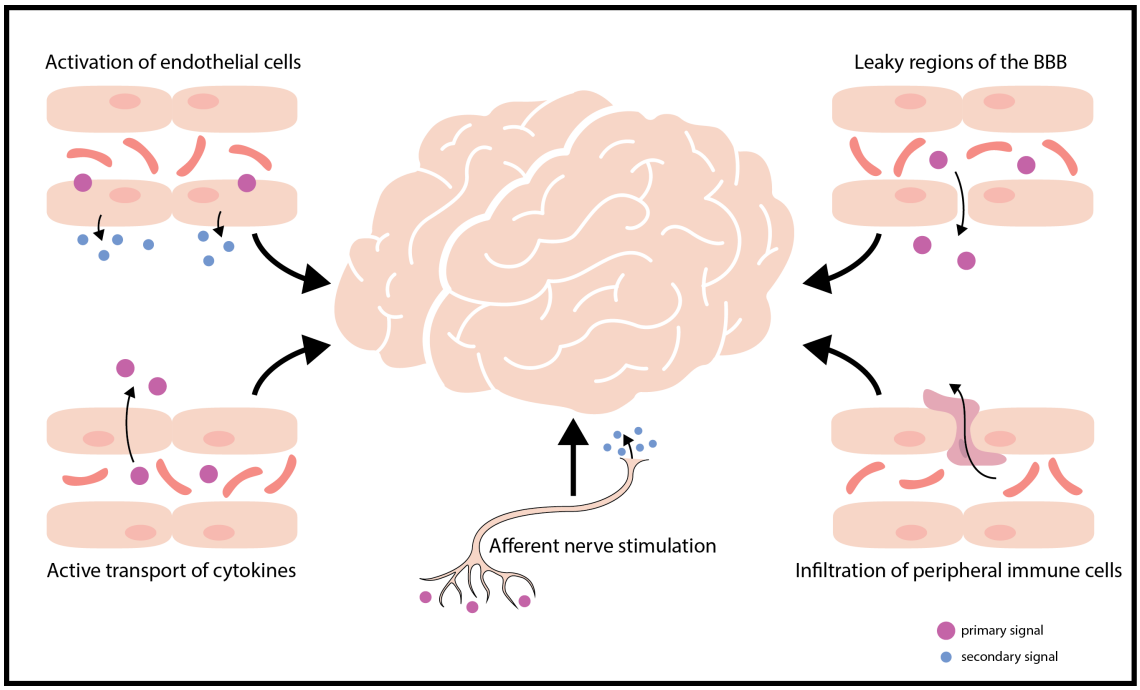

Figure 1.2. Inflammatory signalling from the periphery into the brain.
The five mechanisms by which systemic inflammatory signals are thought to be transmitted across the BBB and into the CNS. *Wickens original artwork.*

1.3.3.2 Neurotransmission

The severity of depressive symptoms induced during IFN-α treatment in cancer patients has been shown to correlate with the reduction of circulating tryptophan (Capuron et al., 2002). This indicates that IFN-α may exert its depressive actions by reducing the availability of the precursor to serotonin, tryptophan, and in turn reduce serotonin neurotransmission. The processing of tryptophan can follow two routes: into serotonin or into kynurenine. The conversion of tryptophan to kynurenine can be performed by indoleamine 2,3 dioxygenase (IDO); an enzyme which is highly induced

by inflammatory cytokines, including IFN-α, IL-1β and TNF-α (Figure 1.3) (Campbell et al., 2014). Cytokines have been shown in rodents to mediate the increased expression of IDO, contributing to inflammation-induced depressive-like behaviours (O'Conner et al., 2009a; O'Conner et al., 2009b). LPS-induced expression of IDO in monocytes is mediated through inflammatory signalling pathways including NF-κB and p38 MAPK (Fujigaki et al., 2006). p38 MAPK activity also mediates the proinflammatory cytokine-induced activity of serotonin transporters, which reduces synaptic serotonin levels (Zju et al., 2006). In mice, systemic LPS has been shown to increase kynurenine levels within the brain, as well as quinolinic acid, presumably by IDO activation and tryptophan metabolism towards the kynurenine pathway (Lawson et al., 2013a; Walker et al., 2013; Dobos et al., 2012; O'Connor et al., 2009a). Blocking the activity of IDO, either by genetic knockout or pharmacological inhibition, results in protection from centrally administered LPS-induced depressive-like behaviour in mice (Lawson et al., 2013b; Parrott et al., 2013; Corona et al., 2013), suggesting the behaviours are mediated by IDO activation and subsequent neuroinflammation within the brain. In humans, tryptophan depletion has been shown to increase depressive symptoms in patients, though this finding was only observed in around one third of patients (Delgado et al., 1994). IFN-α treatment in humans has also been shown to enhance circulating levels of kynurenine and reduce levels of tryptophan and serotonin, alongside the increase in depressive symptoms (Bonaccorso et al., 2002). These findings demonstrate the potential of proinflammatory cytokines to diminish serotonin neurotransmission. Whilst tryptophan depletion has been shown to enhance depressive behaviour, the effect of kynurenine alone also has the ability to induce depressive-like behaviour in mice (O'Connor et al., 2009a). In addition, when tryptophan is metabolised into kynurenine, it can subsequently be metabolised into quinolinic acid in microglia cells (Heyes et al., 1996). Quinolinic acid is an NMDA receptor agonist that can be used in high doses to induce excitotoxicity in neurodegenerative disease mouse models (Sanberg et al., 1989). Quinolinic acid is increased in microglia in the anterior cingulate cortex of depressed suicide brains, and the level of CSF quinolinic acid is associated with cytokine-induced depression (Steiner et al, 2011; Raison et al., 2010).

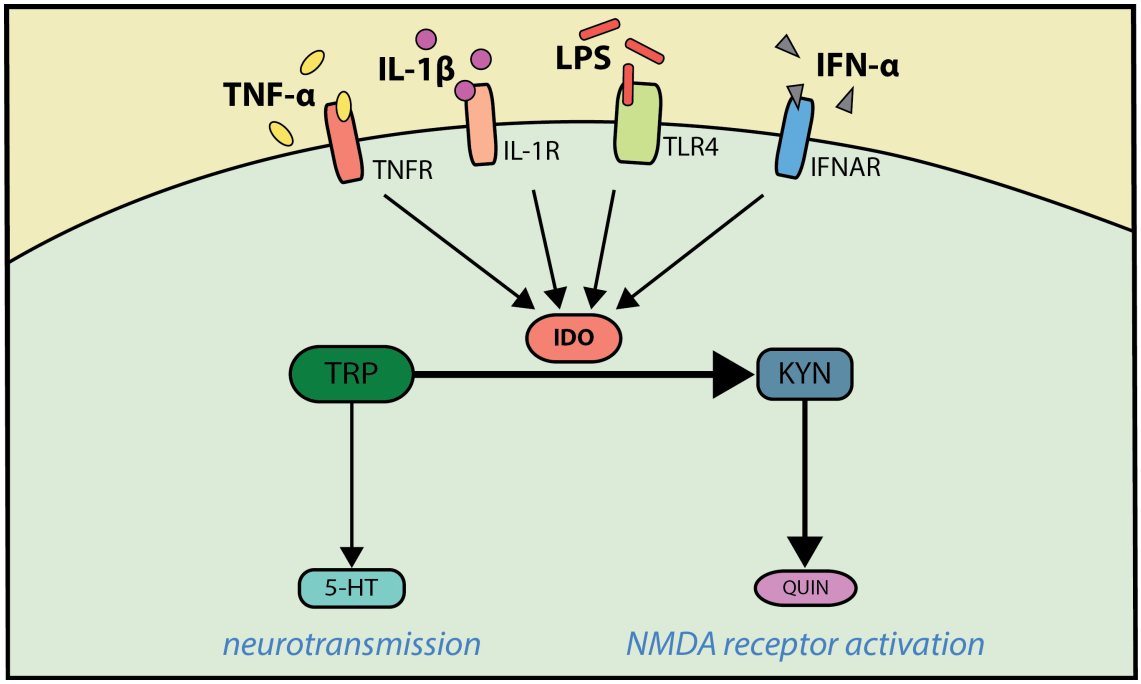

Figure 1.3. IDO signalling.

Indoleamine 2,3 dioxygenase (IDO) converts tryptophan (TRP) to kynurenine (KYN). This reduces the processing of TRP towards 5-HT. KYN can be metabolized towards the production of NMDA receptor agonist quinolinic acid (QUIN). Inflammatory cytokines (including TNF-α, IL-1β and IFN-α) and LPS can enhance IDO expression and activity. *Wickens original artwork.*

In *in vitro* experiments, cytokines have been shown to induce the release of glutamate from astrocytes, which would contribute to excitotoxicity within the CNS (Ida et al., 2008). Dopaminergic signalling has also been implicated in cytokine-induced depression. IFN-α treatment in humans causes a reduction in the activity of the enzyme tetrahydrobiopterin (BH4), which converts phenylalanine to tyrosine, a dopamine precursor. Following IFN-α treatment, CSF tyrosine is decreased, whilst phenylalanine and the inactive oxidised form of BH4 is increased (Felger et al., 2013). Cytokine-induced activity of nitric oxide synthase (NOS) and the production of nitric oxide (NO) is thought to increase BH4 oxidation and reduce the availability of BH4 and dopamine in rats (Kitagami et al., 2003). Together, these findings support the role of inflammatory cytokines in reduced monoamine production as well as enhanced excitotoxicity and glutamatergic signalling within the depressed brain.

1.3.3.3 HPA axis

Paradoxically, depression is associated with inflammation as well as increased levels of cortisol, which is anti-inflammatory. However, cortisol fails to exert anti-inflammatory effects due to impaired GR feedback (Figure 1.4) (Pace and Miller, 2009). Whilst IFN-α treatment can acutely induce HPA axis hyperactivity with increased levels of ACTH and cortisol, this response is not present after chronic treatment, indicating cytokines do not induce sustained cortisol expression (Capuron et al., 2003). Instead, the actions of inflammation on the HPA axis are thought to primarily be through impairing GR function and inhibiting the anti-inflammatory actions of cortisol (Pariante, 2006). Proinflammatory cytokines, such as IL-1α, TNF-α and IFN-α, have been shown to inhibit GR translocation to the nucleus and subsequent GR-mediated gene expression via the activation of glucocorticoid response elements (GRE) (Pariante et al., 1999; Kino et al., 2003; Hu et al., 2009). Furthermore, antidepressant compounds are able to enhance dexamethasone-induced GR translocation and gene expression by inhibiting active transport of dexamethasone or cortisol from the cell (Pariante et al., 2001). p38 MAPK has been implicated in the process of cytokine-induced GR dysfunction, with p38 MAPK inhibition reversing the cellular effects of IL-1α (Wang et al., 2004). Other cytokine-induced inflammatory signalling proteins, including NF-κB, c-Jun amino-terminal kinase (JNK) and signal transducer and activator of transcription 5 (STAT5), have also been shown to impair GR expression, translocation and/or function (Pace and Miller, 2009; Hu et al., 2009). These data indicate that the induction of proinflammatory cytokines can impair the inhibitory feedback role of GR receptors by altering downstream signalling pathways.

1.3.3.4 Neurogenesis and neuroplasticity

Reduced adult neurogenesis has been implicated in the pathology of depression (Sahay et al., 2007). Much work focuses on the hippocampus, due to its role in learning and memory, its apparent atrophy in MDD and the relatively high basal level of adult neurogenesis (Sapolsky, 2001). For example, depression is associated with reduced hippocampal and frontal lobe volume as assessed by magnetic resonance imaging (Frodl et al., 2006; Videbech and Ravnkilde, 2004). Such findings are interpreted as an indirect measure of impaired adult neurogenesis in depressed patients.

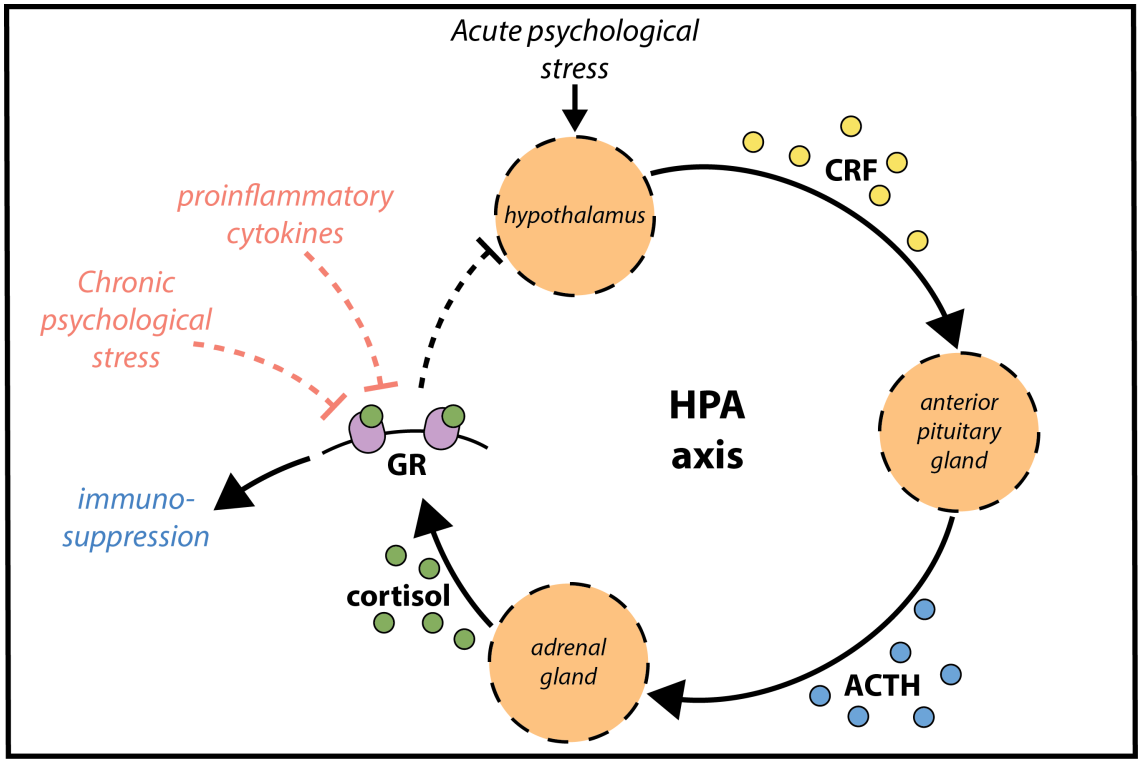

Figure 1.4. HPA axis.

Psychological stress stimulates hypothalamic-pituitary-adrenal (HPA) axis activity. Corticotrophin-releasing factor (CRF) is released from the hypothalamus and stimulates adrenocorticotrophic hormone (ACTH) release from the anterior pituitary gland. ACTH stimulates cortisol release from the adrenal gland, which binds glucocorticoid receptors (GR) to inhibit HPA activity and suppress the immune system. Chronic psychological stress and proinflammatory cytokines can impair GR function, increasing HPA activity yet reducing the anti-inflammatory activity of cortisol. *Wickens original artwork.*

In animal models, proinflammatory cytokines have been shown to have negative effects on neurogenesis (Song and Wang, 2011). LPS, inflammatory cytokines (including TNF-α and IL-1β) and chronic stress have all been shown to reduce neurogenesis in the hippocampus of mice (Iosif, 2006; Koo and Duman, 2008; Monje et al., 2003). IL-1R-knockout or the administration of an IL-1R antagonist can reverse both the depressive behaviours and the reduced neurogenesis induced by chronic stress (Koo and Duman, 2008). In IL-1R knockout mice, chronic stress also failed to increase levels of corticosterone, the murine analogue of cortisol, and the depressive-like behaviour was attenuated. Subsequently, the direct administration of chronic corticosterone induced depressive-like behaviour and reduced neurogenesis in both IL-1R knockout and wildtype mice (Goshen et al., 2008). These data indicate a role of HPA axis activity in IL-1-mediated suppression of neurogenesis and increased depressive-like behaviour. IL-1β has been shown to regulate anti-neurogenic effects of IFN-α treatment in the mouse hippocampus (Kaneko et al., 2006). Furthermore,

mechanisms by which IL-1β inhibits neurogenesis may be via the neurotoxic effects of the kynurenine-quinolinic acid pathway following IDO activation, as inhibition of kynurenine 3-monooxygenase prevents quinolinic acid production and enhances neurogenesis (Zunszain et al., 2012). These data demonstrate the ability of inflammation and the production of inflammatory cytokines to inhibit neurogenesis, alongside altering GR function and monoamine neurotransmission, supporting the hypothesis of inflammation-induced pathophysiological changes in depression.

1.4 The NLRP3 inflammasome

The primary function of the innate immune system is to detect and remove pathogens or damaged tissue. Immune cells, including macrophages and microglia, express the necessary receptors for the detection of a range of stimuli and the machinery necessary for the induction of an inflammatory response (Kettenmann et al., 2011). First identified in 2002, the inflammasome is an intracellular multi-protein complex that, upon activation and assembly, leads to the production of the proinflammatory cytokines IL-1β and IL-18 (Martinon et al., 2002). These cytokines are important to many inflammatory processes, such as the recruitment of immune cells. The NLRP3 inflammasome is the most regularly studied inflammasome, though there are a number of other inflammasomes formed with other NLR proteins (Figure 1.5A) (Tschopp et al., 2003). The NLRP3 inflammasome is expressed in many tissues, including the CNS, and has been studied extensively due to its activity in response to a broad range of stimuli (Ying et al., 2009). The activity of the NLRP3 inflammasome signalling is dependent upon two stages: firstly, the upregulation of the necessary proteins (priming), and secondly, the assembly of the inflammasome resulting in its activation. The NLRP3 inflammasome is important in the innate immune response, responding to a wide range of stimuli including pathogen-associated molecular patterns (PAMPs) and danger-associated molecular patterns (DAMPs). The activation and induction of an inflammatory response via the actions of IL-1β and IL-18 ultimately lead to the clearance of pathogenic material or damaged tissue.

1.4.1 Components

NOD-like receptors (NLRs) are a family of pathogen-recognition receptors (PRRs) that can sense a range of intracellular stimuli in response to PAMPs and

DAMPs (Davis et al., 2011). There are a number of NLRs that result in the formation of different inflammasomes, sensitive to specific stimuli (Figure 1.5A). NLRs contain a NACTH nucleotide-binding domain (NBD), a leucine-rich repeat (LRR) and a variable N-terminus. There are a number of NLRs that have an N-terminal pyrin domain, including NLRP3 (also referred to as NOD-, LRR- and pyrin domain-containing 3) (Ting et al., 2008). The NBD required for the oligomerisation of NLRP3, whilst the LRR is considered to be the ligand-interaction domain, though an official ligand has not yet been identified. Due to the wide range of stimuli NLRP3 responds to, it is likely there is a converging intermediate signalling process responsible for the induction of NLRP3 inflammasome activation. Finally, the pyrin domain allows for pyrin-pyrin interactions, vital in the formation of the inflammasome (Martinon et al., 2002).

Along with NLRP3, there are two other proteins in the NLRP3 inflammasome (Figure 1.5B). ASC (apoptosis speck-like protein containing a CARD or PYCARD) is an adaptor protein that consists of a pyrin domain and a CARD (caspase activation and recruitment domain). The pyrin domain interacts with the pyrin domain of NLRP3, whilst the CARD domain enables interaction with other CARD domains (Agostini et al., 2004). The third and final component of the NLRP3 inflammasome is procaspase-1, which contains a CARD domain that can interact with the CARD domain of ASC. Procaspase-1 is the precursor to caspase-1. NRLP3 inflammasome assembly induces the auto-cleavage of procaspase-1 and the formation of the active caspase-1. Subsequently, caspase-1 can cleave proIL-1β and proIL-18 into their mature and biologically active forms, IL-1β and IL-18. These inflammatory cytokines are then rapidly secreted from the cell to propagate the inflammatory response (Schroder and Tschopp, 2010).

Other inflammasomes include NLRP1, NLRP6, NLRP7 and NLRP12, which all contain a LRR, a NBD and a pyrin domain. NRLC4 contains a CARD domain instead of a pyrin domain, whilst NLRP1 has both a pyrin domain and a CARD domain. This enables NLRP1 and NLRC4 to directly interact with procaspase-1 without ASC, though ASC interaction allows for a greater magnitude of response due to the formation of large protein filaments to amplify capsase-1 activity (Faustin et al., 2007). In addition to the NLR inflammasomes, there is the absent in melanoma 2 (AIM2) inflammasome which contains a DNA-sensing HIN domain and a pyrin domain for ASC interaction. NLRP1, NLRC4 and AIM2 inflammasome expression has all been reported within the CNS (Yin et al., 2009; Denes et al., 2015).

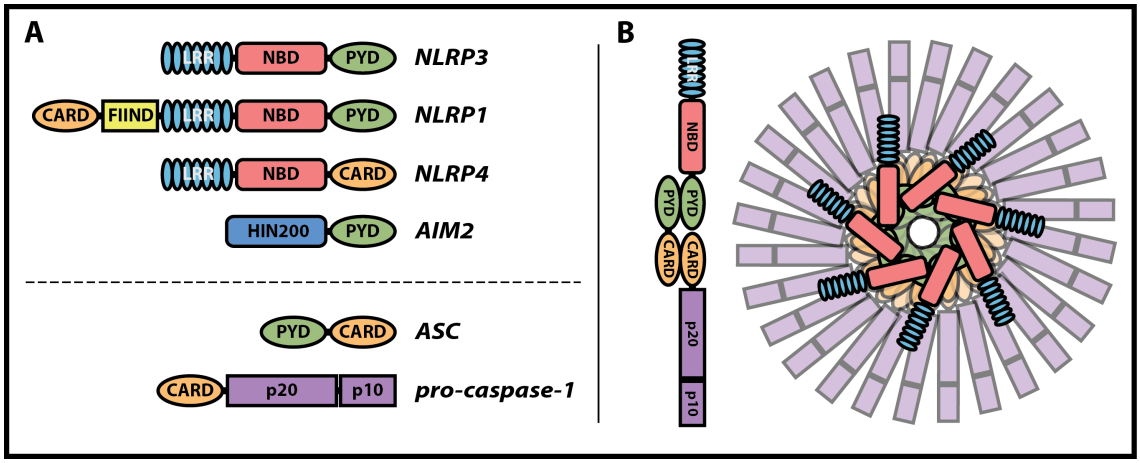

Figure 1.5. The inflammasomes.

Components of the NLRP3, NLRP1, NLRP4 and AIM2 inflammasomes (**A**). NLRP3 contains a pyrin domain (PYD), a nucleotide-binding domain (NBD) and a leucine-rich repeat (LRR). AIM2 contains a DNA-sensing HIN domain. NLRP3 stimulation leads to the activation of the NLRP3 inflammasome (**B**). NLRP3 oligomerises and its PYD domain interacts with the PYD domain of ASC and enables the formation of large ASC filaments, amplifying the inflammasome response. The CARD domain of ASC interacts with the CARD domain of procaspase-1, allowing autocleavage and the production of active caspase-1. *Wickens original artwork.*

1.4.2 Priming

The activity of the NLRP3 inflammasome is dependent upon two distinct signalling pathways that converge: priming and activation. Both are necessary but not sufficient for inflammasome activation and IL-1β production (Bauernfeind et al., 2009).

The priming step, referring to the upregulation of NLRP3 and proIL-1β, is dependent upon NF-κB signalling (Figure 1.6). Toll-like receptors (TLRs) are a family of receptors that recognise a range of microbial molecular patterns and culminate in the activation of the transcription factor NF-κB (Kawai and Akira, 2007). TLRs can respond to bacterial, fungal and viral components (Akira and Takeda, 2004). LPS is a component of the Gram-negative bacterial cell wall and is recognised by the TLR4 receptor. LPS-TLR4 signalling activates downstream signalling molecules, including myeloid differentiation primary response gene 88 (MyD88), resulting in NF-κB disinhibition via the phosphorylation of the inhibitor of NF-κB (IκB) proteins. Subsequently, NF-κB components can translocate to the nucleus and induce transcription (Lawrence, 2009). Inhibition of NF-κB dose-dependently reduces NLRP3 inflammasome priming (Bauernfeind et al., 2009). Priming is also induced in response to endogenous signals. Proinflammatory cytokines, such as TNF-α IL-1β, can induce NF-κB signalling and have been shown to enable ATP-induced NLRP3 inflammasome

activation by inducing NF-κB-mediated protein expression (Franchi et al., 2009). NF-κB inhibition abrogates extracellular ATP-induced inflammasome activation following priming with both TNF-α and LPS, indicating that both stimulants converge onto NF-κB signalling in order to prime cells (Franchi et al., 2009). In addition to *de novo* protein synthesis, the NLRP3 inflammasome can also be primed via the process of deubiquitination of NLRP3. This is thought to be the early stage of priming following TLR4 or ATP signalling (Juliana et al., 2012). Therefore, there are two sources of functional NLRP3 following stimulation: the deubiquitination enables rapid immediate availability of NLRP3, whilst *de novo* protein synthesis takes place for more delayed availability.

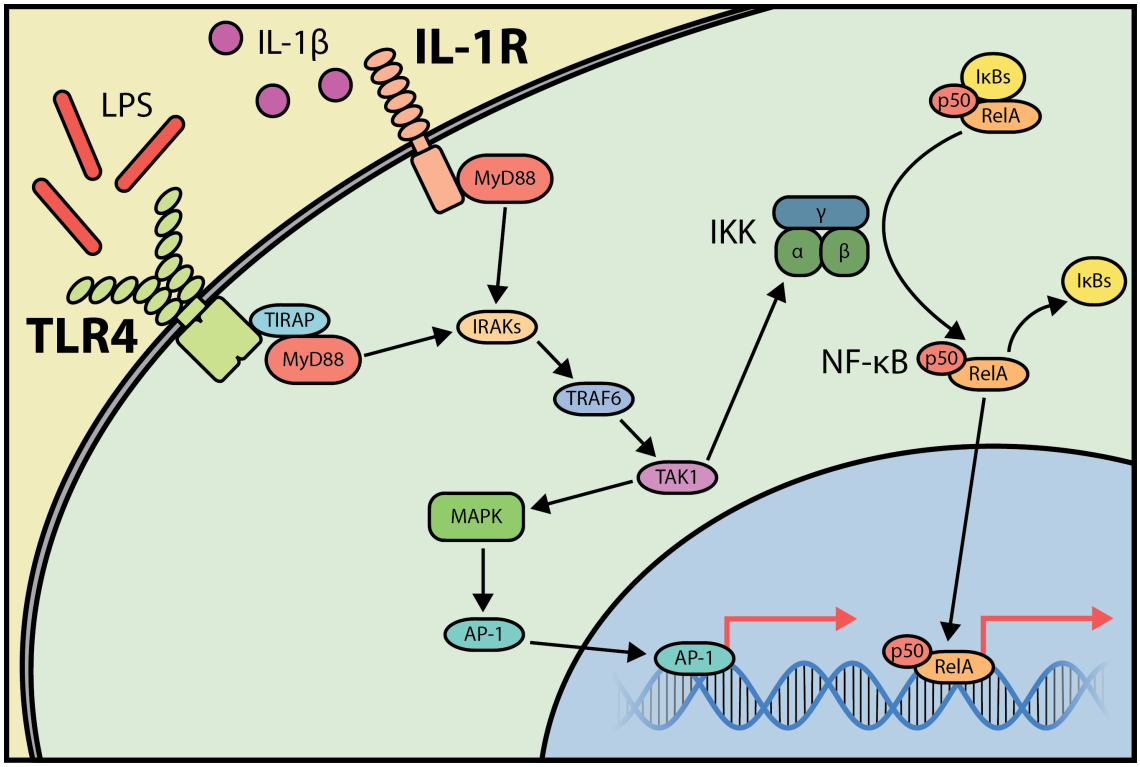

Figure 1.6. Cell priming.

LPS- and IL-1β-induced protein expression via TLR4 and IL-1R, respectively. MyD88 activation leads to the recruitment of IRAK and TRAF6, and the activation of TAK1. TAK1 activates the IKK complex, which phosphorylates IκB and allows NF-κB translocation to the nucleus. TAK1 also leads to MAPK phosphorylation and the activation of AP-1. Both NF-κB and AP-1 induce transcription of proinflammatory proteins. *Wickens original artwork.*

1.4.3 Activation

Activation of the inflammasome refers to the assembly of the inflammasome following the stimulation, which enables the production of IL-1β and IL-18 via caspase-1 activity (Figure 1.7) (Martinon et al., 2002). Upon activation of the NLRP3 inflammasome, ASC dimerises and forms large filament aggregates within the cell, which can be detected via immunofluorescence and often referred to as ASC-specks (Fernandes-Alnemri et al., 2007; Lu et al., 2014). This speck formation has been shown to be dependent upon both priming and inflammasome activation (Bauernfeind et al., 2009). Linear ubiquitination of ASC, via the linear ubiquitination assembly complex (LUBAC), has been show to be necessary for assembly of the NLRP3 inflammasome in macrophages following stimulation with the ionophore nigericin (Rodger et al., 2014). The function of ASC aggregation is to amplify inflammasome activation and cytokine production. In addition, oligomeric NLRP3 inflammasome particles are released from macrophages into the extracellular space following ATP or nigericin stimulation, where caspase-1 activity continues and further amplifies the local inflammatory response extracellularly (Baroja-Mazo et al., 2014).

Exogenous PAMPs that have been shown to activate the NLRP3 inflammasome include influenza, adenovirus, *Staphylococcus aureus*, *Neisseria gonorrhoeae* and some bacterial pore-forming toxins such as nigericin (Allen et al., 2009; Muruve et al., 2008; Mariathasan et al., 2006; Duncan et al., 2009; Walev et al., 1995). Sterile signals that activate the NLRP3 inflammasome include endogenous stimuli such as extracellular ATP, Aβ, uric acid, high glucose or cholesterol crystals, as well as exogenous stimuli such as asbestos and silica (Mariathasan et al., 2006; Halle et al., 2008; Martinon et al., 2006; Duewell et al., 2010; Cassel et al., 2008; Dostert et al., 2008; Trueblood et al., 2011). Due to the wide range of stimuli that can induce NLRP3 inflammasome activation, it is assumed that these stimuli converge onto certain intracellular signals that indicate stress or damage and subsequently activate the inflammasome.

The resulting activation of caspase-1 can lead to a form of cell-programmed inflammation-associated cell death, called pyroptosis (Miao et al., 2011). Pyroptosis in macrophages has been shown to be dependent upon ASC and caspase-1 and the processing of gasdermin D (GSDMD), which causes the formation of membrane pores, cell swelling and rupture (Sborgi et al., 2016). Non-canonical pathways for NLRP3 inflammasome activation have been reported to involve the activation of caspase-11 in response to cytosolic triggers including LPS, in the absence of TLR4 activation (Kayagaki et al., 2011). LPS that has entered the cell can bind directly to the CARD

domain of caspase-11 and culminates in the activation of the NLRP3 inflammasome and caspase-1 through mechanisms currently unknown (Kayagaki et al., 2013). Whilst caspase-11 is not required for ATP-induced IL-1β production, it is required for *E. coli* activation of caspase-1, and caspase-11 knockout provided protection from lethal doses of LPS in mice (Kayagaki et al., 2011).

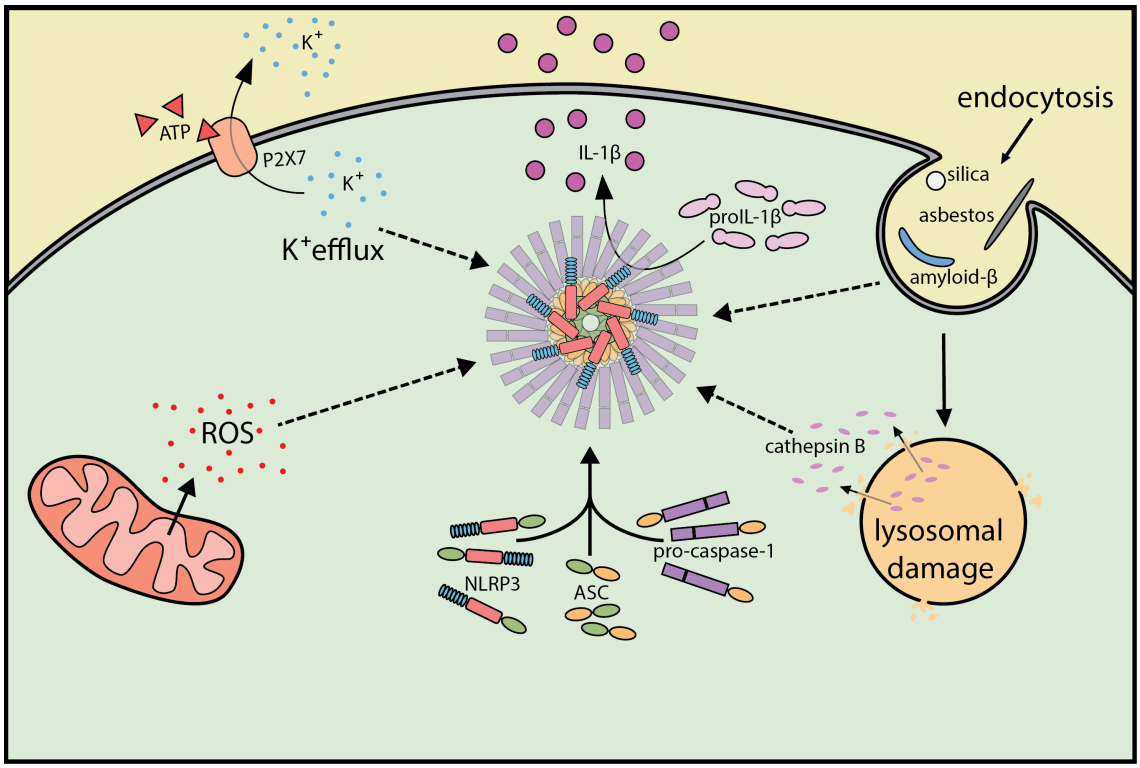

Figure 1.7. NLRP3 inflammasome activation.

Mechanisms of activation for the NLRP3 inflammasome include P2X7 receptor-mediated potassium efflux, ROS generation, endocytosis (including silica, asbestos and amyloid-β) and the release of cathespin B following lysosomal damage. *Wickens original artwork.*

1.4.3.1 Potassium efflux and P2X7

Intracellular signals that are thought to mediate NLRP3 inflammasome activation following stimulation include potassium (K^+) efflux, the generation of reactive oxygen species and lysosomal damage, with many activators stimulating more than one of these cellular processes (Guo et al., 2015). Inflammasome activation via K^+ efflux is mediated primarily by the P2X7 receptor. P2X receptors are trimeric ligand-gated cation channels that, upon interaction with extracellular ATP, enable calcium (Ca^{2+}), sodium (Na^+) and K^+ movement between the cytosol and extracellular space

(Suprenant et al., 1996). The P2X7 receptor responds to high extracellular concentrations of ATP, with an EC_{50} of 160 μM in mice (Vitiello et al., 2012; Donnelly-Roberts et al., 2009). The inhibition of the P2X7 receptor blocks ATP-induced NLRP3 inflammasome activation and IL-1β release in neutrophils, monocytes and microglia (Karmakar et al., 2016; Piccini et al., 2008; Murphy et al., 2012). THP-1 monocytes lysed in low K^+ buffers (< 70 mM) exhibit spontaneous inflammasome assembly and activation, as demonstrated by immunoprecipitation (Pétrilli et al., 2007). When the K^+ concentration of the lysis buffer was raised above 70 mM, NLRP3 inflammasome assembly and activity did not occur. This suggests that ATP-induced K^+ efflux lowers the cytosolic K^+ concentration from 140-150 mM to below 70 mM, the threshold for NLRP3 inflammasome activation. In addition, increasing the extracellular K^+ can inhibit K^+ efflux and NLRP3 inflammasome activity. Raising the extracellular K^+ concentration from 5 mM to 30 mM inhibited NLRP3 inflammasome activation in bone marrow-derived macrophages (BMDMs) by ATP, nigericin, lysosomal destabilization (by Leu-Leu methyl ester hydrobromide), alluminium, silica and crystals (Muñoz-Planillo et al., 2013).

ATP is released by many cells as a DAMP in response to infection or damage and acts as a local signalling molecule, exerting autocrine and paracrine functions directed towards mediating an immune system response (Praetorius and Leipziger, 2009). Extracellular ATP release has also been shown to mediate NLRP3 inflammasome activation induced by uric acid crystals, silica, alum crystals and nigericin (Muñoz-Planillo et al., 2013; Riteau et al., 2012). Whilst high concentrations of ATP act as a proinflammatory danger signal by binding the P2X7 receptor (Piccini et al., 2008), other P2X receptors (P2X1 and P2X4) can respond to lower concentrations of ATP and have different roles in immune signalling, such as T cell activation (Woehrle et al., 2010). P2X4 receptors have also been reported to mediate high glucose-induced NLRP3 inflammasome activation in epithelial cells (Chen et al., 2013). High extracellular Ca^{2+} can also induce NLRP3 inflammasome activation via calcium-sensing receptors (Rossol et al., 2012; Muñoz-Planillo et al., 2013). The role of intracellular Ca^{2+} in NLRP3 inflammasome activation is controversial. Some reports state that inhibition of cytosolic Ca^{2+} signalling attenuates ATP-induced NLRP3 inflammasome signalling (Murakami et al., 2012). However, Ca^{2+} signalling in ATP-induced NLRP3 inflammasome activation is reportedly neither necessary nor sufficient (Katsnelson et al., 2015). As well as inducing K^+ efflux, extracellular ATP has been shown to induce the formation of pores via P2X7 receptor interaction, which enables the movement of large molecules up to 1 kDa across the lipid membrane (Pelegrin and Surprenant, 2006; Kanneganti et al., 2007). This can be demonstrated by the uptake of large-molecule dyes, and could enable the entry of PAMPs and DAMPs into the cell for

cytosolic interactions. These pores are formed by pannexins, as inhibition of pannexin-1 (Panx1) blocks P2X7 receptor-mediated uptake of dye, and has been shown to be important in ATP-induced release of IL-1β (Pelegrin and Surprenant, 2006). Conversely, pannexin-1-knockout macrophages have been reported to have impaired ATP release as a DAMP, but unaffected ATP-induced inflammasome activation (Qu et al., 2011). However, examination of the Panx1 knockout mouse strain has revealed only a 70 % reduction in Panx1 mRNA expression (Hanstein et al., 2013).

1.4.3.2 Reactive oxygen species

The generation of reactive oxygen species (ROS) is considered a vital signal in NLRP3 inflammasome response to cell stress (Tschopp and Schroder, 2010; Harijith et al., 2014). The production of ROS such as superoxide (O_2^-•) and hydroxyl radicals (OH•) occurs primarily within the mitochondrial electron transport chain as a by-product of cellular respiration (Figure 1.8). ROS generation can also be a result of enzymes such as NADPH oxidases (NOXs) with a direct role in cell signalling (Bedard and Krause, 2007). ROS levels are normally controlled by the induction of antioxidant proteins, such as superoxide dismutase (SOD). High levels of ROS are associated with cellular stress and can lead to cell damage and cell death (Fleury et al., 2002). Inhibition of ROS, both general ROS and NOX-dependent ROS, reduces NLRP3 inflammasome activity (Bauernfeind et al., 2011). However, this was reported to be a result of reduced expression of inflammatory protein such as NLRP3 and not reduced inflammasome activity. These findings indicate that ROS can increase NLRP3 inflammasome activity by enhancing cell priming.

However, a number of studies have reported that ROS signalling is required for NLRP3 inflammasome activation. ATP stimulation and activation with particulates, such as asbestos and silica, have all been shown to induce the generation of ROS (Cruz et al., 2007; Dostert et al., 2008). Blocking NOX-mediated ROS generation can inhibit ATP- or nigericin-mediated activation of the NLRP3 inflammasome and IL-1β release in macrophages (Cruz et al., 2007; Hewinson et al., 2008). Silica-induced NLRP3 inflammasome activation has been shown to require NOX-mediated ROS signalling, which is upstream of inflammasome activity as demonstrated by silica-induced ROS in NLRP3$^{-/-}$ macrophages (Cassel et al., 2008). Mitochondrial ROS has also been shown to be important in NLRP3 inflammasome activity, with enhanced mitochondrial ROS resulting in increased NLRP3 inflammasome activity (Zhou et al., 2011). ATP and nigericin have been shown to induce lysosomal damage and inflammasome activation via mitochondrial ROS (Heid et al., 2013). Blocking

mitochondrial ROS via a mitochondria-targeted antioxidant can inhibit ATP-induced NLRP3 inflammasome activation (Nakahira et al., 2011). Mitochondrial ROS-mediated NLRP3 inflammasome activity is also responsible for the release of mitochondrial DNA into the cytosol, which was shown to further enhance IL-1β release in macrophages (Nakahira et al., 2011). Subsequently, ATP-induced IL-1β release is attenuated in macrophages lacking mitochondrial DNA (Shimada et al., 2012).

Whilst ROS have repeatedly been shown to be important in NLRP3 inflammasome activation, the mechanisms by which ROS can cause activation are unclear. ROS have also been shown to interact with proteins that directly alter NLRP3 inflammasome function. ROS oxidise thioredoxin (TRX), causing it to dissociate from TRX-interacting protein (TXNIP) and, subsequently, TXNIP associates with NLRP3 leading to NLRP3 inflammasome activation. Furthermore, TXNIP knockout can impair IL-1β secretion, whilst TRX knockout enhances IL-1β secretion in macrophages, demonstrating the role of ROS-TXNIP-NLRP3 signalling in IL-1β production (Zhou et al., 2010). However, this finding was not replicated with $TXNIP^{-/-}$ macrophages in another research group (Masters et al., 2010). TXNIP can also translocate to the mitochondria, bind TRX2 and cause enhanced ROS generation (Li et al., 2009; Lane et al., 2013). In addition, ATP-induced ROS generation was shown to stimulate extracellular signal-regulated protein kinases 1 and 2 (ERK1/2) phosphorylation and PI3K activation, which can mediate processes such as apoptosis and metabolism (Cruz et al., 2007). Contradicting the theory of ROS generation stimulating NLRP3 inflammasome activity, $SOD1^{-/-}$ macrophages exhibit enhanced superoxide production and reduced caspase-1 and NLRP3 inflammasome activity in response to ATP, nigericin and *S. aureus* (Meissner et al., 2008). Increased superoxide levels resulted in caspase-1 inactivation via oxidation. In addition, $SOD\text{-}1^{-/-}$ provided protection from LPS-induced septic shock. Cell-type, ROS-type and spatio-temporal differences in ROS may contribute to these differences.

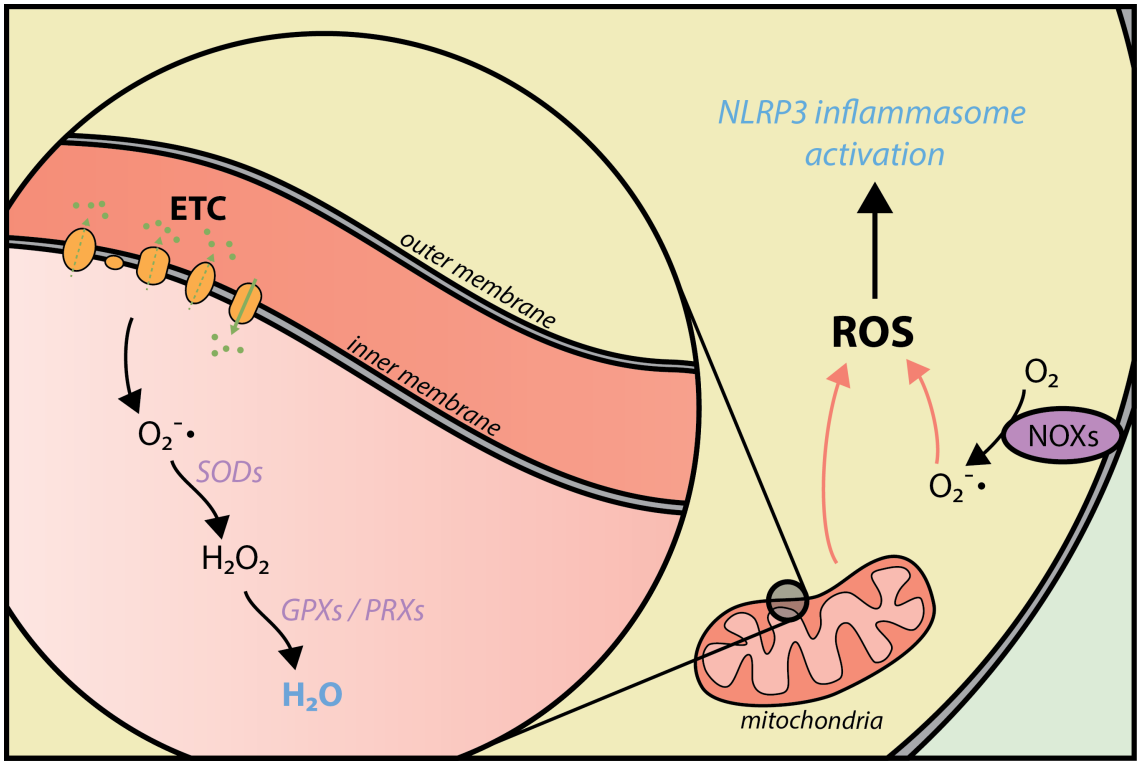

Figure 1.8. ROS generation.

Reactive oxygen species (ROS) are generated in the mitochondria as a by-product of the electron transport chain (ETC). Superoxide radicals ($O_2^{-}\bullet$) are produced following the reduction of oxygen (O_2). Superoxide can be converted to hydrogen peroxide (H_2O_2) by superoxide dismutases (SODs), which can then be reduced to water (H_2O) by glutathione peroxidases (GPXs) or peroxiredoxins (PRXs). Superoxide can also be generated in the cytosol by membrane-bound NADPH oxidases (NOXs). ROS generation can induce NLRP3 inflammasome activation. *Wickens original artwork.*

1.4.3.3 Lysosomal damage

In addition to ROS and K^+ efflux, lysosomal rupturing can result in NLRP3 inflammasome activation. Lysosomes mediate the degradation and digestion of intracellular waste material and of material phagocytosed from outside of the cell. Phagocytosis of certain NLRP3 inflammasome activators, including amyloid-β, asbestos and silica, have been shown to induce lysosomal damage in macrophages and microglia, leading to the activation of the NLRP3 inflammasome (Halle et al., 2008; Hornung et al., 2008; Dostert et al., 2009). In addition, inhibition of phagocytosis with cytochalasin D (which impairs actin filament assembly) can block amyloid-β- and silica-mediated inflammasome activation and subsequent IL-1β release (Halle et al., 2008; Hornung et al., 2008). Imaging of macrophage endolysosomes reveals crystal-induced leakage of lysosomal contents (Hornung et al., 2008). It has been reported that the release of cathepsin B (a lysosomal protease usually contained within the lysosome)

contributes to this activation. Inhibition of cathepsin B (selective inhibitor CA-074-Me) can inhibit crystal-induced NLRP3 inflammasome activation (Hornung et al., 2008), though contrasting data have been reported using cathepsin B knockout macrophages (Dostert et al., 2008). Whilst ATP and nigericin causes lysosomal rupturing after NLRP3 inflammasome activation, lysosomal rupturing alone (via lysosomal destabilising agent LLOMe) can also trigger inflammasome activation (Lima et al., 2013). It has been reported that the ATP- and nigericin-induced lysosomal damage is a result of mitochondrial ROS generation (Heid et al., 2013). These findings indicate agents that induce lysosomal damage, such as amyloid-β, can induce inflammasome activation via mechanisms independent of K^+ efflux.

1.5 Modeling inflammation and depression

1.5.1 The validity of modeling depressive-like behaviour in mice

The validity of any animal model is based on three main concepts: construct validity, face validity and predictive validity (Willner and Mitchell, 2002). Construct validity refers to the methodological approach used to induce and assess a disease-like state, face validity refers to the similarity between the model and the disease condition, both behaviourally and neuropathologically, and predictive validity refers to the ability of a model to respond to pharmacological treatments in a similar way to the human condition (Willner and Mitchell, 2002).

Animal models are an integral part of studying mood disorders and the underlying pathophysiology (Krishnan et al., 2011; Nestler and Hyman, 2010). However, modeling depression in rodents entails greater difficulties in comparison to a purely physical or genetic disorder. Whilst construct validity can be accomplished with relative ease in genetic conditions, modeling a psychiatric disorder like depression is difficult as the etiology is unclear and no disease-causing genes have been identified (Nestler and Hyman, 2010). Neurobiological and behavioural changes have to be induced by environmental or pharmacological manipulation. In addition, any behavioural assessment in mice following a particular manipulation is dependent upon locomotion, which is subsequently interpreted to indirectly represent a particular emotional state. Therefore, the construct validity of behavioural paradigms used in models of mood disorders is also weak. For face validity, many symptoms apparent in depression cannot be modeling in rodents, such as guilt or suicidal thoughts. Therefore, there is a focus on specific behavioural components, such as anhedonic

and behavioural despair. Predictive validity has been established with many antidepressants in mice (Lucki et al., 2001), though many argue that assessing the behavioural effects of antidepressant compounds is not a model of depression, but just a comparison of behaviour output to a reference compound (Nestler and Hyman, 2010).

A complete model of depression cannot be attained. Depression is a multifaceted disorder with great variability in an individual's symptoms, biochemistry and treatment response, and no reliable biomarkers that can be modeled. This obstacle is overcome in part by creating models of specific aspects of disease, such as certain symptoms or pathophysiological processes. By doing so, research into mood disorders is broken down into 'endophenotypes' as opposed to trying to replicate a depression as a whole (Slattery et al., 2014). For example, to study the inflammation exhibited in a subpopulation of depressed patients, inflammation can be induced environmentally or artificially (the independent variable) and behavioural and biochemical output can be assessed (the dependent variable). Whilst considering the limitations in construct and face validity, a greater understanding of the neurobiological processes that contribute to behaviour and pathophysiology associated with depression can be attained.

1.5.2 Inflammation-based models of depressive-like behaviour in mice

There are several ways to study inflammation and its influence on behaviour in mice. The most straightforward route is the direct administration of an inflammatory agent that induces an inflammatory response. LPS induces a broad inflammatory response when administered *in vivo* and can be administered systemically to induce depressive-like behaviours (O'Connor et al., 2009a). Such models assess a transient period of inflammation (further discussed in Section 3.1.1). Repeated LPS can also be used to model sustained inflammation (Kubera et al., 2013), though repeated LPS does induce tolerance (Engeland et al., 2001). In addition, LPS can be administered directly into the CNS via *intracerebroventricular* (*i.c.v.*) injection, enabling neuroinflammation to be assessed without systemic inflammation (Lawson et al., 2013b). To study a specific inflammatory signalling pathway, proinflammatory cytokines, such as TNF-α, can also be administered to induce depressive-like behaviour (Kaster et al., 2012). Poly(I:C), a synthetic double-stranded RNA agonist for TLR3, can also be used to stimulate viral infection-induced inflammation (Gibney et al.,

2013). Such approaches enable consistent induction of predictable inflammatory signalling, and can therefore be replicated and dissected. An alternative approach to studying inflammation *in vivo* is stress-induced inflammation, which would have greater construct validity, as it is an endogenous inflammatory process. For example, chronic stress can increase serum cytokine levels, microglia activation and depressive-like behaviours in mice (Alcocer-Gómez et al., 2015). However, such approaches have greater variability, due to protocol differences and individual differences.

1.5.3 Assessing depressive-like behaviour

1.5.3.1 Forced swim test

The forced swim test (FST) is a behavioural paradigm used to assess the antidepressant efficacy of drugs (Lucki et al., 2001). The FST has also been used to infer pro-depressive behaviours in response to a variety of pharmacological and environmental interventions (O'Reilly et al., 2006; O'Connor et al., 2009a; Bogdanova et al., 2013). The test consists of placing a rodent in a cylinder of water for whilst behaviour is recorded and scored. First developed for rats in 1978, the FST measures time spent immobile to assess escape-directed behaviour and behavioural despair (Porsolt et al., 1978), and has since been adapted for use with mice (Lucki et al., 2001). The longer the mouse spends immobile, the greater the depressive-like behaviour. This has been interpreted as a reduction in motivation to escape a negative environment.

The FST is regularly used in drug development as many current antidepressants can reduce immobility times (Lucki et al., 2001). This predictive validity is seen with a range of acutely administered SSRI antidepressant drugs, including fluoxetine and citalopram, as well as other monoamine reuptake inhibitors, such as bupropion, and TCAs, such as imipramine and desipramine (David et al., 2003; Lucki et al., 2001). However, there are some significant flaws in the FST in drug development. The FST is based on the ability of current antidepressants to reduce immobility, and as animal models are often defined by this predictive validity, new drugs are generally similar to existing drugs, which are only effective in 50 – 60 % of MDD patients (Hendrie et al., 2013). Antidepressant-like activity in the FST can also be observed in mice following treatment with the NMDA receptor antagonist ketamine, which has been shown to exert rapid antidepressant activity in humans (Fond et al., 2014; Koike et al., 2013).

However, the FST is sensitive to the strain of mouse used as different strains have different baseline behaviours and different response profiles to antidepressant drugs (David et al., 2003; Lucki et al., 2001). The FST can also be used as an endpoint readout in other models of depression, including chronic mild stress (Zhang et al., 2015), maternal separation (Desbonnet et al., 2010) or inflammation-based models such as LPS (O'Connor et al., 2009a) or poly(I:C) (Gibney et al., 2013), which can all induce increases in immobility. This demonstrates the ability of the FST to assess both anti- and pro-depressive interventions. As the readout is highly dependent on locomotion, the effect any intervention has on locomotor activity should be assessed to avoid false positives or negatives.

1.5.3.2 Sucrose preference test and female urine sniffing test

Reward-seeking behaviours, such as the sucrose preference test (SPT) and the female urine sniffing test (FUST), allow an endpoint measurement that can assess natural hedonic behaviours (Lewis et al., 2005; Mendleson et al., 1989). The SPT gives mice a choice between water and a palatable sucrose or saccharin solution, whereby mice exhibit a preference for the sweet solution (Lewis et al., 2005), demonstrating hedonic behaviour. The test was originally used to show a reduced sucrose preference following chronic mild stress, which was reversible with desipramine (Willner et al., 1987). The SPT has since been used in inflammation-based models of depression (Frenois et al., 2007) and exhibited predictive validity with chronic SSRI treatment, including citalopram and fluoxetine (Rygula et al., 2006; Muscat et al., 1992). One advantage of the SPT over the FST is that it allows for behavioural assessment over extended periods of time, as mice can be constantly housed with water and sucrose.

The FUST is a recently developed behavioural task that assesses hedonic behaviour in the form of sexual motivation. Male mice are exposed to water or female urine and an exploratory preference towards the female urine is observed (Malkesman et al., 2010). It was also shown that mice have a greater preference for female urine over novel odours, eliminating novelty as a factor. This task has been validated in a learned helplessness model of depression, where mice show a reduction in urine sniffing (Malkesman et al., 2010), but has not yet been assessed in other models of depression. Furthermore, this reduction in urine sniffing can be reversed following chronic treatment with citalopram, demonstrating predictive validity (Malkesman et al., 2010). A similar paradigm that assesses social interaction with female versus male intruders is based upon the same sexual motivation concept, but utilises mice instead of urine (Ago et al., 2015). The preference for female interaction over male interaction,

which only develops once sexually mature, was abolished after castration and was reduced in an acute inflammation model of depression (Ago et al., 2015). These tasks allow an alternative social hedonic behaviour to be assessed that is based upon the innate influence of pheromones. These tasks also allow assessment at a specific time point, as opposed to relatively long test periods of the SPT.

1.6 Aims of thesis

The NLRP3 inflammasome is important in the inflammatory response and has been previously shown to mediate depressive-like behaviours in a chronic stress model in mice. It was hypothesized that NLRP3 inflammasome signalling is important in the development of LPS-induced depressive-like behaviours in mice. To test this hypothesis, LPS-based mouse models of depressive-like behaviour were tested and developed, before using NLRP3$^{-/-}$ mice to investigate the role of NLRP3 in LPS-induced behavioural changes.

Neuroinflammation is mediated by microglia, which exist in low O_2 conditions within the brain. It was hypothesized that in 5 % O_2 conditions, similar to the *in vivo* microenvironment, inflammatory signalling in microglia would differ from that seen in 20 % O_2. To test this hypothesis, BV2 microglia and primary microglia were exposed to differing lengths of 5 % O_2 before microglia function and NLRP3 inflammasome activity was assessed.

Aims:

1 – To model LPS-induced depressive-like behaviours in mice

2 – To study NLRP3 inflammasome function in microglia and the effect of 5 % O_2 hypoxia

3 – To investigate the involvement of NLRP3 in microglia function and inflammation-induced depressive behaviour using NLRP3$^{-/-}$ mice

Chapter 2: Methods

2.1 In vivo methods

2.1.1 Animals – Janssen Pharmaceutica

Experiments were performed on 10-14 week old male C57BL/6J mice obtained from Charles River (France). Mice were normally housed in groups of 2-4 except when singly housed as indicated in the test. Cages (L x W x H: 36 X 20 X 13 cm) contained wood shavings, nesting material and a plastic shelter (Mouse hut, Bio-Serve; L x W x H: 9.5 x 7.6 x 4.8 cm), with access to food and water *ad libitum.* Mice were under a 12-hour light cycle, with normal lighting conditions being lights on at 06:00 h and reversed lighting conditions being lights on at 18:00 h, with 30 min dim/rise phases. In some experiments, reversed lighting conditions were used and mice were habituated to these conditions for two weeks prior to the experiments. Temperature was maintained at 22 ± 2 °C and humidity at 50 ± 2 %. All mice were acclimatised to the animal facility for a minimum of 2 weeks and handled daily for one week prior to random assignment to treatment groups and experimentation. All protocols were approved by the Institutional Ethical Committee on Animal Experimentation, in compliance with Belgian law (Royal Decree on the protection of laboratory animals dd. April 6, 2010) and conducted at Janssen Pharmaceutica facilities accredited by the Association for the Assessment and Accreditation of Laboratory Animal Care.

2.1.2 Animals – University of Bath

Experiments were performed on 10-14 week old male C57BL/6J or NLRP3 homozygous knockout mice on a C57BL/6J background (B6.129S6-Nlrp3$^{<tm1Bhk>}$/J - ref:021302; Jackson Laboratory, Maine, US via Charles River, Margate, UK). Both NLRP3$^{+/+}$ and NLRP3$^{-/-}$ mice were maintained in homozygous colonies (Figure 2.1). All F1 generation mice were genotyped and mated. Homozygous F2 littermates were mated to produce mice for all behavioural experiments. Mice used for primary microglia cultures were F2 or F3. Mice were normally housed in groups of 3-4 except when singly housed as indicated in the test. Cages (L x W x H: 35 X 20 X 15 cm) contained wood shavings, nesting material and a plastic shelf, with food and water available *ad libitum*. Mice were under a 12-hour light cycle (lights on at 07:00 h). Temperature was maintained at 21 ± 1 °C and humidity at 50 – 60 %. Mice were handled daily for one week prior to random assignment to treatment groups and experimentation. All procedures were carried out under a Home Office project license held in accordance with the Animals (Scientific Procedures) Act 1986 and European Directive 2010/63/EU.

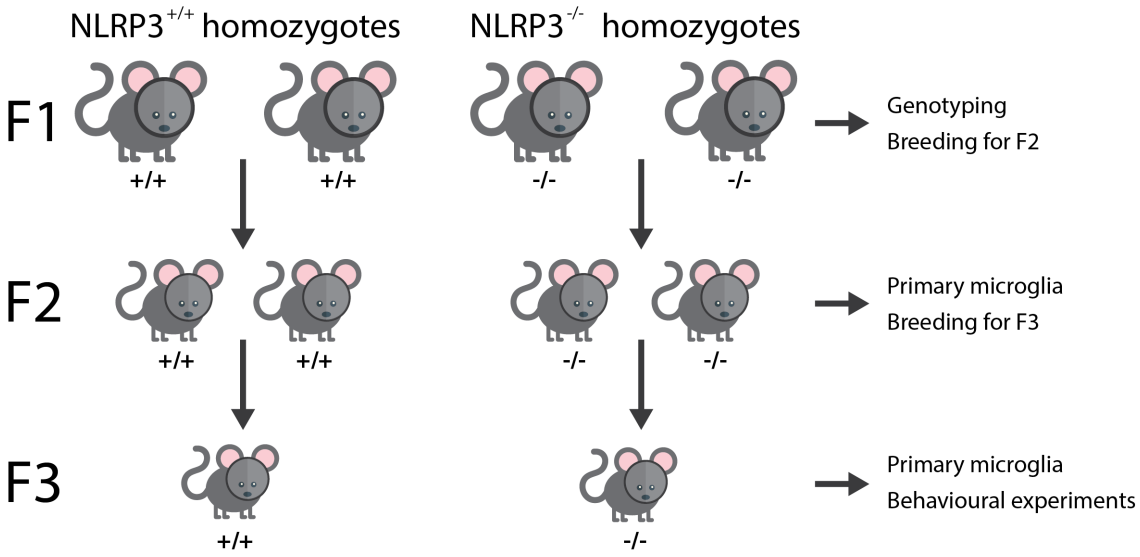

Figure 2.1. Breeding plan for NLRP3$^{+/+}$ and NLRP3$^{-/-}$ mice.

First generation mice were genotyped and maintained in homozygous colonies. Primary microglia were obtained from F2 and F3 mice, and behavioural experiments were carried out on F3 mice. *Wickens original artwork*.

2.1.3 Treatments

Lipopolysaccharide (LPS) from *Escherichia coli* (serotype 055:B5, Sigma-Aldrich) was prepared fresh in sterile saline (0.9 % NaCl) prior to intraperitoneal injection at a volume of 10 ml/kg. LPS doses were selected based on previously observed acute LPS-induced depressive-like behaviours in mice (O'Connor et al., 2009a).

For acute studies, mice were injected with 0.415 or 0.83 mg/kg LPS or saline. For repeated LPS studies, there were four different groups that were treated for 3 or 5 days: control (saline was injected each day); acute LPS (LPS was administered only on the final day); constant dose (CD) LPS (0.83 mg/kg LPS was injected each day) or increasing dose (ID) LPS (Figure 2.2). For ID LPS, the following doses of LPS were used: 0.052 / 0.104 / 0.208 / 0.415 / 0.83 mg/kg (5-day) or 0.208 / 0.415 / 0.83 mg/kg (3-day). Body weights were recorded daily prior to injections, which took place between 09:00 – 18:00 h.

TREATMENT GROUP	5-day		3-day		
Saline	SAL	SAL	SAL	SAL	SAL
Acute LPS	SAL	SAL	SAL	SAL	0.83
CD LPS	0.83	0.83	0.83	0.83	0.83
ID LPS	0.05	0.1	0.21	0.42	0.83

Figure 2.2. Schedule for 3-day and 5-day repeated injection experiments.

Mice were divided into four treatment groups: saline, acute LPS, constant dose (CD) LPS and increasing dose (ID) LPS. Mice were injected daily with either saline (SAL) or LPS (0.05 – 0.83 mg/kg; *i.p.*).

Drugs with known antidepressant activity were used as positive controls in these experiments (Table 2.1). In the forced swim test drugs were administered 30 min prior to testing (ketamine / bupropion / desipramine / fluoxetine). When ketamine was investigated for its role in alleviating acute LPS-induced depressive-like behaviour, administration occurred either 24 h or 30 min prior to testing.

When investigating the effect of centrally administered LPS, mice were injected with 100 ng of LPS (1 µl) or saline, via direct injection or cannula into the lateral ventricle (see Section 2.1.4 and 2.1.5).

Compound	*Source*	*Doses (mg/kg)*	*Route*
Lipopolysaccharide	Sigma	0.05-0.83	*i.p.*
Ketamine	Lipomed	5-10	*s.c.*
Desipramine	Sequoia Research Products	10-20	*i.p.*
Bupropion	Janssen Research Foundation	10-20	*i.p.*
Fluoxetine	Abcam	20	*i.p.*

Table 2-1. Compounds used for *in vivo* assessment.

2.1.4 Intracerebroventricular injection – Janssen Pharmaceutica

Mice were administered the opioid analgesic Dipidolor (Janssen, BE) 30 min prior to surgery (4 mg/kg; subcutaneously). Mice were then anaesthetised with 5 % isoflurane (Abbott IsoFlo, 100 % w/w). Once unconscious, the mouse's head was shaved and iso-Betadine (10% povidone-iodine; Meda) was applied topically. Opticrom Ad Eye Ointment (Ecuphar) was applied to the eyes to avoid drying. Mice were then transferred to a stereotaxic frame and isoflurine was kept at 2 %. Once the mouse was fixed into position, an incision was made along the scalp to expose the skull. Xylocaine (10 % lidocaine; Astrazeneca) was topically applied to the exposed tissue for local anaesthesia. A hole was drilled through the skull to allow injection at the following coordinates: lateral 1.5 mm / posterior 0.6 mm / dorsal 2.3 mm with respect to Bregma. Coordinates were tested on a culled mouse by injecting a dye (Figure 2.3A). Saline or LPS (10 ng) was injected at a volume 1 µl at a rate of 1 µl/min using a Hamilton syringe. Following injection, the syringe was carefully withdrawn and the scalp was joined back together using Vetbond glue (3M). Mice were placed in a clean cage and allowed to recover at a temperature of 27-28 °C for 24 h. Mice were tested at either 6 or 24 h after surgery in the OFT and FST.

2.1.5 Intracerebroventricular cannulation – Janssen Pharmaceutica

Mice were prepared for surgery as described for ICV injection (Section 2.1.4). After drilling a hole at the appropriate location in the skull of the mouse, the guide cannula was inserted to the appropriate depth (2.3 mm dorsal). An anchoring screw was attached to the opposite side of the skull. Veterinary cement was then used to fix the cannula in place, with the anchoring screw minimizing movement of the cannula. The scalp was joined back together over the cement with veterinary glue and the dummy cannula was inserted into the guide cannula. Mice were placed in a clean cage and allowed to recover at a temperature of 27-28 °C for 24 h. Mice were given 2 weeks to recover from surgery before being anaesthetized with isoflurane (5 %) prior to injection. The dummy cannula was replaced with the injection cannula and saline or LPS (10 ng) was injected at a volume 1 µl at a rate of 1 µl/min using a Hamilton syringe. After injection, the dummy cannula was replaced into the guide cannula and mice were returned to their home cage. Mice were tested either 6 or 24 h later in the OFT and FST. After experimentation, mice were culled and a blue dye was injected to observe the location of the cannula (Figure 2.3B).

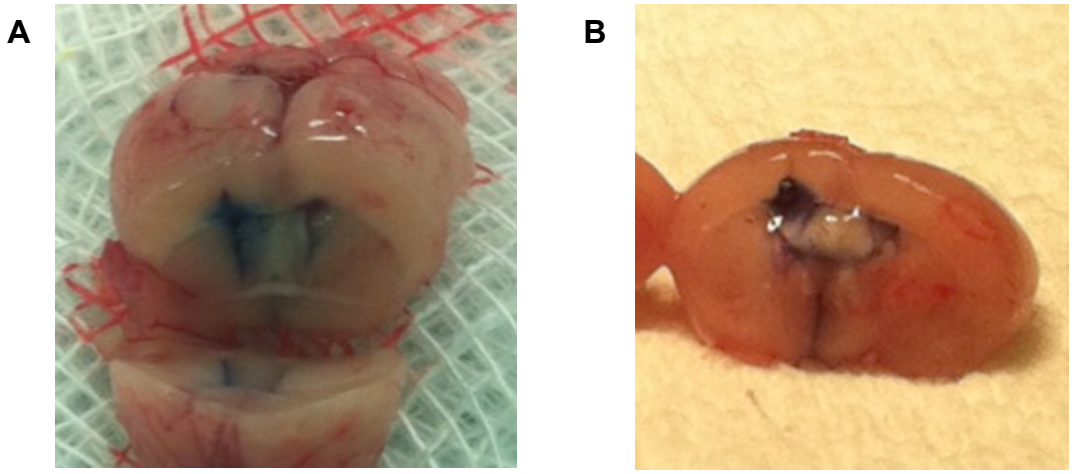

Figure 2.3. ICV injection of dye.

Direct injection of dye post-mortem at the following coordinates: lateral 1.5 mm / posterior 0.6 mm / dorsal 2.3 mm with respect to Bregma (A). Mice with cannulas implanted were injected with a dye post-mortem (B). Both brains show injection of dye into the lateral ventricle and diffusion across the ventricle.

2.1.6 Behavioural assessment

Mice were moved into experimental rooms ≥1 h prior to experimentation to allow habituation and returned to their home cage after testing, unless stated otherwise. No mouse underwent testing in more than two behavioural paradigms, with an interval of at least 12 h. In LPS experiments, mice were typically tested in the OFT and subsequently in the FST, or just in the SPT / FUST alone.

2.1.7 Open Field Test (OFT) – Janssen Pharmaceutica

The OFT protocol used was as described previously (Biesmans et al., 2013). The experimental apparatus consisted of 4 separate arenas (each 40 X 40 X 40 cm), allowing 4 mice to be tested simultaneously. Locomotor activity was assessed as a measure of sickness behaviour in a 10 min OFT under low light conditions (2-3 lux). An infrared camera, mounted above each arena, tracked the mice using Noldus EthoVision (version 6.1). Tracking began 2 seconds after the detection of a mouse in the arena and the total distance travelled was recorded. Arenas were cleaned with 70 % ethanol in between each mouse.

2.1.8 Open Field Test (OFT) – University of Bath

The OFT protocol used was as described previously (Almatroudi et al., 2015). The experimental apparatus consisted of a single arena (L x W x H: 41 X 41 X 38 cm) with 32 infrared lasers (16X x 16Y) to detect locomotion (SmartFrame Open Field System, Kinder Scientific). Locomotor activity was assessed as a measure of sickness behaviour in a 10 min OFT under low light conditions (<10 lux). Infrared beam breaks within the arena was used to track mice using Kinder Scientific MotorMonitor software. Tracking began 2 seconds after a mouse was placed in the arena and the total distance travelled recorded. Arenas were cleaned with 70 % ethanol in between each mouse.

2.1.9 Forced swim test (FST) – Janssen Pharmaceutica

The FST protocol used was as described previously (Biesmans et al., 2013). The experimental apparatus consisted of 4 separate cylinders (11 cm diameter and 10 cm deep water), which were automatically washed and filled with water at 24-25 ˚C between each mouse. Mice were placed in the cylinders for 6 min, whilst a fixed camera perpendicular to the cylinder was used to capture 4 mice simultaneously. Immobility was manually scored, blind to treatment, over the 6 min test period. For automated scoring (pharmacological validation and *i.c.v*. LPS experiments), movement was tracked using Noldus EthoVision (version 9.0) for 6 min beginning 2 seconds after detection of a mouse and immobility was scored.

2.1.10 Forced swim test (FST) – University of Bath

The FST protocol used was as described previously (Almatroudi et al., 2015). The experimental apparatus consisted of a glass cylinder (22 cm diameter), which was cleaned with 70 % ethanol and filled with water (23 cm deep) at 25 ± 1 ˚C between each test. Mice were placed in the cylinders for 6 min, whilst a camera placed perpendicular to the cylinder was used to record the mice. Immobility was manually scored, blind to treatment, over the 6 min test period.

2.1.11 Rotarod – Janssen Pharmaceutica

Mice were assessed in two test sessions: a 'baseline' test immediately prior to LPS or saline administration and a final test at either 6, 24 or 48 h after treatment. Mice first underwent four training sessions in succession the day before treatment where mice were placed on the rotarod for 5 min each time at progressively faster speeds: 16, 20 and 24 revolutions per minute (rpm), and finally an accelerating speed from 0-40 rpm (Med Associates, model CT-ENV-575M-X5). During training, mice that had fallen off the rotarod were placed back on. Subsequently, the baseline test and final test sessions were 5 min at an accelerating speed of 0-40 rpm. Latency to fall off the rotarod was recorded automatically via infrared cameras and mice were not replaced back onto the rotarod once off (Figure 2.4).

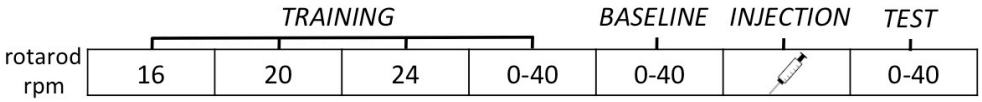

Figure 2.4. Rotarod protocol.

Mice underwent 4 training sessions of increasing difficulty. A baseline trial was measured prior to injection and a final test trial was measured at either 6, 24 or 48 h post-administration of either saline or LPS (0.83 mg/kg; *i.p.*). rpm – revolutions per minute.

2.1.12 Sucrose consumption – University of Bath

Preliminary experiments were conducted to establish a palatable sucrose solution for C57BL/6J mice, since strain differences in sucrose sensitivity have been reported (Lewis et al, 2005). Mice were deprived of water for 4 h prior to experimentation (16:30 – 20:30). Bottles containing water or a sucrose solution (2.5 or 5 % in tap water) were placed in the cage for 1 h (20:30 – 21:30). The test portion of the experiment was carried out at the start of the dark phase (lights out at 19:00), as this is when mice will normally drink. Bottles were weighed before and after testing to calculate the total amount of liquid consumed.

2.1.13 Sucrose Preference Test (SPT) – Janssen Pharmaceutica

The SPT protocol used was as described previously (Biesmans et al., 2013). Animals were housed individually in customized Plexiglas cages (35 X 31 X 16 cm; Techniplast, Italy) that fitted two water bottles. Bottles were filled with either tap water (W) or 2.5 % sucrose dissolved in tap water (S) during the habituation phase prior to a testing phase. During the habituation phase, mice were housed with W/W or W/S alternating for 24 h periods over 4 days. Bottles were removed at the same time every morning (09:00-10:00) and consumption determined by weighing the bottles. Mice were then weighed and placed back in their cage with fresh pre-weighed bottles containing the appropriate solutions. The test phase was carried out for 2 days immediately following the administration of LPS or saline (Figure 2.5). Total consumption was calculated (water and sucrose consumption combined) as well as the preference for sucrose (sucrose consumption as percentage of total consumption). In the event of leaking bottles, values were replaced by the mean of all bottles for the appropriate solution for that time period. This happened in less than 5 % of all bottle measurements.

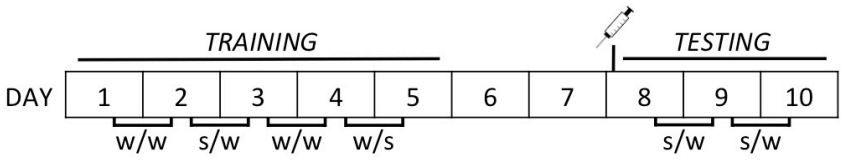

Figure 2.5. Sucrose preference test.

Mice underwent 4x 24 h training sessions prior to testing with access to two water bottles either both containing water (W/W) or one water and one 2.5 % sucrose solution (W/S). For the test period, mice were injected with saline or LPS (0.83 mg/kg; *i.p.*) and allowed access to water and sucrose (W/S) for 24 h sessions. Volume consumed from each bottle at the end of 24 h session was measured by weighing bottle before and after session.

2.1.14 Female Urine Sniffing Test (FUST) – Janssen Pharmaceutica

The FUST has previously been validated using the learned helplessness (LH) model of depressive behaviour and the action of the antidepressant citalopram in mice (Malkesman et al., 2010). Prior to the experiment, adult female mice were housed in groups of 4 in metabolic cages with grid floors for 2 h to collect urine (approximately 1 - 2 ml per cage). 4 cotton-bud applicators (Assistent, Germany; product code 4302) were

soaked in test tubes containing female urine or water immediately prior to and during the experiment.

Under normal light levels, male mice were weighed and placed individually in a novel cage (with wood shavings only) containing two dry cotton-bud applicators for the 30 min habituation phase. The applicators (15 cm long) were fixed in place by a custom-made device that clips onto the cage and points the applicators down at an angle of 45 degrees, with the cotton-buds 2.5 cm above the cage floor and 15 cm apart, and cage lids on (Figure 2.6). The protocol used here was adapted from Malkesman *et al*. (2010) to incorporate one test period with two applicators (water and urine) as opposed to two test periods each with one applicator. For the test phase, the applicators and the holding device was removed (whilst the mouse was still in the cage) and replaced with a new holding device with two new applicators: one soaked in water and the other soaked in female urine (left versus right was randomized to avoid positional preference). Timing and live manual scoring of behaviour began immediately after the addition of the new applicators. During the test phase, time spent sniffing each applicator. Sniffing was scored when the mouse was sniffing the bud of the applicator directly from close range (biting the applicator is not counted) with an observation timer for 3 min. Total times spent sniffing each applicator was recorded. Mice were then returned back to their home cage and the applicators placed back into the appropriate test tube for re-use. Greater time spent sniffing female urine over water reflects a sex-driven hedonic behaviour. In a validation experiment to confirm a sexual bias, male urine was also tested in direct comparison with female urine or water.

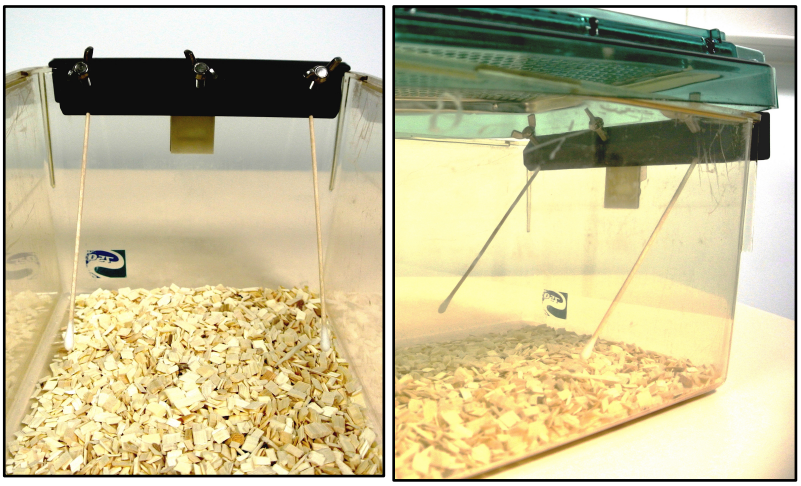

Figure 2.6. The female urine sniffing test.

Mice were exposed to two cotton buds soaked in ether water or female urine. Time spent sniffing was recorded.

2.1.15 Statistical Analysis

In vivo data were analysed using a Student's *t*-test or a one-way analysis of variance (ANOVA) followed by Dunnett's posthoc test or two-way ANOVA followed by Bonferroni or Dunnett posthoc tests for multiple comparisons where appropriate ($p < 0.05$). All data are represented as mean ± SEM.

2.2 Tissue genotyping

2.2.1 DNA extraction

DNA samples were prepared from ear clippings taken from NLRP3$^{+/+}$ and NLRP3$^{-/-}$ mice as previously describes (Truett et al., 2000). Tissue samples were lysed in an alkaline lysis buffer (0.5 ml; 25 mM sodium hydroxide; 0.2 mM EDTA; pH 12). Samples were boiled at 95°C for 1 h before being cooled to 4°C. An equal volume of neutralization buffer (0.5 ml; 40 mM tris; pH 5) was added. Samples were centrifuged (10 min; 1400 G; 4°C) and supernatants were collected and stored at -80°C for analysis at a later time.

2.2.2 Polymerase chain reaction (PCR)

PCR was used to identify the presence of NLRP3 or a previously validated internal positive control (GRCm38) provided by Jackson Laboratories (Yu et al., 2013) in DNA samples obtained from mice. A *Taq* DNA Polymerase kit (New England Biolabs) was used with gene-specific primers outlined in Table 2. 2. 4 µl of a master mix containing *Taq* DNA polymerase, dNTPs and primers in a buffer (outlined in Table 2.3) was added to 1 µl of each sample in 0.2 ml PCR tubes. Volume was adjusted to 20 µl with DNase free water and PCR was performed: 30 seconds at 95°C, 40 cycles of 15 seconds at 95°C / 30 seconds at 60°C / 30 seconds at 68°C, 5 min at 68°C and cooled to 4°C until removed. PCR products were kept at 4°C until gel electrophoresis.

2.2.3 Gel electrophoresis

10 µl of PCR product was added to 2 µl of 6X loading dye (New England Biolabs; B7021S). Samples were run alongside a 100 – 1000 bp DNA ladder (Thermo Scientific; SM0241) on a 1.5 % agarose gel containing ethidium bromide (2 drops of 0.625mg/ml; Severn Biotech Ltd; 14485) at 90 volts for 1 h. Gels were visualized using GeneSnap (SynGene) software.

Target	*Primer sequence*	*Amplicon length (base pairs)*	*Reference*
NLRP3	Forward: AGAAGAGTGGATGGGTTTGCT Reverse: GCGTTCCTGTCCTTGATAGAG	1228	PrimerBlast
GRCm38 (control)	Forward: CTAGGCCACAGAATTGAAAGATC Reverse: GTAGGTGGAAATTCTAGCATCAT	324	Jackson Laboratories

Table 2-2. PCR primers for genotyping.

NLRP3 primers were designed via PrimerBlast and compared with a positive internal control obtained from Jackson Laboratories genotyping protocols (primer references: oIMR7338 and oIMR7339) and developed by the Genome Reference Consortium.

Component	*Source*	*Product code*	*Volume (per sample)*	*Final conc.*
10X Taq buffer (Mg-free)	New England Biolabs	M0320	2.5 µl	1X
25 mM $MgCl_2$	New England Biolabs	M0320	1.5 µl	1.5 mM
10 mM dNTPs	Thermo Scientific	R0191	0.5 µl	200 µM
10 mM forward primer	Sigma	-	0.5 µl	0.2 µM
10 mM reverse primer	Sigma	-	0.5 µl	0.2 µM
Taq DNA Polymerase	New England Biolabs	M0320	0.125 µl	1.25 units
Nuclease-free water	Thermo Scientific	R0581	18.4 µl	-
DNA sample	-	-	1 µl	-

Table 2-3. PCR mastermix.

Components of the mastmix used for the PCR reaction.

2.3 In vitro methods

2.3.1 Immortalized cell lines

The BV2 cell line (gift from Prof. Michel Mallait, Hôpital de le Pitié-Salpêtrière, Paris, France) is an immortalized murine microglial cell line, first obtained from /6 mice (Blasi et al., 1990). BV2 microglia were cultured as described previously, with modifications (Sheng et al., 2011). Briefly, BV2 microglia were maintained in culture medium consisting of Dulbecco's modified eagles medium/nutrient mixture F12 (DMEM/F12) with 4.5 g/L D-glucose, 10 % fetal bovine serum (FBS), 100 units/ml penicillin, 100 µg/ml streptomycin and 0.25 µg/ml amphotericin B (Gibco, Life Technologies, UK). The J774.2 cell line (Health Protection Agency, Salisbury, UK) is an immortalized murine macrophage cell line. J774.2 macrophages were maintained in culture medium consisting of DMEM/F12 with 10 % fetal bovine serum (FBS), 100 units/ml penicillin, 100 µg/ml streptomycin and 2 mM L-glutamine. Cell lines were routinely cultured at 37 ˚C in 5 % CO_2/air). For experiments, BV-2 and J774.2 cells were plated in 24-well clear plates (0.5 x 10^6 cells per well) or 96-well black plates (0.1 x 10^6 cells per well) 24 h before testing.

2.3.2 Neonatal primary microglia

Primary neonatal mouse microglia cells were obtained from C57BL/6J pups (P0-2) using the low trypsinisation method described previously (Saura et al., 2003). Newborn mouse pups (male and female) were euthanized via cervical dislocation before whole brains were collected. In ice-cold phosphate buffered saline (PBS), the cortices were dissected and the meninges were removed prior to mincing with scissors. The tissue was centrifuged (150 G; 3 min) and PBS removed before the tissue underwent enzymatic dissociation with 12 ml of 0.25 % (v/v) trypsin with 0.5 ml of DNase I (30 Units final concentration) for 15 min in a shaking water bath (37 ˚C). DMEM/F12 with 10 % fetal bovine serum (FBS), 100 units/ml penicillin, 100 µg/ml streptomycin and 0.25 µg/ml amphotericin B (Gibco, Life Technologies, UK) was added and tissue was mechanically dissociated by pipetting. Cells were centrifuged (350 G; 7 min) and resuspended in fresh DMEM/F12 medium before being passed through a 70 µm cell strainer. The mixed cell population was plated in at a density of 300,000 cells/well in a clear 12 well plate coated with poly-D-lysine (20 µg/ml). Fresh DMEM/F12 medium was added once a week for 3 weeks. After 21 days *in vitro* (DIV) from plating, the conditioned medium was collected from the mixed cell culture and the

cells were washed with serum-free medium before being incubated with diluted trypsin (0.0625% v/v) for 20 min at 37 ˚C to remove the upper astrocytic layer without detaching the majority of lower layer adhered microglia. Cells were then washed with complete medium twice and conditioned medium was re-added. Experimentation took place 24 h later.

2.3.3 Cell stimulation

In order to prime cells, primary microglia, BV2 microglia and J774.2 macrophages were treated with lipopolysaccharide (LPS; Escherichia coli; serotype 055:B5) or left untreated as a control. To stimulate inflammasome activation following LPS priming, cell medium was replaced with a microglia extracellular solution buffer: 130 mM NaCl, 3 mM KCl, 1 mM $MgCl_2$, 2 mM $CaCl_2$, 10 mM HEPES, 10 mM glucose, pH 7.3 with NaOH (Toulme et al., 2010). Cells were incubated for 30 min in the presence or absence of 5mM ATP. The irreversible caspase-1 inhibitor Ac-YVAD-cmk was used to assess inflammasome function and applied during the 4 h LPS priming step prior to ATP stimulation, with DMSO as a vehicle control.

2.3.4 Western Blotting

Cells were treated with a lysis buffer containing 1 % (v/v) Triton X-100 and protease inhibitor cocktail (2 mM AEBSF, 0.3 mM aprotinin, 130 mM bestatin hydrochloride, 14 mM E-64, 1 mM EDTA and 1 mM leupeptin hemisulfate salt) in a buffered saline (150 mM NaCl, 20 mM Tris pH 7.4, 1 mM $MgCl_2$, 1 mM $CaCl_2$) and the cell lysates were collected. Samples were then centrifuged at 3000 rpm (1400 G) for 10 min at 4 °C and supernatants were stored at -20 ˚C. Laemmli loading buffer (2X) was added to samples before being heated at 100 ˚C for 5 min to denature the protein. Samples were resolved by electrophoresis (200 V for 30 min) on 12 % SDS PAGE gels (Mini Protean Tetra-Cell, Bio-Rad). Protein was then transferred to a nitrocellulose membrane (150 mA for 120 min; Mini Trans-Blot Cell, Bio-Rad). Membranes were blocked with 5 % milk (w/v; Sigma, UK) in PBS containing 0.1 % Tween-20 for 1 h at ambient room temperature before being incubated with the primary antibody overnight on a rocker at 4 °C in 2.5 % milk (w/v). The primary antibodies used were as follows: mouse anti-IL-1β (1 µg/ml; Thermo Scientific), mouse anti-β-actin (2.1 µg/ml; Abcam), rabbit anti-β-actin (2.1 µg/ml; Abcam), mouse anti-NLRP3 (0.5 µg/ml; Adipogen), rabbit anti-P2X7 (0.6 µg/ml; Alomone) and rabbit anti-ASC (1 µg/ml; Santa Cruz). Membranes

were washed 3 times in PBS-0.1 % Tween-20 for 5 min at ambient room temperature before secondary antibody incubation.

For quantitative fluorescent analysis, membranes were incubated with fluorescent secondary antibodies (donkey anti-mouse IRDye 800CW or donkey anti-rabbit IRDye 680RD; 0.1 µg/ml; Li-cor) at ambient room temperature on a rocker for 45 min, before being washed at least 3 times in PBS-0.1 % Tween-20 (v/v). Infrared fluorescence was detected to provide a signal proportional to protein concentration, allowing protein quantification (Odyssey CLx, Li-cor). All values are given relative to β-actin levels of the same blot.

For semi-quantitative densitometry analysis, membranes were incubated with HRP secondary antibodies (rabbit anti-mouse or swine anti-rabbit, 1.3 µg/ml; Dako, UK) at room temperature on a rocker for 1 h, before being washed 3 times in PBS-0.1 % Tween-20. Antibody binding was detected via enhanced chemiluminescence using ImageQuant-RT ECL (Biological Industries, UK) and quantified using ImageQuant TL software (GE Healthcare). To evaluate equal loading of proteins, the blots were stripped by incubating membranes in 0.77 % (v/v) 2-mercaptoethanol at 50 °C with agitation for 40 min. Membranes were then washed, blocked with 5 % milk in PBS-0.1 % Tween-20 for 1 h and re-probed for β-actin using the same method as previously described.

2.3.5 Detection of cytokine secretion

Following ATP stimulation in cell cultures, supernatants were collected and centrifuged (10 min; 1400 G) at 4 °C and stored at -20 ˚C. Samples were subsequently assessed using commercially available IL-1β ELISA kits (eBioscience, USA) or V-PLEX proinflammatory panel 1 kit (TNF-α & IL-6, Meso Scale Discovery, UK) according to the manufacturers instructions. Standards were provided by the manufacturer. Absorbance measurements performed using a FLUOstar Optima plate reader (BMG Labtech, Germany) for IL-1β ELISAs and a MSD Sector Imager 6000 (Meso Scale, US) for the Mesoscale mouse proinflammatory cytokine plate.

2.3.6 Immunocytochemistry

Sterile glass cover slips were treated with poly-D-lysine (20 µg/ml; ≥1 h; 37 ˚C) before being washed with sterile water and PBS. Mixed glia cells were then plated onto

PDL-coated cover slips following isolation from brain tissue and microglia were isolated after 3 weeks via mild trypsinisation, as previously described. Cells were washed with PBS and treated with 4 % formaldehyde (w/v) and 2 % Triton X-100 (v/v) in PBS for 30 min to fix and permeabalise cells before being blocked for 1 h with 3 % (w/v) milk in PBS with 0.2 % Triton X-100 at room temperature. After being washed 3 times in PBS-0.1 % Tween-20, cells were incubated with the primary antibody diluted in antibody diluent (1 % milk in PBS with 0.1 % triton X-100) at 4 °C overnight. Primary antibodies include mouse anti-IL-1β (10 µg/ml), mouse anti-NLRP3 (5 µg/ml), rabbit anti-CD11b (10 µg/ml) or rabbit anti-GFAP (10 µg/ml). Cells were washed 3 times PBS-0.1 % Tween-20 for 5 min and incubated with secondary antibody Alexa Fluor 488 secondary goat anti-rabbit antibody (2 µg/ml), Alexa Fluor 488 secondary rabbit anti-mouse (2 µg/ml) and/or Alexa Fluor 647 secondary donkey anti-mouse (2 µg/ml) in antibody diluent for 1 h at room temperature. Cells were washed 3 times in PBS-0.1 % Tween-20 and incubated with 600 nM DAPI for 20 min before being washed again and mounted onto glass slides with 7 µl mowiol and left to dry overnight. Confocal images were obtained with a Zeiss LSM510 Meta confocal microscope (Zeiss Plan Apochromat 63x / 1.4 oil Ph3 microscope objective). The primary antibody was omitted for negative. Images were processed using ImageJ software (version 1.46r).

2.3.7 Fluorescent measurements

BV-2 cells were plated on 96-well black plates at 100,000 cells per-well 24 h prior to experiments. Primary microglia were isolated 24 h prior to experiments in 24-well clear plates. Cell medium was replaced with a microglia extracellular solution buffer (see above) containing 25 µM ethidium bromide. P2X7 receptor antagonist A-740003 or DMSO as a vehicle control was used to assess ATP-P2X7 activity. Fluostar Optima plate reader (BMG Labtech, Germany) at 37 ˚C was used to measure ethidium fluorescence (F) at 525 nm (excitation wavelength) and 605 nm (emission wavelength) every 60 seconds. 5 initial readings were averaged for a baseline (F_0) before ATP (5 mM) or buffer was added to each well. For a final maximal reading (F_{max}), Triton X-100 was added to each well (0.2 % v/v) to lyse cells for 10 min for a final maximal reading. Fluorescence values were then calculated as a percentage of the maximal response as follows: $\boldsymbol{y = ((F - F_0) / F_{max}) * 100}$

2.3.8 Reactive oxygen species (ROS) measurement

Primary microglia were isolated 24 h prior to experiments in 24-well clear plates and primed with LPS for 4 h. Cells were loaded with 2',7'-dichlorofluorescin diacetate (20 μM; H_2DCFDA) in serum-free medium for 40 min. Cells were then washed and microglia extracellular solution buffer containing 25 μM ethidium bromide was added. Fluostar Optima plate reader (BMG Labtech, Germany) at 37 ˚C was used to measure DCF fluorescence at 485 nm (excitation) and 520 nm (emission) every 60 seconds, as well as ethidium fluorescence (F) at 525 nm (excitation) and 605 nm (emission). 5 initial readings were averaged for a baseline (F0) before ATP (0 – 5 mM) or buffer was added to each well.

2.3.9 Cell density assessment

To assess cell density of mixed glia and microglia cultures, cells were cultured in 24-well plates for 1-3 weeks. DNA content was assessed using the CyQuant NF Cell Proliferation Assay Kit (Thermo Fisher, UK). Cell medium was aspirated and replaced with CyQuant dye reagent in Hank's balanced salt solution (HBSS), prepared according to the manufacturers instructions, for a 1 h incubation period at 37 ˚C. Fluorescence was measured with excitation at 485 nm and emission detection at 530 nm using a CLARIOstar plate reader (BMG Labtech, Germany).

2.3.10 LDH release

Necrotic/pyroptotic cell death was assessed by lactate dehydrogenase (LDH) release into the supernatant using the CytoTox 96 Non-radioactive Cytotoxicity Assay kit (Promega, UK). Following cell stimulation with LPS and/or ATP, supernatants were collected and centrifuged (10 min; 1400 G). Samples (50 μl) were then transferred to a 96-well plate and incubated with the assay substrate for 30 min at room temperature before the stop solution (1 M acetic acid) was added. Absorbance (490 nm) was then measured with a FLUOstar Optima plate reader (BMG Labtech, Germany).

2.3.11 Data Analysis

All *in vitro* data were expressed as the mean ± SEM of n ≥ 3 independent biological repeats. Data distribution was assumed to be normal, though not formally tested. Statistical analysis was carried out with a one-way or two-way ANOVA. If ANOVA assessment revealed significance ($p < 0.05$), Tukey or Dunnett post hoc analysis was carried out.

2.3.12 Reagents and consumables

Reagents for cell culture	*Source*	*Product code*
Lipopolysaccharides, from Escherichia coli 055:B5	Sigma, UK	L2880
DMEM (F-12)	Gibco, UK	11520396
DMEM (F-12) + glucose	Gibco, UK	11594486
FBS	Gibco, UK	11533387
Penecillin / streptomycin	Gibco, UK	11548876
Penecillin / steptomycin / amphotericin B	Gibco, UK	11570486
Glutamine	Gibco, UK	25030024
Trypsin (2.5 % v/v)	Gibco, UK	10590046
Trypsin (0.25 % v/v)	Gibco, UK	11570626
Phosphate buffered saline	Gibco, UK	11590476
Sterile water	Gibco, UK	15230089
Poly-D-lysine	Sigma, UK	P1024
Deoxyribonuclease I	Sigma, UK	D5025
Phosphate buffered saline tablets	Sigma, UK	P4417
HBSS	Gibco, UK	11530476
12 well clear cell culture plates	Greiner BioOne	665-180
24 well clear cell culture plates	Greiner BioOne	662-160
96 well black cell culture plates	Greiner BioOne	655-086
Cell scraper	Fisher Scientific	08-100-241
Cell strainer 100um	Fisher Scientific	FB35181
T25 cell culture flask	BD Bioscience	353109
T75 cell culture flask	BD Bioscience	353136
T175 cell culture flask	BD Bioscience	353112
DAPI	Sigma, UK	5748

Table 2-4. Reagents and consumables for cell culture.

Drugs	*Source*	*Product code*
DMSO	Sigma, UK	D8418
A-740003	Sigma, UK	A0862
Ac-YVAD-cmk	Sigma, UK	SML0429
Ketamine	Sigma, UK	K2753
Desipramine	Sigma, UK	D3900

Table 2-5. Drugs used for *in vitro* assessment.

Reagents for SDS page and transfer	*Source*	*Product code*
Tris(hydroxymethyl)amino-methane	Sigma, UK	252859
Sodium dodecyl sulfate	Sigma, UK	L3771
30 % (w/v) acrylamide	National Diagnostics	EC-890
Ammonium persulfate	Acros Organics	AC327081000
TEMED	Fisher Scientific	T/P190/04
Glycine	Sigma, UK	G8898
Methanol	Sigma, UK	34860
Nitrocellulose membrane	Bio-Rad	162-0112
Skimmed milk powder	Sigma, UK	70166
PageRuler Prestained Protein Ladder	Fisher Scientific	11812124
Protease inhibitor cocktail	Sigma, UK	P2714
BSA	Sigma, UK	A7906
EZ enhanced chemiluminescence (ECL)	Biological Industries	20-500-120
Laemmli sample buffer (2X)	Sigma, UK	S3401

Table 2-6. Reagents for SDS page and transfer.

Antibodies	*Source*	*Product code*
Primary antibodies		
anti-β-actin (mouse host)	Abcam	ab6276
anti-β-actin (rabbit host)	Abcam	ab8227
anti-proIL-1β	Fisher Sci.	10405184
anti-NLRP3	Adipogen	AB-20B-0014-C100
anti-ASC	Santa Cruz	Sc-22514-R
anti-P2X7	Alomone Labs	APR-004
anti-CD11b	Abcam	Ab75476
Anti-GFAP	Abcam	Ab7260
Secondary antibodies		
IRDye 800CW Donkey anti-mouse (fluorescent)	Li-cor	925-32212
IRDye 680RD Donkey anti-rabbit (fluorescent)	Li-cor	926-68073
polyclonal rabbit anti-mouse (HRP)	Dako, UK	P0260
polyclonal swine anti-rabbit (HRP)	Dako, UK	P0217
Alexa Fluor 488 rabbit anti-mouse	Invitrogen	A11059
Alexa Fluor 488 goat anti-rabbit	Invitrogen	A21206
Alexa Fluor 647 donkey anti-mouse	Abcam	Ab150103

Table 2-7. Primary and secondary antibodies.

Assays	*Source*	*Product code*
Bradford	Sigma, UK	B6916
Mouse IL-1β ELISA Ready-SET-Go!	Affymetrix eBioscience	88-7013-88
CyQuant NF Cell Proliferation Assay Kit	Life Technologies	C35007
CytoTox 96 non-redioactive Cytotoxicity assay	Promega, UK	G1780
MSD mouse pro-inflammatory cytokine plate	Meso Scale Discovery	K15048D-1
H2DCFDA	Fisher Scientific	D399

Table 2-8. Assay kits.

Chapter 3: Modeling LPS-induced depressive-like behaviours in mice

3.1 Introduction

In order to investigate the effects of inflammation in depression, inflammatory insults can be assessed in mice via behavioural and molecular analysis (see Section 1.5.2). Inflammatory agents used include LPS, Bacillus Calmette-Guerin (BCG), proinflammatory cytokines and poly(I:C) (Kaster et al., 2012; O'Connor et al., 2009b; Cunningham et al., 2007). Alternatively, neuroinflammation has been demonstrated in chronic stress models of depression. In this thesis, LPS has been used to study inflammation and depressive-like behaviour.

3.1.1 Acute LPS model of inflammation-induced depression

LPS is a component of the Gram-negative bacterial cell wall and is recognised by the TLR4 receptor on immune cells. LPS induces a robust inflammatory response and the production of pro-inflammatory cytokines both *in vivo* and *in vitro* (O'Connor et al., 2009a; Hanisch, 2002; Lee et al., 1993). Acute administration of LPS in mice has been used to assess inflammation-induced sickness, consisting of reductions in a range of behaviours including locomotor activity, exploratory behaviour, social and sexual behaviour, food and water consumption, self-grooming and impairments in learning and memory (Dantzer, 2001). These behavioural effects of LPS can be observed when administered both systemically and centrally into the lateral ventricle of the brain, with the latter enabling one to assess neuroinflammation in isolation from systemic inflammation (Lawson et al., 2013b). Sickness behaviours peak at around +6 h, and are generally considered to have disappeared by +24 h post-administration, although sickness behaviours have been observed at +24 h time-points and later (Biesmans et al., 2013; Godbout et al., 2008; Lawson et al., 2013a; Corona et al., 2010). Sickness behaviours in LPS studies are typically assessed by observing distance travelled, such as in an open field, but have also been measured by food/water consumption or social interaction (O'Connor et al., 2009a; Henry et al., 2008; Couch et al., 2016).

Sickness behaviour is paralleled with an increase in pro-inflammatory cytokines in the blood and brain, including TNF-α, IL-1β and IL-6, and reductions in brain BDNF (Biesmans et al., 2013; Zhang et al., 2016; Yang et al., 2016; O'Connor et al., 2009a; Lawson et al., 2013a). Cytokine expression in response to endotoxin exposure is broadly similar in mice to that of humans, though mice require a higher dose of endotoxin (Copeland et al., 2005). In humans, an acute LPS insult (0.8 ng/kg) induced

increased serum levels of TNF-α and IL-6 (Hannestad et al., 2011). Sickness behaviours are considered to mimic the behavioural changes experienced in humans during illness whilst the immune system is activated (Dantzer, 2001). Such behaviours are thought to have evolutionary benefits in conserving energy, limiting danger and avoiding exposure to more pathogens (Miller and Raison, 2016).

Typically, depressive-like behaviours are assessed at +24 h after LPS administration, when the overt symptoms of sickness have subsided (O'Connor et al., 2009a). At this point, subtle changes in behaviour can be assessed without the confounding effect of reduced locomotion. Increased immobility in the FST or TST and anhedonia in the SPT are often observed at +24 h, though high doses of acute LPS can cause depressive-like behaviours to last up to 1 month post-administration (Anderson et al., 2016; Anderson et al., 2015). In humans, acute LPS (0.8 ng/kg) can also induce mild depressive-like symptoms, which can be attenuated with citalopram pretreatment (Hannestad et al., 2011). Acute LPS models of depressive-like behaviour do not intend to model depression as a whole, but rather focus on an endophenotype observed in depressed patients in an attempt to understand some of the underlying molecular processes contribute to depression pathology.

A literature search of “lipopolysaccharide + depression + mice” returned 59 studies that assessed depressive-like behaviour following LPS administration in wildtype adult mice (neonatal/juvenile mice not included). Of the 59 studies, 54 were acute intraperitoneal (*i.p.*) administration of LPS (Table 3.1). In the last two years there has been a significant rise in the usage of the acute LPS model of depression, as 50 % (27) of the studies identified were been published in 2015/16, with 30 % (16) being used to assess the antidepressant activity of natural products (Table 3.1). Whilst 26 experiments reported depressive-like behaviour in the absence of sickness behaviour, 15 experiments showed either no significant depressive-like behaviour or the presence of sickness behaviour at the same time-point at which depressive-like behaviour was assessed, failing to rule out the confounding influence of sickness. A further 16 experiments failed to report any sickness behaviour assessment at all. Despite the inconsistencies in acute LPS studies, LPS induces a replicable and robust sickness behaviour, which has usually subsided by +24 h, when depressive-like behaviours are typically observed.

Treatment with SSRI antidepressants, including fluoxetine and paroxetine, have been shown to inhibit the development of acute LPS-induced depressive like behaviours in mice (Li et al., 2016; Yao et al., 2015; Dong et al., 2016; Ohgi et al., 2013). Ketamine administration has also been shown to attenuate LPS-induced

depressive-like behaviours in mice, without affecting sickness behaviour (Walker et al., 2013). These findings support the idea that excessive glutamatergic signalling and excitotoxicity plays a key role in inflammation-induced depression.

The acute LPS model has very low construct validity, with a single high dose inflammatory insult not replicating the chronic and subtle nature of inflammation in depression. Several recent studies have attempted to model chronic inflammation in mice using repeated LPS administration. In mice, 10 consecutive injections of high dose LPS (0.83 mg/kg) (Guo et al., 2014) or 8 injections (every other day) of low dose LPS (0.1 mg/kg) (Xie et al., 2012) resulted in the development of depressive-like behaviours. In rats, 7 injections (every other day) of 0.5 mg/kg LPS resulted in depressive-like behaviours in the FST and SPT (Guo et al., 2016). These sustained inflammation-based model of depressive-like behaviour in mice have greater face validity than acute LPS, as they better represent the sustained inflammation associated with the human condition.

3.1.2 Environmental factors influencing depressive-like behaviour

As detailed in Table 3.1, LPS doses used to provoke depression-related behaviours range from 0.1 – 5 mg/kg. However, information on the housing conditions, including light phase and group or individual housing, are often partially or completely absent from reports. Depressive-like behaviours can be sensitive to a range of factors, including animal strain, gender, social isolation, lighting, experimenter handling and diet (Bogdanova et al., 2013). As nocturnal animals, rodents naturally exhibit increased locomotion during the dark-phase of the light cycle (Kopp et al., 1998). Changes in locomotion may influence behaviours that require movement, including the FST. Unnatural manipulation of the circadian rhythm by extending the light period can increase FST immobility in mice (Fonken et al., 2009). Changes in locomotion, anxiety- and depressive-like behaviour following chronic stress in rats has been shown to be influenced by the light cycle (Huynh et al., 2011). In addition, female rats have been shown to exhibit increased FST immobility in the dark cycle, whilst male rats are unaffected (Verma et al., 2010). Social isolation in rats has returned mixed findings, with some studies reporting increased depressive-like behaviours (Kokare et al., 2010; Brenes et al., 2008), whilst others report no depressive-like behaviour (Hall et al., 1998) (Fischer et al., 2012). Increased immobility has been reported in female mice following isolation, which was reversible with fluoxetine (Martin and Brown, 2010). In a learned helplessness model of depression, group housing of mice attenuated

depressive behaviour (Chourbaji et al., 2005). Furthermore, the behavioural response to acute inflammation has been shown to be influenced by group housing, whereby an increase in inflammation-induced FST immobility is seen in group-housed CD-1 mice, but not when individually housed (Painsipp et al., 2011). No increase in immobility was reported in group or individually housed C57Bl/6J mice (Painsipp et al., 2011). Due to the sensitivity of depressive-like behaviour, such changes in experimental conditions may account for some of the variation seen throughout the literature.

3.1.3 Aims of Chapter 3

The aim of this chapter was to assess the acute LPS model of depressive-like behaviour in a number of behavioural tasks, including the FST, SPT and FUST. The influence of environmental conditions on behaviour following acute LPS was assessed, including light cycle and group / individual housing. The effect of ketamine on sexual motivation in the FUST was also investigated. Sickness and depressive-like behaviour was assessed following central administration of LPS directly into the lateral ventricle, thereby avoiding systemic inflammation. Finally, repeated LPS administration was used to develop a novel model of sustained inflammation-induced depressive-like behaviour. All experiments in this chapter were carried out at Janssen Pharmaceutica, except the preliminary sucrose consumption test of different sucrose concentrations (Figure 3.4).

	Experimental conditions						*Depressive-like behaviour*			*Sickness*		
Author	**Strain**	**Age/ weight**	**Housing**	**Light**	**Dose mg/ kg**	**n size**	**FST**	**TST**	**Sucrose preference**	**Loco-motion**	**Food/water consumption**	**Social behaviour**
Renault *et al*. 2006	CD1-Swiss	9-11 wks	G	R	0.2	9-10	24h↑					
Frenois *et al*. 2007	CD1	35-40 g	I	N	0.83	10-12	24h↑	24h↔	0-48h↓	23h↔		
Henry *et al*. 2008	BALB/c	12 wks	I	-	0.33	15			24-39h↓			24h↔
Godbout *et al*. 2008	BALB/c	12-24 wks	I	R	0.33	8-14	24h↑			24h↓	24h↓	
O'connor *et al*. 2009	CD1	35-40 g	I	N	0.83	11-14	24h↑	24h↑		24h↔		
Viana *et al*. 2010	CF1	25-30 g	-	N	0.45	6-8		24h↑	0-24h↓	24h↔		
	C57BL/6	25-30 g	-	N	1	6-8		24h↑				
de Paiva *et al*. 2010	Swiss	22-30 g	-	N	0.1	8-10	2h↑	2h↑		2h↓	2h↓	
Corona *et al*. 2010	C57BL/6	12-24 wks	-	N	0.5	10-16		48h↔		48h↓		24h↔
Zhu *et al*. 2010	C57BL/6J	7-12 wks	-	N	0.2	6-10		1h↑		0-4h↔		
Painsipp *et al*. 2011	C57BL/6J	16-24 wks	G	N	0.83	7-8	24h↓					
	C57BL/6J	16-24 wks	I	N	0.83	7-8	24h↔		Day26↓		24h↓	
	CD1	16-24 wks	G	N	0.83	7-8	24h↑					
	CD1	16-24 wks	I	N	0.83	7-8	24h↔		Day26↓		24h↓	
Park *et al*. 2011	CD1	9-10 wks	G	R	0.83	5-6	30h↑			27h↓		
Kang *et al*. 2011	CD1	10-12 wks	I	N	0.8	6-10	22h↑	24h↑	0-24h↓	<22h↔		
Salazar *et al*. 2012	C57BL/6J	-	I	R	0.83	6-20			0-24h↓	24h↓		
Walker *et al*. 2013	C57BL/6J	12 wks	I	N	0.83	>6	28h↑		24-28h↓	24h↔		
Custodio *et al*. 2013	Swiss	22-24 g	G	R	0.5	8-10	24h↑			24h↔		
Lawson *et al*. 2013	C57BL/6J	>10 wks	I	N	0.83	6	24h↔		24h↔	24h↓		
Ohgi *et al*. 2013	BALB/c	8 wks	-	N	0.5	6-12		24h↑		24h↔		
Biesmans *et al*. 2013	NMRI	10 wks	G	N	0.63-1.25	10	24h↔	24h↔	0-72h↓	24h↓		
Martin-de-saavedra *et al*. 2013	Swiss	12-16 wks	-	-	0.1	7		2h↑				
Mello *et al*. 2013	Swiss	20-30 g	G	R	0.5	6-10	24h↑			24h↔		
Zhang *et al*. 2014	BALB/c	8 wks	G	N	0.8	8-10	24h↑		24-25h↓			

	Experimental conditions						*Depressive-like behaviour*			*Sickness*		
Author	**Strain**	**Age/ weight**	**Housing**	**Light**	**Dose mg/ kg**	**n size**	**FST**	**TST**	**Sucrose preference**	**Loco-motion**	**Food/water consumption**	**Social behaviour**
Renault *et al*. 2006	CD1-Swiss	9-11 wks	G	R	0.2	9-10	24h↑					
Frenois *et al*. 2007	CD1	35-40 g	I	N	0.83	10-12	24h↑	24h↔	0-48h↓	23h↔		
Henry *et al*. 2008	BALB/c	12 wks	I	-	0.33	15			24-39h↓			24h↔
Godbout *et al*. 2008	BALB/c	12-24 wks	I	R	0.33	8-14	24h↑			24h↓	24h↓	
O'connor *et al*. 2009	CD1	35-40 g	I	N	0.83	11-14	24h↑	24h↑		24h↔		
Viana *et al*. 2010	CF1	25-30 g	-	N	0.45	6-8		24h↑	0-24h↓	24h↔		
	C57BL/6	25-30 g	-	N	1	6-8		24h↑				
de Paiva *et al.* 2010	Swiss	22-30 g	-	N	0.1	8-10	2h↑	2h↑		2h↓	2h↓	
Corona *et al.* 2010	C57BL/6	12-24 wks	-	N	0.5	10-16		48h↔		48h↓		24h↔
Zhu *et al.* 2010	C57BL/6J	7-12 wks	-	N	0.2	6-10		1h↑		0-4h↔		
Painsipp *et al.* 2011	C57BL/6J	16-24 wks	G	N	0.83	7-8	24h↓					
	C57BL/6J	16-24 wks	I	N	0.83	7-8	24h↔		Day26↓		24h↓	
	CD1	16-24 wks	G	N	0.83	7-8	24h↑					
	CD1	16-24 wks	I	N	0.83	7-8	24h↔		Day26↓		24h↓	
Park *et al.* 2011	CD1	9-10 wks	G	R	0.83	5-6	30h↑			27h↓		
Kang *et al.* 2011	CD1	10-12 wks	I	N	0.8	6-10	22h↑	24h↑	0-24h↓	<22h↔		
Salazar *et al.* 2012	C57BL/6J	-	I	R	0.83	6-20			0-24h↓	24h↓		
Walker *et al.* 2013	C57BL/6J	12 wks	I	N	0.83	>6	28h↑		24-28h↓	24h↔		
Custodio *et al*. 2013	Swiss	22-24 g	G	R	0.5	8-10	24h↑			24h↔		
Lawson *et al.* 2013	C57BL/6J	>10 wks	I	N	0.83	6	24h↔		24h↔	24h↓		
Ohgi *et al.* 2013	BALB/c	8 wks	-	N	0.5	6-12		24h↑		24h↔		
Biesmans *et al.* 2013	NMRI	10 wks	G	N	0.63-1.25	10	24h↔	24h↔	0-72h↓	24h↓		
Martin-de-saavedra *et al.* 2013	Swiss	12-16 wks	-	-	0.1	7		2h↑				
Mello *et al.* 2013	Swiss	20-30 g	G	R	0.5	6-10	24h↑			24h↔		
Zhang *et al.* 2014	BALB/c	8 wks	G	N	0.8	8-10	24h↑		24-25h↓			

	Experimental conditions						*Depressive-like behaviour*			*Sickness*		
Author	**Strain**	**Age/ weight**	**Housing**	**Light**	**Dose mg/kg**	**n size**	**FST**	**TST**	**Sucrose preference**	**Loco-motion**	**Food/water consumption**	**Social behaviour**
Shaikh *et al.* 2016	Swiss	25-30 g	-	-	0.4	8	2h↑				24h↓	24h↔
Dong *et al.* 2016	C57BL/6N	8 wks	-	N	0.5	9-10	27h↑	27h↑		24h↔		
Tao *et al*. 2016	ICR	18-22 g	-	-	0.5	10	24h↑	24h↑				
Zhang *et al.* 2016	ICR	-	-	-	0.5	10	24h↑	24h↑	0-24h↓	24h↔		
Sriram *et al.* 2016	Swiss	25-30 g	G	R	1	6-8	24h↑	24h↑	24-48h↓			
Sulakhiya *et al*. 2016	Swiss	22-28 g	-	-	0.83	8	24h↑	24h↑				
Anderson *et al.* 2016	C57BL/6	8-13 wks	G	-	5	10-11		1month↑				

Table 3-1. of studies that utilised acute LPS administration to assess depressive-like behaviour in adult mice.

A Web of Science search of "lipopolysaccharide + depression + mice" returned 54 articles that assessed at least one depressive-like behaviour after a single intraperitoneal administration of LPS. Arrows indicate whether the measured behaviour was increased (↑), decreased (↓), or was not statistically different (↔). FST and TST measurement is immobility. Blue (■) indicates either the presence of depressive-like behaviour or the absence of sickness behaviour, whilst red (■) indicates either no depressive-like behaviour or the presence of sickness behaviour. In order to exclude overt sickness as a confounding factor in depressive-like behaviours, sickness should be assessed during or before the time-point at which depressive-like behaviour is assessed. G – group housed; I – individually housed; N – normal light cycle; R – reversed light cycle.

3.2 Results

3.2.1 Pharmacological validation of depressive-like behaviour in mice

In preliminary experiments, the FST was pharmacologically validated using a range of antidepressant drugs with proven clinical efficacy and pre-clinical efficacy in the mouse FST. Time spent immobile was assessed in control adult male C57BL/6J mice in the FST 30 min after the administration of antidepressants including desipramine, ketamine, bupropion, and fluoxetine (Figure 3.1A-D). Bupropion (one-way ANOVA, $F_{(2,27)} = 5.477$, $p = 0.01$) and ketamine (one-way ANOVA, $F_{(2,27)} = 10.83$, $p < 0.001$) both revealed a significant effect on time spent immobile during a 6 minute FST. 20 mg/kg bupropion and 10 mg/kg ketamine significantly reduced FST immobility ($p < 0.01$ & $p < 0.001$, respectively), indicating anti-depressant activity. Desipramine (one-way ANOVA, $F_{(2,24)} = 1.388$, $p = 0.2688$) and fluoxetine (*t* test, $p = 0.4492$) failed to significantly affect immobility time.

Bupropion and ketamine were subsequently assessed in a 10-minute OFT in low light, 30 min after administration, to measure the effect on locomotion (Figure 3.1E-F). Bupropion induced a significant increase in distance travelled (*t* test, $p < 0.001$), whilst ketamine had no effect on distance travelled (*t* test, $p = 0.5789$) compared to saline treated controls. Neither bupropion (*t* test, $p = 0.4211$) nor ketamine (*t* test, $p = 0.8342$) affected time spent in the centre of the OFT (Figure 3.1G-H), though it should be noted that a low level of light (2 – 3 lux) was used, so the centre of the maze was not aversive as required for assessing anxiety-like behaviours per se.

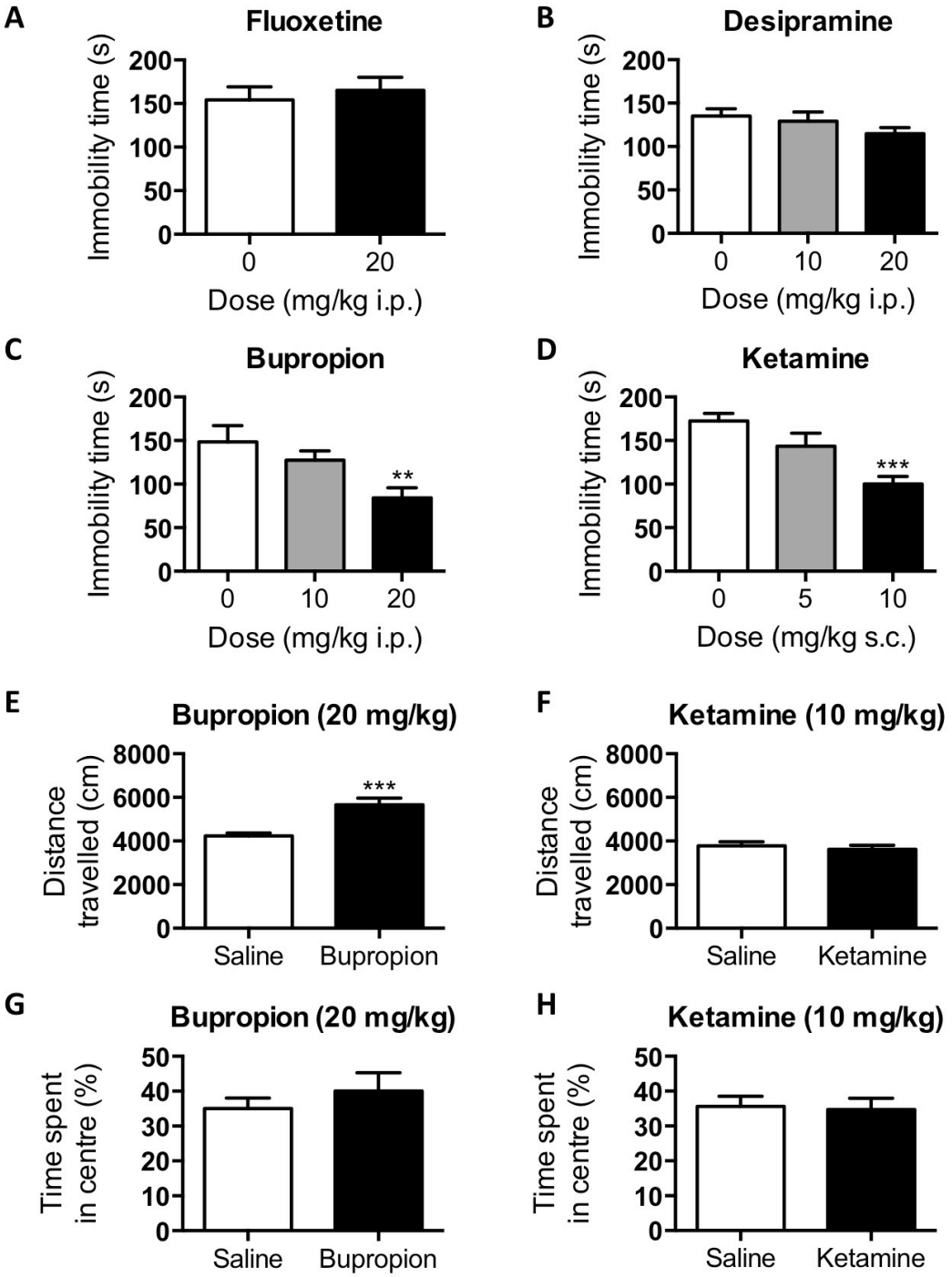

Figure 3.1. Pharmacological validation of antidepressant compounds in the forced swim test and open field test in adult male C57BL/6J mice.

Fluoxetine (*i.p.*; **A**), desipramine (*i.p.*; **B**), bupropion (*i.p.*; **C**) and ketamine (*s.c.*; **D**) were all tested for 6 min in the FST, 30 min after administration. Total distance travelled in a 10 min OFT (**E**, **F**). Time spent in the centre of the OFT (**G**, **H**). Values shown are mean ± SEM of n=8-10 per group. $^{**}p < 0.01$, $^{***}p < 0.001$ compared to saline injected controls. Data was analysed by Students *t*-test (**A**, **E** - **H**) or one-way ANOVA with Dunnett's posthoc test (**B** - **D**).

3.2.2 Assessment of acute LPS induced depressive-like behaviours

3.2.2.1 Effect of housing and lighting conditions on acute LPS-induced behaviours

The influence of housing and lighting conditions on acute LPS-induced behaviours has not been systematically studied. Mice were housed either in groups or individually and then tested during the light phase (lights on 06:00 h) or the dark phase (lights off at 06:00 h, behaviours assessed under red light) of the light cycle (Figure 3.2). As an indication of sickness behaviour, body weight and total locomotion in the OFT was monitored (Figure 3.2A-B). A two-way ANOVA revealed a significant effect of treatment ($F_{(2,161)}$ = 337.3, p < 0.001) and housing ($F_{(3,161)}$ = 4.923, p < 0.01) on body weight change at +24 h after injection, but no interaction between the two ($F_{(6,161)}$ = 1.807, p = 0.101). All LPS-treated mice showed a significant reduction in body weight, following acute LPS administration at both doses (all p < 0.001), compared to saline-treated controls. A two-way ANOVA revealed a significant effect of treatment ($F_{(2,133)}$ = 284.7, p < 0.001) and housing ($F_{(3,133)}$ = 5.56, p < 0.01) on distance travelled in the OFT at +6 h after injection, but no interaction between the two ($F_{(6,133)}$ = 1.695, p = 0.127). A significant reduction in the total distance travelled in the OFT was seen 6 h after acute administration of LPS, at both 0.42 and 0.83 mg/kg, in all housing conditions when compared to saline-treated controls (all p < 0.001). There was no significant difference between housing conditions in LPS-treated mice. However, in saline-treated mice, the mice group-housed and tested in the dark travelled further than mice group-housed and tested in the light (p < 0.05). On average, locomotion was reduced to 40 % and 32 % of control following 0.42 and 0.83 mg/kg LPS, respectively, consistent with a pronounced sickness behaviour 6 h following acute LPS administration. Furthermore, acute LPS treatment did not significantly influence the time spent in the centre portion of the OFT, indicating that LPS did not induce anxiety-like behaviour, though the OFT setup was not optimised to detect anxiety-related behaviours (Figure 3.2C).

Depressive-like behaviour was subsequently assessed in the FST, 24 h after acute LPS administration because overt sickness behaviour is often no longer present at this time (Figure 3.2D) (O'Connor et al., 2009a). A two-way ANOVA revealed a significant effect of treatment ($F_{(2,131)}$ = 3.334, p < 0.05), though posthoc comparisons between saline and LPS groups did not reveal any significant differences. There was no significant effect of housing ($F_{(3,131)}$ = 0.4783, p = 0.6979) on FST immobility and no significant interaction between the two ($F_{(6,131)}$ = 1.665, p = 0.1345). Following post hoc analysis, no group showed a significant increase in FST immobility following LPS

administration compared to saline-treated mice. In subsequent experiments with acute LPS all mice were group housed and tested in the light phase unless otherwise stated.

3.2.2.2 Time course of acute LPS-induced behaviours

Having established evident sickness behaviour at +6 h in the OFT, the duration of this behaviour was investigated (Figure 3.3A). At +24 h after injection, there was a significant effect of LPS on distance travelled in the OFT (one way ANOVA, $F_{(3,68)}$ = 6.458, $p < 0.001$). Both 0.42 and 0.83 mg/kg LPS produced a significant reduction in total distance travelled in the OFT to 81 ± 3 % (n = 17) and 79 ± 5 % (n = 18) of control, respectively ($p < 0.01$ and $p < 0.001$, respectively). 0.21 mg/kg LPS did not significantly affect distance travelled. There was a significant effect of LPS on immobility in the FST at +48 h after injection (one way ANOVA, $F_{(2,25)}$ = 7.727, $p < 0.01$), although no group exhibited significantly greater immobility levels compared to control (Figure 3.3B). The rotarod test was also used to assess motor coordination at +6, +24 and +48 h after acute LPS administration in separate groups of mice (Figure 3.3C). A two-way ANOVA revealed a significant effect of treatment ($F_{(1,54)}$ = 13.22, $p < 0.001$), but no significant effect of treatment time ($F_{(5,54)}$ = 0.07, p = 0.9964) or interaction between the two ($F_{(5,54)}$ = 1.045, p = 0.4008). Posthoc analysis revealed a reduction in post-LPS performance compared to baseline performance +6 h after LPS administration ($p < 0.05$), but not at +24 h or +48 h after administration.

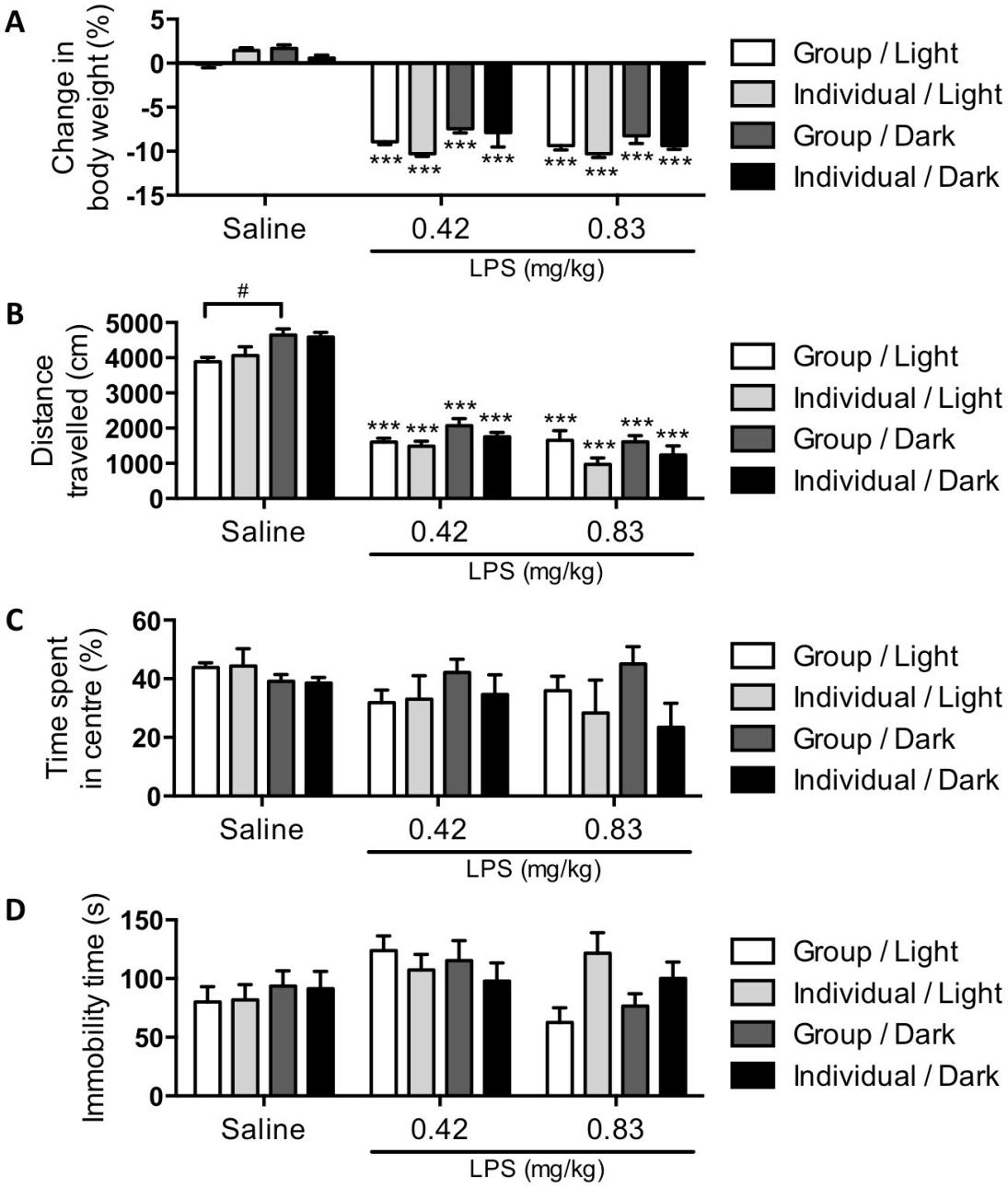

Figure 3.2. Sickness and depressive-like behaviour following acute LPS in adult male C57BL/6J mice.

Change in body weight +24 h after LPS or saline administration (**A**). Distance travelled (**B**) and time spent in the centre (**C**) of the OFT was assessed +6 h post-administration of LPS. Time spent immobile in the FST +24 h post-administration of LPS (**D**). Mice were group housed (n=3/4 per cage) or individually housed ("Group" & "Individual"). Behaviours were assessed during the light (lights on 06:00 hr) or the dark (lights off 06:00 hr) phase ("Light" & "Dark"). Values shown are mean ± SEM of n=10-15 per group. ***$p < 0.001$ compared to saline injected controls, $^{\#}p < 0.05$. Data was analysed by two-way ANOVA with Bonferroni's posthoc test.

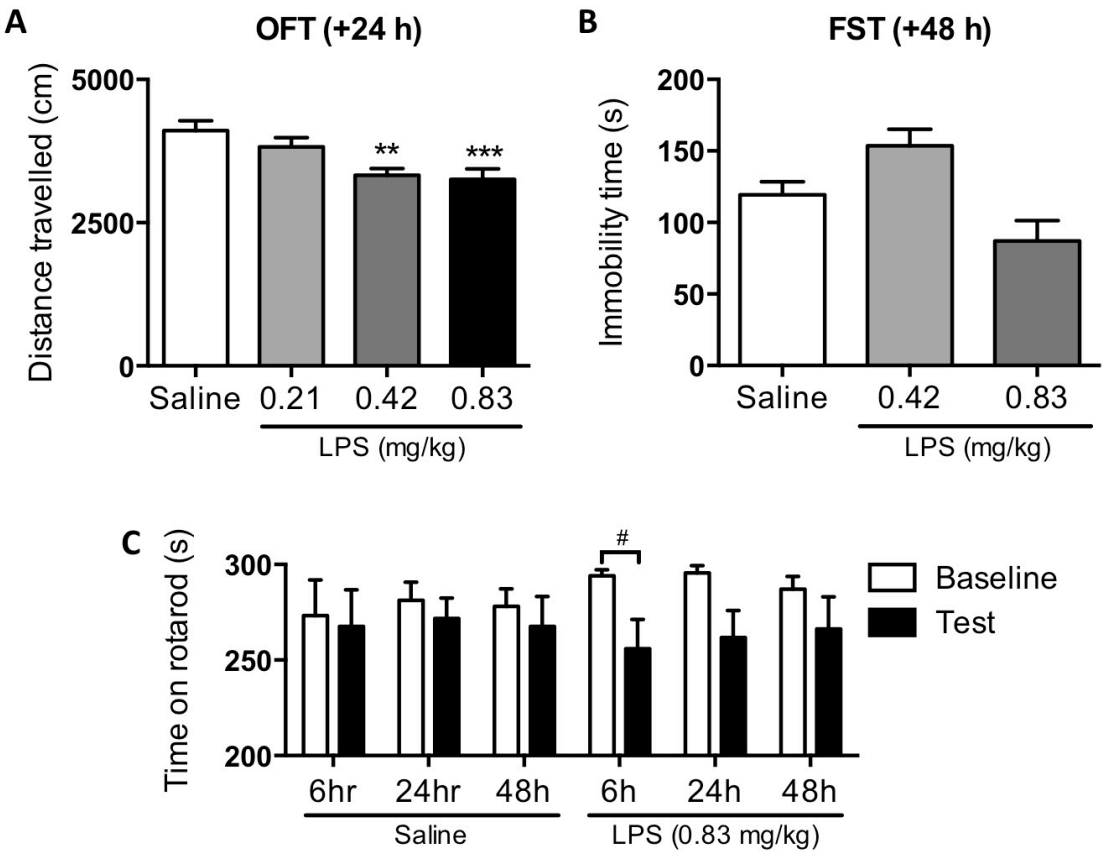

Figure 3.3. Time course of behavioural effects of acute LPS administration in adult male C57BL/6J mice.

Distance travelled in the OFT +24 h post-administration of saline or LPS (**A**). Time spent immobile in the FST (**B**) +48 h post-administration of saline or LPS (n=9-18 per group, $^{**}p < 0.01$, $^{***}p < 0.001$ compared to saline injected controls). In a separate group of animals, motor coordination in a 3 min rotarod test was examined at 6, 24 or 48 h post-administration of saline or LPS (**C**; n=10 per group, $^{\#}p < 0.05$ compared to pre-treatment baseline performance). Mice were group housed (n=3/4 per cage) and behaviour assessed in the light cycle. All values are mean ± SEM and analysed by one-way ANOVA with Dunnett's posthoc test (**A**, **B**) or two-way ANOVA with Bonferroni's posthoc test (**C**).

3.2.2.3 Effect of acute LPS on anhedonic behaviours

The SPT and FUST were used as additional methods of testing depressive-like behaviours, in particular, hedonic behaviour. In a preliminary experiment carried out at the University of Bath, the palatability of sucrose was assessed in adult male C57BL/6J mice in a sucrose consumption test (Figure 3.4B). Following a 4 h food and water restriction, there was a significant effect of sucrose on volume consumed (one way ANOVA; $F_{(2,9)} = 10.89$; $p = 0.004$). Mice consumed significantly more 2.5 % or 5 % sucrose solution when compared to mice that had just water ($p < 0.01$ & $p < 0.05$,

respectively). These data indicate that 2.5 % sucrose solution is enough to induce a significant preference and a hedonic behaviour.

In the SPT (performed at Janssen Pharmaceutica), mice have a choice between two bottles: one containing water and one containing sucrose dissolved in water). During the 4 days training prior to LPS administration, mice had access to either two water bottles (days 1 & 3), or water and sucrose (days 2 & 4). There was a significant effect of day on preference (one way repeated measures ANOVA, $F_{(2.4,109.2)}$ = 382.4; p < 0.001; Figure 3.4C). Mice exhibited a significant preference for 2.5 % sucrose solution over water (~90%; p < 0.001) compared to the preference of right over left when only water was available (50%). This indicates that there was no positional preference of bottles. In addition, there was a significant effect of day on total volume consumed (one way repeated measures ANOVA, $F_{(2,91.8)}$ = 50.82; p < 0.001; Figure 3.4D). A significant increase in total volume consumed was observed on training days 2 and 4, which included sucrose solution (p < 0.001 for both), as well as training day 3, which did not include sucrose solution (p < 0.001). The increase seen on day 3 could be explained by an increase in mice sampling the water bottles in anticipation of sucrose solution.

A two-way repeated measures ANOVA revealed a significant effect of treatment ($F_{(2,43)}$ = 4.941, p = 0.0117) and time ($F_{(1,43)}$ = 8.513, p = 0.0056) on sucrose preference following acute LPS administration, as well as a significant interaction between the two ($F_{(2,43)}$ = 4.515, p = 0.0166; Figure 3.4E). A significant effect of treatment ($F_{(2,43)}$ = 34.31, p < 0.001) and time ($F_{(1,43)}$ = 28.65, p < 0.001) on total volume consumed was also observed following acute LPS administration, as well as a significant interaction between the two ($F_{(2,43)}$ = 10.53, p < 0.001; Figure 3.4F). Both doses of LPS tested, 0.415 and 0.83 mg/kg, produced a significant reduction in volume consumed to 56 ± 7 % (n = 16) and 42 ± 5 % (n = 15) of control and sucrose preference to 81 ± 6 % (n = 16) and 79 ± 4 % (n = 15) of control, respectively, in the first 24 h after injection (all p < 0.001). No significant reductions in volume consumed or sucrose preference was observed from 24-48 h after injection.

The FUST was used to assess sexually motivated behaviour at +6 h and +24 h (separate groups of mice) after acute LPS administration (0.42 & 0.83 mg/kg; Figure 3.5B-C). The task was first validated by assessing the preferences of male mice for female urine over male urine or water (Figure 3.5A). A two-way repeated measures ANOVA revealed a significant effect of odour ($F_{(1,30)}$ = 55.81, p < 0.001) on sniffing behaviour in the FUST. Male mice had a preference for sniffing at female urine over male urine and water (p < 0.001 for both). No preference for male urine over water was

observed, indicating the preference towards female urine is likely sex-based and not novelty-based.

Acute LPS-induced behavioural changes were then assessed in the FUST. At +6 h after saline or LPS administration, a two-way repeated measures ANOVA revealed a significant effect of treatment ($F_{(2,17)}$ = 19.06, p < 0.001) and odour ($F_{(1,17)}$ = 33.35, p < 0.001) on FUST sniffing behaviour, and a significant interaction between treatment and odour ($F_{(2,17)}$ = 11.51, p < 0.001). Saline-injected control mice spent significantly more time sniffing urine when compared to water (p < 0.001), but this was not seen in LPS-treated mice (Figure 3.5B). Furthermore, time spent sniffing urine was significantly reduced to 23 ± 8 % (n = 7) and 17 ± 6 % (n = 7) following 0.42 or 0.83 mg/kg LPS treatments, respectively, when compared to control mice (p < 0.001 for both). Similarly, a two-way repeated measures ANOVA revealed a significant effect of treatment ($F_{(2,17)}$ = 7.06, p = 0.0059) and odour ($F_{(1,17)}$ = 85.66, p < 0.001) on FUST sniffing behaviour at +24 h after saline or LPS administration, and a significant interaction between treatment and odour ($F_{(2,17)}$ = 6.932, p = 0.0063). Again, saline-injected control mice spent significantly more time sniffing urine compared to water (p < 0.001) and this effect was also evident in both 0.42 and 0.83 mg/kg LPS treated groups (p < 0.001 and p < 0.05, respectively; Figure 3.5C). However, at +24 h post-LPS administration, time spent sniffing urine was significantly reduced to 62 ± 10 % (n = 7) and 44 ± 7 % (n = 7) following 0.42 or 0.83 mg/kg LPS treatments, respectively, when compared to control mice (p < 0.01 and p < 0.001, respectively). In addition, there was not a significant effect of LPS treatment on time spent sniffing water. These results demonstrate that acute LPS administration produced a significant effect on hedonic behaviour in both the SPT and FUST +24 h post-administration.

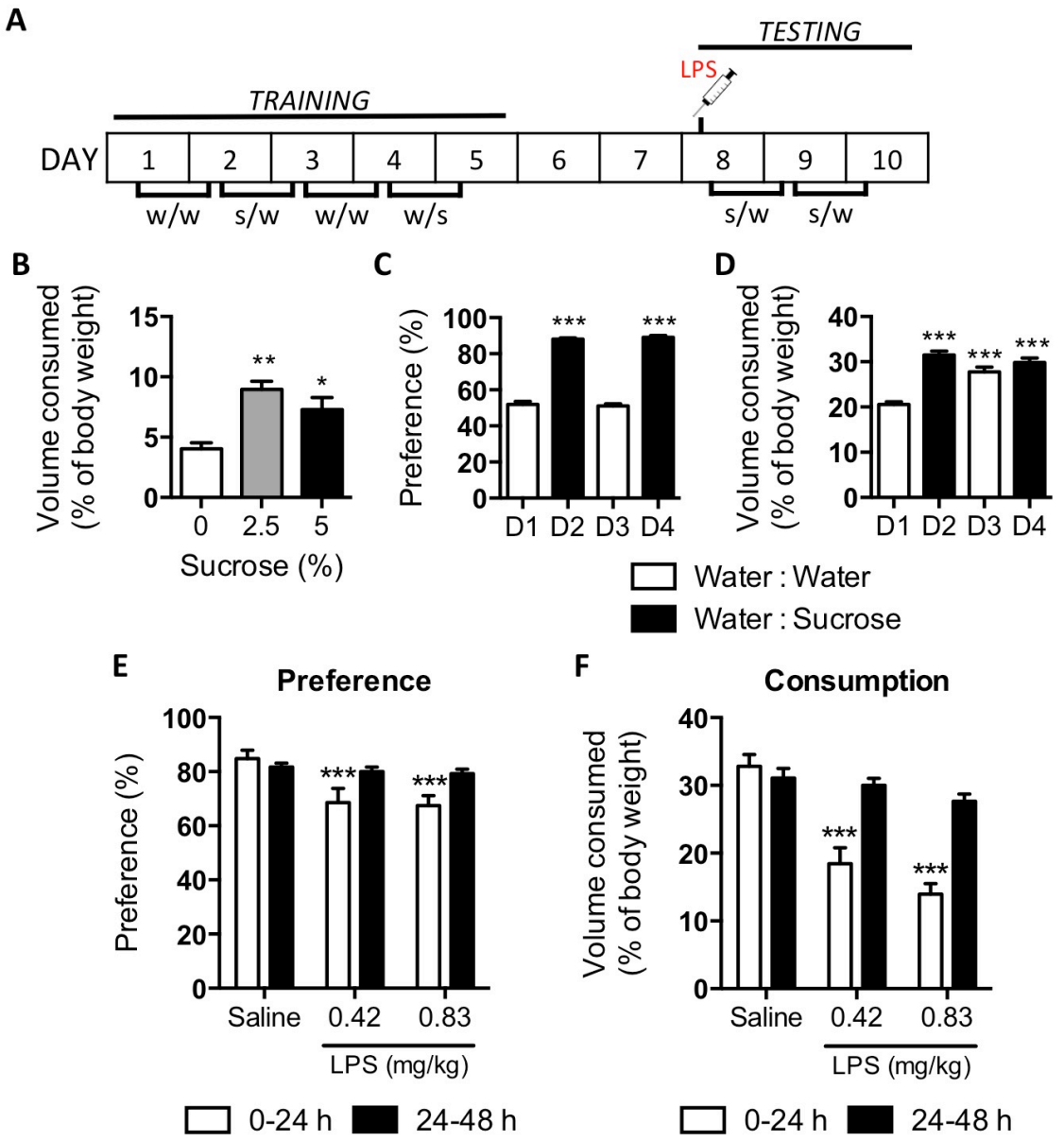

Figure 3.4. Effects of acute LPS administration in the sucrose preference test in adult male C57BL/6J mice.

Mice were given the choice of two bottles containing either water (w) or sucrose solution (s) during the SPT (**A**). Consumption of sucrose solutions (0, 2.5 or 5 %) was measured (**B**; n=4 per group, *$p < 0.05$, **$p < 0.01$ compared to 0 % sucrose). During the 4-day SPT training, mice were given either two water bottles (Days 1 & 3), or one water bottle and one 2.5 % sucrose solution (Days 2 & 4). Preference of sucrose solution over water or left water bottle over right water bottle was calculated (**C**), as well as total consumption (**D**). Following LPS or saline administration, sucrose preference (**E**) and total consumption (**F**) was recorded during 0-24 h and 24-48 h (n=15-16, ***$p < 0.001$ compared to saline injected controls). Mice were singly housed throughout the experiment, lights on at 06:00 h. Values shown are mean ± SEM and analysed by one-way repeated measures ANOVA with Dunnett's posthoc test (**B**) or two-way repeated measures ANOVA with Dunnett's posthoc test (**C** - **F**).

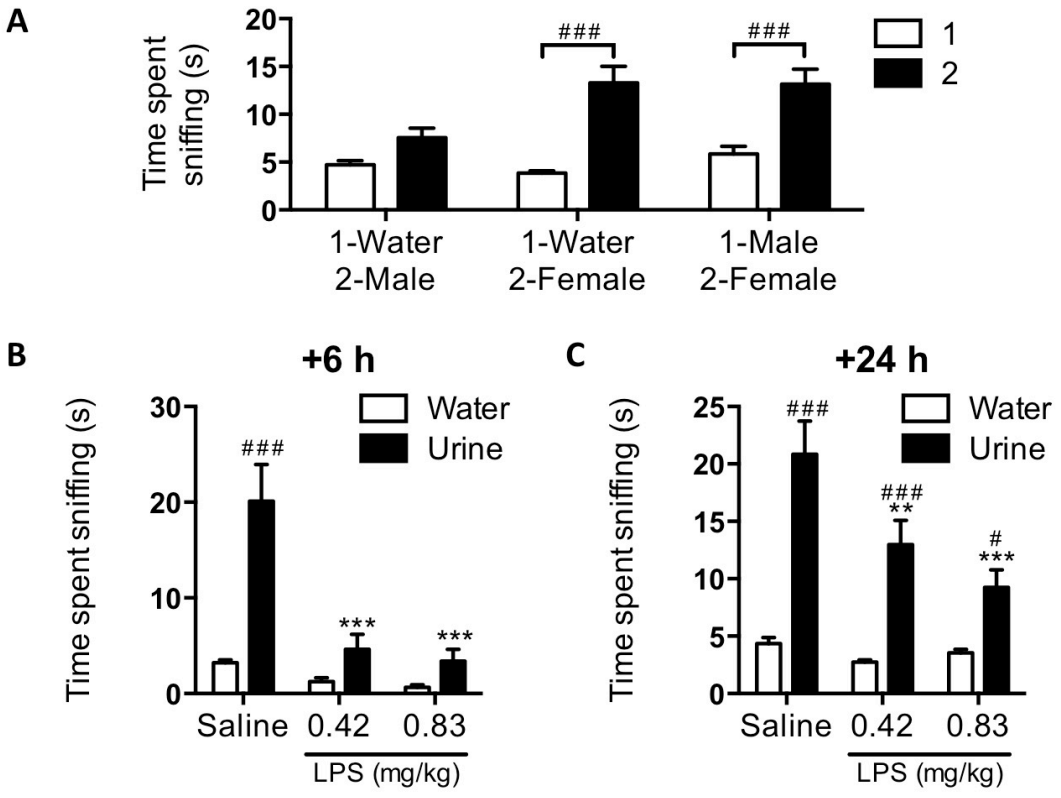

Figure 3.5. Effects of acute LPS administration on sexual motivation in the female urine sniffing test in adult male C57BL/6J mice.

During a 3 min FUST test period, time spent sniffing water, male urine or female urine soaked cotton buds was assessed to validate sex-driven behaviour (**A**). FUST behaviour was assessed at +6 h (**B**) and +24 h (**C**) post-administration of saline or LPS. Mice were group housed (n=3/4 per cage) and behaviour assessed during the light phase. Values shown are mean ± SEM of n=6-7 per group. $^{**}p < 0.01$, $^{***}p < 0.001$ compared to urine sniffing saline injected controls) and $^{\#}p < 0.05$, $^{\#\#\#}p < 0.001$ within group comparison vs water. Data was analysed by two-way repeated measures ANOVA with Bonferroni's posthoc test.

3.2.3 The effect of ketamine on LPS-induced depressive-like behaviour

In preliminary experiments, ketamine exhibited antidepressant-like activity in the FST without affecting locomotion (Figure 3.1). The potential antidepressant activity of ketamine on LPS-induced depressive-like behaviour was assessed in the FUST at +24 h post-LPS administration. Ketamine (10 mg/kg; *s.c.*) was administered 30 min before the FUST (Figure 3.6A). A two-way repeated measures ANOVA revealed a significant effect of odour on FUST behaviour ($F_{(1,24)}$ = 73.03, p = 0.009) and a significant interaction between treatment and odour ($F_{(3,24)}$ = 4.833, $p < 0.001$), though no significant effect of treatment alone ($F_{(3,24)}$ = 2.87, p = 0.0575). All mice showed a

significantly greater time spent sniffing female urine compared to water ($p < 0.001$ for saline treated controls; $p < 0.05$ for all other groups), indicating sexual motivation. LPS alone significantly reduced time spent sniffing urine when compared to saline treated control mice ($p < 0.01$). Interestingly, ketamine alone significantly reduced time spent sniffing urine ($p < 0.01$), indicating a pro-depressive-like effect. Mice administered LPS 24 h before testing and ketamine 30 min before testing still exhibited a significant reduction in time spent sniffing urine ($p < 0.01$), with no significant difference between LPS alone and LPS with ketamine. These data suggest that ketamine administered 30 min prior to the FUST failed to abrogate the depressive-like effects of acute LPS administered 24 h prior. Furthermore, ketamine alone induced depressive-like behaviour, though alongside LPS, it did not enhance the depressive-like effects of LPS.

Subsequently, ketamine (10 mg/kg; *s.c.*) was administered alongside LPS, 24 h prior to the FUST, in an attempt to block the development of inflammation-induced depressive-like behaviour in the FUST (Figure 3.6B). A two-way repeated measures ANOVA revealed a significant effect of odour ($F_{(1,37)} = 131.9$, $p < 0.001$) and treatment ($F_{(3,37)} = 4.868$, $p = 0.0059$), with a significant interaction between odour and treatment ($F_{(3,37)} = 3.611$, $p = 0.022$). All mice showed a significantly greater time spent sniffing female urine compared to water ($p < 0.01$ for LPS alone; $p < 0.001$ for all other groups). LPS alone significantly reduced the time spent sniffing urine ($p < 0.001$). Ketamine alone, administered alongside LPS 24 h prior to testing, did not significantly alter the time spent sniffing urine when compared to saline treated controls. When ketamine was co-administered with LPS, there was still a significant reduction in time spent sniffing female urine compared to the control mice ($p < 0.05$), and no significant difference compared to LPS alone. These findings suggest ketamine failed to reverse or attenuate the depressive-like effect of acute LPS on FUST behaviour in adult male mice.

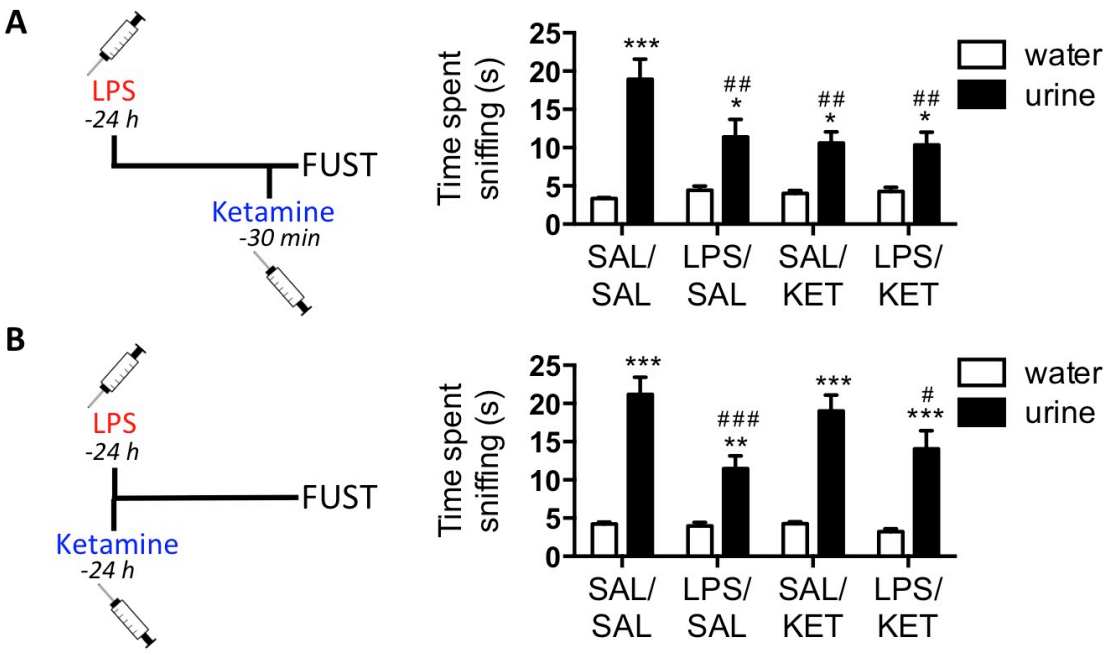

Figure 3.6. Effects of ketamine on acute LPS-induced depressive-like behaviour in the female urine sniffing test in adult male C57BL/6J mice.

LPS (0.83 mg/kg; *i.p.*) was administered 24 h prior to the FUST. Ketamine (10 mk/kg; *s.c.*) was administered either 30 min (**A**) or 24 h (**B**) before the FUST. Mice were group housed (n=3/4 per cage) and behaviour assessed in the light cycle. Values shown are mean ± SEM of n=7-11 per group. $^{*}p < 0.05$, $^{***}p < 0.001$ compared to urine sniffing saline injected controls; $^{\#}p < 0.05$, $^{\#\#}p < 0.01$, $^{\#\#\#}p < 0.001$ within group comparison vs water. Data was analysed by two-way repeated measures ANOVA with Bonferroni's posthoc test.

3.2.4 Intracerebroventricular (ICV) administration of LPS

By administering LPS directly into the CNS, the influence of peripheral inflammation can be avoided and neuroinflammation can be assessed in isolation. Here, LPS (100 ng) was administered directly into the lateral ventricle of the brain (lateral 1.5 mm / posterior 0.6 mm / dorsal 2.3 mm with respect to Bregma) via intracerebroventricular (ICV) injection in an attempt to induce a depressive-like behaviour in mice (Section 2.1.12). Firstly, central administration of LPS during surgery was assessed, with mice receiving an injection of LPS or saline (1 µl) directly into the lateral ventricle and tested in the OFT and the FST at +6 h and +24 h, respectively, or +24 h and +48 h, respectively. Body weight following LPS was significantly reduced at +24 h compared to saline treated mice (92 ± 1 %; n = 12; *t* test, $p < 0.001$; Figure 3.7E). Distance travelled in the OFT was significantly reduced at +6 h after administration (33 ± 3 %; n = 4; *t* test, $p < 0.001$; Figure 3.7A), and was not significantly reduced after +24 h after administration (72 ± 10 %; n = 6; *t* test, $p = 0.0989$; Figure 3.7B). When tested in the FST, no significant increase in immobility was observed at

+24 h (*t* test, $p = 0.535$; Figure 3.7C) or +48 h (*t* test, $p = 0.454$; Figures 3.7D). In order to avoid any confounding factors of carrying out behavioural tests within 24 h of surgery, ICV administration via a cannula surgically implanted 2 weeks prior was also tested (Section 2.1.13). Body weight following LPS was significantly reduced at +24 h compared to saline treated mice (92 ± 2 %; n = 6; *t* test, $p < 0.001$; Figure 3.8B). Distance travelled in the OFT at +6 h was significantly reduced in LPS treated mice compared to saline treated mice (50 ± 12 %; n = 6; *t* test, $p = 0.0027$; Figure 3.8A). At +24 h, FST immobility was not significantly different between LPS and saline treated mice (*t* test, $p = 0.341$, n = 6; Figure 3.8C).

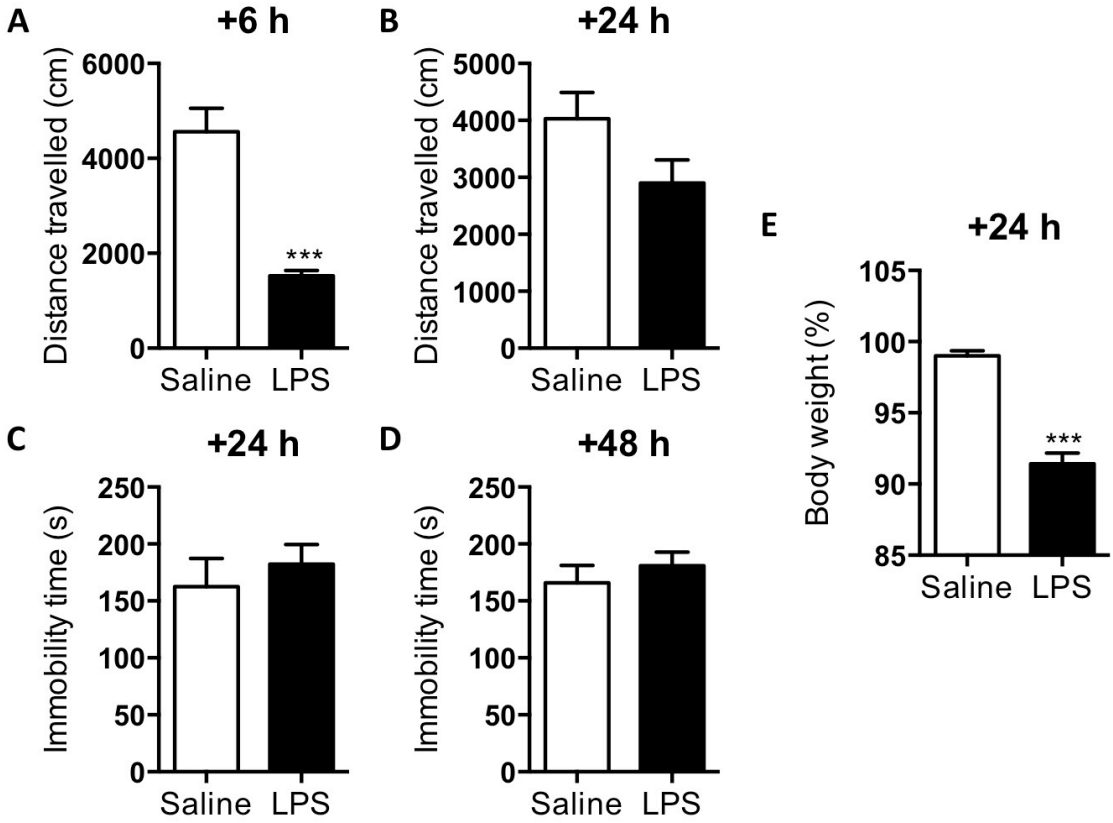

Figure 3.7. Effects of *i.c.v.* injection of LPS on open field test and forced swim test behaviour in adult male C57BL/6J mice.

LPS (100 ng) or saline was injected directly into the lateral ventricle during surgery. Distance travelled in the OFT at +6 h (**A**) and +24 h (**B**) after saline or LPS administration. Time spent immobile in the FST at +24 h (**C**) or +48 h (**D**). Body weight +24 h after saline or LPS administration (**E**). Mice were individually housed and behaviour assessed in the light cycle. Values shown are mean ± SEM of n=4-6 per group. ***$p < 0.001$ compared to saline injected controls. Data was analysed by Students *t*-test.

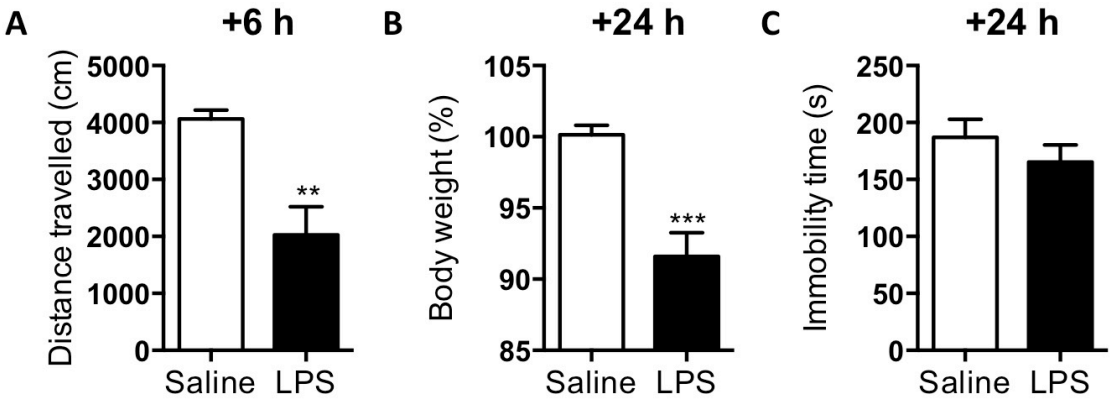

Figure 3.8. Effects of *i.c.v.* administration of LPS via cannula on open field test and forced swim test behaviour in C57BL/6J mice.

LPS (100 ng) or saline was injected directly into the lateral ventricle via a cannula surgically implanted 2 weeks prior to injection. Distance travelled in the OFT at +6 h after saline or LPS administration (**A**). Body weight at +24 h after saline or LPS administration (**B**). Time spent immobile in the FST at +24 h after saline or LPS administration (**C**). Mice were individually housed and behaviour assessed in the light cycle Values shown are mean ± SEM of n=6 per group. $^{**}p < 0.01$, $^{***}p < 0.001$ compared to saline injected controls. Data was analysed by Student's *t*-test.

3.2.5 A repeated LPS model of depressive-like behaviour in mice

In order to develop a protocol for assessing the effects of a period of sustained inflammation on depression-related behaviours, repeated daily dosing with LPS was carried out. A 3-day and 5-day model tested with four groups: saline treated controls, acute LPS (0.83 mg/kg), constant dosing (CD) of 0.83 mg/kg and increasing dosing (ID) doubling up to 0.83 mg/kg on final day. Sickness behaviour was assessed by tracking body weight and assessing locomotor behaviour in the OFT at +6 h after the final injections. Depressive-like behaviour in the FST was investigated at +24 h after the final injection.

3.2.5.1 Effects of repeated daily LPS administration for 3 days

In the 3-day experiment, there was a significant interaction between treatment and time on body weight (two way repeated measures ANOVA, $F_{(9,156)} = 84.54$, $p < 0.001$; Figure 3.9B). Body weight at the start of the experiment was similar in all groups: 24.5 ± 0.5 g (n = 14) for saline, 24.2 ± 0.3 g (n = 14) for acute LPS, 24.6 ± 0.3 g (n = 14) for CD LPS and 24.9 ± 0.5 g (n = 14) for ID LPS. At +24 h after the final

injection, there was a significant effect of treatment of body weight (one way ANOVA, $F_{(3,52)} = 78.82$, $p < 0.001$; Figure 3.9C). Body weight at +24 h was increased by +0.4% for the saline group, reduced by -8.6% for acute LPS, by -12.1% for CD LPS and by -11.9% for ID LPS, with the reductions in body weight for all LPS treatments being statistically significant compared to saline-treated controls ($p < 0.001$ for all). In addition, the reduction in body weight observed in CD and ID LPS was significantly greater than that seen in acute LPS ($p < 0.01$ for both).

A significant effect of treatment on distance travelled in the OFT was observed at +6 h after administration (one way ANOVA, $F_{(3,52)} = 107.9$, $p < 0.001$; Figure 3.9D). A significant reduction in the distance travelled in the OFT was evident for all LPS-treated groups in the 3-day experiment (all $p < 0.001$). Taken together, the reduction in body weight and the reduction in locomotion are consistent with sickness behaviour following LPS administration. Interestingly, the CD LPS mice showed an attenuated reduction in locomotion (61 ± 3 % of control; n = 14) that was significantly different from that seen in either the ID LPS (38 ± 2 % of control; n = 14) or acute LPS (37 ± 3 % of control; n = 13) treated mice ($p < 0.001$ for both). This observation may reflect the development of tolerance to CD LPS in sickness behaviour as repeated stimulation with high dose LPS resulted in attenuated sickness behaviour.

Depressive-like behaviour was assessed in the FST at +24 h after the final injection (Figure 3.9E). After the 3-day LPS treatment, there was a significant effect of LPS on FST immobility (one way ANOVA, $F_{(3,52)} = 3.919$, $p < 0.05$). Only ID LPS treatment caused a significant increase in immobility (166 ± 10 % of control; n = 14) compared to control ($p < 0.0\,5$).

A

TREATMENT	DAY 1	DAY 2	DAY 3
Saline	SAL	SAL	SAL
Acute LPS	SAL	SAL	0.83
CD LPS	0.83	0.83	0.83
ID LPS	0.21	0.42	0.83

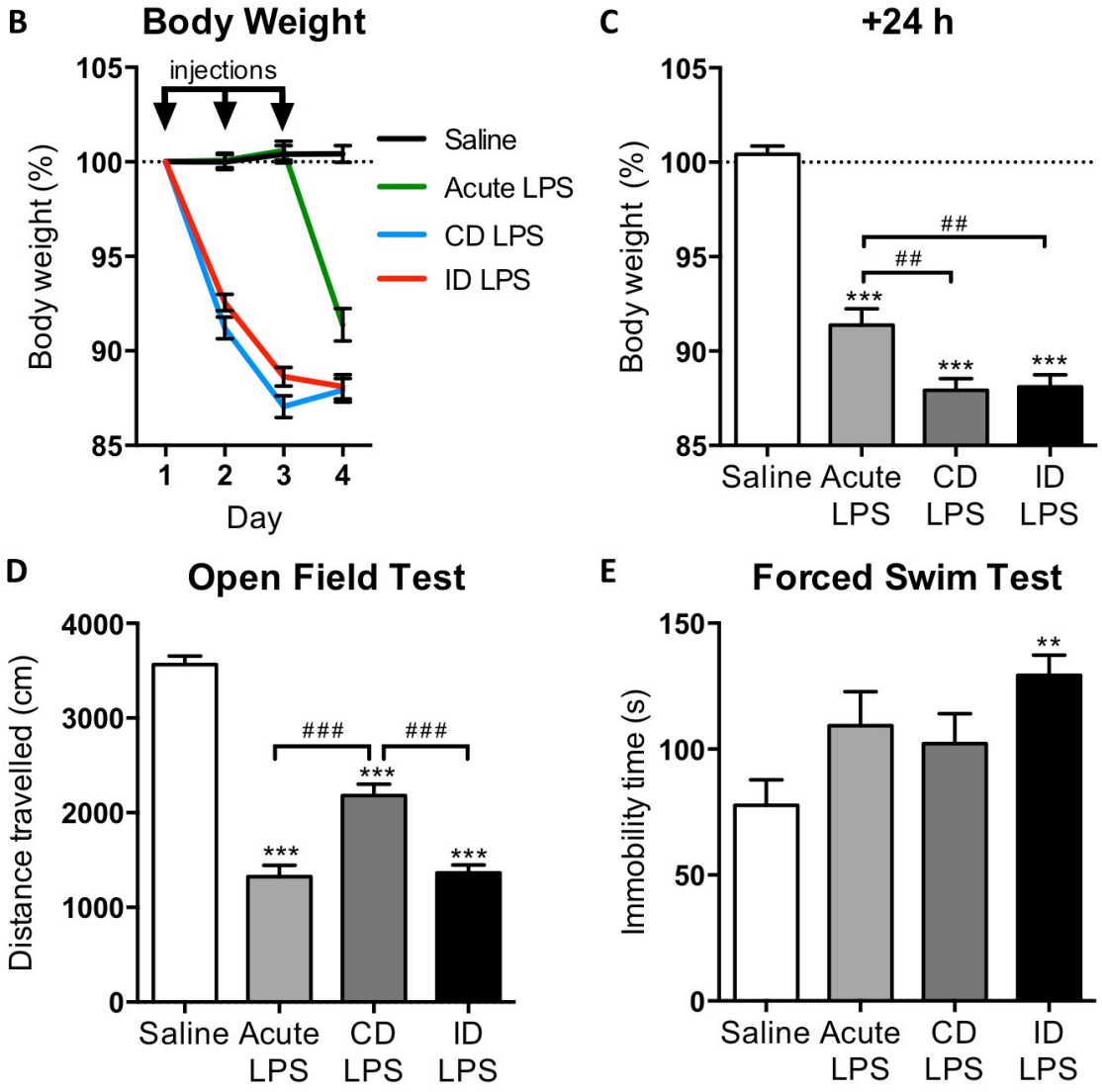

Figure 3.9. Effects of repeated 3-day LPS administration on body weight and behaviour in adult male C57BL/6J mice.

Mice were treated with saline or LPS for 3 consecutive days. The four groups were constant dose (CD) LPS; increasing dose (ID) LPS; acute LPS; saline controls (**A**). Body weight throughout the 3-day injection schedule was tracked (**B**), and body weight at +24 h after the final injection is shown (**C**). Distance travelled in the OFT at +6 h after final injection (**D**). Time spent immobile in the FST at +24 h after final injection (**E**). Values shown are mean ± SEM of n=13-15 per group. Data was analysed by one-way ANOVA with Bonferroni's posthoc test. $^{**}p < 0.01$, $^{***}p < 0.001$ compared to saline injected controls; $^{\#\#}p < 0.01$, $^{\#\#\#}p < 0.001$.

In a separate group of mice, the effect of 3-day CD LPS (0.83 mg/kg) administration was tested in the SPT. Saline treated mice were compared to 3-day CD LPS-treated mice to assess the development of LPS tolerance in the SPT. During the 4 days training prior to LPS administration, mice had access to either two water bottles (days 1 & 3), or water and sucrose (days 2 & 4). There was a significant effect of day on preference (one way repeated measures ANOVA, $F_{(2.1,46.7)}$ = 106.4; p < 0.001; Figure 3.10B). Mice exhibited a significant preference for 2.5 % sucrose solution over water (~90%; p < 0.001) compared to the preference of right over left when only water was available (50%). This indicates that there was no positional preference of bottles. In addition, there was a significant effect of day on total volume consumed (one way repeated measures ANOVA, $F_{(2.1,45.8)}$ = 117.2; p < 0.001; Figure 3.10C). A significant increase in total volume consumed was observed on training days 2 and 4, which included sucrose solution (p < 0.001 for both.

A two-way repeated measures ANOVA revealed a significant effect of treatment on sucrose preference ($F_{(1,13)}$ = 31.6; p < 0.001) and a significant interaction between treatment and time ($F_{(2,26)}$ = 4.195; p = 0.0264; Figure 3.10D). After LPS administration on Day 1 and Day 2, sucrose preference was significantly reduced (p < 0.001 for both). On Day 3, after the third LPS injection, mice did not show a significant reduction in sucrose preference. A two-way repeated measures ANOVA revealed a significant effect of treatment ($F_{(1,13)}$ = 37.77; p < 0.001) and time ($F_{(2,26)}$ = 59.28; p < 0.001) on total volume consumed, and a significant interaction between treatment and time ($F_{(2,26)}$ = 12.03; p < 0.001; Figure 3.10E). Total volume consumed was also significantly reduced after the first and second injections on Day 1 and 2 (p < 0.001 & p < 0.01, respectively). On Day 3, after the third LPS injection, mice did not show a significant reduction in consumption. These findings support the suggestion that repeated CD LPS resulted in the development of tolerance.

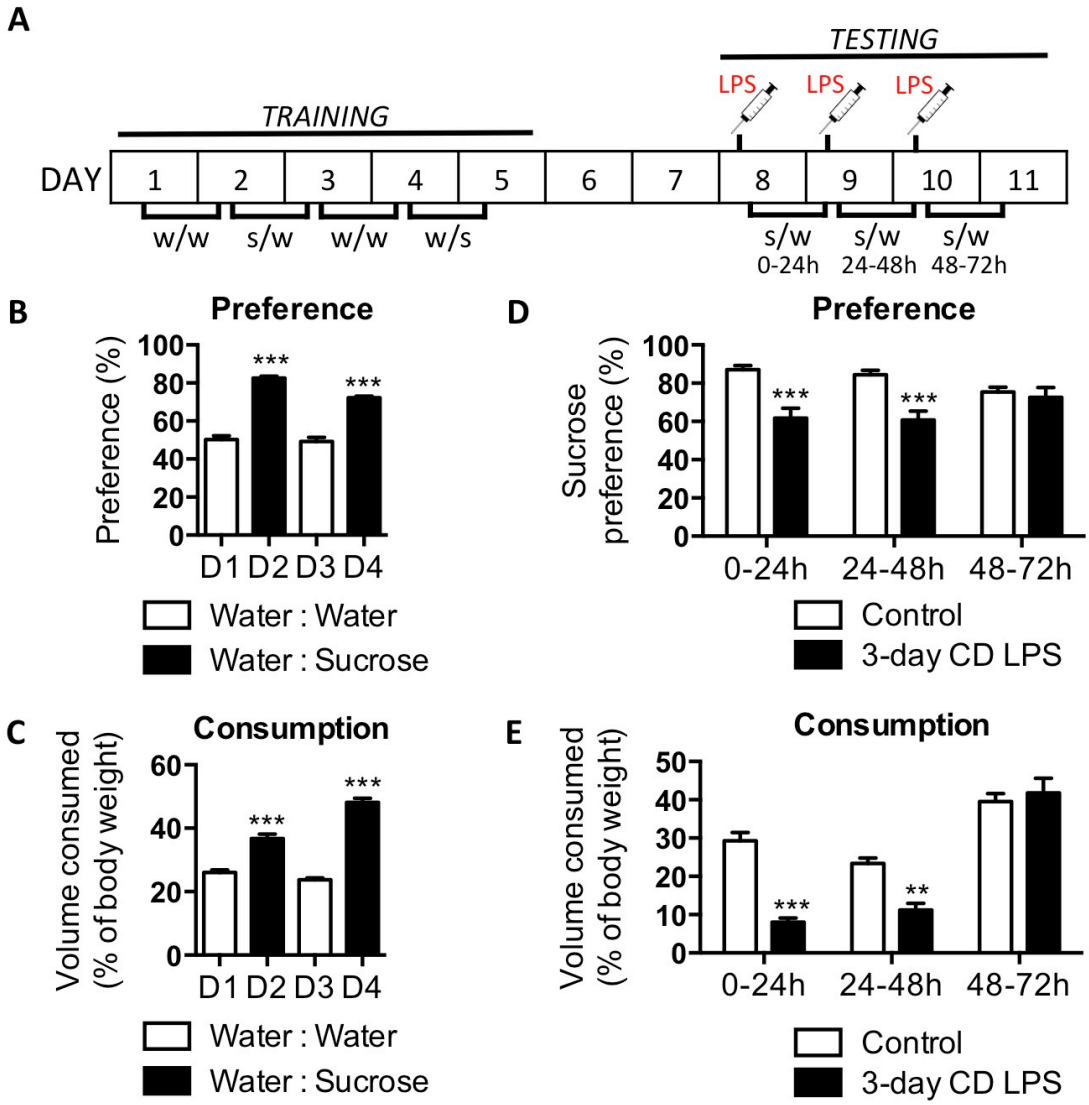

Figure 3.10. Effects of repeated 3-day constant dose LPS administration on the sucrose preference test in adult male C57BL/6J mice.

Mice were given the choice of two bottles containing either water (w) or sucrose solution (s) during the SPT (**A**). SPT training took place before mice were treated with saline or 0.83 mg/kg constant dose (CD) LPS for 3 consecutive days. During the 4-day SPT training, mice were given either two water bottles (Days 1 & 3), or one water bottle and one 2.5 % sucrose solution (Days 2 & 4). Preference of sucrose solution over water or left water bottle over right water bottle was calculated (**B**), as well as total consumption (**C**). Sucrose preference (**D**) and total consumption (**E**) was measured for 24 h windows beginning immediately after injection. Values shown are mean ± SEM of n=7-8 per group. Data was analysed by one-way repeated measures ANOVA with Dunnett's posthoc test (**B** & **C**), or two-way repeated measures ANOVA with Bonferroni's posthoc test (**D** & **E**). $^{**}p < 0.01$, $^{***}p < 0.001$ compared to saline injected controls, or to Day 1 in SPT training.

3.2.5.2 Effects of repeated daily LPS administration for 5 days

In the 5-day experiment, again there was a significant interaction between treatment and time on body weight (two way repeated measures ANOVA, $F_{(15,330)}$ = 137.8, $p < 0.001$; Figure 3.11B). Body weight at the start of the experiment was similar in all groups: 25.1 ± 0.3 g (n = 20) for saline, 24.7 ± 0.3 g (n = 19) for acute LPS, 24.7 ± 0.3 g (n = 20) for CD LPS and 25.1 +/- 0.4 g (n = 11) for ID LPS. At +24 h after the final injection, there was a significant effect of treatment of body weight (one way ANOVA, $F_{(3,66)}$ = 71.01, $p < 0.001$; Figure 3.11C). Body weight at +24 h was increased by 1.8% in the saline group and reduced by -7.1% for acute LPS, by -6.0% for CD LPS and by -4.5% for ID LPS, with the reductions in body weight for all LPS treatments being statistically significant compared to saline-treated controls ($p < 0.001$ for all; Figure 3.10C). The reduction in body weight observed in CD and ID LPS was significantly attenuated when compared to acute LPS ($p < 0.001$ & $p < 0.01$, respectively), indicating the development of LPS tolerance.

A significant effect of treatment on distance travelled in the OFT was observed at +6 h after administration (one way ANOVA; $F_{(3,66)}$ = 31.47, $p < 0.001$; Figure 3.11D). A significant reduction in the distance travelled in the OFT was evident for all LPS-treated groups in the 5-day experiment (all $p < 0.001$). The reduction in body weight and the reduction in locomotion indicate the presence of sickness behaviour during the 5-day LPS administration. However, the reduction in locomotion observed following acute LPS (47 ± 3 % of control; 19) was significantly greater than the reductions seen in both CD LPS (76 ± 3 % of control; n = 20; $p < 0.001$) and ID LPS (72 ± 8 % of control; n = 11; $p < 0.01$). This finding suggests the development of tolerance to both constant and increasing doses of LPS in sickness behaviour. There was no significant effect of LPS on FST immobility at +24 h after the final injection in the 5-day experiment (Figure 3.11E; $F_{(3,62)}$ = 1.716, $p = 0.1728$).

A

TREATMENT	DAY 1	DAY 2	DAY 3	DAY 4	DAY 5
Saline	SAL	SAL	SAL	SAL	SAL
Acute LPS	SAL	SAL	SAL	SAL	0.83
CD LPS	0.83	0.83	0.83	0.83	0.83
ID LPS	0.05	0.1	0.21	0.42	0.83

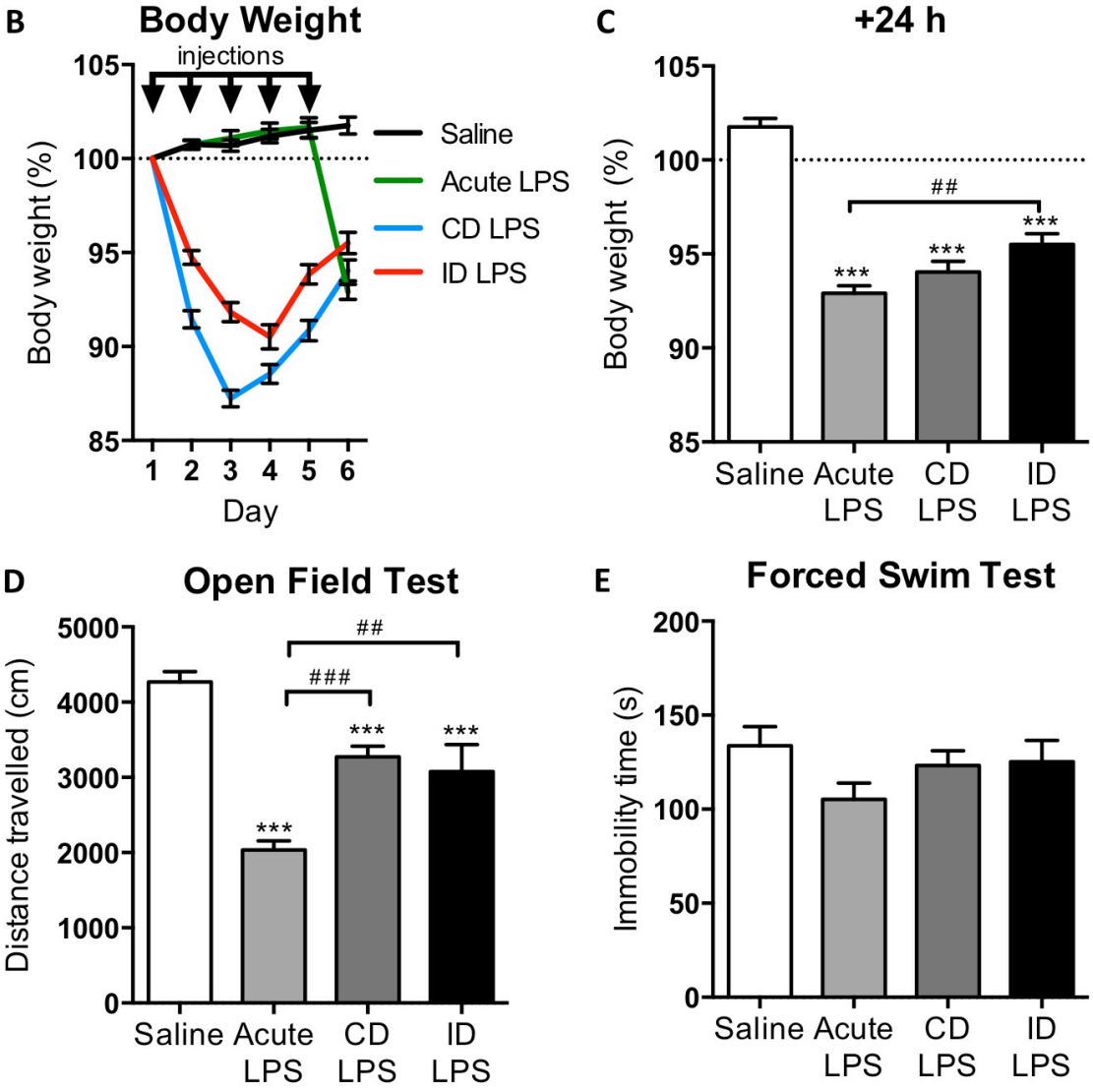

Figure 3.11. Effects of repeated 5-day LPS administration on body weight and behaviour in adult male C57BL/6J mice.

Mice were treated with saline or LPS for 5 consecutive days. The four groups were constant dose (CD) LPS; increasing dose (ID) LPS; acute LPS; saline controls (**A**). Body weight throughout the 5-day injection schedule was tracked (**B**), and body weight at +24 h after the final injection is shown (**C**). Distance travelled in the OFT at +6 h after final injection (**D**). Time spent immobile in the FST at +24 h after final injection (**E**). Values shown are mean ± SEM of n=11-20 per group. Data was analysed by one-way ANOVA with Bonferroni's posthoc test. ***p < 0.001 compared to saline injected controls; $^{\#\#}p$ < 0.01, $^{\#\#\#}p$ < 0.001.

3.3 Summary of findings

- Acute LPS (0.42 – 0.83 mg/kg; *i.p.*) induced a robust sickness behaviour that was not influenced by light phase or group / individual housing, but failed to produce a depressive-like behaviour.
- Depressive-like behaviours were observed in the SPT and, for the first time, in the FUST following acute LPS (0.42 – 0.83 mg/kg; *i.p.*).
- Reduced locomotion was observed at +24 h after acute LPS administration (0.42 – 0.83 mg/kg; *i.p.*), indicating the presence of sickness and a potentially confounding factor.
- Ketamine (10 mg/kg; *s.c.*) failed to inhibit the depressive-like effects of acute LPS (0.83 mg/kg; *i.p.*) in the FUST.
- ICV LPS (100 ng) also induced sickness behaviour and failed to produce a depressive-like behaviour in the FST.
- A 3-day increasing dose LPS protocol (0.21 – 0.83 mg/kg; *i.p.*) induced a depressive-like behaviour in the FST, whilst avoiding the development of LPS tolerance seen in OFT locomotion.
- Extending this protocol to 5-day increasing dose LPS (0.05 – 0.83 mg/kg; *i.p.*) enabled the development of LPS tolerance and failed to induce a depressive-like behaviour in the FST.

3.4 Discussion

Acute LPS is regularly used to study inflammation-induced depressive-like behaviours in mice (O'Connor et al., 2009a). In this chapter, various acute LPS-induced behavioural changes were assessed in adult male C57BL/6J mice, as well as the influence of lighting and social isolation on such behaviours. Systemic acute LPS (0.42 & 0.83 mg/kg; *i.p.*) failed to induce a depressive-like behaviour in the FST, regardless of environmental adjustments. Systemic acute LPS did induce anhedonic depressive-like behaviours in the FUST and SPT. However, reduced locomotion was observed in the OFT at +24 h after systemic LPS administration, indicating the presence of sickness. Central acute LPS also induced sickness and failed to induce a depressive-like behaviour in the FST. In an attempt to model sustained inflammation and induce depressive-like behaviour, a novel protocol for repeated LPS administration was developed and assessed. A 3-day increasing dose LPS protocol induced the development of depressive-like behaviour in the FST, whilst circumventing the development of tolerance in the OFT.

3.4.1 Pharmacological validation of behavioural tests

The FST was pharmacologically validated with ketamine (10 mg/kg) and bupropion (20 mg/kg), both of which have been previously shown to exhibit antidepressant-like activity in the FST (Browne and Lucki, 2013; David et al., 2003). Ketamine did not influence distance travelled in the OFT, whilst bupropion increased distance travelled. Consistent with this finding, it has been reported that 16 mg/kg bupropion increased locomotion in C57BL/6J mice, though doses as low as 2 mg/kg were shown to reduce FST immobility (David et al., 2003). An increase in locomotion is therefore a confounding factor for its antidepressant activity in the FST. Ketamine has been shown to attenuate depressive-like behaviours induced by acute LPS when co-administered (Walker et al., 2013). Consistent with some studies in C57BL/6J mice, both fluoxetine (20 mg/kg) and desipramine (10 – 20 mg/kg) failed to exert antidepressant-like activity in the FST (Lucki et al., 2001; David et al., 2003). The utility of the FST is based upon its predictive validity for classical antidepressants, though its predictive validity is strain-dependent and can be variable across studies (Lucki et al., 2001). The TST has previously demonstrated predictive validity with a range of antidepressant drugs in C57BL/6J mice, including desipramine and citalopram, and may therefore provide an alternative to the FST for assessing depressive-like behaviour in mice (Ripoll et al.,

2003). The SPT was not pharmacologically validated here, but has been previously with chronic treatment of SSRIs and TCAs (Willner et al., 1987; Muscat et al., 1992). Whilst the FUST has been previously pharmacologically validated with chronic citalopram (Malkesman et al., 2010), it was shown here that acute ketamine (10 mg/kg) induced a pro-depressive effect in the FUST when administered 30 min prior to testing. This novel finding was unexpected and suggests the test may be more sensitive to chronic treatment.

3.4.2 Acute LPS model of depressive-like behaviour

3.4.2.1 Acute LPS induced sickness

Acute LPS is known to induce a transient profile of sickness behaviours, including reduced exploratory behaviour and reduced food and water consumption (Dantzer, 2001). Consistent with the robust induction of sickness behaviour detailed in the literature (Table 3.1), all LPS treatments here induced a reduction in locomotion at +6 h and a reduction body weight +24 h after administration. However, sickness behaviour, as assessed by OFT hypolocomotion, was still present at +24 h and is therefore a confounding factor to depressive-like behaviours assessed at that time-point. Within the literature, acute LPS (0.2 to 0.83 mg/kg) is regularly used to assess depressive-like behaviours at +24 h, with many reporting no significant effect in locomotion (Frenois et al., 2007; O'Connor et al., 2009a; Viana et al., 2010; Walker et al., 2013; Custódio et al., 2013; Ohgi et al., 2013; Mello et al., 2013; Sulakhiya et al., 2014; Wang et al., 2014; André et al., 2014; Ji et al., 2014; Medeiros et al., 2015; Yao et al., 2015; Couch et al., 2015; Sriram et al., 2015; Zhang et al., 2015). Conversely, a number of studies have reported the presence of significant hypolocomotion in the OFT at +24 h after LPS, including lower doses of 0.5 and 0.63 mg/kg, consistent with the findings presented here (Biesmans et al., 2013; Corona et al., 2010; Godbout et al., 2008; Lawson et al., 2013a; Salazar et al., 2012). Evidently, there is a great amount of variation in the literature regarding the time course of LPS-induced hypolocomotion. One factor may be the technology used to assess locomotion. The data presented here were assessed using infrared tracking, similar to earlier studies that also reported reduced locomotion (Salazar et al., 2012; Biesmans et al., 2013). However, of the acute LPS studies detailed in Table 3.1, almost all studies that assessed OFT locomotion used manual scoring of line crossings, which may be insensitive to the small reductions in locomotion. Only one study used distance-tracking software and reported no significant effect of acute LPS (0.8 mg/kg) on locomotion at +24 h

(Medeiros et al., 2015). Three studies also utilised a system of infrared beams that also reported no significant effect of acute LPS (0.5 mg/kg) at +24 h (Ohgi et al., 2013; Yao et al., 2015; Dong et al., 2016). Other measures of sickness, such as food consumption and social interactions, have also been reported to be significantly decreased at +24 h and beyond (Godbout et al., 2008; Painsipp et al., 2011; Jangra et al., 2014; Shaikh et al., 2016; Yang et al., 2016). It was also shown here that performance on the rotarod was impaired at +6 h after LPS, but not at +24 h. This finding is consistent with other studies that have reported no significant effect of LPS on rotarod performance at +24 h (Krzyszton et al., 2008; Custódio et al., 2013). Therefore, hypolocomotion in the OFT does not translate to reduced performance on the rotarod, suggesting that there is no locomotor deficit at 24 h, but rather a reduction in exploratory behaviour, a hallmark of sickness. Overall, these data demonstrate the variability of the reported LPS-induced sickness time-course.

Throughout the literature, the environmental conditions used for acute LPS studies, such as the light cycle and group or individual housing, vary and are often not reported (Table 3.1). Of the 54 studies detailed, 17 studies used group housing, 12 used individual housing, whilst 25 did not report housing. 28 of the studies had a normal light cycle and tested in the light phase and 10 studies did the opposite. 16 studies did not report lighting conditions. Mice are nocturnal and exhibit increased locomotion throughout the dark phase (Kopp et al., 1998). Based on this, it might be expected that LPS-treated mice assessed during the dark phase will travel further than LPS-treated mice assessed during the light phase. Here, the light phase used for testing had no effect on LPS-induced sickness, indicating that whilst the natural locomotion of mice may be influenced by the light phase, the sickness induced by high-dose LPS is not sensitive to such environmental changes. Low dose LPS (0.01 mg/kg) has been shown to induce the expression of IL-1β, IL-6 and TNF-α in the hippocampus of rats at +3 h when administered during the light phase but not the dark phase of the light cycle (Fonken et al., 2016). Similarly, LPS-induced neuroinflammation following inescapable foot shock stress is also sensitive to the light cycle, with enhanced neuroinflammation when stress was administered during the light phase. Such findings indicate the light phase could increase LPS-induced neuroinflammation, though this theory did not translate into enhanced LPS-induced hypolocomotion during the light phase. The effects of the light cycle on LPS-induced hypolocomotion in a non-novel open field apparatus has been assessed in rats using a lower dose of 0.2 mg/kg LPS (Franklin et al., 2003). Rats were administered LPS at either the onset or 2 h into the light phase or the dark phase of the light cycle, and locomotion was assessed at +2 h. Similar to the findings detailed here, reductions in body weight were significant in all groups and LPS-induced reductions in locomotion were not significantly altered by the

light phase in which locomotion was tested. However, these experiments used rats and tested locomotion at a +2 h time-point, and therefore are not directly comparable to the findings presented here. Whilst baseline behaviour is influenced by the light cycle, the robust sickness induced by LPS appears to be not overtly affected. There was also no effect of group / individual housing on OFT locomotion. Some studies have shown that social isolation, used as a stressor, can enhance locomotion and depressive-like behaviour (Ieraci et al., 2016), whilst others have shown no effect of social isolation on locomotion in mice (Arndt et al., 2009).

3.4.2.2 Acute LPS-induced depressive-like behaviour

Acute administration of LPS failed to induce a depressive-like behaviour in the FST, regardless of light phase or group / individual housing. This finding is incongruent with the majority of, but not all, published acute LPS studies. As in this thesis, acute LPS does not consistently induce depressive-like behaviours (Painsipp et al., 2011; Corona et al., 2013; Biesmans et al., 2013; André et al., 2014; Couch et al., 2016). In previous experiments conducted at Janssen, using the same experimental equipment as in this thesis, LPS doses as high as 1.25 mg/kg failed to induce depressive-like behaviour in NMRI mice in both the FST and TST at +6 h and +24 h after administration (Biesmans et al., 2013). Systemic 0.83 mg/kg LPS has also failed to induce a significant increase in FST immobility in acute LPS studies with C57BL/6J mice (Lawson et al., 2013a; André et al., 2014). In addition, some studies have reported group / individual housing to influence the development of FST depressive-like behaviours following acute LPS treatment. LPS (0.83 mg/kg) increased FST immobility in group housed CD1 mice, but not in individually housed CD1 mice (Painsipp et al., 2011). LPS also failed to increase FST immobility in individually housed C57BL/6J mice, and actually reduced FST immobility in group housed C57BL/6J mice (Painsipp et al., 2011). Social isolation can be used as a stressor in mice, inducing an increased baseline TST immobility in C57BL/6J mice (Ieraci et al., 2016). As chronic stress can induce neuroinflammation (Alcocer-Gómez et al., 2015), social isolation may also be expected to influence LPS-induced behaviours. These findings contrast the data presented here that suggest housing conditions can influence the development of acute LPS-induced depressive-like behaviour. Direct comparisons between acute LPS studies within the literature can be difficult due to the number of variables within the protocol. Alongside lighting, housing and dose (all detailed in Table 3.1), other variables include FST cylinder diameter, handling protocols and environmental enrichment. Nevertheless, no FST depressive-like

behaviours were observed in any of the housing or lighting conditions tested in this thesis following acute LPS.

Whilst acute LPS failed to induce increased immobility in the FST, reduced pleasure-seeking behaviours were observed in the SPT, which assesses the preference for a palatable substance (Papp et al., 1991). C57BL/6J mice exhibited a preference for 2.5 % sucrose solution, consistent with previous findings (Lewis et al., 2005). Acute LPS reduced sucrose preference and consumption during the 0-24 h test period, consistent with previous acute LPS studies using the same test window (Zhang et al., 2016; Jaehne et al., 2015; Salazar et al., 2012). The reduced overall consumption in this first test window can be attributed to sickness, consistent with previous acute LPS studies (Painsipp et al., 2011; Jangra et al., 2014). However, during this test period, a preference for sucrose is still present following LPS administration at around 70 %, indicating an attenuated hedonic behaviour, as opposed to complete anhedonia. If robust sickness were present for the entire 24 h window, no sucrose preference would be expected. Therefore, it could be argued that during the first test period, mice exhibit an attenuated sucrose preference and a depressive-like behaviour that is not entirely due to sickness. A reduced sucrose preference was not observed during the 24-48 h test period. However, such large test periods make the separation of sickness and depressive-like behaviour difficult. If a depressive-like behaviour is present around the +24 h mark, it may not be observable as the anhedonia is confounded by sickness in the 0-24 h period, and the anhedonia strength may be weakened during the 24-48 h period. Shorter test windows of 12 h, 4 h or 1 h may be better to identify a depressive-like behaviour at more specific time points and have been used previously following acute LPS administration (Henry et al., 2008; Walker et al., 2013; Li et al., 2015). Furthermore, the concentration of sucrose used is important in the anhedonic response, as a high sucrose concentration (10 %) can overcome LPS-induced anhedonic behaviours in NMRI mice that are seen with lower sucrose concentrations (Biesmans et al., 2013).

Acute LPS also induced a depressive-like behaviour in the FUST. The FUST is a behavioural paradigm that enables the assessment of an alternative innate hedonic behaviour based on sexual motivation (Malkesman et al., 2010). Whilst the creators of the FUST used novel odours to demonstrate the preference for female urine was not novelty-based, it was not established whether the preference was sex-based or just social interaction-based. By directly comparing male and female urine in the FUST, it was shown here that the preference for female urine is sex-driven. The test has not previously been used in the acute LPS model of depression, but has been validated in the learned helplessness model of depression and pharmacologically validated with

chronic citalopram in C57BL/6J mice (Malkesman et al., 2010). In addition, the FUST has been used to evaluate the role of the neurokinin-1 receptor in depressive-like behaviour, whereby knockout C57BL/6 mice exhibit diminished sexual motivation (Berger et al., 2012). Following LPS, the preference for female urine sniffing is abolished at +6 h, and is only partially restored at +24 h. As the time spent sniffing water is unaffected, this indicates there is a depressive-like behaviour with no overt effect of sickness. The effect of acute LPS (0.5 mg/kg) has recently been assessed in a novel, but similar, behavioural test that assesses social interaction of a male mouse with a female or male intruder mouse as a direct comparison, called the female encounter test (Ago et al., 2015). Acute LPS reduced the social interaction preference for females over males at +24 h in CD1 mice, indicating a reduction in sexual motivation and supporting the findings presented in this thesis. In contrast to our findings and the findings in the female encounter test, acute low-dose LPS (0.05 – 0.25 mg/kg) in males rats did not impair sexual behaviours (sexual mounts) in at +2 h to +6 h (Avitsur et al., 1997). A higher dose may be required to reduce sexual behaviour. In addition, the FUST and female encounter test only measure interaction with a stimulus (urine or a mouse in a separated cage) and not direct sexual behaviours such as mounting. The data presented here demonstrates an LPS-induced reduction in sexual motivation and depressive-like behaviour in the FUST at +24 h, without overt sickness behaviour present. No later time points were assessed. As opposed to the SPT protocol used here, the FUST enabled assessment of anhedonic behaviour at a specific time-point and avoided the potentially confounding factor of a 24 h test period in the SPT.

3.4.3 Ketamine failed to abrogate the depressive effects of acute LPS

Ketamine can exert rapid antidepressant activity in humans (Berman et al., 2000) and has been shown to successfully treat patients with TRD (aan het Rot et al., 2010). Ketamine has also been shown to have antidepressant-like activity in rodents (Browne and Lucki, 2013), similar to findings presented earlier in the FST (Section 3.2.1). LPS was administered 24 h before testing, whilst ketamine was administered either 30 min before testing (as this time-point demonstrated antidepressant-like activity in the FST) or 24 h before testing, to test whether it could protect against LPS-induced effects. In both experiments, ketamine failed to abrogate the depressive-like effect of LPS. This contrasts a previous study that reported ketamine reversed the depressive-like behaviours induced by acute LPS (0.83 mg/kg) in the FST and SPT

(Walker et al., 2013). The mechanisms by which ketamine was hypothesised to abrogate the effects of acute LPS was the inhibition of excitotoxicity by inhibiting the glutamatergic NMDA receptor and enhancing AMPA signalling (Walker et al., 2013). Furthermore, when administered 30 min before testing, ketamine caused a significant reduction in female urine sniffing, demonstrating a pro-depressive effect. These findings show that whilst ketamine could influence FUST behaviour, it could not abrogate the LPS-induced reduction. The effects of ketamine on sexual behaviour has not previously been studied, though ketamine has been shown to induce impairments in an odour-based memory task (Rushforth et al., 2011). SSRI antidepressants would usually be more typical drugs to test, but many SSRIs, such as fluoxetine, have been shown to be ineffective in the FST in C57BL/6J mice (Section 3.2.1; Lucki et al., 2001). Earlier work has shown predictive validity in 129S1/SVlmJ mice in the FUST with chronic citalopram, suggesting the model may be more sensitive to chronic treatment (Malkesman et al., 2010). The FUST appears to have poor predictive validity in comparison to the FST, but a greater face validity as sexual dysfunction is associated with depression (Baldwin, 2001).

3.4.4 Centrally administered LPS

The advantage of centrally administered LPS compared to systemically administered LPS is that direct administration within the CNS enables one to study the influence of neuroinflammation on behaviour, circumventing the transmission of a systemic inflammatory insult from the periphery into the brain. Furthermore, LPS does not cross the BBB well (Banks and Robinson, 2010), and so by administering LPS centrally, TLR4 activation within the CNS can be investigated, as opposed to a broader inflammatory response. Central LPS-induced behavioural changes were caspase-1-dependent in mice. However, caspase-$1^{-/-}$ did not protect against systemic LPS (Lawson et al., 2013a). These findings demonstrate differences between central and peripheral LPS administration on behaviour and the potential compensatory mechanisms that may occur during systemic LPS administration.

Here, central administration of LPS, either via direct injection during surgery or via cannula injection, sickness was observed at +6 h but no depressive-like behaviour in the FST at +24 h. An earlier study has shown that surgical injection of a far greater dose of 5 μg LPS induced a significant increase in FST immobility 3 days after administration, without any confounding hypolocomotion (Dobos et al., 2012). Inhibiting IDO activity reversed the LPS-induced depressive-like behaviour. The same LPS dose

has been used prior to SPT assessment and revealed a significant effect of LPS on sucrose preference, though no significant effect between groups (van Buel et al., 2015). Both of these studies used higher doses of LPS and assessed depressive-like behaviours several days after administration, allowing mice to overcome the effects of surgery. Here, behavioural tests were carried out as early as +6 h after surgery. Whilst saline-treated mice exhibited normal behaviour, the behavioural effects of LPS may be influenced by the invasive surgical procedure for *i.c.v.* injection. The implantation of a cannula overcame this problem, but still failed to induce a depressive-like behaviour in the FST. In contrast to these findings, previous studies using cannulas to inject LPS into the lateral ventricle have used the same dose (100 ng), but reported significant depressive-like behaviours in the FST and SPT in the absence of overt sickness behaviour (Lawson et al., 2013a; Fu et al., 2010). The clear induction of sickness in body weight loss and hypolocomotion demonstrates centrally administered LPS exerted its inflammatory actions within the brain and influenced behaviour, but the FST failed to detect any changes in behaviour. These findings indicate further variability between studies of acute LPS-induced depressive-like behaviour. Automated software was used to detect FST immobility in central LPS administered mice, as earlier validated with bupropion and ketamine. Manual scoring may provide a more sensitive analysis that could detect subtle behavioural changes. However, manual scoring was utilised for the systemic acute LPS experiments earlier but still failed to detect a depressive-like behaviour in the FST.

3.4.5 Acute LPS as a model of depressive-like behaviour

The popularity of systemic LPS administration is due to its well-characterised ability to induce a broad inflammatory response *in vivo* that can transmit a signal across the BBB, incorporating the upregulation of various pro-inflammatory proteins within the brain and microglia activation (O'Connor et al., 2009a). Behavioural measures can be used to investigate the transient rise and fall of sickness as an indirect measure of inflammation. As demonstrated in this thesis, the reported behavioural time-course of LPS-induced sickness behaviour is inconsistent across the literature and can be confounding in the assessment of depressive-like behaviours (Table 3.1). The separation of sickness and depressive-like behaviour can be difficult due to the overlap of behaviours. However, behavioural time-courses must be established prior to further behavioural assessment to avoid the confounding influence of sickness. Similarly to LPS-induced sickness, LPS-induced depressive-like behaviours exhibit considerable variability between studies (Table 3.1), and between

behavioural paradigms, as demonstrated in this thesis. Furthermore, many studies fail to report the environmental conditions in which mice are housed and tested in, which can influence the subtle changes in behaviour being assessed in models of depressive-like behaviour (Bogdanova et al., 2013). The FST has poor face validity, and FST scoring is a variable factor due to its subjectivity. This subjectivity can be eliminated with the use of mouse tracking software, though such software may not be sensitive enough to discriminate accurately between different behaviours in the FST. Accordingly, the acute LPS experiments here also assessed using automated software, though no significant depressive-like behaviours were observed. More objective measures, such as the FUST and SPT may provide a more robust behavioural profile.

The findings presented here, along with the variability within the literature (Table 3.1), demonstrate that acute LPS is not a very robust or consistent model of depression. Furthermore, the inflammation exhibited by many depressed patients is a chronic condition that can predict the onset of depression or depressive symptoms years in advance (Zalli et al., 2016). For this reason, whilst acute inflammatory insults can provide insight into the mechanisms of peripheral inflammation, neuroinflammation and the influence on behaviour, it does not model sustained inflammation or accurately represent the human condition.

3.4.6 Repeated LPS model of depressive-like behaviour

In an attempt to model sustained inflammation and induce depressive-like behaviour, a novel protocol for repeated LPS administration was developed. It was found that a 3-day increasing dose LPS protocol induced the development of depressive-like behaviour, whilst circumventing the development of tolerance. 5-day LPS protocols failed in producing a depressive-like behaviour. This model enables the study of a period of sustained inflammation on depressive-like behaviours and therefore could have greater translatability than the acute LPS model. There is high variability between acute LPS studies (Table 3.1) and the few studies that utilise repeated LPS to model depressive-like behaviour exhibit even greater variation.

3.4.6.1 Sickness following repeated LPS

The primary restriction in using repeated LPS to induce an inflammatory response in mice is the development of tolerance towards LPS. Tolerance is a transient period of desensitisation whereby a pyrogen induces a diminished inflammatory response, whilst a normal response can be reinstated following a period of non-exposure (Beeson, 1947). Repeated exposure to LPS results in an attenuated sickness response as well as a reduced induction of pro-inflammatory cytokines (Zeisberger and Roth, 1998). In this thesis, repeated administration of constant dose (CD) LPS (0.83 mg/kg) for 3 or 5 consecutive days induced the development of 'behavioural tolerance', evident as attenuated locomotor reductions in response to repeated LPS. Congruent with this, LPS-induced anhedonic behaviour in the SPT was no longer present following the third injection in the CD paradigm. The development of tolerance and attenuated or absent hypolocomotion has been reported before following numerous repeated LPS protocols in rats (Franklin et al., 2003; Franklin et al., 2007) and in mice (Engeland et al., 2001; Kohman et al., 2010). In CF-1 mice, repeated administration of 0.05 – 0.2 mg/kg LPS (3 injections over one week) resulted in an attenuated locomotor reduction after the second administration and no reduction after the third (Engeland et al., 2001). In BALB/c mice, 4 daily consecutive injections of 3 μg LPS (~0.1 mg/kg) completely abolished the hypolocomotion in the OFT at +3 h induced by a single administration of LPS (Kohman et al., 2010). These data confirm the ability of repeated LPS to rapidly and consistently induce the development of tolerance. In the data presented here, whilst the reduced locomotion was attenuated after 3- and 5-day LPS administration, a significant reduction was still present. This could be due to the high dose of LPS used in this CD paradigm in comparison to other repeated LPS studies.

Though neuroinflammation was not assessed here, repeated administration of LPS can also alter the inflammatory profile within the brain. Repeated injections (3 over 24 h) of high dose LPS (3 mg/kg) has been shown to enhance IL-6 and TNF-α expression and reduce IL-1β expression in comparison to a single dose in mice (Erickson and Banks, 2011). Two consecutive injections of 0.83 mg/kg LPS in mice causes a significantly greater increase in brain kynurenine and quinolinic acid when compared to a single dose of LPS, as well as an increased kynurenine/tryptophan ratio (Larsson et al., 2016). Similar findings were observed in rats following LPS administration (0.5 mg/kg) every other day for 2 weeks, increasing kynurenine and reducing the kynurenine/tryptophan ratio (Guo et al., 2016). These findings indicate that repeated LPS administration may enhance kynurenine pathway induction, inducing excitotoxicity and depleting tryptophan levels.

By using a novel paradigm of progressive increasing dose (ID) of LPS in the 3-day experiment, the tolerance to repeated administration of LPS was overcome somewhat. Mice undergoing ID LPS exhibited a similar level of reduced locomotion compared to acute LPS treated mice. In addition, the weight loss is greater than acute LPS treated mice. These findings indicate repeated injections in the 3-day ID LPS mice caused further weight loss and sickness behaviour in the OFT similar to acute LPS, as LPS tolerance had not developed. However, in the 5-day experiment, the reduced locomotion following ID LPS was attenuated compared to acute LPS, similar to CD LPS. In addition, the body weight of mice following 5-day ID LPS was greater than acute LPS treated mice, indicating mice had begun eating normally and gaining weight, even during LPS treatments. This indicates the development of behavioural tolerance. These findings suggest that whilst increasing the LPS dose over three days delays the development of LPS tolerance, over 5 days the development of tolerance cannot be avoided by increasing the dose protocol.

3.4.6.2 Depressive-like behaviour following repeated LPS

3-day ID LPS was the only treatment group to exhibit a depressive-like behaviour in the FST. Depressive-like behaviour in the FST, TST and/or the SPT has been reported in mice following varying repeated LPS protocols. In Swiss mice, 8 injections (every other day) of 0.1 mg/kg LPS resulted in a depressive-like behaviour in the TST, with no effect of OFT line crossing (Xie et al., 2012). In rats, 7 injections (every other day) of 0.5 mg/kg LPS resulted in depressive-like behaviours in the FST and SPT (Guo et al., 2016). In ICR mice, 10 consecutive injections of 0.83 mg/kg LPS induced a depressive-like behaviour in the FST (Guo et al., 2014). In these studies, the development of LPS tolerance is neither discussed nor assessed. LPS tolerance is consistently reported following repeated LPS, and therefore it would be assumed that LPS tolerance was developed in these models (Franklin et al., 2003; Engeland et al., 2001). If so, the level of LPS-induced inflammation would not be constant, but diminish over time. However, depressive-like behaviours are still reported, though the time-point at which behaviours were assessed after LPS injection was not clear. A study that used a protocol of 4 daily consecutive LPS injections (1 mg/kg) in rats showed an induction of depressive-like behaviour in a 15 minute FST, though body weight began to rise after the initial weight loss following the first LPS administration, indicating the development of tolerance (Bay-Richter et al., 2011). However, locomotion assessed +2 h after the first, second and third injections did not appear to show a diminished effect. A recent chronic intermittent LPS study that administered 0.25 mg/kg LPS to C57Bl/6

mice twice a week for up to 12 weeks (Krishna et al., 2016). After 6 and 12 weeks, increased FST immobility was reported. Decreased locomotion was observed at 6 weeks and increased locomotion was observed at 12 weeks. The treatment also caused persistent microglia activation. This chronic intermittent model demonstrates a sustained effect of repeated LPS and the induction of depressive-like behaviour, with greater face validity than acute LPS studies (Krishna et al., 2016).

Together, these studies show that repeated administration of the same dose of LPS can induce depressive-like behaviours, in contrast to the findings presented here with 3-day and 5-day CD LPS. However, the variation in dosing and timing make direct comparisons difficult. The only study to use changing doses of LPS is a 4-month study that showed a 5-day rising and falling of LPS doses, once a month, induced SPT anhedonia in female mice in the final weeks (Kubera et al., 2013). This study incorporates extended periods of rest between each 5-day LPS treatment, which may avoid the development of LPS tolerance, as well as using a rising and falling LPS dose. However, sustained anhedonic behaviour was observed only in the final month, and only in female mice, even after the protocol was adapted in male mice to 5 injections over 10 days instead of 5 days. Whilst this model has more face validity, in that it assesses chronic inflammation, the article does not report if the behaviour was sustained beyond the final 2 weeks of the 4-month protocol, and fails to report any FST or TST data, though one would expect such experiments to have been carried out in such a longitudinal study.

Injections can act as a stressor (Ryabinin et al., 1999), and repeated injections may influence depressive-like behaviour in the FST. When comparing the 3-day and 5-day LPS experiments, the FST immobility is similar, though the immobility of saline controls is ~80 seconds and ~135 seconds in the 3-day and 5-day experiments, respectively. In addition, the saline-treated controls in the acute LPS experiments show FST immobility at ~80 seconds. Physical restraint for injection has been shown to act as a stressor in rodents, increasing corticosterone and CRF levels (Harbuz et al., 1994) (Balcombe et al., 2004). Repeated restraint stress can be used to model depressive-like behaviours in mice, though these stressors are typically around 2 h restraints in a restraint device (Alcocer-Gómez et al., 2015). The repeated stress of injection in the 5-day experiment may increase FST immobility and therefore mask the depressive effects of LPS treatment.

Here, a novel 3-day protocol of increasing LPS dose partially addresses some of the drawbacks of the acute LPS model of depressive-like behaviour. Whilst 3 days of

inflammation is not chronic, it is sustained and enables the biochemical and behavioural assessment of sustained inflammation. Furthermore, the increasing dose circumvents the development of behavioural tolerance observed in earlier studies in response to LPS (Engeland et al., 2001; Franklin et al., 2003). This protocol may provide an alternative method for studying the sustained inflammation present in depression. In order to develop the model, further time points would need to be assessed to show the time course of behavioural changes, and the ability of chronic antidepressant treatment should be tested to provide predictive validity. In addition, other behaviours could be assessed, such at the TST, SPT, FUST, as well as pro-inflammatory markers within the brain.

An ideal model would be one that involves chronic low-grade inflammation. Such models could be developed based upon a study that used very low LPS doses (1 μg/kg) over 10 consecutive days (Tarr et al., 2012). A progressively increasing sickness behaviour in the OFT was observed, though no depressive-like behaviour was assessed. The same dose administered 4 times over a month can also progressively induce anxiety-like behaviour in the light-dark box, indicating sensitisation to LPS (Banasikowski et al., 2015). Whilst these studies are not assessing depressive-like behaviour, the development of a similar chronic model may provide greater insight into inflammation-associated depression. Another approach is the use of poly(I:C), a synthetic double-stranded RNA agonist for TLR3. Poly(I:C) has been show to induce an acute immune response that is not diminished upon secondary stimulation (Cunningham et al., 2007). Furthermore, acute poly(I:C) has been shown to induce sickness and depressive-like behaviours in a similar fashion to acute LPS (Gibney et al., 2013). Therefore, poly(I:C) could be a viable tool for inducing sustained inflammation to study inflammation-induced depressive-like behaviour in mice. Though the separation of sickness and depressive-like behaviour is still necessary in the use of poly(I:C), similar to acute LPS.

Chapter 4: NLRP3 inflammasome function in microglia and the effect of hypoxia

4.1 Introduction

4.1.1 Microglia

Within the CNS, the innate immune system is mediated by microglia, which respond to a wide range of stimuli. BV2 cells are an immortalised murine microglia cell line that have been previously utilised to assess NLRP3 inflammasome activity and IL-1β production (Shi et al., 2012). Whilst BV2 microglia are a useful tool for studying microglia, primary murine microglia provide greater validity (Henn et al., 2009). There are a number of methods for the isolation of primary microglia. The most common method of isolation from mixed glia cultures incorporates an extended period of shaking to detach and harvest microglia. However, the physical stress exerted on mixed glia cultures induces amoeboid microglia morphology and has been shown to induce the release ATP in astrocytes (Praetorius and Leipziger, 2009; Coco et al., 2003; Kettenmann et al., 2011). The retraction of microglia processes can occur via adenosine 2A receptor stimulation following extracellular ATP degradation, promoting the amoeboid morphology (Orr et al., 2009). Alternatively, primary microglia can be isolated with the use of mild trypsin, which causes the astrocytic layer to detach, leaving microglia attached in the well (Saura et al., 2003). This process avoids the mechanical stress and any potential release of ATP and microglia activation (Praetorius and Leipziger, 2009).

4.1.2 NLRP3 inflammasome in microglia and disease

NLRP3 signalling in microglia has been widely studied due to the growing understanding of neuroinflammation and its role in numerous neurological diseases. Microglia express the components for NLRP3 inflammasome signalling and respond to many stimuli, similar to macrophages (Shi et al., 2012). Some reports demonstrate astrocytes do not to express a functional NLRP3 inflammasome, indicating microglia are responsible for IL-1β production within the CNS (Gustin et al., 2015). However, this is controversial as Aβ has been shown by others to induce IL-1β release in astrocytes (Couturier et al., 2016). In addition, some studies have indicated NLRP3 inflammasome activity in neurons (de Rivero Vaccari et al., 2008; Compan et al., 2012). Inflammasome activity and microglia activation is a feature seen in various neurological diseases and infections (Walsh et al., 2014a). Bacterial infections, such as *S. aureus*, induce NLRP3 inflammasome activation and IL-1β release in microglia with partial dependency on local ATP stimulation of P2X7 receptors (Hanamsagar et al.,

2011). NLRP3 expression and activity is induced following a cerebral ischemia reperfusion model of stroke, and NLRP3$^{-/-}$ protects against neurovascular damage (Yang et al., 2014). Furthermore, the NLRP3-induced neuronal damage was mediated by microglia activation. Neurodegenerative prion proteins activate microglia and induce inflammasome signalling, whilst the blockade of K^+ efflux and ROS signalling can attenuate NLRP3 inflammasome activation (Shi et al., 2012). It has also been shown that NLRP3 activation is important in Alzheimer's disease. Aβ can lead to microglia recruitment and NLRP3 inflammasome signalling (Khoury et al., 2007; Halle et al., 2008). In addition, mouse models of Alzheimer's disease show increased microglia activation and NLRP3$^{-/-}$ microglia exhibited a more anti-inflammatory phenotype, with increased IL-4 and reduced NOS2 expression (Heneka et al., 2014). Subsequently, NLRP3-knockout led to an increase in Aβ clearance and improved performance in cognitive tasks, demonstrating the potential negative effects of excessive NLRP3 inflammasome signalling in microglia.

Depression, which is associated with inflammation, has also been hypothesised to involve inflammasome signalling (Iwata et al., 2013). Microglia activation is a feature of the acute LPS model of depression in mice, as demonstrated by the increased expression of microglia marker ionised calcium-binding adapter molecule 1 (Iba-1) in brain regions such as the hippocampus and prefrontal cortex (Biesmans et al., 2013; Wang et al., 2014; van Buel et al., 2015). Microglia activation plays a critical role in responding to systemic inflammation following acute LPS and propagating that inflammatory response within the brain and influencing behaviour. Minocycline, a brain permeable anti-inflammatory drug, has been shown to inhibit LPS-induced microglia activation by reducing NF-κB signalling, the expression of pro-inflammatory cytokines and inhibiting morphological changes associated with activation (Kobayashi et al., 2013; Fan et al., 2007). Pre-treatment with minocycline has also been shown to attenuate LPS-induced sickness and depressive-like behaviours (Henry et al., 2008; O'Connor et al., 2009a; Fan et al., 2007). Reducing LPS-TLR4 signalling can also inhibit LPS-induced microglia activation and sickness behaviours. By blocking the LPS receptor TLR4 or the downstream messenger MyD88, the expression of TNF-α and p38 MAPK can be completely inhibited, as well as maintaining a resting microglia morphology and preventing the reduced locomotion sickness behaviour (Hines et al., 2013). These findings affirm the role microglia play in peripherally induced neuroinflammation and the resulting changes in behaviour.

4.1.3 The hypoxic brain

The level of oxygen (O_2) availability within the body is highly variable, depending on the metabolic activity of the tissue. Atmospheric partial pressure of O_2 (PO_2) at sea level is 160 mmHg, constituting 21 % of the atmosphere. Once inspired, the increase in CO_2 and water vapour within the lungs reduces the PO_2, and the availability of O_2 within body tissue is considerably lower that the atmospheric level, as the level of available O_2 falls further once it passes into the bloodstream and into tissue (Figure 4.1) (Masamoto and Tanishita, 2009). Furthermore, the brain is highly metabolic, accounting for 20 % of metabolism within the body, and subsequently the availability of O_2 from cerebral vessels is lower than other tissues. Early invasive recordings using O_2-sensitive probes reported the partial pressure of O_2 to be lower than atmospheric PO_2 (Ivanovic, 2009). Such recordings have been done in humans during surgery, with brain tissue PO_2 reportedly averaging 27.6 mmHg, equivalent to 3.6 % (Hemphill et al., 2005). O_2 sensitive probes have also been used to measure O_2 availability in rodents. Cerebral arterial PO_2 is measured to be 90-110 mmHg and venous PO_2 is measured to be 30-40 mmHg (Nwaigwe et al., 2000; Erecińska and Silver, 2001). Brain tissue is reported to be even lower. For example, hypothalamic measurements were 11-16 mmHg, hippocampal measurements were 20.3 mmHg and thalamic measurements were 26 mmHg, with overall ranges comparable to 0.5 – 7 % O_2 (Cater et al., 1961; Nwaigwe et al., 2000; Ivanovic, 2009). Although measurements were variable and averages were potentially overestimated due to the presence of blood vessels, the overall conclusion of these findings is that the brain exists in a relatively low O_2 environment (Ndubuizu and LaManna, 2007). However, recent advances in technology allow the measurement of PO_2 *in vivo*, accurately and non-invasively. The method by which this is done is two-photon imaging using phosphorescent probes that quench in an O_2-dependent manner, enabling capillary and tissue PO_2 to be measured (Sakadzić et al., 2010; Lecoq et al., 2009). This technique has recently been further developed to be used in awake mice, and reports a capillary PO_2 of 36 mmHg and an interstitial PO_2 in olfactory bulb and somatosensory cortex of 23 mmHg, equivalent to 3 % O_2 (Lyons et al., 2016). Such findings confirm the relative hypoxic environment in which the brain exists. However, nearly all *in vitro* research that studies the function of CNS cells, such as neurons, microglia and astrocytes, is in cells cultured in atmospheric (~20 %) O_2 conditions. This environment should be considered hyperoxic relative to the *in vivo* microenvironment, and conversely, hypoxia could be considered as *in situ* normoxia (Ivanovic, 2009). Furthermore, PO_2 is lower in the liquid phase of cell media than atmospheric PO_2, with 37 mmHg PO_2 (5 %) conditions reportedly resulting in 20 mmHg PO_2 (~2.6 %) in

cultures of 50,000 astrocytes (Bambrick et al., 2011). This finding suggests a ~5 % O_2 incubation of microglia cultures may provide conditions more similar to the 23 mmHg PO_2 reported in the mouse cortex (Lyons et al., 2016). Changes to the availability of O_2 may have effects on the functioning of a cell. When investigating microglia immune function *in vitro*, whether in relation to depression, Alzheimer's disease, infection or any other neurological disease, the effect of a hyperoxic environment needs to be considered.

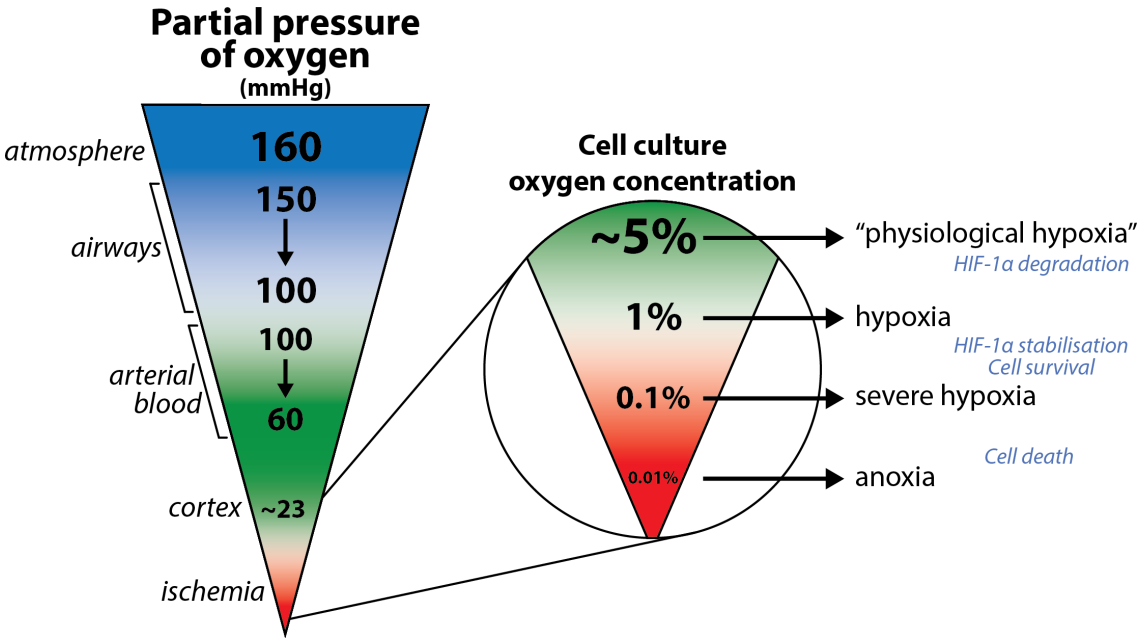

Figure 4.1. O_2 concentration in tissue *in vivo*.

The partial pressure of O_2 falls as it moves from the atmosphere and into tissue. Atmospheric PO_2 at sea level is 160 mmHg, or 21 %. The PO_2 falls within the lungs due to an increase in CO_2 and H_2O, and falls further to between 60 – 100 mmHg in arterial blood. PO_2 has been recorded as 23 mmHg in the cortex (Lyons et al., 2016). At O_2 concentrations below 5 %, HIF-1α protein is stabilised and an enhance cell survival and inflammation (Jiang et al., 1996; Mazure et al., 2010). Severe hypoxic conditions can induce cell death (Shimizu et al., 1996). *Wickens original artwork.*

4.1.4 Oxygen, metabolism and ROS generation

O_2 is required by all cells in the human body to undergo aerobic cellular respiration for the production ATP. Via the process of glycolysis, the Krebs cycles and the electron transport chain, glucose and O_2 produce water, CO_2 and generates ATP. ATP in turn provides the energy required for most cellular processes. Therefore, O_2 availability to cells in culture is critical. However, during the electron transport chain process within the mitochondria, O_2 can accept free electrons resulting in the formation of superoxide radicals ($O_2^-\bullet$). These radicals have the potential to cause significant

damage within the cell due to their oxidative ability, and so they are tightly regulated enzymes such as superoxide dismutase (SOD), which converts O_2^-• to hydrogen peroxide (H_2O_2). H_2O_2 can then be processed into H_2O and O_2 via catalase, or into another ROS, hydroxyl radicals (OH•), as a result of partial reduction (Turrens, 2003). The over-production of ROS is considered 'oxidative stress', and whilst ROS can have detrimental effects within a cell, they also act as important signalling molecules, in particular within the innate immune system. For example, increased ROS levels is involved in NLRP3 inflammasome activation, which can be abrogated by inhibiting ROS signalling (Cruz et al., 2007).

4.1.5 Hypoxia and inflammation

The association between O_2 availability and mitochondrial ROS generation is generally considered linear. Increasing O_2 causes an increase in mitochondrial O_2^-• and H_2O_2 (Boveris and Chance, 1973; Turrens et al., 1982; Murphy, 2009), whilst mitochondrial ROS production can fall during hypoxia, as O_2 is the substrate for ROS generation (Hoffman et al., 2007; Kussmaul and Hirst, 2006). However, there is considerable data that demonstrate that in severe hypoxia (≤1 % O_2) mitochondrial ROS signalling increases (Guzy et al., 2005; Desireddi et al., 2010; Hernansanz-Agustín and Izquierdo-Álvarez, 2014). Mitochondrial ROS generation is an important signalling messengers for a number of cellular responses in hypoxia, including the activation of transcription factors and signalling molecules (Sena and Chandel, 2012; Waypa et al., 2016). An initial burst of ROS production in acute hypoxia has been reported which subsequently diminishes (Hernansanz-Agustín and Izquierdo-Álvarez, 2014). Whilst the mechanisms by which hypoxia can induce ROS signalling is unclear, low O_2 (~1 %) has been shown to increase the expression of TLR4, proinflammatory cytokines and chemokines in immune cells and microglia (Ock et al., 2007; Blengio et al., 2013; Kim et al., 2010).

Acute hypoxia can affect most cells types by altering ion movement and metabolism, though long-term effects of hypoxia are thought to be mediated primarily through the activity of hypoxia-inducible factor 1 (HIF-1) (Mukandala et al., 2016). HIF-1 is a transcription factor that can induce the expression of proteins involved in cell migration, metabolism, growth and apoptosis, transport and angiogenesis (Schofield and Ratcliffe, 2004). HIF-1α is one of the most characterised proteins involved in cell signalling under low O_2 conditions and is a transcription factor formed of two subunits, HIF-1α and HIF-1β. HIF-1β is constitutively expression, whilst HIF-1α is sensitive to O_2

concentration and is rapidly degraded in high O_2 conditions (Huang et al., 1996). HIF-1α activity is controlled post-translationally via prolyl hydroxylases (PHD), which is dependent upon O_2 for HIF-1α hydroxylation under normoxic conditions, leading to its ubiquitination via a von Hippel-Lindau (pVHL)-E3 ligase complex and its subsequent degradation (Figure 4.2) (Masson et al., 2001; Jaakkola et al., 2001; Tanimoto, 2000). Under low oxygen levels, PHD activity is reduced and stabilised HIF-1α translocates to the nucleus and form a dimer with HIF-1β to induce transcription at genes contained a hypoxia-response element (HRE). ROS signalling in hypoxia is thought to contribute to the PHD inhibition and HIF-1α stabilisation (Guzy et al., 2005; Chandel et al., 2000). NF-κB and MAPK induction, as demonstrated by IL-1 and LPS stimulation, can also induce HIF-1α stabilization (Frede et al., 2006; Bonello et al., 2007). HIF-1α stabilisation has also been reported to be mediated by mitochondrial ROS, whereby HIF-1α induces REDD1 expression, which suppresses mitochondrial ROS generation and inhibits HIF-1α stabilisation in a negative feedback loop (Horak et al., 2010).

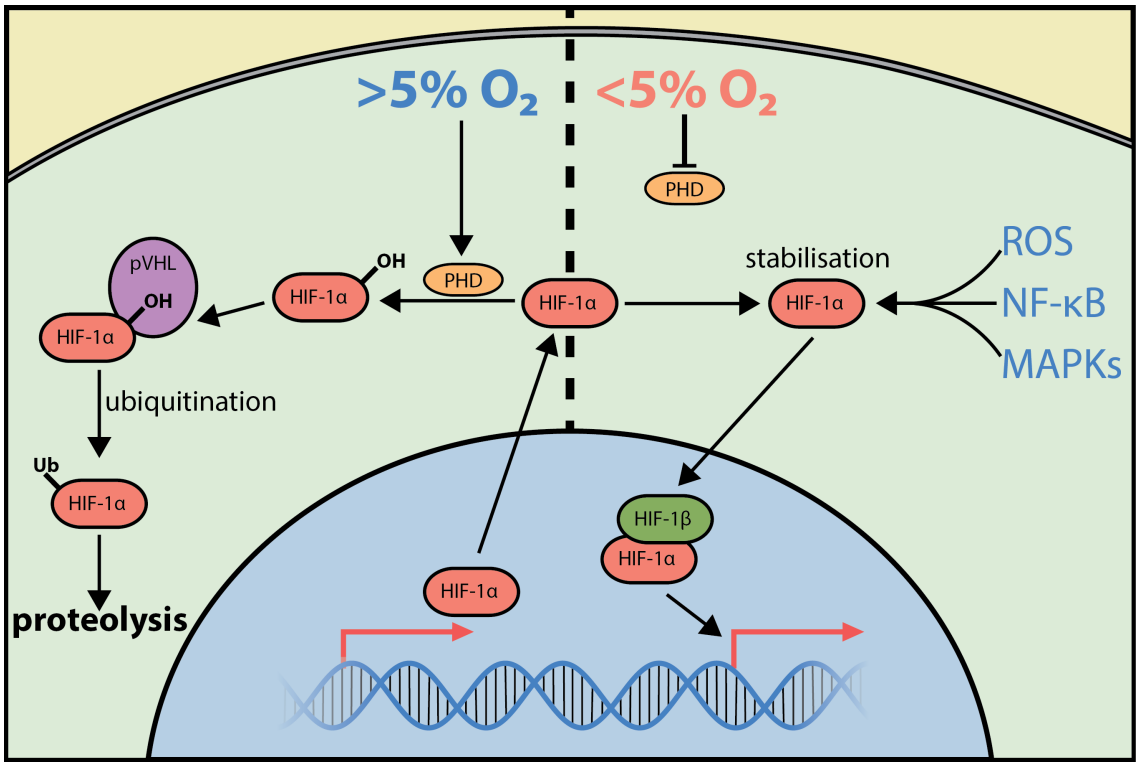

Figure 4.2. HIF-1α degradation and stabilisation.

HIF-1α is constitutively expressed. In high-oxygen conditions, hydroxylation of HIF-1α via prolyl hydroxylases (PHD) leads to ubiquitination via the von Hippel-Lindau (pVHL) ubiquitination complex and, ultimately, its degradation. In low oxygen conditions, PHD activity is reduced, leading to the stabilisation of HIF-1α and its translocation to the nucleus, where it forms a dimer with HIF-1β to induce transcription at hypoxia-response elements (HREs). ROS, NF-κB and MAPK activity can also lead to HIF-1α stabilisation. *Wickens original artwork.*

Hypoxia can have detrimental effects within the CNS, involving neuroinflammation, neurotransmission and excitotoxicity. Acute hypoxia induces inflammatory signalling processes in microglia. Severe hypoxia (≤0.2 % O_2) has been shown to induce microglia activation and inflammatory signalling, including p38 MAPK and NF-κB activation, nitric oxide (NO) production and TNF-α secretion (Guo and Bhat, 2006; Park et al., 2002; Lu et al., 2006). The activation of NF-κB in hypoxia was observed in microglia and not astrocytes, inducting the inflammatory response in hypoxia is primarily microglia-mediated (Guo and Bhat, 2006). The induction of iNOS (inducible nitric oxide synthase) and NO in microglia is reportedly dependent of PI3K signalling and the activation of HIF-1α (Lu et al., 2006). Minocycline, an anti-inflammatory drug that has been shown to inhibit microglia activation, can inhibit the hypoxia-induced p38 MAPK activation and the production of NO and inflammatory cytokines (Suk, 2004).

Overall, these data indicate that severe hypoxia can induce ROS signalling, HIF-1α expression and proinflammatory signalling. However, most studies that assess the effect of hypoxia on inflammation use very low concentrations of O_2, usually in an attempt to mimic ischemia. Hypoxia is not usually used to replicate the *in vivo* microenvironment within the brain. HIF-1α stabilisation is induced at around 5 % O_2 and increases as O_2 concentration decreases, showing maximal expression at 0.5 % O_2 (Jiang et al., 1996). Above 5 % O_2, HIF-1α is degraded, with astrocytes cultured at 5 % O_2 demonstrating no HIF-1α protein (Liu et al., 2006). A more physiologically relevant cell culture environment would be closer to this level, similar to the *in situ* microenvironment and therefore able to detect more subtle changes in O_2, and not just massive reductions from a hyperoxic state (21 %) to severe ischemia (1 % O_2). However, microglia function and inflammatory signalling has yet to be fully examined within this range of O_2 concentration.

4.1.6 Aims of Chapter 4

The aims of this thesis chapter were to first characterise NLRP3 inflammasome expression and activity in BV2 microglia and primary microglia isolated by mild trypsinisation, and to study the influence of mild hypoxia. Whilst NLRP3 inflammasome signalling has been demonstrated in microglia before, it has not been characterised in primary microglia isolated by mild trypsinisation. Subsequently, 5 % O_2 incubation was utilised to assess the effect of moderate hypoxia on NLRP3 inflammasome priming and activity, in an attempt to better replicate the natural conditions of microglia within the

brain. O_2 availability within the brain is considered to range between 0.5 and 7 %, depending on the region and its metabolic activity (Ivanovic, 2009). Nevertheless, cell culture is routinely performed using ~20 % O_2, which would be a hyperoxic environment. O_2 concentration can influence O_2-dependent cell signalling, including ROS generation and the stabilisation of HIF-1α (Mukandala et al., 2016). Generally, experiments that examine hypoxic conditions utilise O_2 concentrations below 1 % to model ischemia and reperfusion. Such conditions have been shown to induce ROS generation and cytokine production (Suk, 2004). The use of a 'moderate' hypoxic environment to replicate the *in vivo* microenvironment has not previously been studied, and inflammasome signalling in mild hypoxia has not previously been assessed in microglia. Incubation periods in low O_2 of 4 h, 24 h and 3 weeks were employed to study cytosolic protein expression, cytokine secretion and P2X7 receptor activity. Necrotic cell death was also studied to investigate ATP-induced pyroptosis. In addition, the influence of ketamine on NLRP3 inflammasome activity was assessed, as ketamine has been shown to attenuate LPS-induced neuroinflammation and depressive-like behaviour (Walker et al., 2013).

4.2 Results

4.2.1 NLRP3 inflammasome function in BV2 microglia and the effects of acute hypoxia on LPS-induced priming

4.2.1.1 Stimulation of BV2 microglia with lipopolysaccharide (LPS)

To study microglia function and NLRP3 inflammasome activity, microglia require priming in order to upregulate proteins required for inflammasome activation. Here, we stimulated our microglia with LPS, which is regularly used to stimulate innate immune responses from immune cells. The cells used here are a commonly used immortalized murine microglia cell line (BV2) with a previously established LPS response (Henn et al., 2009). In order to determine an effective concentration of LPS to use for cell stimulation, BV2 microglia were stimulated with 0.01 – 1 µg/ml LPS for 4 h. A range of LPS concentrations were tested to ensure the selected LPS concentration used for future experiments induced the expression of NLRP3 (Figure 4.3A) and proIL-1β (Figure 4.3B) with the potential for increased expression. Quantitative measurement of protein was possible via infrared fluorescent western blot analysis. LPS stimulation had a significant effect on NLRP3 (one way ANOVA, $F_{(3,8)} = 7.045$, $p = 0.0124$) and proIL-1β (one way ANOVA, $F_{(3,8)} = 8.515$, $p = 0.0072$) expression. All doses of LPS induced a significant increase in the protein expression of both NLRP3 (estimated molecular weight: 118 kDa) and proIL-1β (estimated molecular weight: 31 kDa) when compared to control levels ($p < 0.05$ for 0.01 & 0.1 µg/ml, $p < 0.01$ for 1 µg/ml). The middle dose of 0.1 µg/ml LPS was selected to be used for future experiments as it induced a significant increase in proIL-1β and NLRP3 expression but still had the capacity for further increased expression of proIL-1β, allowing the study of both increases and decreases in protein expression.

4.2.1.2 Spatial expression of NLRP3 and proIL-1β in BV2 microglia

Following activation by PAMPs, such as LPS, microglia alter their protein expression. CD11b is an membrane-bound antigen expressed by microglia which is upregulated following activation and is commonly used to confirm microglia phenotype (Roy et al., 2006). Increased CD11b is reported in neuroinflammation and is thought to be involved with changes in morphology and motility (Rock et al., 2004). Fluorescent imaging of BV2 microglia via immunocytochemistry confirmed the expression of CD11b. Following LPS stimulation (0.1 µg/ml; 4 h), CD11b expression is upregulated

(Figure 4.4A). BV2 microglia exhibited a basal level of NLRP3 expression, which was increased following 4 h stimulation with LPS (Figure 4.4B). ProIL-1β was not detectable in the absence of LPS, and expression was induced following LPS stimulation (Figure 4.4C). A Z-stacked image of a CD11b-stained BV2 microglia shows extended processes that are an indicator of resting ramified microglia (Figure 4.4E; (Stence et al., 2001).

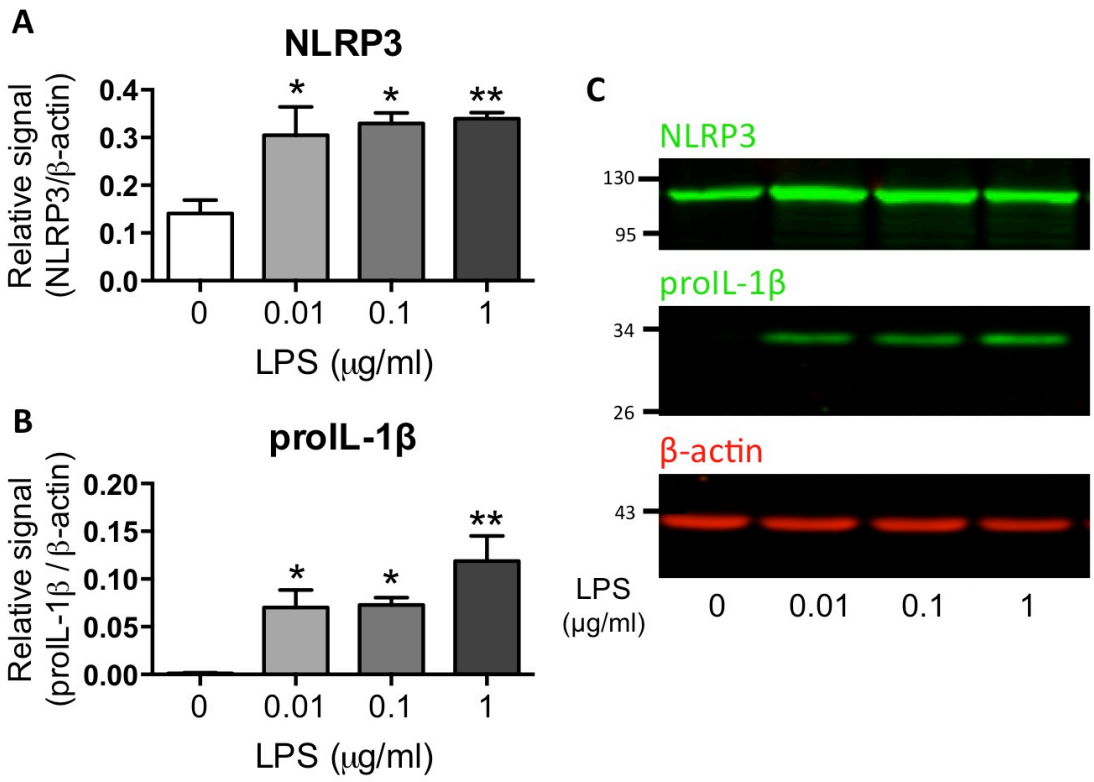

Figure 4.3. Western blot analysis of protein expression in BV2 microglial cells following LPS stimulation.

NLRP3 (**A**; green) and proIL-1β (**B**; green) expression was assessed relative to β-actin by quantitative western blotting (**C**) following stimulated with 0.1-1 μg/ml LPS (4 h). Histograms represent fluorescence intensity relative to β-actin (red). Data shown are mean ± SEM (n=3) and analysed by one-way ANOVA with Dunnett posthoc analysis. *$p < 0.05$, **$p < 0.01$, both compared to control.

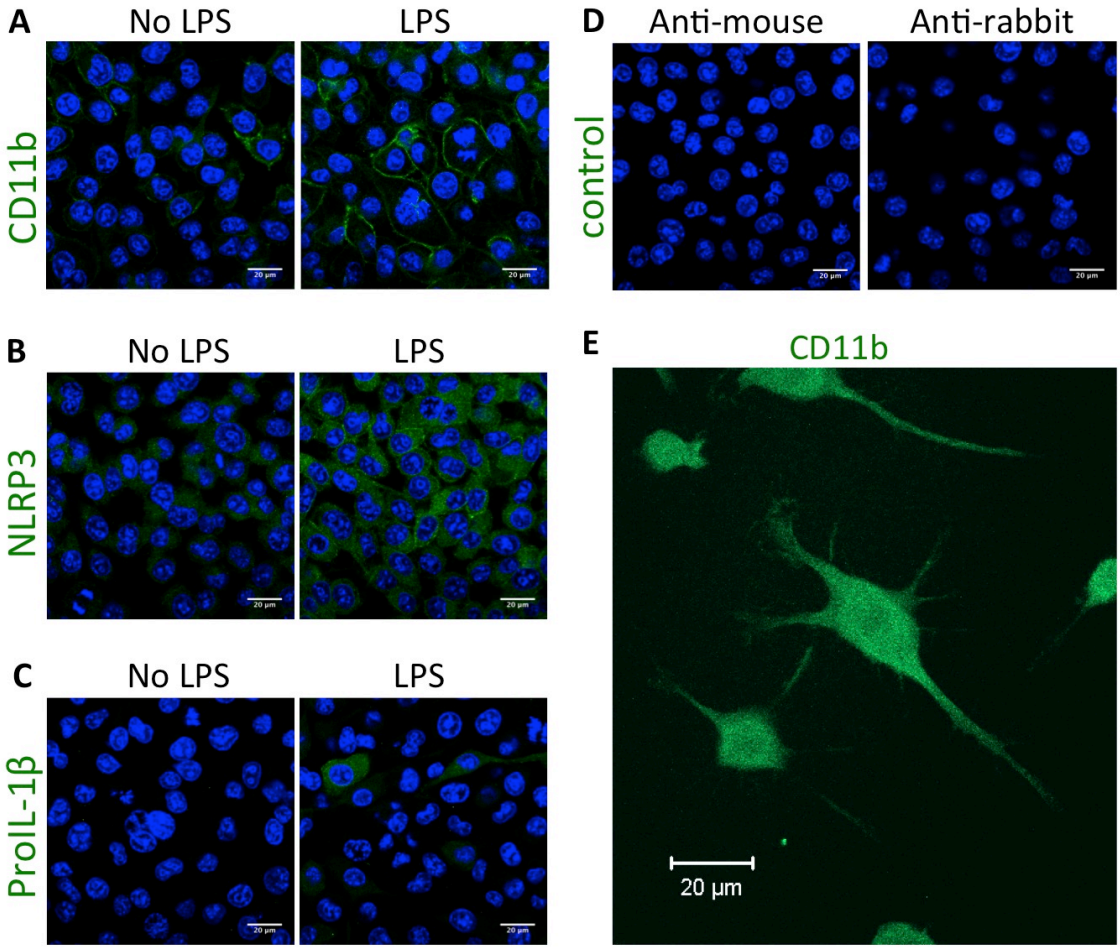

Figure 4.4. Confocal micrographs of BV2 microglial cells.

The expression of microglial marker CD11b (**A**), NLRP3 (**B**) and proIL-1β (**C**) were assessed following LPS stimulation (0.1 µg/ml, 4 h). Primary antibodies were omitted for negative controls (**D**). Cells were counterstained with nuclear marker DAPI (blue). Z-stacked image of an unstimulated BV2 microglia (**E**).

4.2.1.3 Time dependent protein expression in BV2 microglia

The time course of LPS-induced expression of NLRP3 (Figure 4.5A), proIL-1β (Figure 4.5B) and P2X7 (Figure 4.5C) in BV2 microglia was quantified using multiple time points (0, 1, 2 and 4 h). LPS stimulation has a significant effect of NLRP3 (one way ANOVA, $F_{(3,8)} = 14.43$, $p = 0.0014$) and proIL-1β (one way ANOVA, $F_{(3,8)} = 4.281$, $p = 0.0444$) expression, but not on P2X7 expression (*t* test, $p = 0.9527$). BV2 microglia exhibit a basal level of NLRP3 expression, and upon LPS stimulation, the level of NLRP3 increases in an LPS time-dependent manner, with a significant increase at 2 h ($p < 0.01$) and 4 h ($p < 0.01$). Whilst there is no basal expression of proIL-1β, expression can be seen after 1 h LPS stimulation, and a significant increase can be observed after 4 h ($p < 0.05$). The stimulation of the ATP-gated receptor P2X7 has

been shown to mediate ATP-induced inflammasome activation in macrophages (Kahlenberg and Dubyak, 2004). Confirming previous studies (Gendron and Chalimoniuk, 2003), BV2 cells express the P2X7 receptor (estimated molecular weight: 75 kDa), necessary for ATP-induced inflammasome activation. LPS stimulation did not alter P2X7 expression levels.

4.2.1.4 P2X7 receptor activity in BV2 microglia

Extracellular ATP-induced uptake of ethidium is an indicator of P2X7 receptor function, with ATP-P2X7 activation (EC_{50}: 214 μM for YOPRO dye uptake) resulting in the formation of pores and allowing the entry of large molecules (Chessell et al., 1998). Functional P2X7 receptor activity in BV2 cells, necessary for ATP-induced inflammasome activation, was assessed. When stimulated with high doses of ATP (≥1 mM) in calcium and magnesium containing buffer, ethidium uptake and fluorescence in BV2 cells rapidly increases, indicating functional P2X7 receptor activity (Figure 4.6A). Fluorescence values were normalised to a maximal signal (following cell lysis with triton X-100). At 20 min post-administration of ATP, a significant effect of ATP on ethidium uptake was observed (Figure 4.6B; one way ANOVA, $F_{(5,12)} = 72.76$, $p < 0.001$). BV2 microglia exhibit a significant increase in ethidium uptake with 1, 3 and 5 mM ATP ($p < 0.01$, $p < 0.001$ and $p < 0.001$, respectively). A-740003 is a selective P2X7 receptor antagonist that can block mouse- and human-P2X7 agonist-evoked dye uptake (Donnelly-Roberts et al., 2009) and IL-1β release in human THP-1 cells (Honore et al., 2006). A significant effect of treatment on ethidium uptake was observed (Figure 4.6C; one way ANOVA, $F_{(5,12)} = 38.18$, $p < 0.001$). When BV2 microglia were incubated with A-740003 ethidium fluorescence was significantly reduced at 10 μM (56 ± 9 %; n = 3; $p < 0.001$) and 30 μM (32 ± 2 %; n = 3; $p < 0.001$). In addition, whilst a significant effect of treatment was observed, LPS stimulation for 4 h prior to experimentation did not alter ATP-induced ethidium uptake (Figure 4.6D; one way ANOVA, $F_{(3,12)} = 74.13$, $p < 0.001$), nor did LPS stimulation influence the activity of the P2X7 receptor antagonist, A-740003 (Figure 4.6E; one way ANOVA, $F_{(3,8)} = 19.22$, $p < 0.001$).

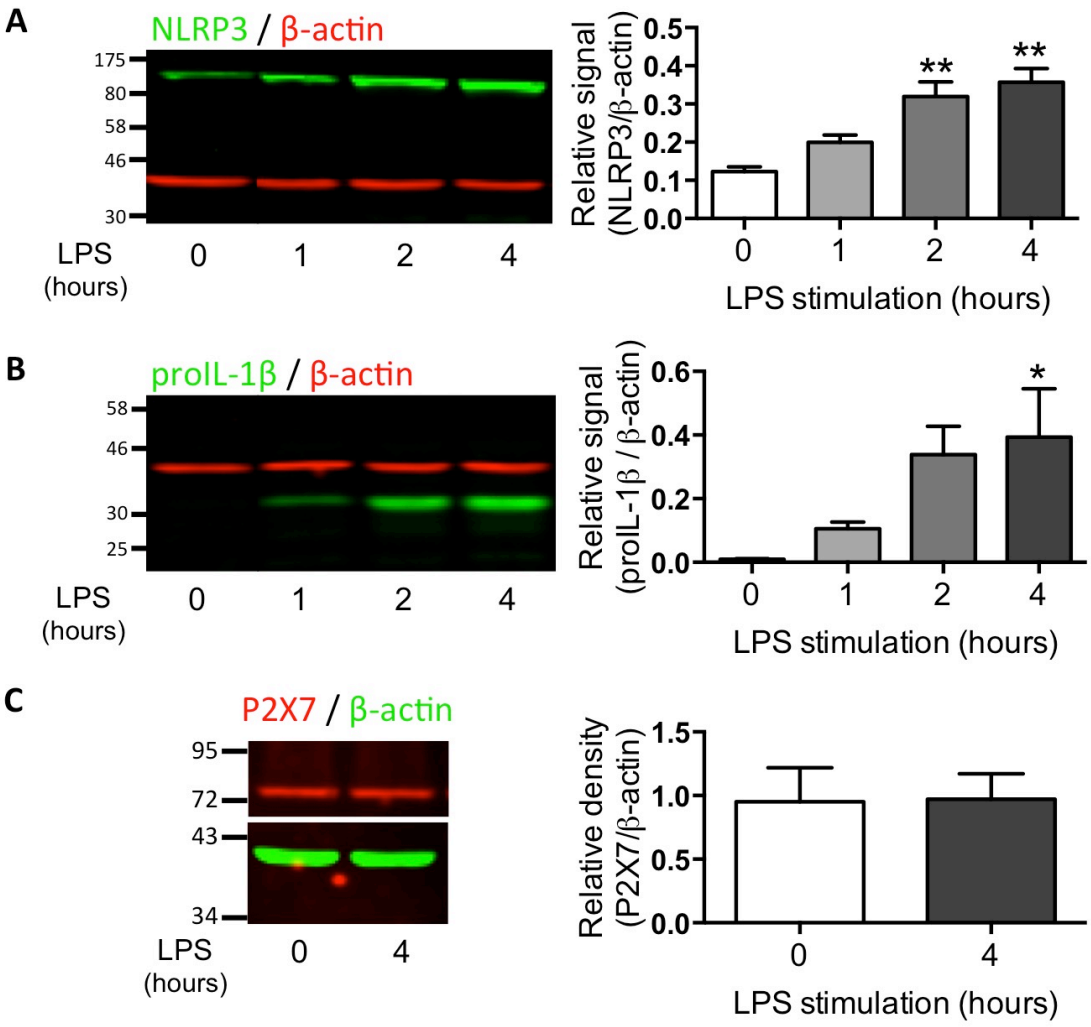

Figure 4.5. Western blot analysis of protein expression in BV2 microglial cells following LPS stimulation.

NLRP3 (**A**; green), proIL-1β (**B**; green) and P2X7 (**C**; red) expression following 0-4 h LPS stimulation (0.1 µg/ml). Histograms represent fluorescence intensity relative to β-actin. Data shown are mean ± SEM (n=3-4) and analysed by one-way ANOVA with Dunnett posthoc analysis (**A** & **B**) or Student's *t*-test (**C**). *$p < 0.05$, **$p < 0.01$, both compared to control.

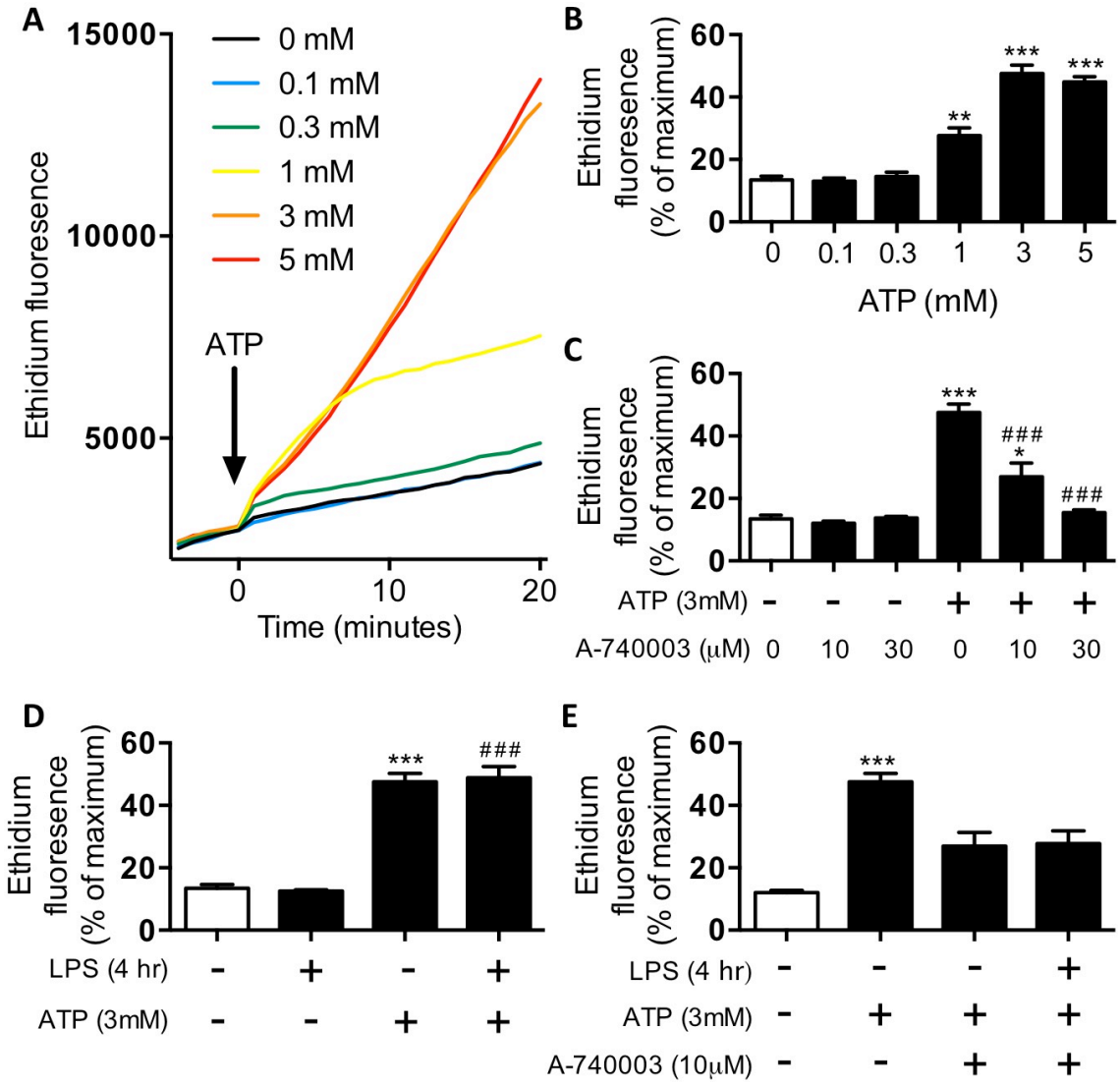

Figure 4.6. P2X7 receptor-mediated uptake of ethidium in BV2 microglia.

Raw ethidium fluorescence following stimulation with ATP (0.1 – 5 mM; **A**) and analysed following 20 min ATP stimulation (**B**). P2X7 receptor inhibition with selective antagonist A-740003, added 5 min before ATP (10 and 30 μM; **C**). The effect of LPS stimulation (0.1 μg/ml; 4 h) on P2X7 activity (**D**) and on A-740003 inhibition of the P2X7 receptor (**E**). Values are 20 min post-ATP addition and represent % of a maximal fluorescence signal after lysing cells with 0.2 % Triton X-100 (**B**-**E**). Data represent mean ± SEM (n=3) and analysed by two-way ANOVA with Tukey's post hoc test. *p < 0.05, **p < 0.01, ***p < 0.001, all compared to control; $^{\#}p < 0.05$, $^{\#\#}p < 0.01$, $^{\#\#\#}p < 0.001$ compared to +ATP.

4.2.1.5 The effect of acute 5 % O_2 hypoxia on BV2 microglia priming

O_2 partial pressure measurements taken within the brain indicate that the microenvironment in which microglia exist is hypoxic when compared to the approximately 20 % O_2 conditions commonly used in cell culture (Lyons et al., 2016). To study microglia in conditions that better mimic the *in vivo* microenvironment (Ivanovic, 2009), cells were exposed to 5 % O_2 for 5 h and stimulated with LPS (0.1 µg/ml; 4 h) before proIL-1β (Figure 4.7A) and NLRP3 (Figure 4.7B) expression was assessed. A two-way ANOVA revealed a significant effect LPS ($F_{(1,8)}$ = 426.5, p < 0.001) and hypoxia ($F_{(1,8)}$ = 62.98, p < 0.001) on proIL-1β expression, and a significant interaction between LPS and hypoxia ($F_{(1,8)}$ = 62.12, p < 0.001). A two-way ANOVA also revealed a significant effect LPS ($F_{(1,8)}$ = 157.4, p < 0.001) on NLRP3 expression and a significant interaction between LPS and hypoxia ($F_{(1,8)}$ = 7.096, p = 0.0286), but no significant effect of hypoxia alone ($F_{(1,8)}$ = 5.135, p = 0.0532). Stimulation with LPS resulted in a significant increase in proIL-1β expression (p < 0.001) and NLRP3 expression (p < 0.001) in comparison to control. However, when incubated in hypoxic (5 % O_2) conditions 1 h prior to and during LPS stimulation, the cytosolic levels of proIL-1β (45 ± 3 %; n = 3; p < 0.001) and NLRP3 (74 ± 5 %; n = 3; p < 0.05) were significantly lower compared to 20 % O_2. This finding suggests that acute exposure to low O_2 attenuates TLR4-mediated priming of microglia cells.

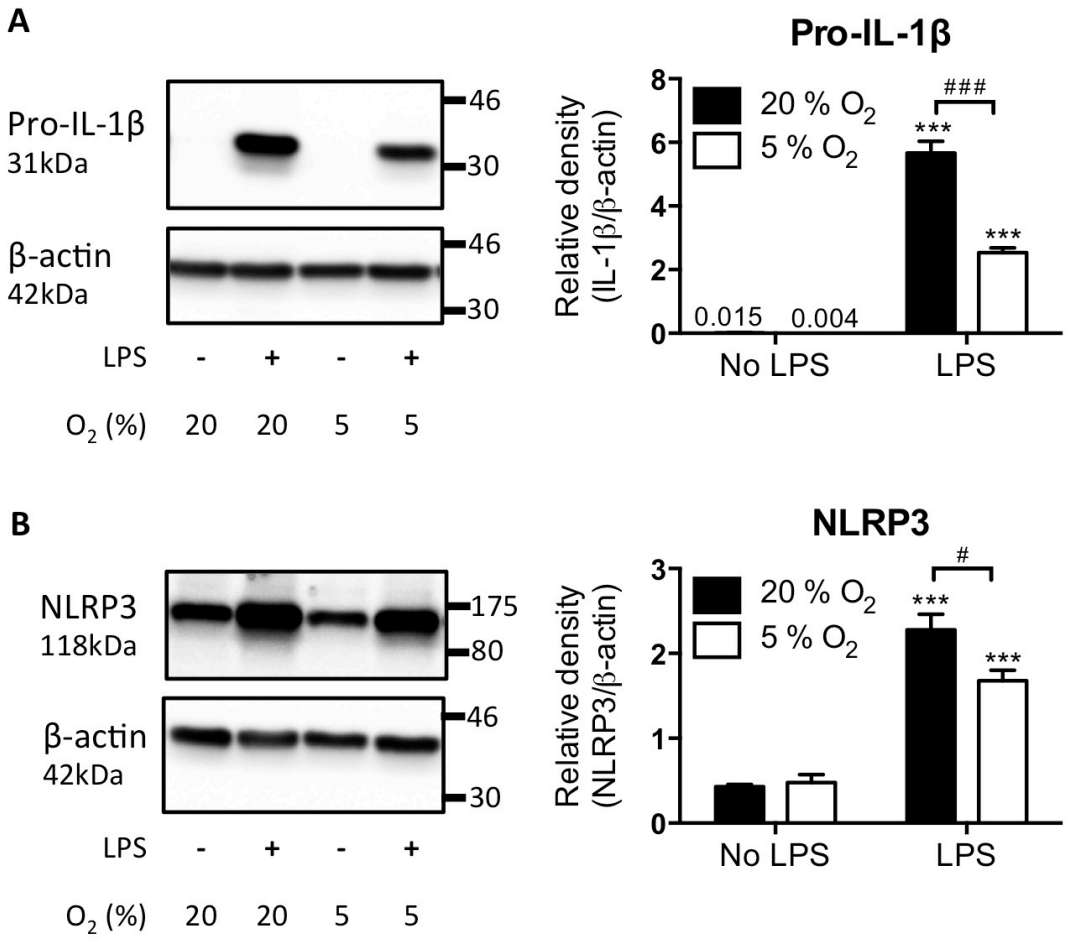

Figure 4.7. ProIL-1β and NLRP3 protein expression in BV2 microglia under normoxia and acute low oxygen conditions.

Cytosolic proIL-1β (**A**) and NLRP3 (**B**) expression with and without LPS stimulation (4 h; 0.1 μg/ml) in 5 or 20 % O_2 (5 h) in BV2 microglia. Histograms represent density relative to β-actin. Data represent mean ± SEM (n=3) and analysed by two-way ANOVA with Tukey posthoc analysis. ***$p < 0.001$ compared to no LPS; $^{\#}p < 0.05$.

4.2.1.6 BV2 microglia priming response to TNF-α and IL-1β stimulation

In order to understand if this phenomenon of attenuated NLRP3 and proIL-1β expression under acute hypoxia was specific to TLR4 signalling, BV2 microglia were incubated with proinflammatory murine cytokines IL-1β and TNF-α, which both also induce NF-κB signalling via their respective receptors and in turn induce the expression of inflammatory proteins (Verstrepen et al., 2008). NLRP3 (Figure 4.8B) and proIL-1β (Figure 4.8C) expression was assessed after 4 h stimulation with LPS (0.1 µg/ml), IL-1β (1- 10 ng/ml) and/or TNF-α (1- 10 ng/ml). A two-way ANOVA revealed a significant effect of LPS treatment ($F_{(5,24)}$ = 94.46, p < 0.001) and hypoxia ($F_{(1,24)}$ = 13.11, p = 0.0014) on NLRP3 expression, and a significant effect of hypoxia on the LPS response ($F_{(5,24)}$ = 5.168, p = 0.0023). A two-way ANOVA revealed a significant effect of LPS treatment ($F_{(5,24)}$ = 19.23, p < 0.001) on proIL-1β expression, with a significant effect of hypoxia on the LPS response ($F_{(5,24)}$ = 3.14, p = 0.0255), but no significant effect of hypoxia alone ($F_{(1,24)}$ = 3.14, p = 0.0891). Whilst LPS still induced a significant increase in proIL-1β and NLRP3 expression (p < 0.001 for both), both IL-1β and TNF-α failed to induced expression, contrasting previous findings that shown microglia activation with IL-1β and TNF-α (Sheng et al., 2011).

4.2.1.7 Inflammasome activity in BV2 microglia

The danger associated molecular pattern, extracellular ATP, is a potent activator of the NLRP3 inflammasome and regularly used to study inflammasome activity (Mariathasan et al., 2006). IL-1β release following ATP stimulation (5 mM; 30 min) was assessed in LPS-primed (0.1 µg/ml; 4 h) BV2 microglia and J774.2 macrophages as a positive control (Figure 4.9). A two-way ANOVA revealed a significant effect ATP ($F_{(1,12)}$ = 5.008, p = 0.045) and cell type ($F_{(1,12)}$ = 4.946, p = 0.0461) on IL-1β secretion. Whilst the expression of ATP-receptor P2X7, NLRP3 and the IL-1β precursor protein has been demonstrated, ATP failed to induce IL-1β secretion in LPS-primed BV2 microglia detected by ELISA. Conversely, LPS-primed J774.2 macrophages secreted a significant level of IL-1β (p < 0.05) when stimulated with ATP under the same conditions. These data suggest that unlike previous literature, these BV2 microglia do not have a functional NLRP3 inflammasome (Kaushik et al., 2012; Shi et al., 2012).

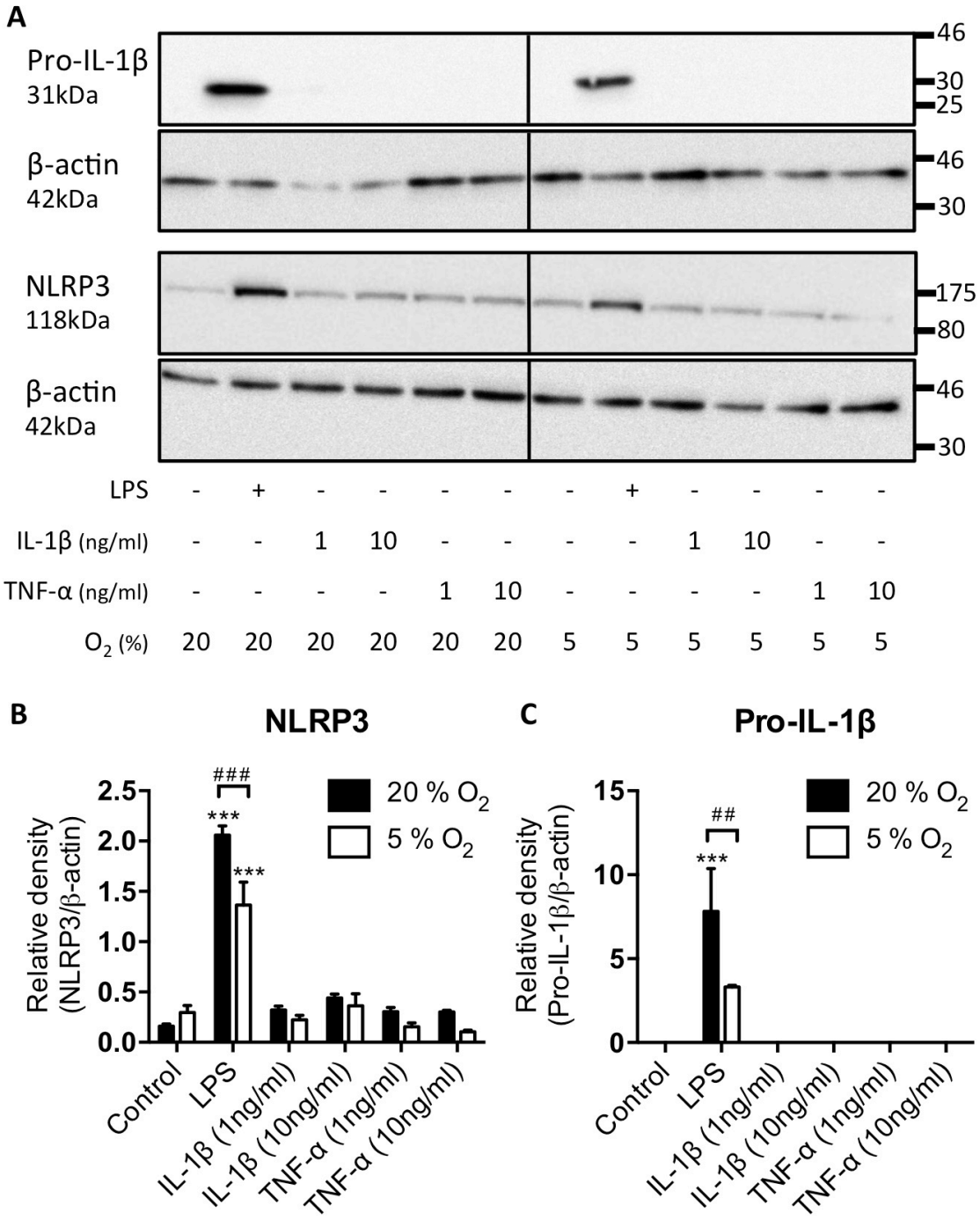

Figure 4.8. ProIL-1β and NLRP3 protein expression in BV2 microglia following stimulation with proinflammatory cytokines.

Cytosolic expression of NLRP3 and proIL-1β expression assessed by western blotting (**A**) following stimulation with LPS (4 h; 0.1 µg/ml), IL-1β (4 h; 1 and 10 ng/ml) or TNF-α (4 h; 1 and 10 ng/ml) in 5 or 20 % O2 (5 h) in BV2 microglia. Histograms represent density relative to β-actin for proIL-1β (**B**) and NLRP3 (**C**). Data represent mean ± SEM (n=3) and analysed by two-way ANOVA with Tukey post hoc analysis. $^{***}p < 0.001$ compared to control; $^{\#\#}p < 0.01$, $^{\#\#\#}p < 0.001$.

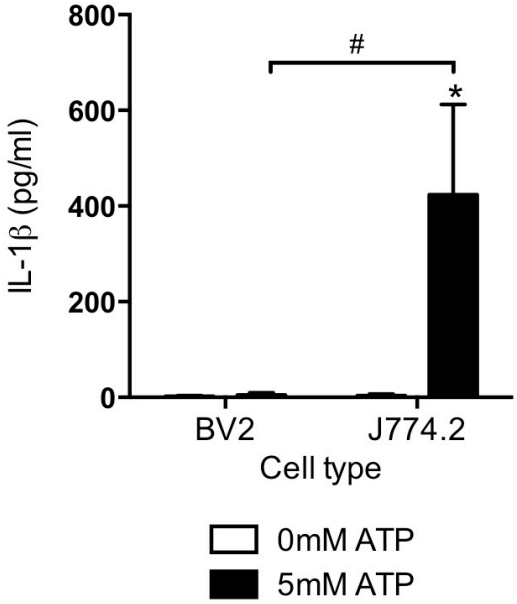

Figure 4.9. ATP-induced IL-1β release from BV2 microglia and J774.2 macrophages.

ELISA detection of IL-1β release following ATP stimulation (5 mM; 30 min) in LPS primed (0.1 µg/ml; 4 h) BV2 microglia and J774.2 macrophages. Data shown are mean ± SEM (n=3) and analysed by two-way ANOVA with Tukey's posthoc analysis. *p < 0.05 compared to control. $^{\#}p$ < 0.05.

4.2.1.8 BV2 microglia cell death

Lactate dehydrogenase (LDH) is an important cytosolic enzyme that is released during cell death as a cell dies as the membrane degrades (Korzeniewski and Callewaert, 1983). The release of LDH was assessed in LPS (0.1 µg/ml; 4 h) and ATP (5 mM; 30 min) stimulated BV2 microglia (Figure 4.10B) to investigate if the cells exhibit a normal cell death response to stimulation when compared to macrophages (Figure 4.10A). LPS / ATP stimulation had a significant effect of LDH release in J774.2 macrophages (one way ANOVA, $F_{(3,8)}$ = 9.933, p = 0.0045), but not in BV2 microglia (one way ANOVA, $F_{(3,8)}$ = 2.474, p = 0.1359). When stimulated with both LPS and ATP, J774.2 macrophages released LDH (p < 0.01), an indicator of cell death. However in BV2 cells, LDH secretion was not significantly affected by LPS and/or ATP stimulation, with a baseline level of LDH release noticeably higher that of J774.2 macrophages. This finding suggests that BV2 microglia have a diminished pyroptotic response to ATP stimulation.

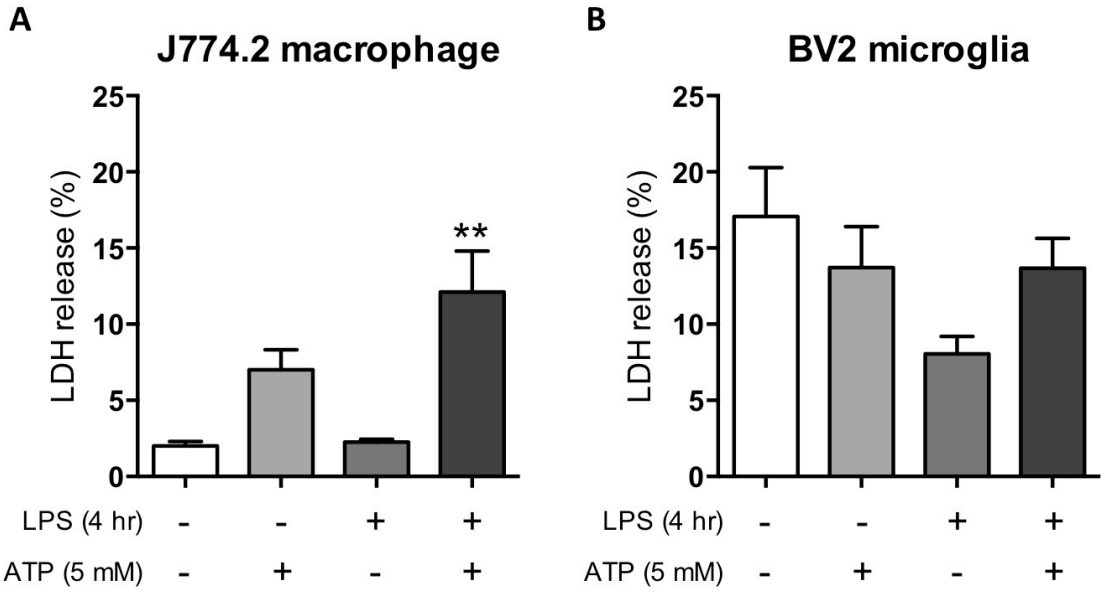

Figure 4.10. Cell death in J774.2 macrophages and BV2 microglia.

The release of lactate dehydrogenase (LDH), an indicator of necrotic cell death, in J774.2 macrophages (**A**) and BV2 microglia (**B**) following LPS (0.1 µg/ml; 4 h) and ATP (5 mM; 30 min) stimulation. Data represent mean ± SEM (n=3) and analysed by one-way ANOVA with Dunnett posthoc analysis. $^{**}p < 0.01$ compared to control.

4.2.1.9 ASC expression in BV2 microglia

ASC is a critical component of the NLRP3 inflammasome that bridges NLRP3 to procaspase-1, allowing inflammasome assembly and procaspase-1 autocleavage. The production of caspase-1 in turn cleaves proIL-1β resulting in the mature bio-active form, IL-1β (Schroder and Tschopp, 2010). Following the absence of ATP-mediated IL-1β secretion ASC expression was assessed via western blotting. It was found that whilst J774.2 macrophages expressed ASC protein, BV2 microglia did not (Figure 4.11A), which elucidates the absence of secreted IL-1β and cell death following ATP stimulation. Whilst ASC protein could not be detected, PCR revealed the presence of ASC mRNA (Figure 4.11B), suggesting ASC protein expression may be inhibited at a translational level or that the level of ASC protein is below the detectable range.

Due to the unusual phenotype of the BV2 cells, with the absence of ASC protein expression, the lack of IL-1β secretion, the failed priming with inflammatory cytokines and the cell death response to stimulation, all future experiments were carried out with primary microglia isolated from C57BL/6J mice in order to confidently assess normal microglia function.

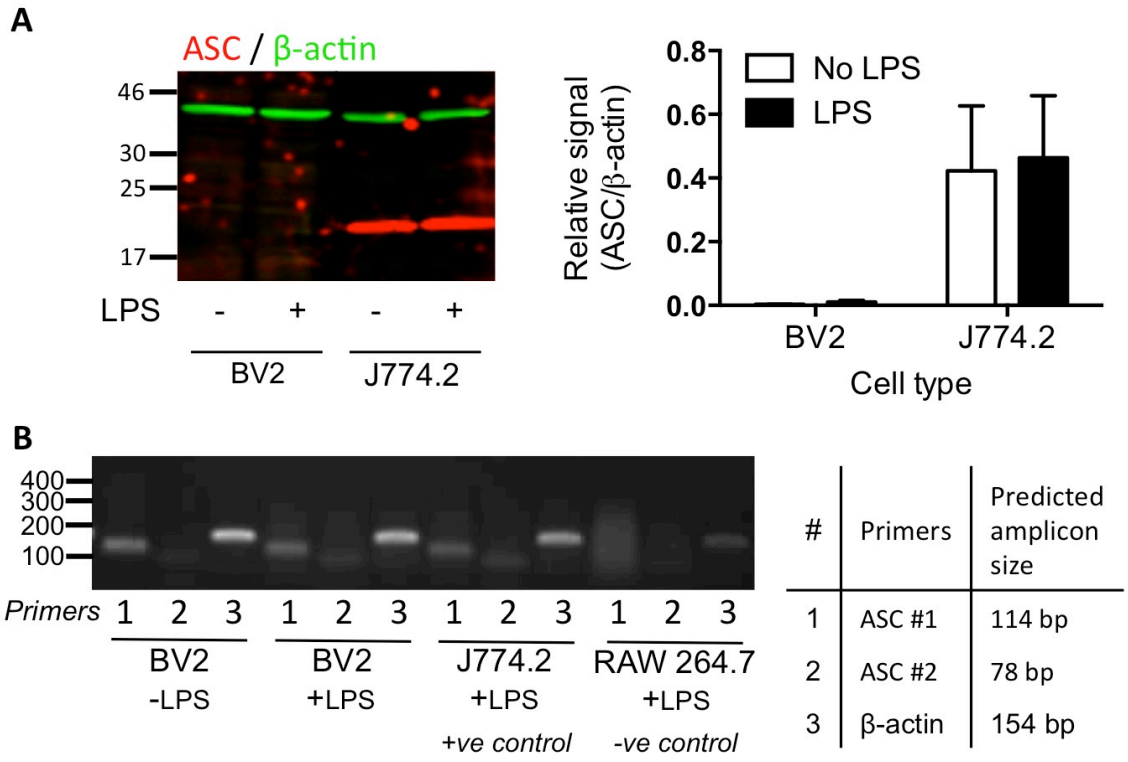

Figure 4.11. ASC protein and mRNA expression in BV2 microglia and J774.2 macrophages.

Western blot analysis of ASC expression (red) in BV2 microglia and J774.2 macrophages (**A**) with and without LPS stimulation (0.1 μg/ml; 4 h). Histogram represents fluorescence intensity relative to β-actin (green). PCR analysis of ASC mRNA in BV2 microglia and J774.2 or RAW264.7 macrophages (**B**). Two separate sets of ASC primers were used (#1 & #2), and a β-actin primer (#3) as a control. Data shown are mean ± SEM (n=3) and analysed by two-way ANOVA.

4.2.2 Characterisation of NLRP3 inflammasome function in neonatal primary microglia isolated by mild trypsinisation

4.2.2.1 Isolation of primary microglia

The majority of primary microglia cultures are obtained by an extended period of shaking of mixed glia cultures, ranging from 15 min to 5 h (Parvathenani et al., 2003; Liu et al., 2001). The shaking process causes microglia to enter an amoeboid form whereby cells retract their projections to allow free movement and detach from the surface of the well to be harvested and re-plated (Giulian and Baker, 1986). The primary disadvantage of shaking is the mechanical stress that is placed upon the cells. The retraction of projections is an indicator of microglia activation (Kettenmann et al., 2011) and potentially extracellular ATP (Orr et al., 2009), though this phenotype allows the isolation of detached microglia in the supernatant. This process may alter microglia behaviour and affect microglia stimulation during experimentation the following day. In an attempt to avoid potential mechanical stress and activation of microglia, we used a method of mild trypsin to isolate primary microglia (Figure 4.12A) (Saura et al., 2003). After 3 weeks in culture, a layer of astrocytes form in the mixed glial cultures, which overlay microglia (Figure 4.12C) (Sheng et al., 2011). By using a low concentration of trypsin for a brief period (10 – 20 min), the astrocytic layer becomes detached and can be removed, leaving microglia still adhered to the surface of the well (Figure 4.12D). The conditioned media from the mixed glia culture is then added back to the well. Confocal imaging showed that before isolation, there are many GFAP-positive cells, indicating the presence of astrocytes (Figure 4.12E). Following isolation, only GFAP-negative / CD11b-positive cells remain, demonstrating a pure culture of primary microglia (Figure 4.12G). The primary microglia exhibit numerous projections, demonstrating a resting ramified morphology. LPS stimulation (0.1 μg/ml; 4 h) of primary microglia induced a visible increase in NLRP3 expression from the low basal level of expression detected by immunocytochemistry (Figure 4.13A). A visible upregulation of cytosolic proIL-1β can also be seen following LPS stimulation, with no basal expression (Figure 4.13B). In addition, the microglia morphology following LPS stimulation appeared more rounded with retracted processes.

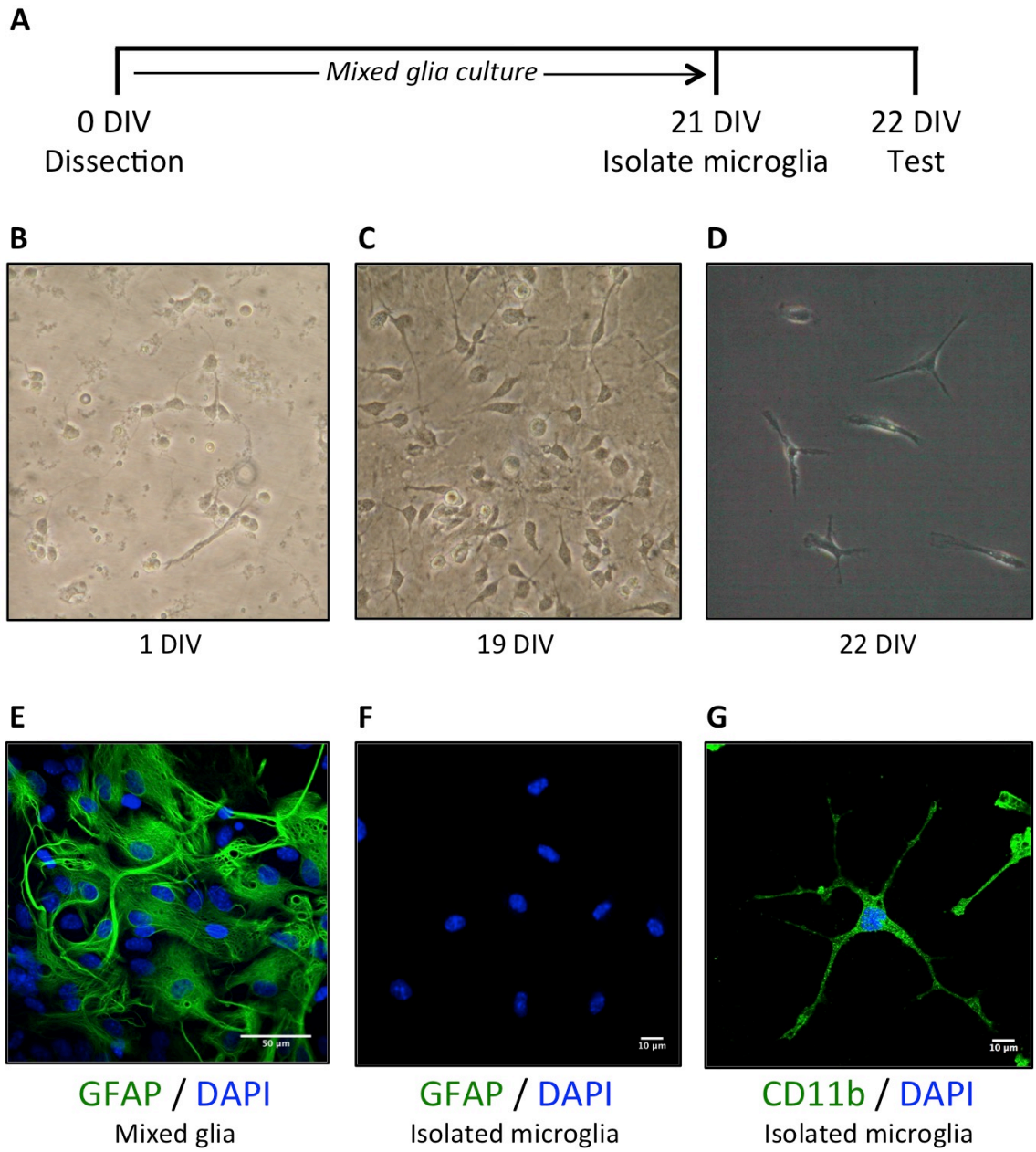

Figure 4.12. Isolation of primary microglia from mixed glia cultures taken from neonatal C57BL/6J mice.

Mixed glial cells are cultured for 3 weeks until microglia are isolated prior to experimentation (**A**). Light microscope images show mixed glia culture from 1 day in vitro (DIV) through to 19 DIV (**C**) and isolated microglia cells via mild trypsinisation at 22 DIV (**D**). Confocal images of mixed glia cultures and isolated microglia with nuclei counterstained in DAPI (blue). Mixed glial cultures contain GFAP-positive (green) astrocytes (**E**). Following mild trypsinisation, GFAP-positive cells are removed where DAPI staining indicates the presence of cells (**F**) leaving only CD11b-positive (green) microglia (**G**). Images are representative of n=3.

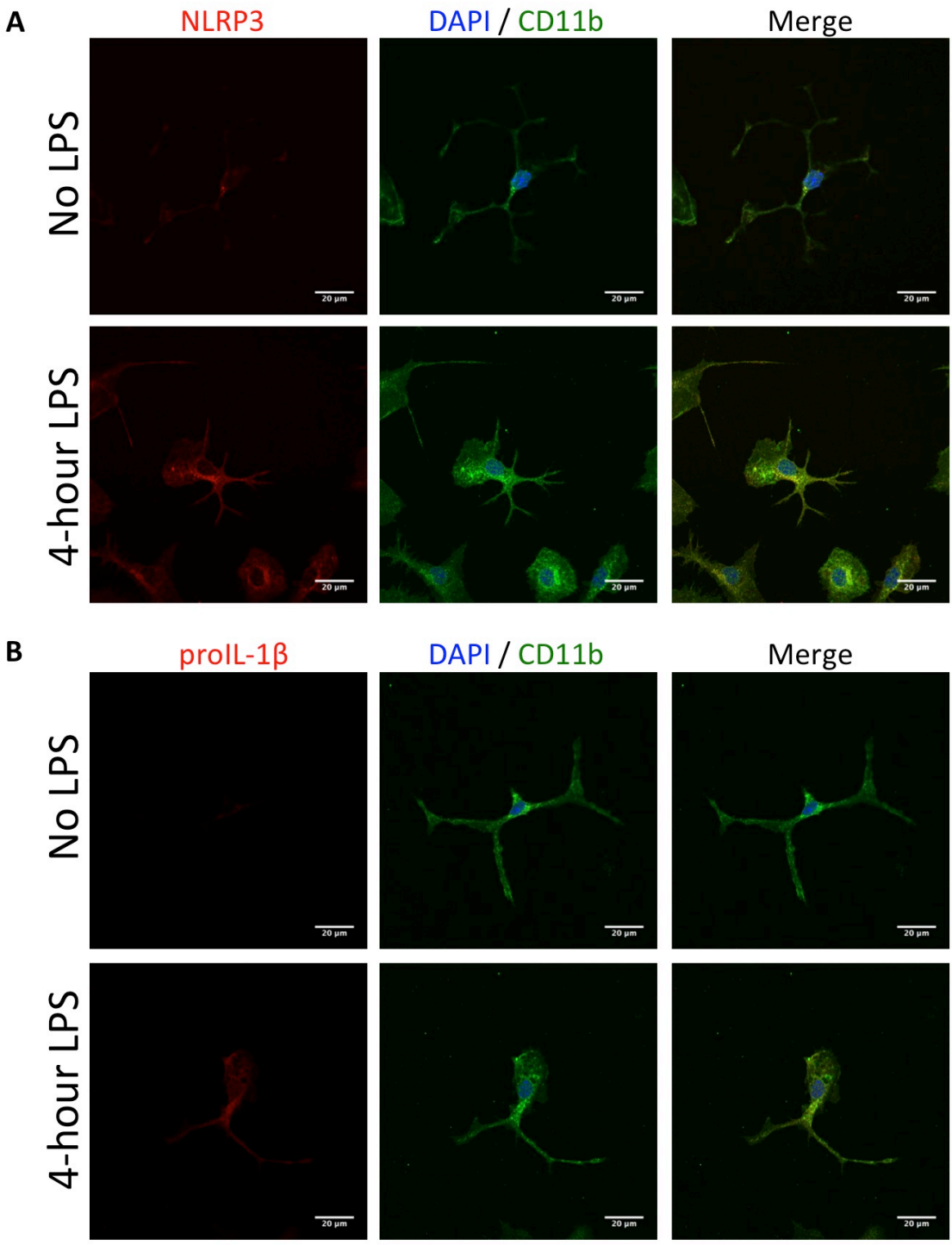

Figure 4.13. Immunocytochemical imaging of NLRP3, proIL-1β and CD11b expression in microglia isolated from neonatal C57BL/6J mice.

NLRP3 (red; **A**), proIL-1β (red; **B**) and CD11b (green) expression following LPS stimulation (4 h; 0.1 µg/ml). The nuclei were counterstained in DAPI (blue). Scale bar is 20 µm. Images representative of n = 3.

4.2.2.2 Protein expression in primary microglia

NLRP3 (Figure 4.14A), proIL-1β (Figure 4.14B), P2X7 (Figure 4.14C) and ASC (Figure 4.14D) expression in trypsin isolated primary microglia was determined. LPS stimulation (0.1 µg/ml; 4 h) had a significant effect on NLRP3 (one way ANOVA, $F_{(3,8)}$ = 6.019, p = 0.019) and proIL-1β (one way ANOVA, $F_{(3,12)}$ = 3.543, p = 0.0481) expression. Similarly to BV2 microglia, primary neonatal microglia show a basal level of NLRP3 protein expression. Following 4 h LPS stimulation, a significant upregulation in NLRP3 is observed (p < 0.01), as well as a significant induction of proIL-1β expression (p < 0.05). In addition, primary neonatal microglia express the adaptor protein ASC, essential for NLRP3 inflammasome assembly, as well as P2X7. A two way ANOVA revealed no effect of LPS stimulation on P2X7 expression ($F_{(1,12)}$ = 0.6439, p = 0.4379) or ASC expression ($F_{(1,12)}$ = 0.4754, p = 0.9473), demonstrating a similar expression pattern to J774.2 macrophages.

4.2.2.3 P2X7 receptor function and inflammasome activity in primary microglia

The P2X7 receptor mediates ATP-induced NLRP3 inflammasome activation (Kahlenberg and Dubyak, 2004). By measuring ATP-induced ethidium uptake, P2X7 receptor function can be assessed (Figure 4.15A). A significant effect of treatment on ethidium uptake was observed (one way ANOVA, $F_{(3,12)}$ = 30.54, p < 0.001). Following stimulation with ATP, primary microglia significantly increase the level of ethidium uptake (p < 0.001). This increase in ethidium fluorescence is significantly attenuated following incubation with the P2X7 receptor specific antagonist A-740003 at 10 µM (79 ± 8 %; n = 4; p < 0.05) and 30 µM (74 ± 3 %; n = 4; p < 0.05), indicating functional P2X7 receptor activity. With ASC expression and functional P2X7 receptor activity confirmed, inflammasome activity and IL-1β secretion was tested. When primed with LPS (0.1 µg/ml; 4 h) and stimulated with ATP (5 mM; 30 min), primary microglia release IL-1β into the supernatant, unlike BV2 microglia (Figure 4.15B). A two-way ANOVA revealed a significant effect ATP ($F_{(1,24)}$ = 24.31, p < 0.001) and LPS ($F_{(3,24)}$ = 13.19, p < 0.001) on IL-1β release, with a significant interaction between LPS and ATP ($F_{(3,24)}$ = 11.64, p < 0.001). IL-1β release was significantly greater than LPS alone (p < 0.001) and ATP alone (p < 0.001). Caspase-1 is the functional enzyme of the NLRP3 inflammasome. To show that the release of IL-1β in primary microglia is a result of NLRP3 inflammasome activity, cells were incubated with the caspase-1 inhibitor Ac-YVAD-cmk (Figure 4.15C). A significant effect of treatment on IL-1β release was

observed (one way ANOVA, $F_{(3,8)}$ = 6.993, p = 0.0126). Ac-YVAD-cmk induced a dose-dependent inhibition of IL-1β secretion, with significant reductions observed at 10 μM (39 ± 13 % of control; n = 3; $p < 0.05$) and 40 μM (17 ± 5 % of control; n = 3; $p < 0.01$), indicating a caspase-1-dependent inflammasome.

4.2.2.4 Primary microglia cell death

To assess necrotic/pyroptotic cell death induced by LPS (0.1 μg/ml; 4 h) and ATP (5 mM; 30 min), LDH release was measured (Figure 4.16). We previously showed that BV2 microglia did not show a significant change in LDH release following stimulation whilst J774.2 macrophages did (Figure 4.10). In primary microglia, a significant effect of LPS / ATP stimulation on LDH release was observed (one way ANOVA, $F_{(3,8)}$ = 7.506, p = 0.0103). Similar to J774.2 macrophages, when stimulated with both LPS and ATP, primary microglia released significant levels of LDH ($p < 0.01$), indicating a pyroptotic response similar to macrophages and contrasting the response observed in BV2.

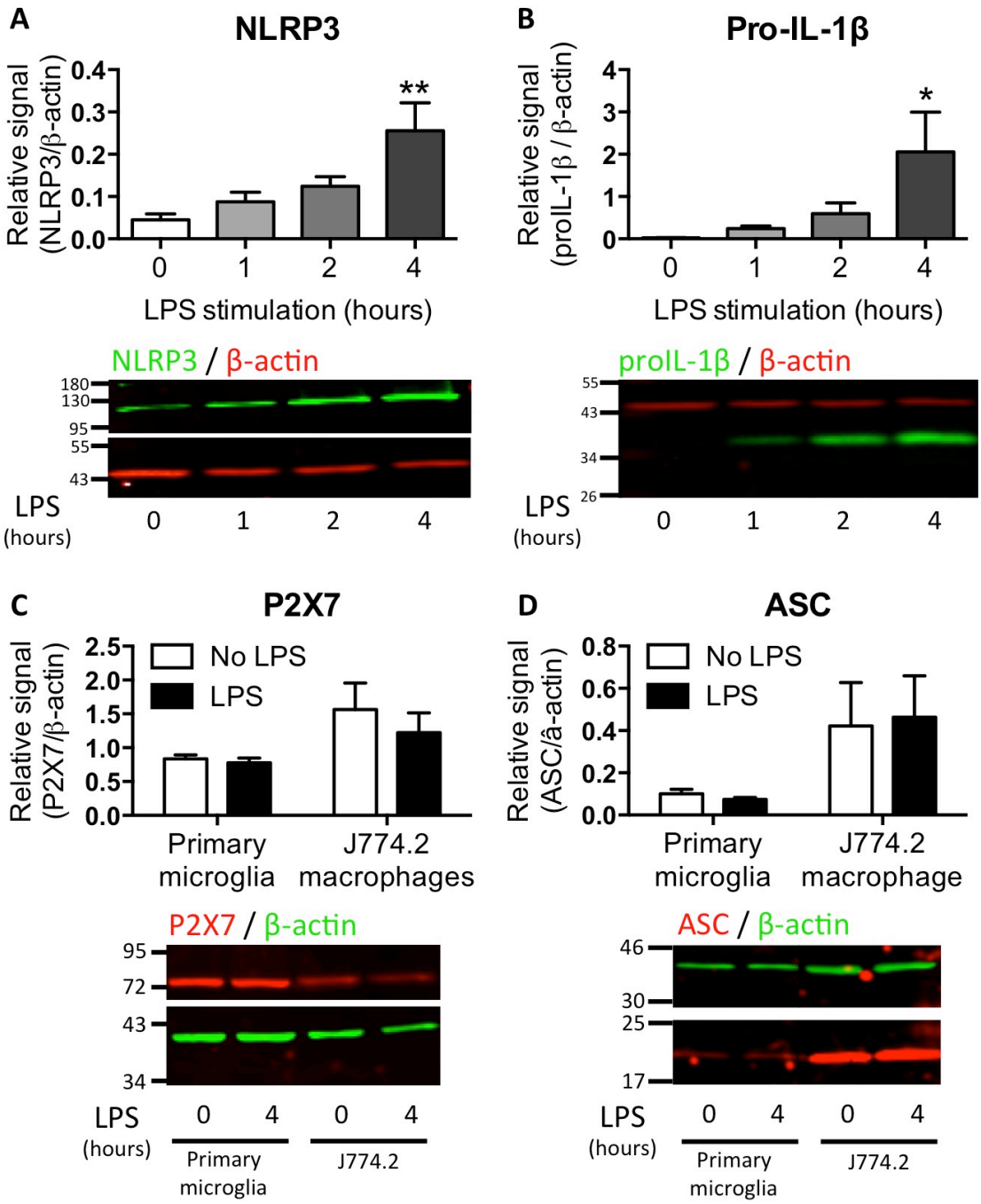

Figure 4.14. Western blot analysis of cytosolic protein expression in primary neonatal microglia isolated from C57BL/6J mice.

NLRP3 (green; **A**) and proIL-1β (green; **B**) expression following LPS stimulation (0 – 4 h; 0.1 µg/ml) in primary microglia. P2X7 (red; **C**) and ASC (red; **D**) expression in primary microglia and J774.2 macrophages following LPS stimulation (4 h; 0.1 µg/ml). Histograms represent fluorescence intensity relative to β-actin. Data shown are mean ± SEM (n=3) and analysed by one-way ANOVA with Dunnett posthoc analysis. *$p < 0.05$, **$p < 0.01$, both compared to control.

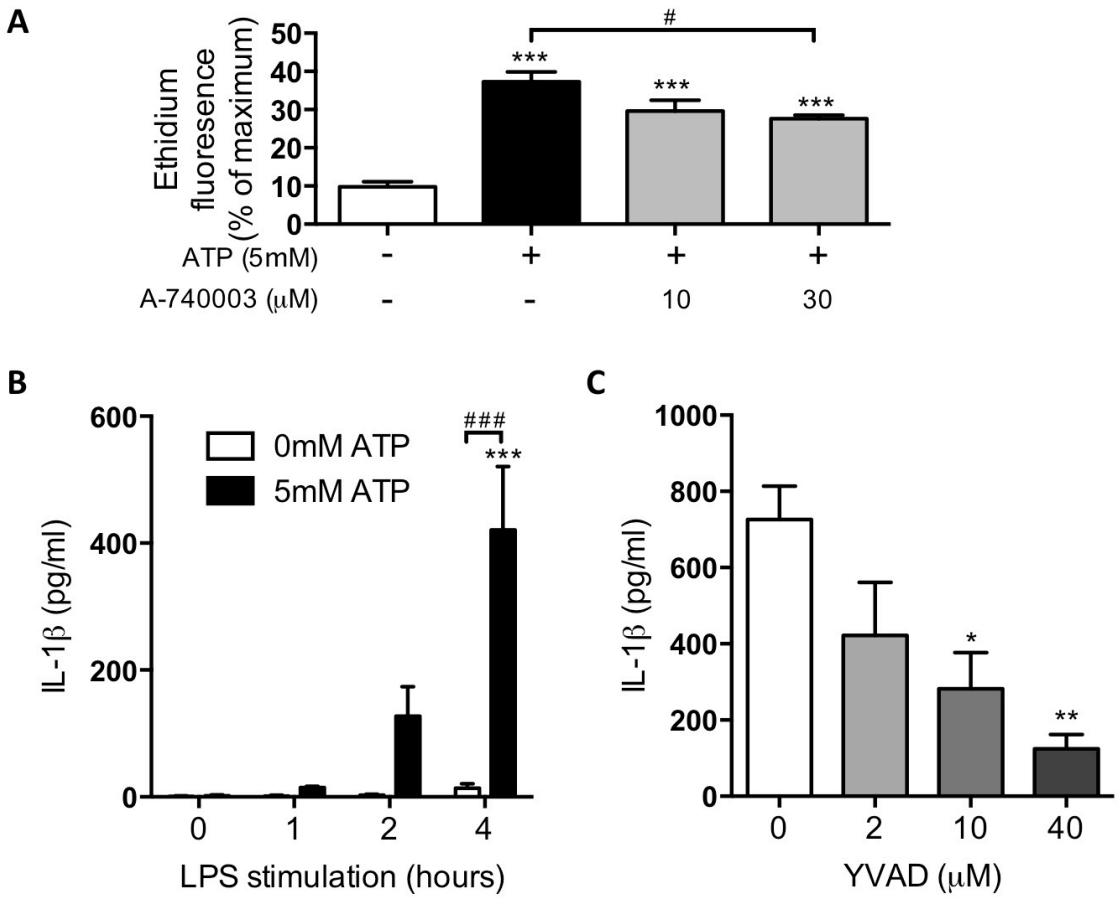

Figure 4.15. P2X7 receptor function and ATP-induced release of IL-1β in neonatal primary microglia isolated from C57BL/6J mice.

Histogram illustrating ethidium fluorescence following 10 min with or without ATP (5 mM) addition in primary microglia. P2X7 receptor inhibition (10 & 30 μM A-740003 added 5 min before ATP addition) (**A**). ELISA detection of IL-1β release following LPS priming (0 – 4 h; 0.1 μg/ml) and ATP stimulation (5 mM; 30 min) (**B**). Caspase-1 inhibition (2 – 40 μM YVAD; 4 h incubation) of IL-1β release from LPS primed (4 h; 0.1 μg/ml) primary microglia detected by ELISA (**C**). Data represent mean ± SEM (n=3) and analysed by one-way ANOVA with Tukey's posthoc test (**A**), two-way ANOVA with Tukey's post hoc test (**B**) or one-way ANOVA with Dunnett's posthoc test (**C**). $^{*}p < 0.05$, $^{**}p < 0.01$, $^{***}p < 0.001$, all compared to control; $^{\#}p < 0.05$, $^{\#\#\#}p < 0.001$ compared to 0 mM ATP.

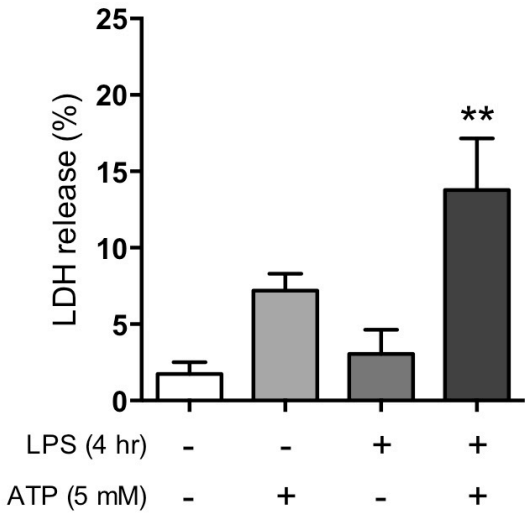

Figure 4.16. Cell death in neonatal primary microglia isolated from C57BL/6J mice.

LDH release following LPS priming (4 h; 0.1 μg/ml) and ATP stimulation (30 min; 5 mM). Data represent mean ± SEM (n=3) and analysed by one-way ANOVA with Dunnett posthoc analysis. ** $p < 0.01$ compared to control.

4.2.2.5 The effect of ketamine of primary microglia function

Ketamine has become a revolutionary new tool in the treatment of treatment-resistant depression, with clinical studies reporting fast-acting improvements in mood following a single dose (Murrough et al., 2013; Berman et al., 2000). In pre-clinical studies, ketamine has been shown to attenuate inflammation-induced depressive-like behaviours in preclinical experiments (Autry et al., 2011; Walker et al., 2013). The antidepressant activity of ketamine in the forced swim test was shown earlier in C57BL/6J mice (Figure 3.1D), but failed to reverse the depressive effects of LPS in the female urine sniffing test (Figure 3.6). Ketamine is a NMDA receptor antagonist and its primary action is stimulating NMDA receptors on neurons, enhancing synaptic protein synthesis and synaptogenesis (Duman et al., 2012). Ketamine has been shown to have anti-inflammatory effects in microglia, including the inhibition of IL-1β release, though the majority of work looking at the effects of ketamine is done in neurons (Chang et al., 2009; Shibakawa et al., 2005). We tested the effects of ketamine on NLRP3 inflammasome expression and function in primary neonatal microglia. Before testing inflammasome function, ketamine-induced cell death was assessed with and without ATP stimulation (5 mM; 30 min) via LDH release (Figure 4.17A). A two-way ANOVA revealed a significant effect of ATP on LDH release ($F_{(1,20)} = 23.68$, $p < 0.001$), but no significant effect of ketamine ($F_{(4,20)} = 0.2277$, $p = 0.9196$), and no interaction between ATP and ketamine ($F_{(4,20)} = 0.056$, $p = 0.9938$). When stimulated with ATP,

LDH release was increased, though ketamine treatment (1-1000 μM) did not alter LDH release in the presence or absence of ATP. This indicates that ketamine does not induce cell death in microglia in a 4 h incubation period. In turn, LPS-induced (0.1 μg/ml; 4 h) expression of proIL-1β (Figure 4.17B) and NLRP3 (Figure 4.17C) was assessed following incubation with ketamine. No significant of ketamine on LPS-induced proIL-1β observed (one way ANOVA, $F_{(4,10)}$ = 2.614, p = 0.0993) or NLRP3 observed (one way ANOVA, $F_{(4,10)}$ = 0.2984, p = 0.8724) expression was observed. Subsequently, the influence of ketamine on ATP-induced IL-1β release was assessed, both when added during the 4 h LPS priming (Figure 4.17D), nor the 30-minute ATP stimulation (Figure 4.17E). No significant of ketamine on ATP-induced IL-1β release was observed when treated during LPS-priming (one way ANOVA, $F_{(4,10)}$ = 2.258, p = 0.135) or ATP-stimulation (one way ANOVA, $F_{(4,10)}$ = 1.677, p = 0.231). These data suggest that ketamine does not directly influence NLRP3 inflammasome expression or ATP-induced inflammasome activity in primary microglia cells. An earlier study showed ketamine inhibited LPS-induced IL-1β secretion, though this was a 12 h LPS stimulation without ATP (Chang et al., 2009). Therefore, our findings indicate the ability of ketamine to attenuate neuroinflammation *in vivo* is independent of P2X7 receptor-mediated NLRP3 inflammasome pathways.

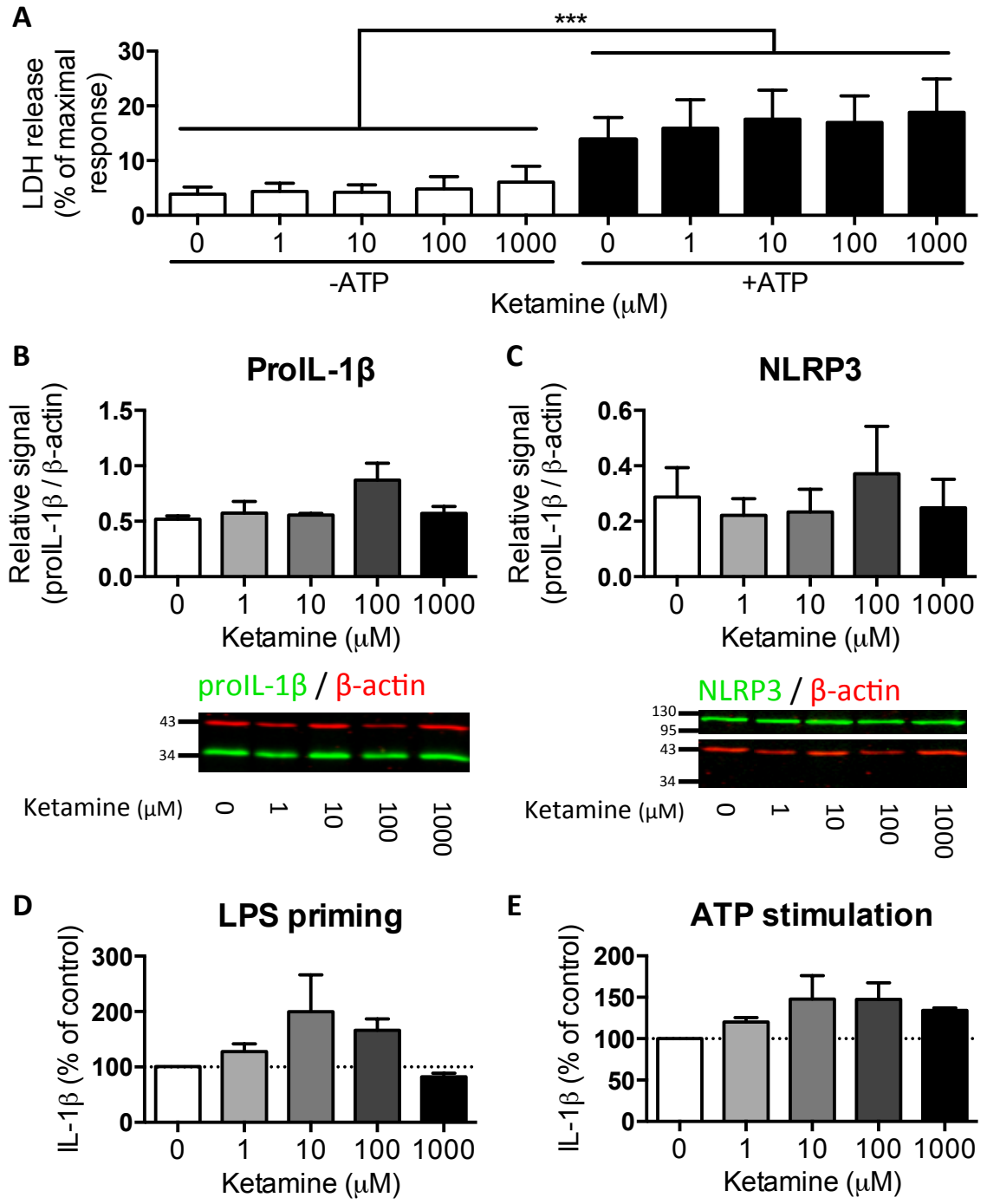

Figure 4.17. The effects of ketamine on cell death and NLRP3 inflammasome expression and activation in neonatal primary microglia isolated from C57BL/6J mice.

LDH release following incubation with ketamine (1 – 1000 μM; 4 h) and ATP stimulation (5 mM; 30 min) in primary microglia (**A**). Expression of proIL-1β (green; **B**) and NLRP3 (green; **C**) in LPS-primed (4 h; 0.1 μg/ml) primary microglia incubated with ketamine. Histograms represent fluorescence intensity relative to β-actin. ATP-induced IL-1β release in LPS-primed primary microglia incubated with ketamine during either the 4 h LPS-priming step (**D**) or the 30-minute ATP stimulation (**E**). Data represent mean ± SEM (n=3) and analysed by two-way ANOVA (A) or one-way ANOVA (B-E) with Dunnett's post hoc tests. ***$p < 0.001$.

4.2.3 The effect of 5 % O_2 on inflammasome function in primary microglia

Brain in microglia will exist in constant state of low O_2 relative to atmospheric O_2 availability (Ivanovic, 2009). In this section, it was asked whether long-term culture under low O_2 would alter the microglia phenotype. As such, primary mixed glia cultures were cultured under low O_2 (5 %) conditions, from immediately after dissection and plating, to sample collection at the end of experiments 3 weeks later. These conditions will be described as chronic hypoxia. Subsequently, mixed glia cultures were incubated in normoxic conditions (20 % O_2 for 3 weeks) before a 24 h incubation in 5 % O_2 hypoxia following microglia isolation. These conditions will be described as acute hypoxia. These conditions were tested to produce an O_2 environment that would theoretically closer represent the natural environment within the brain, reported to be between 0.5 – 7 %, and provide a more realistic insight into microglia function, though not hypoxic enough to induced ischemia (Ivanovic, 2009; Lyons et al., 2016; Ndubuizu and LaManna, 2007; Lecoq et al., 2011).

4.2.3.1 NLRP3 inflammasome expression and activity in chronic 5 % O_2 hypoxia

P2X7 receptor-mediated IL-1β release was assessed in LPS (0.1 μg/ml; 4 h) and ATP (5 mM; 30 min) stimulated primary microglia cultured in either atmospheric O_2 conditions (20 %) or chronic 5 % O_2 (Figure 4.18). A two way ANOVA revealed a significant effect of LPS / ATP treatment ($F_{(3,52)}$ = 38.39, p < 0.001) and hypoxia ($F_{(1,52)}$ = 9.025, p = 0.0041) on IL-1β release, with a significant interaction between treatment and hypoxia ($F_{(3,52)}$ = 14.02, p < 0.001). Whilst LPS / ATP stimulation caused a significant release in IL-1β in 20 % O_2 (p < 0.001), IL-1β release was significantly reduced in microglia cultured in chronic 5 % O_2 (26 ± 4 % of control; n = 10; p < 0.001). Following 4 h LPS stimulation, quantification of proIL-1β (Figure 4.19A), NLRP3 (Figure 4.19B), P2X7 (Figure 4.19C) and ASC (Figure 4.19D) was assessed by western blot. For proIL-1β, a two way ANOVA revealed a significant effect of LPS on expression ($F_{(1,8)}$ = 7.49, p = 0.0256), but no effect of hypoxia ($F_{(1,8)}$ = 0.8922, p = 0.3725) and no interaction between hypoxia and LPS ($F_{(1,8)}$ = 0.8699, p = 0.3783). For NLRP3, a two way ANOVA revealed a significant effect of LPS treatment ($F_{(1,8)}$ = 33.18, p < 0.001) and hypoxia ($F_{(1,8)}$ = 9.555, p = 0.0149) on expression, and a interaction between hypoxia and LPS ($F_{(1,8)}$ = 9.506, p = 0.015). For P2X7, a two way ANOVA revealed no effect of LPS $F_{(1,8)}$ = 0.2569, p = 0.6259) or hypoxia $F_{(1,8)}$ = 1.666, p = 0.2328). For

ASC, a two way ANOVA revealed no effect of LPS $F_{(1,8)}$ = 0.4882, p = 0.5045) or hypoxia $F_{(1,8)}$ = 0.7008, p = 0.4268). The level of cytosolic NLRP3 was significantly greater in microglia cultured at chronic 5 % O_2 than 20 % O_2 ($p < 0.05$), whilst proIL-1β, P2X7 and ASC levels were not significantly affected.

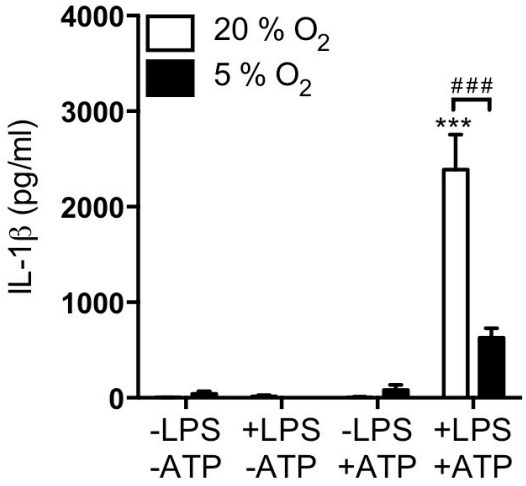

Figure 4.18. The effect of chronic 5 % O_2 availability on IL-1β release in neonatal primary microglia isolated from C57BL/6J mice.

ELISA detection of IL-1β release following LPS priming (4 h; 0.1 μg/ml) and ATP stimulation (30 min; 5 mM) under chronic (3 weeks) 20 % or 5 % O_2. Data represent mean ± SEM (n=10) and analysed by two-way ANOVA with Tukey's post hoc test. ***$p < 0.001$ compared to control; $^{###}p < 0.001$.

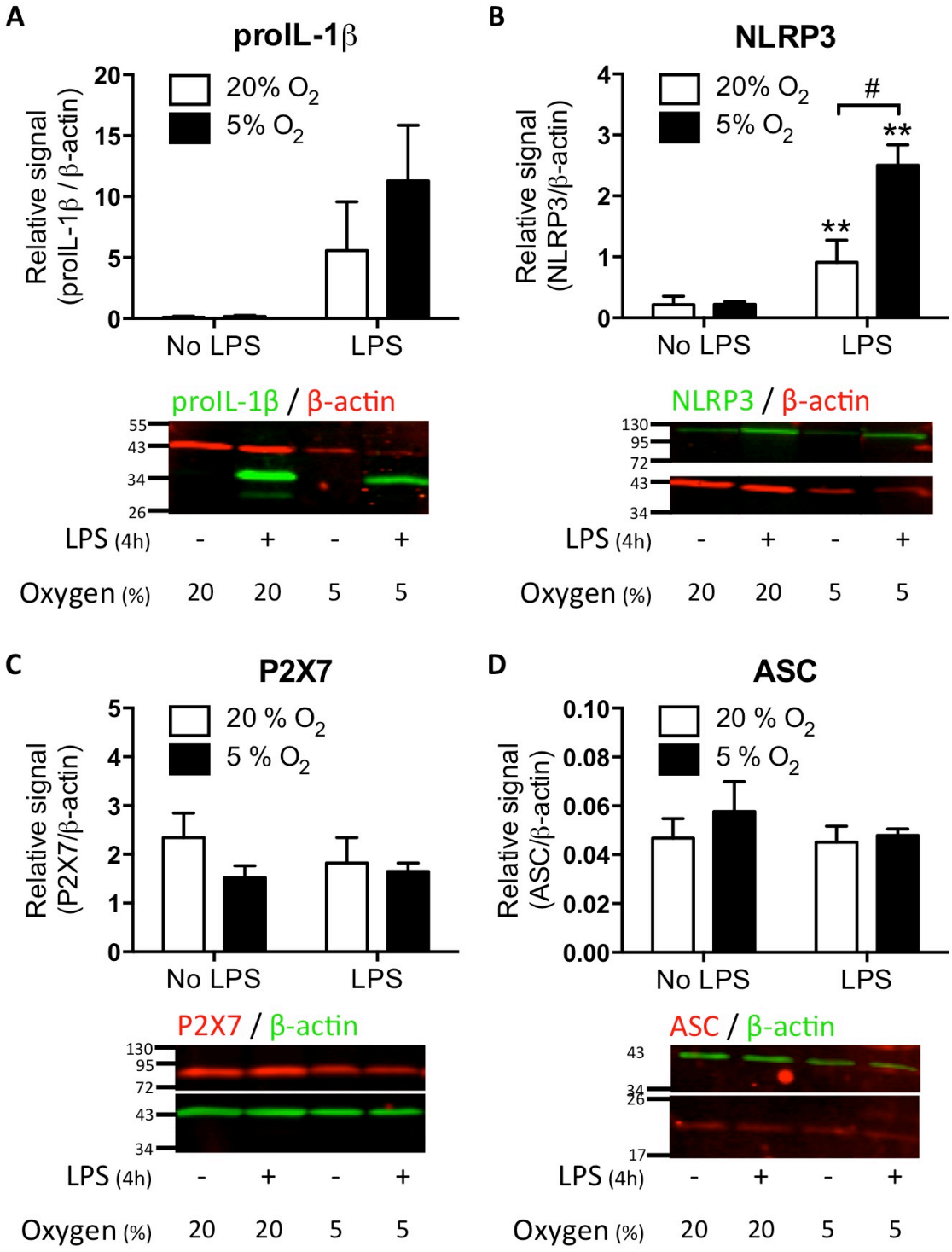

Figure 4.19. Western blot analysis of protein expression primary neonatal microglia isolated from C57BL/6J mice cultured in 20 % or chronic 5 % O_2.

ProIL-1β (green; **A**), NLRP3 (green; **B**), P2X7 (red; **C**) and ASC (red; **D**) expression in the presence and absence of LPS (0.1 µg/ml; 4 h) in primary microglia cultured in chronic (3 weeks) 20 % or 5 % O_2. Histograms represent fluorescence intensity relative to β-actin. Data shown are mean ± SEM (n=3) and analysed by two-way ANOVA with Tukey posthoc analysis. $^{**}p < 0.01$ compared to control; $^{\#}p < 0.05$.

However, when the level of loading control protein β-actin alone was quantified (Figure 4.20A), it showed that there was a significant reduction in β-actin levels in all samples (control and LPS) from chronic 5 % O_2 (23 ± 4 % of control; n = 24; *t* test, $p < 0.001$). β-actin is commonly used at a loading control as the cytosolic levels of the protein is generally unaffected by treatment and is therefore used as a means to assess protein concentration in a sample. This finding suggests that the samples of microglia cultured in 20 % O_2 contain less protein, a consequence of a reduced number of cells. In order to investigate this theory, a DNA content-based assay was used to look at the number of viable cells in the cultures. The assay was carried out on mixed glia cultures at 7, 14, 22 DIV, as well as on isolated microglia cultures on 22 DIV (Figure 4.20B). A significant effect of hypoxia was observed (one way ANOVA, $F_{(4,10)} = 20.65$, $p < 0.001$). Significant reductions in cell number were observed in chronic 5 % O_2 mixed glia cultures at 7 DIV (55 ± 11 %; n = 3; $p < 0.001$), 14 DIV (68 ± 4 %; n = 3; $p < 0.01$), 22 DIV (68 ± 2 %; n = 3; $p < 0.01$), and in isolated microglia (28 ± 6 %; n = 3; $p < 0.001$). This finding would explain why a reduction in IL-1β release is observed in chronic 5 % O_2 following stimulation: a reduced cell number.

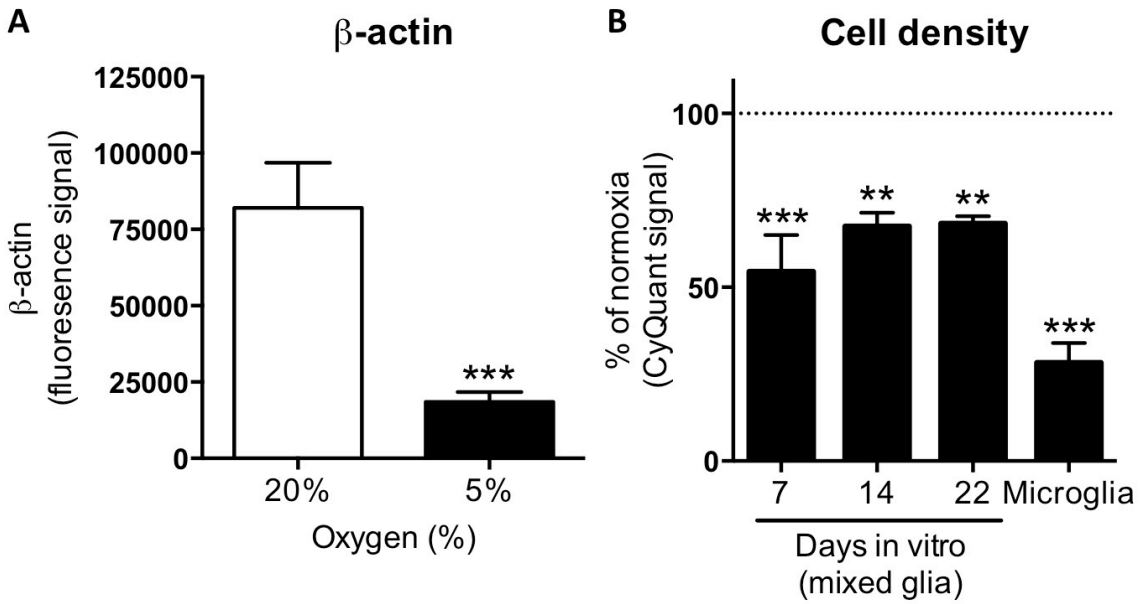

Figure 4.20. Cell density of primary neonatal microglia isolated from C57BL/6J mice cultured in 20 % or chronic 5 % O_2.

Western blot detection of β-actin expression in samples (±LPS) from primary microglia cultured in chronic (3 weeks) 20 % or 5 % O2 (**A**). Cell density assessment with a DNA-based fluorescent probe of primary mixed glia and microglia cultures in chronic 20 % or 5 % O_2 after 7, 14 and 22 days in vitro (DIV) as well as after microglia isolation (**B**). Data shown are mean ± SEM (n=24) and analysed by Student's *t*-test (**A**) or data shown are mean ± SEM (n=3) and analysed by one-way ANOVA with Dunnett's posthoc analysis (**B**). $^{**}p < 0.01$, $^{***}p < 0.001$, all compared to control.

4.2.3.2 Microglia cell density in 24 h 5 % O_2 hypoxia

To avoid the confounding factor of a reduced cell number when cultured under low O_2 conditions, microglia were cultured and isolated under normoxic conditions, and subsequently moved into 5 % O_2 before experimentation 24 h later. This allowed all microglia to proliferate at a similar rate before any change in conditions. In order to first evaluate that the microglia cell number was not affected by 24 h 5 % O_2 hypoxia, the DNA content-based assay was used to assess cell number (Figure 4.21). No significant difference in cell density was observed between 20 % O_2 and 24 h 5 % O_2 (*t* test, $p = 0.4786$). Using this protocol, the difference in proliferation when cultured under chronic 5 % O_2 was eliminated.

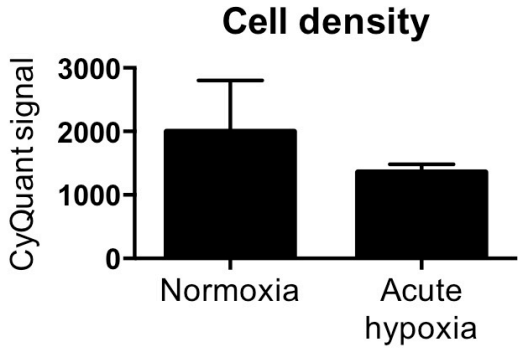

Figure 4.21. Cell density of primary neonatal microglia isolated from C57BL/6J mice in 20 % or acute 5 % O_2 (24 h).

Cell density assessment with a DNA-based fluorescent probe of primary microglia in 20 % or acute 5 % O2 (24 hr). Data shown are mean ± SEM (n=3) and analysed Student's *t*-test.

4.2.3.3 NLRP3 inflammasome expression and activity in primary microglia death in 24 h 5 % O_2 hypoxia

Following LPS priming (0.1 µg/ml; 4 h) of primary microglia exposed to 24 h hypoxia, the protein expression levels of NLRP3 (Figure 4.22A), proIL-1β (Figure 4.22B) and P2X7 (Figure 4.22C) were assessed. For NLRP3 expression, a two way ANOVA revealed a significant effect of LPS ($F_{(1,12)} = 5.861$, $p = 0.0323$) but no effect of hypoxia ($F_{(1,12)} = 0.4022$, $p = 0.5379$). For proIL-1β expression, a two way ANOVA revealed a significant effect of LPS ($F_{(1,12)} = 9.029$, $p = 0.011$) but no effect of hypoxia ($F_{(1,12)} = 0.053$, $p = 0.8224$). For P2X7 expression, a two way ANOVA revealed no significant effect of LPS ($F_{(1,8)} = 0.1295$, $p = 0.7283$) or hypoxia ($F_{(1,8)} = 0.0037$, $p = 0.9632$). Expression levels in 5 % O_2 were not significantly affected when compared to microglia cultured and stimulated in 20 % O_2, indicating a priming response similar to

normoxic conditions. Following LPS (0.1 μg/ml; 4 h) and ATP (5 mM; 30 min) stimulation, IL-1β release was assessed in 20 % O_2 and acute (24 h) O_2 (Figure 4.23A). A two-way ANOVA revealed a significant effect of ATP ($F_{(1,8)}$ = 44.79, p < 0.001) and hypoxia ($F_{(1,8)}$ = 7.514, p = 0.0254) on IL-1β release, and a significant interaction between ATP and hypoxia ($F_{(1,8)}$ = 7.353, p = 0.0266). IL-1β secretion was significantly increased in ATP-treated microglia in 20 % O_2 (p < 0.001) and significantly reduced in acute 5 % O_2 (42 ± 4 % of control; n = 3; p < 0.05), even though cell density is unaffected in 24 h hypoxia (Figure 4.21). To test whether the loss of astrocytes is a factor in the altered inflammasome function of microglia, mixed glia cultures were examined (Figure 4.23B). A two-way ANOVA revealed a significant effect of ATP ($F_{(1,8)}$ = 702.6, p < 0.001) and hypoxia ($F_{(1,8)}$ = 105.5, p < 0.001) on IL-1β release, and a significant interaction between ATP and hypoxia ($F_{(1,8)}$ = 111.5, p < 0.001). A similar pattern of IL-1β release to isolated microglia cultures was observed, with significant increase following ATP in 20 % O_2 (p < 0.001), which was significantly reduced in 24 h 5 % O_2 conditions (45 ± 2 % of control; n = 3; p < 0.001). This finding suggests that reducing the O_2 availability to 5 % inflammasome activity is attenuated shows and that whilst astrocytes have important homeostatic roles within the brain, it is not a factor responsible for this reduction. Our data did show that IL-1β release is higher when mixed glia cultures were stimulated compared to microglia alone, however the process of removing astrocytes also removes a portion of microglia as collateral which would result in an overall lower level of IL-1β release. The release of inflammatory cytokines TNF-α (Figure 4.23C) and IL-6 (Figure 4.23D) was also assessed. A two way ANOVA revealed a significant effect of stimulation on TNF-α release ($F_{(1,8)}$ = 738.8, p < 0.001), but no effect of hypoxia ($F_{(1,8)}$ = 0.264, p = 0.6213) and no interaction between stimulation and hypoxia ($F_{(1,8)}$ = 0.2168, p = 0.6539). Similarly, a two way ANOVA revealed a significant effect of stimulation on IL-6 release ($F_{(1,8)}$ = 121.0, p < 0.001), but no effect of hypoxia ($F_{(1,8)}$ = 1.325, p = 0.283) and no interaction between stimulation and hypoxia ($F_{(1,8)}$ = 1.264, p = 0.2934). A significant increase in TNF-α and IL-6 release was observed following LPS and ATP stimulation (p < 0.001 for all), but no difference between microglia incubation in 20 % O_2 or acute 5 % O_2. These data demonstrate that the reduction seen in ATP mediated IL-1β release in 5 % O_2 is specific to IL-1β and does not affect all other inflammatory cytokines.

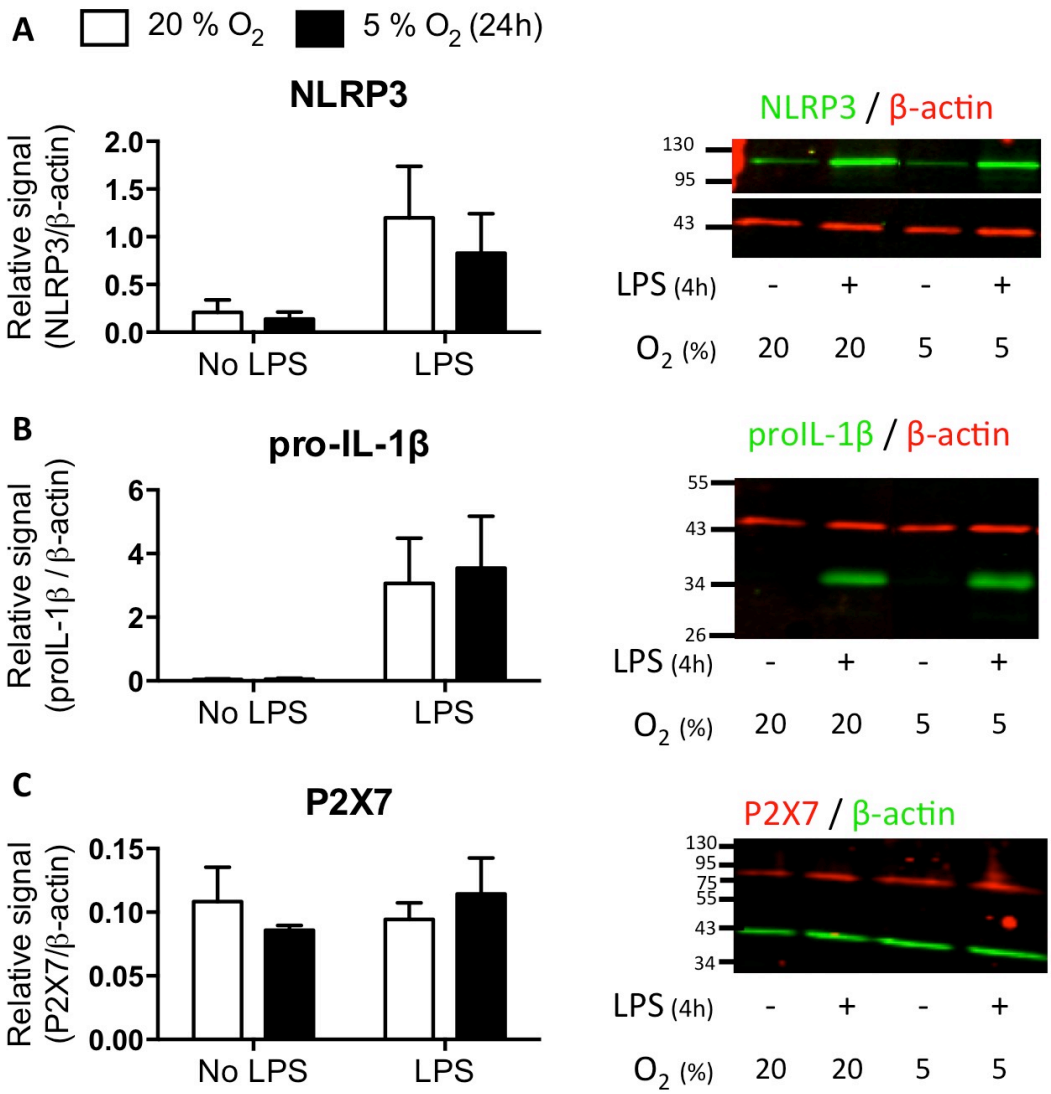

Figure 4.22. Western blot analysis of protein expression in primary neonatal microglia isolated from C57BL/6J mice in 20 % or acute 5 % O_2 (24 h).

NLRP3 (green; **A**), proIL-1β (green; **B**) and P2X7 (red; **C**) protein expression in primary microglia with and without LPS (0.1 µg/ml; 4 hr) in 20 % or acute 5 % O_2 (24 h). Histograms represent fluorescence intensity relative to β-actin. Data shown are mean ± SEM (n=3-4) and analysed by two-way ANOVA with Tukey posthoc analysis.

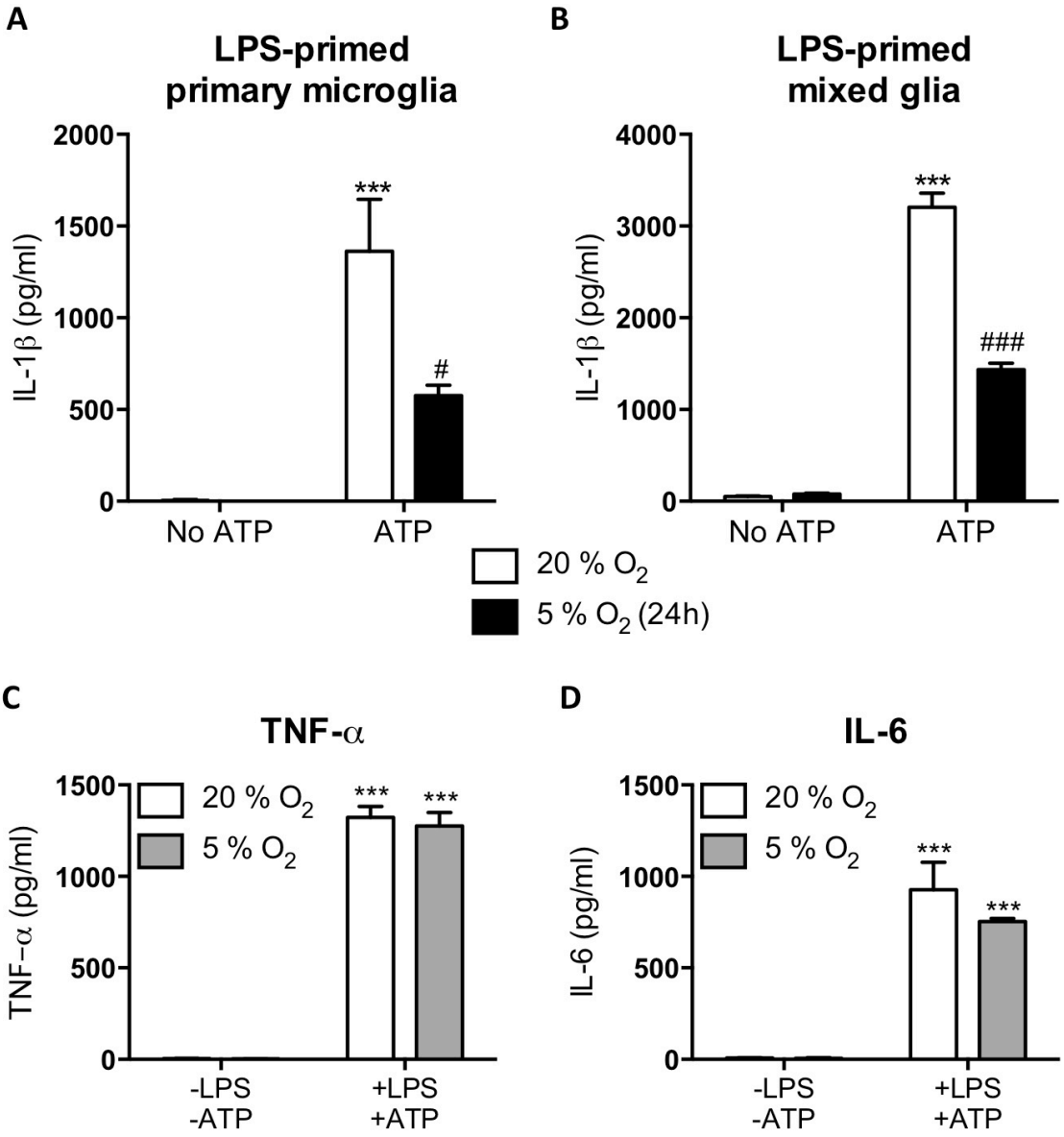

Figure 4.23. The effect of 5 % O_2 on cytokine release in neonatal primary microglia and mixed glia cultures isolated from C57BL/6J mice.

ELISA detection IL-1β release from primary microglia (**A**) and mixed glia (**B**) following stimulation with LPS (0.1 µg/ml; 4 h) and ATP (5 mM; 30 min) in 20 % or 5 % O2 (both chronic and 24 h). TNF-α (**C**) and IL-6 (**D**) release following LPS and ATP stimulation in 20 % or acute 5 % O_2 (24 h). Data represent mean ± SEM (n = 3) and analysed by two-way ANOVA with Tukey's post hoc test. $^{***}p < 0.001$ compared to 20 % O_2 no ATP; $^{\#}p < 0.05$, $^{\#\#\#}p < 0.001$, compared to 20 % O2 no ATP (**A** & **B**). $^{***}p < 0.001$ compared to unstimulated cells (**C** & **D**).

4.2.3.4 Microglia cell death in 24 h 5 % O_2 hypoxia

LDH release following LPS (0.1 µg/ml; 4 h) and ATP (5 mM; 30 min) stimulation was assessed as a measure of cell death to investigate the effect of O_2 conditions on pyroptosis associated with inflammasome activation (Figure 4.24). A two way ANOVA revealed a significant effect of treatment on LDH release ($F_{(1,12)}$ = 15.09, p = 0.0022), but no significant effect of hypoxia ($F_{(1,12)}$ = 1.692, p = 0.2178) and no interaction ($F_{(1,12)}$ = 1.931, p = 0.1899). It was found that, similar to earlier data, microglia cultured in 20 % O_2 significantly increased LDH release when stimulated (533 ± 147 % of control; n = 4; p < 0.01). When stimulated in 5 % O_2, there was not a significant increase in LDH release. However, there was also no significant difference between stimulated microglia in 20 % and 5 % O_2. This finding suggests that a higher O_2 availability may enhance P2X7 receptor-mediated cell death and pyroptosis.

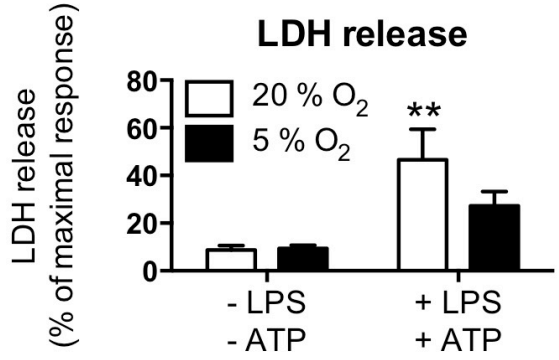

Figure 4.24. Cell death of primary neonatal microglia isolated from C57BL/6J mice in 20 % or acute 5 % O_2 (24 h).

LDH release following LPS (0.1 µg/ml; 4 h) and ATP (5 mM; 30 min) stimulation in primary microglia in 20 % or acute 5 % O2. Data shown are mean ± SEM (n=3) and analysed by two-way ANOVA with Tukey's post hoc analysis (B). **p < 0.01 compared to control.

4.2.3.5 ROS production in LPS-stimulated primary microglia in 24 h 5 % O_2 hypoxia

To try and understand some of the underlying mechanisms underlying the attenuated NLRP3 inflammasome activity observed in primary microglia under 5 % O_2 conditions, ATP-induced production of reactive oxygen species (ROS) was investigated. ROS levels have been shown to be directly linked to O_2 availability and can activate the NLRP3 inflammasome following priming (Zhou et al., 2011; Heid et al.,

2013). After LPS stimulation (0.1 µg/ml; 4 h), cells loaded with DCFDA and stimulated with ATP. DCFDA fluorescence (Figure 25.B) was then measured alongside ethidium fluorescence (Figure 25.A) in the same samples. A two way ANOVA revealed a significant effect of ATP on ethidium uptake ($F_{(3,16)}$ = 36.03, p < 0.001), but no significant effect of hypoxia ($F_{(1,16)}$ = 0.676, p = 4231) and no significant interaction ($F_{(3,16)}$ = 0.1134, p = 0.951). Significant increases in uptake ethidium were seen with 3 and 5 mM ATP in 20 % O_2 (p < 0.01 and p < 0.001, respectively) and in 5 % O_2 (p < 0.05 and p < 0.001, respectively), indicating the activation of the P2X7 receptor is insensitive to low O_2. Whilst a robust signal was detected following the addition of 100 µM hydrogen peroxide (H_2O_2), a two way ANOVA revealed no significant effect of ATP ($F_{(3,16)}$ = 1.215, p = 0.3362) or hypoxia ($F_{(1,16)}$ = 0.5331, p = 0.4759) on DCFDA signal. This result indicates no significant increase in the production of reactive O_2 species following ATP stimulation detectable by DCFDA.

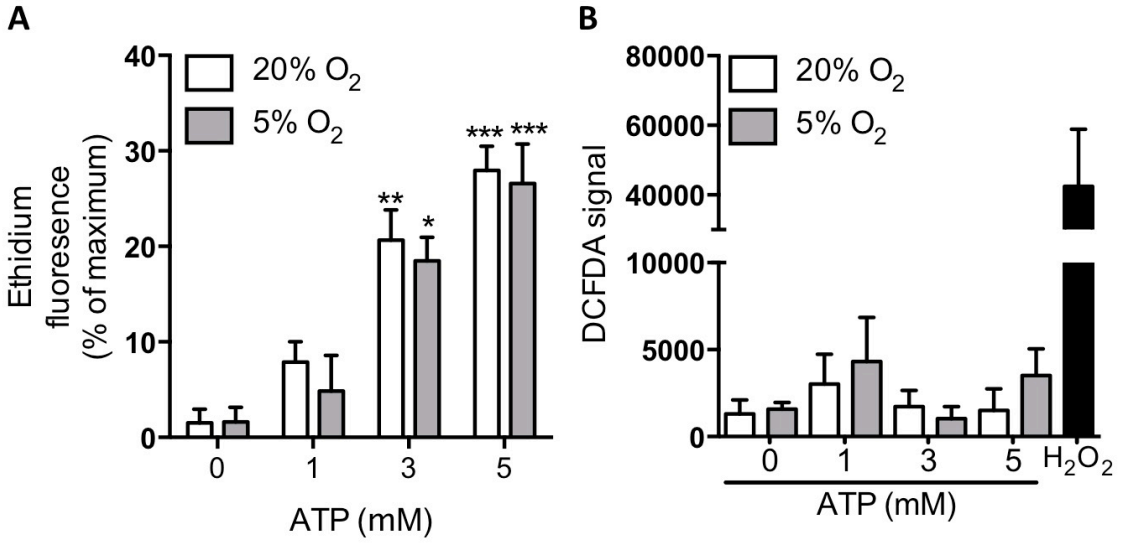

Figure 4.25. P2X7 receptor activation and ROS production following ATP stimulation in LPS-primed primary neonatal microglia isolated from C57BL/6J mice cultured in 20 % or 5 % O_2 (24 h).

Ethidium uptake at 10 min after ATP or control buffer addition (**A**) and ROS generation as detected by DCFDA fluorescence (**B**) in LPS-primed (0.1 µg/ml; 4 h) primary microglia stimulation with ATP (1 – 5 mM ATP) in 20 % or acute 5 % O2 (24 h). 100 µM H_2O_2 used as a positive control. Data shown are mean ± SEM (n=3) and analysed by two-way ANOVA with Tukey posthoc analysis.

4.3 Summary of findings

- BV2 microglia exhibit normal LPS-induced (0.1 μg/ml; 4 h) protein expression and ATP-induced (5 mM; 30 min) P2X7 receptor function, but do not express ASC and do not have a functional NLRP3 inflammasome.
- Under 5 h hypoxia (5 % O_2), LPS-induced (0.1 μg/ml; 4 h) inflammasome protein expression in BV2 microglia is attenuated.
- Primary microglia, isolated via mild trypsinisation, exhibit a ramified morphology, and express a functional NLRP3 inflammasome following LPS (0.1 μg/ml; 4 h) and ATP stimulation (5 mM; 30 min).
- Following chronic hypoxia (3 weeks; 5 % O_2), primary microglia cell number is reduced.
- Following acute hypoxia (24 h; 5 % O_2), primary microglia show attenuated ATP-induced (5 mM; 30 min) IL-1β release and cell death compared to normoxia, but no change in ATP-induced TNF-α or IL-6 release.
- No change in ROS generation was observed in primary microglia following acute hypoxia (24 h; 5 % O_2).

4.4 Discussion

4.4.1 The characterisation of NLRP3 inflammasome expression and activity in BV2 microglia and primary neonatal microglia

4.4.1.1 BV2 microglia

BV2 microglia are a raf/myc-immortalised murine neonatal microglia cell line that are regularly used to study microglia function and neuroinflammation (Blasi et al., 1990). Though BV2 microglia are not commercial available, and therefore not controlled, access to BV2 microglia is usually obtained as gifts from other research labs. As an immortalised cell line, there are a number of differences between BV2 microglia and primary microglia in terms of function and protein expression. This cell line has previously been used to study NLRP3 inflammasome function (Shi et al., 2012). Consistent with other studies, BV2 microglia exhibited CD11b expression, a commonly used marker for identifying microglia, that increased following LPS stimulation (Roy et al., 2006). The upregulation of inflammatory proteins has been previously demonstrated in BV2 microglia, whereby LPS stimulation induces NF-κB activity and protein expression (Lee and Kim, 2012; Liang et al., 2015). P2X7 expression was not altered following LPS stimulation, as P2X7 expression has not been shown to be mediated by NF-κB (Zhou et al., 2009). P2X7 expression has been reported before in microglia (Bartlett et al., 2013). A 16 h LPS stimulation of the N9 microglia cell line caused a significant reduction in P2X7 expression (Bianco et al., 2006). Similarly, long incubation with LPS (3 days) has also been shown to increase P2X7 mRNA expression in macrophages (Humphreys et al., 1998). ATP stimulation induced the uptake of ethidium in a dose-dependent fashion and could be abrogated by P2X7 receptor inhibition, demonstrating functional P2X7 receptor activity and is supported by similar findings in microglia and macrophages (Schilling et al., 1999; Pelegrin and Surprenant, 2006; Bartlett et al., 2013). P2X7 receptor function has been shown to mediate microglia activation and pore formation (Monif et al., 2009), as well as proliferation in early development (Rigato et al., 2012). Taken together, these data confirm the expected pattern of proIL-1β and NLRP3 expression in microglia (Gustin et al., 2015), alongside functional expression of P2X7 receptors. However, ASC protein expression and ATP mediated IL-1β secretion were not detected following LPS / ATP stimulation. ASC expression has previously been observed in BV2 microglia (Shi et al., 2012). IL-1β release has also been reported following ATP, prion and viral stimulation (Liang et al., 2015; Shi et al., 2012; Kaushik et al., 2012). In contrast, some studies have reported impaired IL-1β production following 24-48 h LPS stimulation (Horvath et

al., 2008). Our findings demonstrate the presence of ASC mRNA, and yet no ASC protein, indicating impaired translation and would explain the inability of BV2 microglia to produce mature IL-1β. Consistent with this data, $ASC^{-/-}$ primary microglia failed to secrete IL-1β following stimulation with *S. aureus*, whilst wildtype primary microglia exhibited a strong IL-1β response (Hanamsagar et al., 2011). Differences in the protein expression profile of BV2 microglia may contribute the differences in ASC expression and inflammasome activity, as BV2 microglia only express 17 % of proteins expressed in primary microglia following LPS stimulation (Henn et al., 2009). The lack of ASC protein and IL-1β production makes these BV2 microglia a poor platform for studying ATP-induced NLRP3 inflammasome activity.

Pyroptosis is an inflammatory form of cell death mediated by the activity of caspase-1 and subsequent cell rupture (Miao et al., 2011). The processing of gasdermin-D (GSDMD) to form membrane pores has been shown to be important in macrophage pyroptosis (Sborgi et al., 2016). Though GSDMD has not been studied in activated microglia, an earlier study reported it not to be expressed in the healthy brain (Tamura et al., 2007). BV2 microglia exhibited impaired cell death following stimulation, as assessed by LDH release. Conversely, LDH release from J774.2 macrophages was as expected. A similar pattern of LDH release has been reported in LPS-primed BMDMs, with ATP inducing a significant increase (Yu et al., 2014). An increase in cell death following ATP stimulation has previously been observed in the EOC13 microglia cell line in a P2X7 receptor-dependent manner (Bartlett et al., 2013) These findings indicate BV2 microglia display impaired pyroptosis in comparison to macrophages and microglia cell lines, as well as primary microglia (Brough et al., 2002). As pyroptosis is considered to be dependent upon caspase-1 activity, the lack of ASC protein and the subsequent lack of a functional NLRP3 inflammasome would impair the ability of ATP to induce rapid caspase-1 activity and would therefore impair pyroptosis in these cells. Other inflammasomes also depend of ASC for its functional activity, and ASC has been shown to be necessary for pyroptosis following the activation of the AIM2 and NLRP3 inflammasome (Sagulenko et al., 2013). ASC-knockout was shown to protect macrophages from cell death induced by nigericin and double-stranded DNA. With the use of fluorescent imaging to detect ASC, macrophage stimulation can be shown to induce the formation of a large aggregate of ASC that enables an amplified inflammasome signal (Fernandes-Alnemri et al., 2007). This oligomerisation of ASC provides multiple sites for the interaction with procaspase-1 and its autocleavage (Dick et al., 2016). Without ASC expression, normal pyroptosis in BV2 microglia cannot be studied.

BV2 stimulation with murine IL-1β and TNF-α failed to induce the expression of proIL-1β and NLRP3. Both IL-1β and TNF-α have long been known to bind to their respective receptors and induce NF-κB signalling, resulting in the upregulation of proinflammatory proteins (Li & Verma, 2002). The failure of cytokine-induced priming further demonstrates the atypical phenotype of the BV2 microglia used here. The lack of cytokine-induced priming, absent ATP-induced cell death, ASC protein deficiency and subsequent failed release of IL-1β suggests that for the study of NLRP3 inflammasome activity and neuroinflammation in general, BV2 microglia should be avoided. This sentiment is supported by others, who have demonstrated significant differences in inflammatory signalling in BV2 microglia compared to primary microglia (Horvath et al., 2008).

4.4.1.2 Primary neonatal microglia

As previously mentioned, there are many differences between primary microglia and an immortalised cell line, such as the BV2 microglia. These differences include altered protein expression, increased proliferation and adherence, reduced expression of NO and reduced cytokine expression in BV2 microglia when compared to primary microglia (Horvath et al., 2008). Therefore, BV2 microglia provide only a partial model of primary microglia. In order to study LPS priming and NLRP3 inflammasome signalling, the impaired IL-1β production and altered LPS-induced protein synthesis exhibited by BV2 microglia is a confounding factor (Horvath et al., 2008). Primary microglia can be harvested from the mouse brain through a number of techniques, including separation by density gradient, shaking mixed glia cultures to separate microglia, separation by immunolabeling, or the removal of astrocytes using a low concentration of trypsin (Frank et al., 2006; Giulian and Baker, 1986; Marek et al., 2008; Saura et al., 2003). Overall, the use of primary microglia cultures provides a more accurate model to study microglia function compared to cell lines.

Microglia isolation from mixed glial cultures via mild trypsinisation is an effective way to study primary microglia, that allows proliferation in the presence of astrocytes and isolation without the mechanical stress of vigorous shaking (Saura et al., 2003). Here, the isolation of CD11b-positive / GFAP-negative cells indicated the presence of microglia that exhibited a ramified and branched morphology. This method of isolation has been utilised for a number studies, including LPS-TLR4 signalling and cytokine expression, though NLRP3 inflammasome has not directly been investigated (Yao et al., 2013). The primary microglia isolated here exhibited similar LPS-induced protein expression as BV2 microglia. Importantly, primary microglia did express ASC,

necessary for inflammasome formation. Similar to macrophages, the level of ASC protein was unaffected by LPS stimulation, a finding supported by previous studies in macrophages (Yamamoto et al., 2004). ATP-induced uptake of ethidium has been shown before in microglia cell lines, as well as P2X7 receptor inhibition (Monif et al., 2009; Sanz et al., 2009; Bartlett et al., 2013). However, this has not previously been shown in primary microglia. Here, functional P2X7 receptor activity was observed in primary microglia following ATP stimulation, as well as caspase-1-dependent ATP-induced IL-1β release, consistent with previous findings in macrophages (Cruz et al., 2007). These data demonstrate the ability of these microglia cells to respond to LPS and ATP simulation and exhibit functional NLRP3 inflammasome activity. The expression and activity of the NLRP3 inflammasome in primary microglia has been reported numerous times that have used alternative isolation protocols. These studies include prion protein stimulation, bacterial and viral stimulation, ischemia, and LPS / ATP stimulation (Shi et al., 2012; Hanamsagar et al., 2011; Walsh et al., 2014b; Yang et al., 2014; Gustin et al., 2015).

Primary microglia exhibited increased LDH release following LPS / ATP stimulation similar to macrophages, demonstrating the induction of pyroptosis and cell death. As opposed to BV2 microglia, the primary microglia express ASC and therefore exhibit functional NLRP3 inflammasome activity in response to ATP, inducing caspase-1 activity necessary for pyroptosis (Miao et al., 2011). ATP-induced cell death in primary microglia, as assessed by LDH release, has been demonstrated before (Brough et al., 2002) The data in this thesis demonstrate, for the first time in detail, the characterisation of functional P2X7 receptor activity and NLRP3 inflammasome expression in primary microglia isolated by the technique of mild trypsinisation, as well as a normal ATP-induced pyroptotic response.

4.4.2 Ketamine failed to attenuate NLRP3 inflammasome priming or activation in primary microglia

Ketamine in an NMDA receptor antagonist that has been shown to suppress the depressive behaviours in mice following acute inflammatory insult (Walker et al., 2013). The authors demonstrate the ability of ketamine to abrogate LPS-induced depressive-like behaviour is probably by inhibiting the excitotoxic activity of quinolinic acid, which is upregulated following LPS administration. Microglia convert tryptophan to quinolinic acid, which is enhanced following stimulation (Heyes et al., 1996). In addition, NMDA administration has been shown to induce microglia activation *in vivo*

(Acarin et al., 1996). These data demonstrate an association between excessive glutamatergic signalling and microglia activation. *In vitro*, ketamine has previously been shown to inhibit LPS-induced secretion of TNF-α and IL-1β following extended periods of LPS stimulation (12-24 h) in primary microglia (Shibakawa et al., 2005; Chang et al., 2009). The mechanisms reportedly involved included the inhibition of LPS-induced ERK1/2 and PGE_2 signalling. Similarly, the NMDA receptor antagonist MK-801 also causes a dose-dependent reduction TNF-α release and COX-2 expression in BV2 microglia, measured 24 h after a 1 h LPS treatment (Thomas and Kuhn, 2005). *In vivo*, ketamine suppressed LPS-induced cytokine expression within the intestine via NF-κB inhibition (Sun et al., 2004). In this thesis, it was hypothesised that inhibiting the activity of the NMDA receptor in the microglia culture following LPS stimulation would attenuate microglia activation and ATP-induced NLRP3 inflammasome activity. Ketamine alone did not induce cell death, nor did it affect ATP-induced cell death, consistent with previous data in macrophages (Zhang et al., 2013). However, incubation with ketamine did not alter LPS-induced expression of inflammasome components. Furthermore, incubation with ketamine failed to alter NLRP3 inflammasome activation and IL-1β release. These findings indicate ketamine does not influence NLRP3 inflammasome expression or ATP-induced activity in microglia cells and contrast the earlier studies reporting anti-inflammatory properties of ketamine. However, these studies stimulated microglia for 12 or 24 h, which may result in a slower process of IL-1β release, as LPS can stimulate the release of ATP as a DAMP, which in turn causes inflammasome activation via P2X7 receptor activity (Sperlágh et al., 1998). The application of high concentration ATP after LPS priming accelerates IL-1β processing by enhancing the activation of the NLRP3 inflammasome immediately. This may, therefore, mask any effects ketamine may have of IL-1β production. IL-1β mRNA and protein expression following 4 h LPS stimulation in mixed glial cultures has also been shown to be reduced when incubated with ketamine (1 mM), incongruent with the protein expression observed in this study (Tanaka et al., 2013). This difference may be due to the presence of astrocytes present in the mixed glial culture. Other antidepressants have been shown to directly affect P2X7 receptor function. Whilst ketamine targets glutamate signalling, SSRI antidepressants target serotonergic signalling. The SSRI paroxetine has previously been shown to inhibit ATP-induced ethidium uptake in HEK-293 cells expressing human P2X7 and attenuate ATP-induced IL-1β release in primary monocytes (Dao-Ung et al., 2015). However, the ability to reduce ethidium uptake was only apparent for human P2X7 and not rodent P2X7. Furthermore, fluoxetine failed to suppress ethidium uptake or IL-1β release. Paroxetine, amongst other antidepressants, have also been shown to impair P2X4 mediated calcium signalling (Nagata et al., 2009). Overall, these findings demonstrate

the ability of some SSRI antidepressants to alter P2X7 receptor and IL-1β signalling, though the data here indicates ketamine does not immediately influence NLRP3 inflammasome expression or activity in primary microglia.

4.4.3 The use of primary microglia and BV2 microglia in studying neuroinflammation

The data presented in this thesis provide support for the use of primary microglia isolated via mild trypsinisation for studying NLRP3 inflammasome signalling. This method of isolation, along with the use of protocols such as CD11b-labeled magnetic beads, avoids the mechanical stress of shaking and overt microglia activation (Saura et al., 2003; Marek et al., 2008). A robust NLRP3 inflammasome signalling response can be generated, as well as P2X7 receptor signalling and ATP-induced pyroptosis. However, BV2 microglia present an inconsistent phenotype across the literature and only a partial model for studying microglia function (Horvath et al., 2008). Here, it was shown that BV2 microglia did not express ASC and therefore did not have a functional NLRP3 inflammasome. These conclusions are supported by previous work that show BV2 express only 17 % of the proteins that are observed in primary microglia following LPS stimulation (Henn et al., 2009). BV2 microglia have also been shown to exhibit impaired cytokine production, as well as increased proliferation, increased adherence and decreased NO and cytokine production (Horvath et al., 2008). However, ASC protein has previously been described before, as well as ATP-induced IL-1β expression (Shi et al., 2012). This indicates a variation in the phenotype of BV2 microglia across labs. Such variation may be due to the lack of control over the cell line, as it is not commercially available but shared between labs. Therefore, the age and any further mutations of the cell line are not monitored. In order to avoid any overt confounding factor of BV2 microglia, the cells should be characterised before use. The use of primary microglia provides a more translatable model of microglia function with functional NLRP3 inflammasome activity. Finally, mixed glia cultures may be a useful tool for studying NLRP3 inflammasome signalling, as astrocytes provide homeostatic support to microglia within the CNS and are not thought to express a functional NLRP3 inflammasome, though this is controversial (Gustin et al., 2015; Couturier et al., 2016). If true, IL-1β production could be assessed in microglia using a mixed glia culture that better replicates the environment within the brain.

4.4.4 The effect of O_2 availability on NLRP3 inflammasome signalling in microglia

The availability of O_2 within the brain is considered to range between 0.5 – 7 %, which is significantly lower than atmospheric levels of O_2 (Ivanovic, 2009). In an attempt to model the microenvironment in which microglia exists, a 5 % O_2 environment was utilised for short and extended periods of incubation. Stabilisation of HIF-1α protein has been shown to begin around 5 % O_2, and astrocytes have been show to not express HIF-1α protein at 5 % O_2 (Jiang et al., 1996; Liu et al., 2006). By incubating cells at this O_2 concentration, the role of O_2 availability on NLRP3 inflammasome signalling could be studied in primary microglia and BV2 microglia. However, the majority of hypoxia studies within existing literature use O_2 concentrations below 5 % to model ischemia, making direct comparisons difficult.

4.4.4.1 Brief 5 % O_2 hypoxia (5 h) in BV2 microglia

Whilst the BV2 microglia exhibit impaired inflammasome activity and IL-1β release, LPS priming was shown to be upregulated NLRP3 and proIL-1β (Figure 4.3). The process of LPS priming could subsequently be studied in mild hypoxia. Though basal expression levels were unaffected following a 5 h 5 % O_2 hypoxic incubation period, the LPS-induced expression of both NLRP3 and proIL-1β was attenuated. Whilst inflammation in hypoxia is regularly studied, most studies have utilised a hypoxic atmosphere of ≤ 1 % O_2 as a model of ischemia, and therefore do not represent the environment within the healthy brain. It has been shown that an 8 h hypoxia (<0.2 %) incubation in BV2 microglia attenuated in LPS-induced NF-κB activation, supporting the findings present here (Ock et al., 2007). In addition, a 24 h exposure to 1 % O_2 showed attenuated induction of MyD88 expression and NF-κB activation in hypoxia following LPS stimulation, though this finding was demonstrated in corneal epithelial cells (Pan & Wu, 2012). This article also showed significant reductions in basal TLR4 expression following hypoxia. Conversely, it has been reported that hypoxia can enhance TLR4 and NF-κB signalling. In macrophages, brief hypoxia (2 – 4 h) induced an increase in basal TLR4 expression via HIF-1α activity and enhanced LPS-induced IL-6 and COX-2 expression (Kim et al., 2010). In BV2 microglia and in primary microglia, an 8 h hypoxia exposure induced an upregulation of TLR4 expression and enhanced LPS-induced TNF-α release and increased NF-κB activity (Ock et al., 2007; Guo and Bhat, 2006). 8 h hypoxia also induced p38 MAPK activation in BV2 microglia and primary microglia (Park et al., 2002). These findings demonstrate changes in cell

type, hypoxia duration and hypoxia severity may lead to difference inflammatory responses following stimulation. Many of these pro-inflammatory effects are a result of HIF-1α activity, though HIF-1α stabilisation has been shown to have a threshold of 5 % O_2 and increase as O_2 concentration falls (Jiang et al., 1996). Astrocytes cultured in to 5 % O_2 have been shown not to express HIF-1α (Liu et al., 2006). Therefore, the difference between ≤ 1 % and 5 % O_2 incubation may have significant effects on a cells response to LPS. A study utilising a milder hypoxic model of 3 % O_2 for 24 h in primary microglia demonstrated an increase in IL-1β and TNF-α expression without stimulation (Yao et al., 2013). This is also incongruent with the findings presented here that show no induction of proIL-1β following hypoxia alone, though in this thesis a shorter exposure window of 5 h was used along with a higher O_2 concentration of 5 %. Together, these findings indicate 5 h moderate hypoxia does not alter basal expression of NLRP3 and proIL-1β in BV2 microglia but attenuates expression inducted by LPS, potentially by reducing MyD88 and NF-κB expression and activity (Pan & Wu, 2012).

4.4.4.2 Chronic 5 % O_2 hypoxia (3 weeks) in primary microglia

Though 5 h 5 % O_2 hypoxia was shown to attenuate LPS priming in BV2 microglia, this was a model of acute hypoxia and did not address the sustained hypoxic environment in which microglia exist. Furthermore, primary microglia were used for subsequent experiments as opposed to BV2 microglia in order to study a more accurate model of inflammasome signalling in microglia. From dissection, mixed glia cultures take up to 3 weeks to reach confluency. In an attempt to maintain the low O_2 environment in the brain, cells were cultured and microglia were isolated entirely under 5 % O_2 conditions to maintain constant hypoxia. Under these chronic hypoxia conditions, ATP-induced IL-1β release in LPS-primed cells was significantly attenuated, indicating a diminished ATP-induced inflammatory response. However, the cell number of primary microglia cultured in chronic 5 % O_2 was significantly decreased (Figure 4.19). This was demonstrated by assessment of β-actin levels and by a DNA-content assay that showed the final primary microglia culture in hypoxia had a cell density approximately one third of that apparent in primary microglia cultured at 20 % O_2. These findings indicate that culturing mixed glia in chronic 5 % O_2 impaired proliferation and survival.

Much of the work studying cell proliferation under hypoxic conditions is directed towards understanding tumour growth. Severe hypoxia has been shown to impair cell survival and enhance apoptosis and necrosis (Shimizu et al., 1996; Papandreou et al., 2005). This process involves the breakdown of the mitochondrial membrane and

increased caspase-9 activity (Weinmann et al., 2004). Low levels of O_2 can impair mitochondrial respiration, necessary for the production of ATP, as well as enhance ROS generation (Semenza, 2007). However, less severe hypoxia (~1 – 3 % O_2) is considered to enhance cell survival (Mazure and Pouysségur, 2010). This control of cell survival and proliferation in different O_2 conditions is mediated via the action of HIF-1α, which can help a cell adapt to reduced O_2 environments by reducing mitochondrial O_2 consumption (Carmeliet et al., 1998; Papandreou et al., 2006). Suppression of HIF-1α can result in increased hypoxia-induced cell death (Kilic et al., 2007). These findings contrast the data presented here, as chronic mild hypoxia reduced cell number. However, many of the studies assessing hypoxia are 24 or 48 h incubations at lower O_2 concentration, whilst here, cells were in a mild hypoxic environment for 3 weeks. In addition, culturing primary astrocytes under chronic mild hypoxia of 5 % O_2 does not induce HIF-1α, suggesting HIF-1α signalling is not mediating the change in cell density observed (Liu et al., 2006). In this study, culturing primary astrocytes under chronic mild hypoxia of 5 % O_2 avoided the reduced proliferation of $SOD2^{-/-}$ astrocytes seen in 20 % O_2 (Liu et al., 2006). As $SOD2^{-/-}$ astrocytes cannot neutralise superoxide radicals, this demonstrates that at 20 %, there is excessive superoxide, which inhibits cell survival in $SOD2^{-/-}$ astrocytes. Reducing the O_2 to 5 % reduced superoxide levels and enabled cell survival of $SOD2^{-/-}$ astrocytes. In addition, low-dose H_2O_2 has been shown to enhance cell proliferation in various cells, as low levels of ROS can act as endogenous signalling molecules in healthy cellular function (Liu et al., 2003; Liu et al., 2002; Na et al., 2008; Stone and Collins, 2002). Therefore, it may be that in 20 % O_2 there is an increase in ROS levels due to the greater O_2 availability, enhancing cell proliferation but not inducing oxidative stress. Culturing cells at 5 % O_2 avoids excessive ROS generation (enabling $SOD2^{-/-}$ astrocytes to survive) and may attenuate ROS-enhanced proliferation, without the hypoxia being severe enough to induce oxidative stress itself. However, to make a direct comparison between the effects of O_2 on NLRP3 inflammasome signalling, the same cell density is required. Therefore, a 24 h hypoxia incubation period was utilised following long-term culture in 20 % O_2.

4.4.4.3 Acute 5 % O_2 hypoxia (24 h) in primary microglia

To avoid the confounding factor of altered cell proliferation under 5 % O_2 hypoxia, mixed glia were cultured in 20 % O_2 and transferred to 5 % O_2 incubation immediately after isolation of primary microglia for 24 h prior to sample collection. By doing so, it can be assured a similar cell density is being examined, confirmed

following DNA-content assessment. In accordance, it has been previously demonstrated that low O_2 (3 %) exposure in BV2 microglia does not significantly affect cell viability (Yao et al., 2013). Following 24 h 5 % O_2 incubation, basal and LPS-induced expression of NLRP3, proIL-1β, P2X7 and ASC were unchanged, demonstrating 5 % O_2 hypoxia does not affect LPS-priming in primary microglia. Hypoxia (1 % O_2) has been shown to significantly increase NF-κB-mediated transcription activation in HeLa cells after 48 h, though NF-κB translocation into the nucleus was detected after 4 h. This process was via the phosphorylation of IKK (IκB kinase), which leads to the phosphorylation of IκB and activation of NF-κB (Cummins et al., 2006). Furthermore, 24 h 2 % O_2 in macrophages has been shown to increase LPS-induced expression of NLRP3 and proIL-1β in macrophages, though a far lower concentration of LPS (5 ng/ml) was used (Folco et al., 2014). Conversely, in corneal endothelial cells, hypoxia (1 % O_2 24 h) has been shown to attenuate LPS-induced MyD88 expression and IL-6 secretion (Pan & Wu, 2012). As detailed earlier, hypoxia has been reported to both increase and decrease TLR4 expression, and also induce IL-1β and TNF-α secretion in BV2 microglia (Kim et al., 2010; Pan & Wu, 2012; Ock et al., 2007). Therefore, hypoxia has the capability to alter protein expression, though the data presented here demonstrates that 24 h 5 % O_2 does not change basal expression or LPS-induced expression in primary microglia. For this reason, 5 % hypoxia may be an appropriate and physiologically valid environment to examine microglia function, as LPS-induced inflammatory priming is not enhanced at this point, but further reductions in O_2 can induce inflammatory signalling. In addition, previous studies have shown that 5 % O_2 does not induce HIF-1α stabilisation (Liu et al., 2006; Jiang et al., 1996).

Though the LPS-induced expression of NLRP3 and proIL-1β were unaffected by 24 h 5 % O_2 hypoxia, ATP-induced IL-1β release was significantly attenuated. This reduction was specific for IL-1β, as ATP-induced TNF-α and IL-6 levels were unchanged, indicating 24 h hypoxia specifically suppressed IL-1β processing. In addition, P2X7 receptor-activity as assessed by ethidium uptake was not impaired at 5 % O_2, demonstrating an effect of low O_2 downstream from P2X7. Many studies have shown an altered pattern of cytokine secretion under hypoxic conditions. In the same conditions as described here (24 h; 5 % O_2), LPS-induced IL-6 production was attenuated in placental cells, as well as LPS-induced ROS (Shirasuna et al., 2015). Whilst this demonstrates an anti-inflammatory effect of 5 % O_2 hypoxia, the data here shows that in primary microglia IL-1β and not IL-6 was attenuated by 5 % O_2. In LPS-primed macrophages, stimulation with an NLRP3 inflammasome activator (cholesterol crystals), IL-6 and TNF-α production was unaffected by incubation in 2% O_2, as reported here with ATP stimulation (Folco et al., 2014). However, IL-1β production was enhanced in hypoxia, demonstrating 2% hypoxia enhances NLRP3 inflammasome

activation. This is supported by enhanced LPS-induced IL-1β production following 24 h 3% O_2 hypoxia (Yao et al., 2013). These findings demonstrate NLRP3 inflammasome activity in particular is sensitive to O_2 concentration. Whilst lower levels of O_2 enhance IL-1β production, the data presented here indicates 5 % O_2 attenuates NLRP3 inflammasome activity.

Astrocytes play an important role in homeostasis within the CNS (Gee and Keller, 2005). ATP-induced IL-1β release in mixed glia cultures was tested to assess if astrocytic support abrogated the impaired IL-1β release seen in primary microglia in 5 % hypoxia, however a mixed glia culture did not provide protection from the hypoxia-induced attenuation of IL-1β release. Astrocytes have been shown to not exhibit NLRP3 inflammasome activity and would therefore not contribute to ATP-induced IL-1β production (Gustin et al., 2015). However, there are contrasting studies that report astrocytic production of IL-1β (Couturier et al., 2016). In comparison to primary microglia, all ATP-induced IL-1β production was higher in mixed glia samples, though this was probably due to loss of microglia during the isolation process. This finding indicates the effect of hypoxia on NLRP3 inflammasome function is directly through microglia function, and not through the absence of astrocytic support.

Cell death was significantly increased following ATP stimulation. In 5 % O_2 hypoxia, this increase was not statistically significant. This indicates a potential reduction in ATP-induced pyroptosis under low O_2 conditions. This could be due to a reduction in ROS generation and, subsequently, a reduction in inflammasome signalling and cell death following ATP (Cruz et al., 2007; Heid et al., 2013). In addition, reduced pyroptosis and pore formation via GSDMD, which mediates LDH release in BMDMs, is important in the release of IL-1β as $GSDMD^{-/-}$ macrophages exhibit impaired nigericin-induced release (Shi et al., 2015). Therefore, the reduction in pyroptosis and pore formation may be the reason for reduced IL-1β release, as opposed to attenuated IL-1β processing. However, there was no statistical significance between 20 % O_2 and 5 % O_2 following ATP stimulation. 8 h hypoxia has been shown to enhance LDH release in unstimulated primary microglia (Guo & Bhat, 2006). However this was carried out using ≤0.2 % O_2, which has been shown to induce cell death (Shimizu et al., 1996; Papandreou et al., 2005). In $SOD2^{-/-}$ astrocytes, 5 % O_2 reduced cell death by lowering ROS generation (Liu et al., 2006). Together, these findings indicate that whilst severe hypoxia alone can induce cell death, 5 % O_2 may attenuate ATP-induced cell death. This conclusion would fit with the reduction in ATP-induced NLRP3 inflammasome activity observed in 5 % O_2, as the induction of caspase-1 activity is considered to drive pyroptosis (Miao et al., 2011; Kim et al., 2015).

A reasonable explanation for the attenuated NLRP3 inflammasome activation at 5 % O_2 is a reduction in the level of ROS, a mediator of inflammasome activity. At the same time, 5 % O_2 is not hypoxic enough to induce HIF-1α signalling, oxidative stress and increased ROS generation. Severe hypoxia can induce ROS generation in many cells, including microglia cells, and mediate cell activation and cytokine release (Guo and Bhat, 2006; Park et al., 2002; Lu et al., 2006). The increase in ROS in severe hypoxia can lead to HIF-1α stabilisation (Chandel et al., 2000). In addition, the generation of ROS relative to O_2 availability has been shown to be linear, until severe hypoxia induces an increase (Yao et al., 2013; Hernansanz-Agustín and Izquierdo-Álvarez, 2014). In a study utilising 5 % O_2 for glial cells, it was shown that $SOD2^{-/-}$ astrocytes required 5 % O_2 to survive due to an inability to regulate the generation of superoxide radicals at 20 % O_2 (Liu et al., 2006). Therefore, whilst LPS-induced expression of pro-inflammatory proteins is unaffected at 5 % O_2, a small reduction in ROS signalling may mediate the attenuated ATP-induced IL-1β production. To study this, DCFDA was used to measure intracellular ROS generation. However, in primary microglia cultures, no difference in ROS were detected between 20 % and 5 % O_2, indicating ROS levels are unaffected. ATP stimulation also failed to induce a significant induction of ROS. This is inconsistent with previous reports that demonstrate ATP-induced ROS detection with DCFDA, as ATP has been shown to induce increased levels of ROS in the BV2 microglia, EOC13 microglia, primary microglia and macrophages via P2X7 receptor activation at concentrations between 1 and 3 mM ATP (Bartlett et al., 2013; Spencer et al., 2016; Parvathenani et al., 2003; Cruz et al., 2007). In the same samples in which ROS was measured, ATP-induced ethidium uptake was detected, indicating the presence of functional P2X7 receptor signalling in a dose-dependent manner in primary microglia, though no significant changes in DCFDA signal. This may be due to a weak signal, as primary microglia isolation results in a relatively low density, and measurement had to be done in a clear-bottom 12-well plate due to the mild trypsinisation protocol. The use of DCFDA has several limitations, such as its non-specificity, its susceptibility to self-amplification (as partial oxidisation of DCF can react with O_2 to generate $O\bullet^-$ and, in turn, H_2O_2), and the assumption that all conditions exhibit the same efficiency in DCF radical generation and redox cycling (Kalyanaraman et al., 2012). Therefore, whilst the ethidium-DNA fluorescence is strong enough to produce a detectable signal, the DCFDA fluorescence may have not been. In addition, the primary microglia used here were LPS-primed. Priming BV2 microglia has been shown to enhance the ATP-induced ROS production, and therefore a signal would be expected (Spencer et al., 2016). In order to elucidate the effect of ROS on NLRP3 inflammasome activation in 5 % and 20 % O_2 microglia cultures, a ROS inhibitor could be utilised or an alternative method of ROS detection such as electron

spin resonance, which can enable sensitive detection of short-lived ROS (Kohno, 2010). In addition, other primary microglia preparations could be used to a higher cell density and seeding in a 96-well plate.

4.4.5 Conclusions

The data presented in this chapter demonstrate a NLRP3 inflammasome signalling in primary microglia isolated by mild trypsinisation but not in the BV2 microglia cell line, which exhibited a number of atypical characteristics. In primary microglia, NLRP3 inflammasome signalling and pyroptosis was shown to be attenuated in 5 % O_2, demonstrating a sensitivity to O_2 availability. However, the underlying mechanisms were not elucidated. This use of 'mild hypoxia' may provide a better model for studying neuroinflammation *ex vivo.*

Chapter 5: Investigating the involvement of NLRP3 in microglia function and inflammation-induced depressive behaviour using NLRP3$^{-/-}$ mice

5.1 Introduction

5.1.1 Generation of NLRP3$^{-/-}$ mice

To investigate the role of NLRP3 in microglia function and LPS-induced depressive-like behaviour, NLRP3$^{-/-}$ mice (B6.129S6-Nlrp3^{Tm1Bhk}/J; Jackson Labs, UK) were obtained for behavioural assessment and microglia isolation. The NLRP3$^{-/-}$ mice were first generated by using a neomycin resistance cassette to replace the entire NLRP3 coding sequence in 129S6-derived embryonic stem (ES) cells, and the resulting chimeric males were bred with 129S6/SvEvTac females and subsequently bred to C57BL/6J mice for at least 11 generations (Kovarova et al., 2012). Homozygous NLRP3-knockout mice are fertile and viable, with no identified specific behavioural phenotype. The mice were originally generated to demonstrate the selectivity of NLRP1 in IL-1β production in macrophages stimulated with lethal toxin of *Bacullus anthracis* (Kovarova et al., 2012). It was shown that NLRP3$^{-/-}$ macrophages exhibit normal LDH release following LPS and lethal toxin, and that lethal toxin-induced IL-1β release was NLRP1-dependent and not NLRP3-dependent. In addition, it was shown that IL-1β production in response to the microbial components muramyl dipeptide or peptidoglycan following LPS priming was NLRP3-dependent.

5.1.2 NLRP3 signalling in microglia and disease

Microglia mediate the CNS response to danger and pathogenic signals such as LPS and ATP, which require a functional NLRP3 inflammasome in order to produce the proinflammatory cytokine IL-1β (Gustin et al., 2015). As detailed in Chapter 4 (Section 4.2.2.4), in addition to the production of pro-inflammatory cytokines, ATP-induced inflammasome activation can lead to a form of inflammation-induced cell death in microglia, called pyroptosis (Bergsbaken et al., 2009). NLRP3 inflammasome signalling in microglia has been implicated in the pathophysiology of numerous neurological disorders (Walsh et al., 2014a). Enhanced expression of inflammasome components have been detected in the microglia of HIV-infected people, and HIV infection of microglia cultures enhances ASC translocation, caspase-1 activity and IL-1β release (Walsh et al., 2014b). In modeling brain abscesses, *Staphylococcus aureus* induces NLRP3-mediated IL-1β production in microglia via ATP-dependent means (Hanamsagar et al., 2011). In a G93A-SOD1 transgenic mouse model of amyotrophic lateral sclerosis (ALS), microglia exhibit increased caspase-1 activity and IL-1β production (Meissner et al., 2010). α-synuclein, a hallmark protein of Parkinson's

disease, can also induce IL-1β release in microglia cells in a caspase-1-dependent process via endocytosis and lysosomal damage (Zhou et al., 2016). Microglia exposure to prion peptides (PrP106-126) induces NLRP3 inflammasome activation via K^+ and ROS signalling (Shi et al., 2012). Capsase-1 expression was enhanced in the brains of AD patients, and NLRP3$^{-/-}$ mice exhibit protection from cognitive impairments in a genetic mouse model of AD (APP/PS1). In addition, NLRP3-knockout reduced the level of amyloid-β deposition and enhances amyloid-β phagocytosis in microglia isolated from AD mice (Heneka et al., 2014).

5.1.3 P2X7 receptor and NLRP3 inflammasome signalling in mouse models of depressive-like behaviour

There have been several recent studies investigating the role of NLRP3 in neuroinflammation and depressive-like behaviour in rodents. It has be suggested that inflammasome signalling has a role in the pathology of psychiatric disorders, including depression (Iwata et al., 2013). This is a result of the growing evidence implicating inflammation, and in particular IL-1β signalling, in inflammation-induced and stress-induced models of depression. Inhibiting the activity of IL-1β, through antagonism (IL-1Ra) or genetic knockouts (IL-1R$^{-/-}$ and capsase-1$^{-/-}$), can attenuate or even abolish inflammation-mediated sickness and depressive-like behaviours as well as the depressive-like and antineurogenic effects of chronic stress (Koo and Duman, 2008; Lawson et al., 2013a; Zhu et al., 2010). The central administration of IL-1β alone can induce sickness behaviour similar to LPS, though LPS stimulation is not completely dependent upon IL-1β as other inflammatory cytokines such as TNF-α are thought to compensate (Bluthé et al., 2000). Pharmacological inhibition of caspase-1 has also been shown to abrogate acute LPS-induced depressive-like behaviour in mice (Zhang et al., 2014). Furthermore, the same group showed that pre-treatment with an alternative caspase-1 inhibitor inhibited the depressive-like effects of chronic mild stress (Zhang et al., 2015). Restraint stress-induced depressive behaviours have also been shown to require a functional NLRP3 inflammasome, with NLRP3-knockout mice protected from the depressive effects of stress (Alcocer-Gómez et al., 2015). One study has also shown that peripheral blood mononuclear cells isolated from individuals with depression exhibit elevated levels of ASC mRNA, indicating enhanced inflammasome expression (Momeni et al., 2016).

P2X7 receptor signalling is an important mediator of NLRP3 inflammasome activity. A recent study reported chrysophanol, a Chinese natural medicine, to reduce

P2X7 expression and attenuate LPS-induced depressive-like behaviour, though the detailed mechanisms of action were not elaborated upon (Zhang et al., 2016). Mice lacking P2X7 (deletion of the carboxyl-terminal domain) exhibit an antidepressant phenotype in the TST and FST compared to wildtype mice (Basso et al., 2009). P2X7-knockout mice also show resilience in a repeated FST model of stress, whereas wildtype mice show an increase in immobility following repeated FST exposure (Boucher et al., 2011). These studies indicate the potential of targeting the P2X7 receptor in depression. The SSRI paroxetine has been reported to suppress P2X7 receptor-induced inflammasome activity in human monocytes, demonstrating a link between SSRI antidepressant function and attenuated inflammasome activity (Dao-Ung et al., 2015). Acute restraint stress in rats has been shown to induce an increase in extracellular ATP and glutamate in the hippocampus, and the administration of a selective P2X7 receptor inhibitor (A-804598) blocked the stress-induced expression of pro-inflammatory cytokines and NLRP3 inflammasome activation (Iwata et al., 2016). In addition, chronic treatment with the P2X7 receptor antagonist reversed chronic unpredictable stress-induced depressive-like behaviours. IL-1β inhibition via targeted antibody treatment was also able to reverse the depressive-like behavioural effects of chronic stress (Iwata et al., 2016). These findings demonstrate the importance of stress-induced ATP-P2X7-NLRP3-IL1β signalling in the development of depressive-like behaviour and the ability of psychological stimuli to induce pro-inflammatory signalling within the brain.

5.1.4 Aims of Chapter 5

In this thesis chapter, NLRP3$^{-/-}$ mice were used in the 3-day ID repeated LPS model detailed earlier (Section 3.4.6) to assess the role of NLRP3 in inflammation-induced sickness and depressive-like behaviours. In addition, microglia priming and activation, as well as ATP-P2X7 signalling and cell death were investigated in NLRP3$^{-/-}$ microglia to evaluate the involvement of the NLRP3 inflammasome in these functions.

5.2 Results

5.2.1 Inflammatory signalling in NLRP3$^{-/-}$ primary microglia

5.2.1.1 Validation of NLRP3$^{-/-}$ mice

Four breeding pairs of wildtype C57BL/6J mice (NLRP3$^{+/+}$) and four pairs of NLRP3$^{-/-}$ mice (on a C57BL/6J genetic background) were obtained from Charles River (UK). Genotyping of the first generation (F1) NLRP3$^{-/-}$ and NLRP3$^{+/+}$ mice was carried out (Section 2.2). NLRP3$^{-/-}$ mice samples did not contain the NLRP3 gene but did contain the internal control, whilst NLRP3$^{+/+}$ mice samples contained both genes (Figure 5.1).

5.2.1.2 NLRP3$^{-/-}$ neonatal microglia cultures

Neonatal mixed glia were cultured from NLRP3$^{+/+}$ and NLRP3$^{-/-}$ mice and primary microglia were isolated as described previously, resulting in a CD11b-positive and GFAP-negative culture (Section 2.3.2). Primary microglia were isolated by mild trypsinisation after 21 DIV and tested after 22 DIV. To ensure a similar number of microglia were obtained from NLRP3$^{+/+}$ and NLRP3$^{-/-}$ cultures, cell density was assessed via CyQuant analysis of DNA content (Figure 5.2). No significant difference in cell density was observed between NLRP3$^{-/-}$ and NLRP3$^{+/+}$ microglia cultures (*t* test, $p = 0.4022$), indicating the lack of NLRP3 has not affected the ability of neonatal microglia to survive and proliferate.

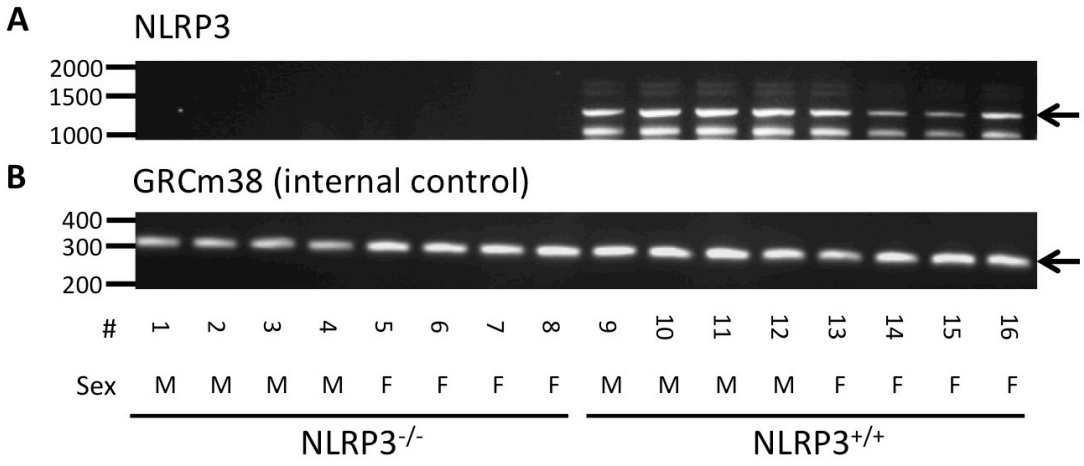

Figure 5.1. Genotyping of NLRP3$^{-/-}$ mice.

DNA isolated from ear clippings of NLRP3$^{+/+}$ and NLRP3$^{-/-}$ F1 mice breeding pairs were genotyped using primers designed to target NLRP3 (**A**) and GRCm38, a validated internal control (**B**).

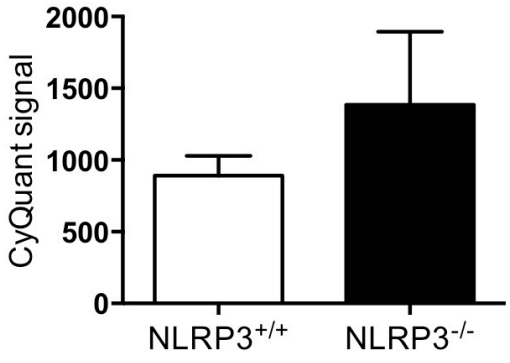

Figure 5.2. The viability of NLRP3$^{-/-}$ primary microglia cultures.

Assessment of NLRP3$^{+/+}$ and NLRP3$^{-/-}$ neonatal primary microglia cultures (22 DIV) with a DNA-based fluorescent probe. Data shown are mean ± SEM (n=3) and analysed by Student's *t*-test.

To confirm the absence of NLRP3 protein in primary microglia cultures, NLRP3 protein expression was assessed via quantitative western blotting (Figure 5.3A). Primary microglia were incubated with or without LPS (0.1 µg/ml; 4 h). A two-way ANOVA revealed a significant effect of LPS treatment ($F_{(1,8)}$ = 20.66, p = 0.0019) and genotype ($F_{(1,8)}$ = 42.17, p < 0.001), with a significant interaction between the two ($F_{(1,8)}$ = 20.28, p = 0.002). NLRP3$^{+/+}$ microglia expressed NLRP3 at a significantly higher level following LPS stimulation compared to unstimulated baseline expression (p < 0.001). NLRP3 expression could not be detected in NLRP3$^{-/-}$ microglia at baseline nor after LPS stimulation. There was a significant difference between NLRP3 expression in LPS stimulated NLRP3$^{+/+}$ and NLRP3$^{-/-}$ microglia (p < 0.001).

Isolated microglia were stimulated with LPS (0.1 µg/ml; 4 h) and ATP (5 mM; 30 min) to assess NLRP3 inflammasome function and IL-1β release (Figure 5.3B). A two-way ANOVA revealed a significant effect of treatment ($F_{(3,16)}$ = 8.896, p = 0.0011) and genotype ($F_{(1,16)}$ = 5.594, p = 0.031), with a significant interaction between the two ($F_{(3,16)}$ = 5.594, p = 0.0081). Stimulation of NLRP3$^{+/+}$ microglia with both LPS and ATP induced a significant release in IL-1β (p < 0.01). The small level of IL-1β observed in the NLRP3$^{-/-}$ microglia is most likely a result of cell death following LPS and ATP stimulation (as demonstrated later by LDH release, Section 5.2.1.4), and in turn the release of cytosolic proIL-1β. Furthermore, there was a significant difference between IL-1β release in stimulated NLRP3$^{+/+}$ and NLRP3$^{-/-}$ microglia (p < 0.01). In addition, the level of IL-6 and TNF-α released in the same samples was assessed (Figure 5.3C-D). A two-way ANOVA revealed a significant effect of treatment ($F_{(1,8)}$ = 35.82, p < 0.001) on IL-6, but no effect of genotype ($F_{(1,8)}$ = 2.502, p = 0.1524). Similarly, a two-way ANOVA revealed a significant effect of treatment ($F_{(1,8)}$ = 40.47, p < 0.001) on TNF-α, but no effect of genotype ($F_{(1,8)}$ = 1.897, p = 0.2058). There were no significant differences in IL-6 or TNF-α release in NLRP3$^{+/+}$ and NLRP3$^{-/-}$ microglia following stimulation.

Together, these data show that NLRP3$^{-/-}$ microglia do not express NLRP3, nor do they exhibit IL-1β release following LPS priming and ATP stimulation *in vitro*. However, the ATP-induced production of other pro-inflammatory cytokines is unaffected.

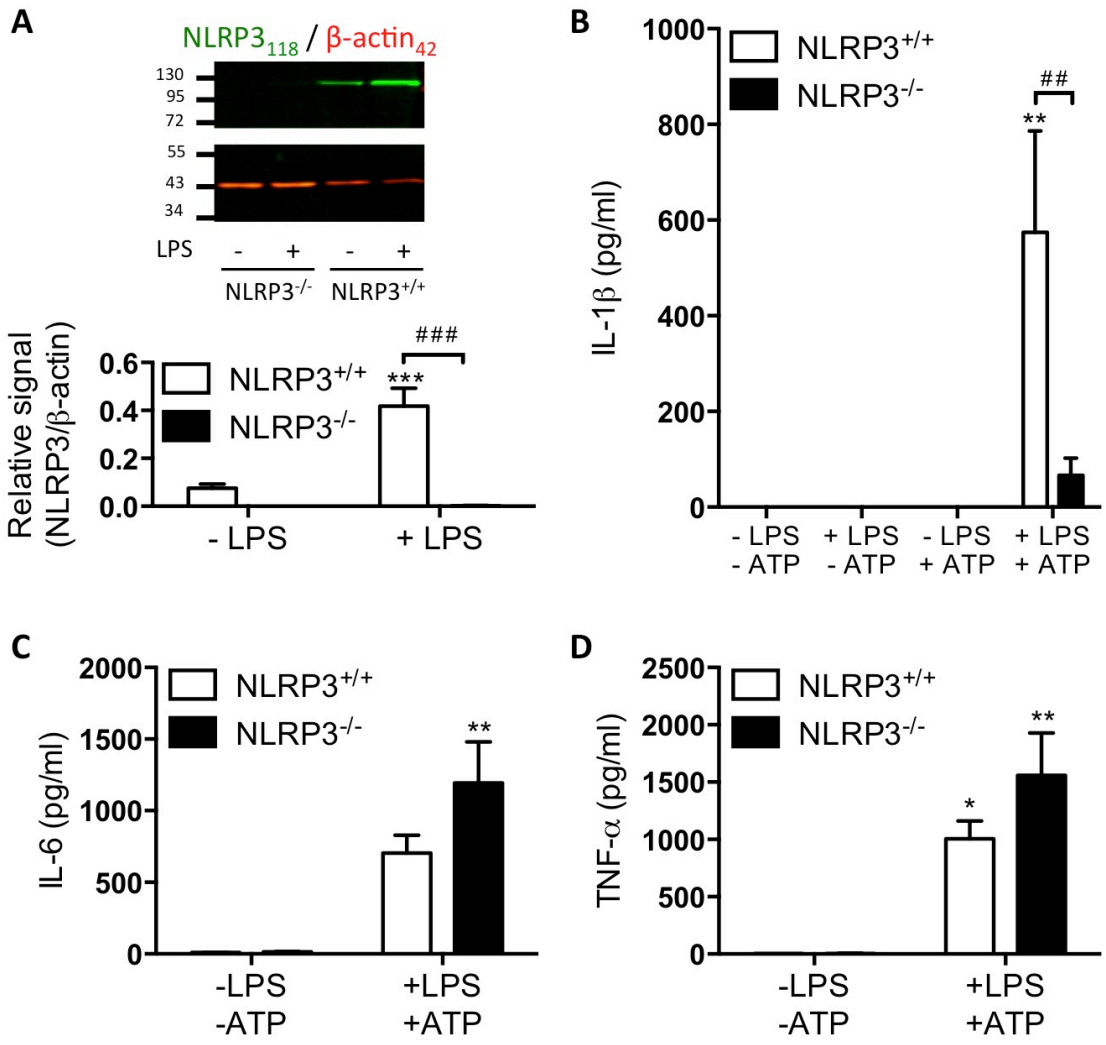

Figure 5.3. Characterisation of neonatal primary microglia isolated from NLRP3-/- mice.

Cytosolic expression of NLRP3 protein was assessed via quantitative western blotting with and without LPS stimulation (0.1 µg/ml; 4 hr) (**A**). The release of IL-1β (**B**), IL-6 (**C**) and TNF-α (**D**) following LPS (0.1 µg/ml; 4 hr) and ATP (5 mM; 30 min) in NLRP3$^{+/+}$ and NLRP3$^{-/-}$ microglia cultures (22 DIV). Data represent mean ± SEM (n=3) and analysed by two-way ANOVA with Tukey's post hoc test. *p < 0.05, **p < 0.01 ***p < 0.001 compared to control; $^{\#}p$ < 0.05 $^{\#\#\#}p$ < 0.001.

5.2.1.3 Protein expression and P2X7 receptor activity in NLRP3$^{-/-}$ neonatal microglia

Quantitative western blotting was used to assess the expression of proIL-1β (Figure 5.4A), ASC (Figure 5.4B) and P2X7 (Figure 5.4C) following LPS stimulation (0.1 µg/ml; 4 h) in NLRP3$^{-/-}$ microglia. A two-way ANOVA revealed a significant effect of LPS treatment ($F_{(1,8)}$ = 10.63, p = 0.0115) on proIL-1β expression, but no effect of genotype ($F_{(1,8)}$ = 2.332, p = 0.1653). A two-way ANOVA revealed no significant effect of LPS treatment ($F_{(1,8)}$ = 0.1433, p = 0.7148) or genotype ($F_{(1,8)}$ = 0.0816, p = 0.7824) on ASC expression. However, for P2X7 expression, a two-way ANOVA revealed no significant effect of LPS treatment ($F_{(1,8)}$ = 1.763, p = 0.2209), but a significant effect of genotype ($F_{(1,8)}$ = 60.62, p < 0.001). P2X7 expression was significantly reduced in NLRP3$^{-/-}$ microglia compared to NLRP3$^{+/+}$ microglia at baseline (58 ± 3 %; n = 3; p < 0.01) and following LPS stimulation (53 ± 4 %; n = 3; p < 0.01). This finding suggests that the basal expression of P2X7, which is not affected by 4 h LPS stimulation, is lower in NLRP3$^{-/-}$ microglia than in NLRP3$^{+/+}$ microglia and may result in a reduced P2X7 receptor-dependent inflammatory signalling.

Subsequently, ATP-induced (5 mM) P2X7 receptor signalling was assessed by ethidium bromide uptake (Figure 5.4D). A two-way ANOVA revealed a significant effect of ATP stimulation ($F_{(1,8)}$ = 27.73, p < 0.001) on ethidium fluorescence at T+10 min, but no effect of genotype ($F_{(1,8)}$ = 0.04506, p = 0.8372). ATP stimulation induced a significant increase in ethidium uptake and fluorescence in NLRP3$^{+/+}$ and NLRP3$^{-/-}$ microglia (p < 0.05 for both). This finding suggests that while the expression level of P2X7 in NLRP3$^{-/-}$ microglia is lower than NLRP3$^{+/+}$ microglia, P2X7 receptor function in response to high-concentration ATP is not significantly affected.

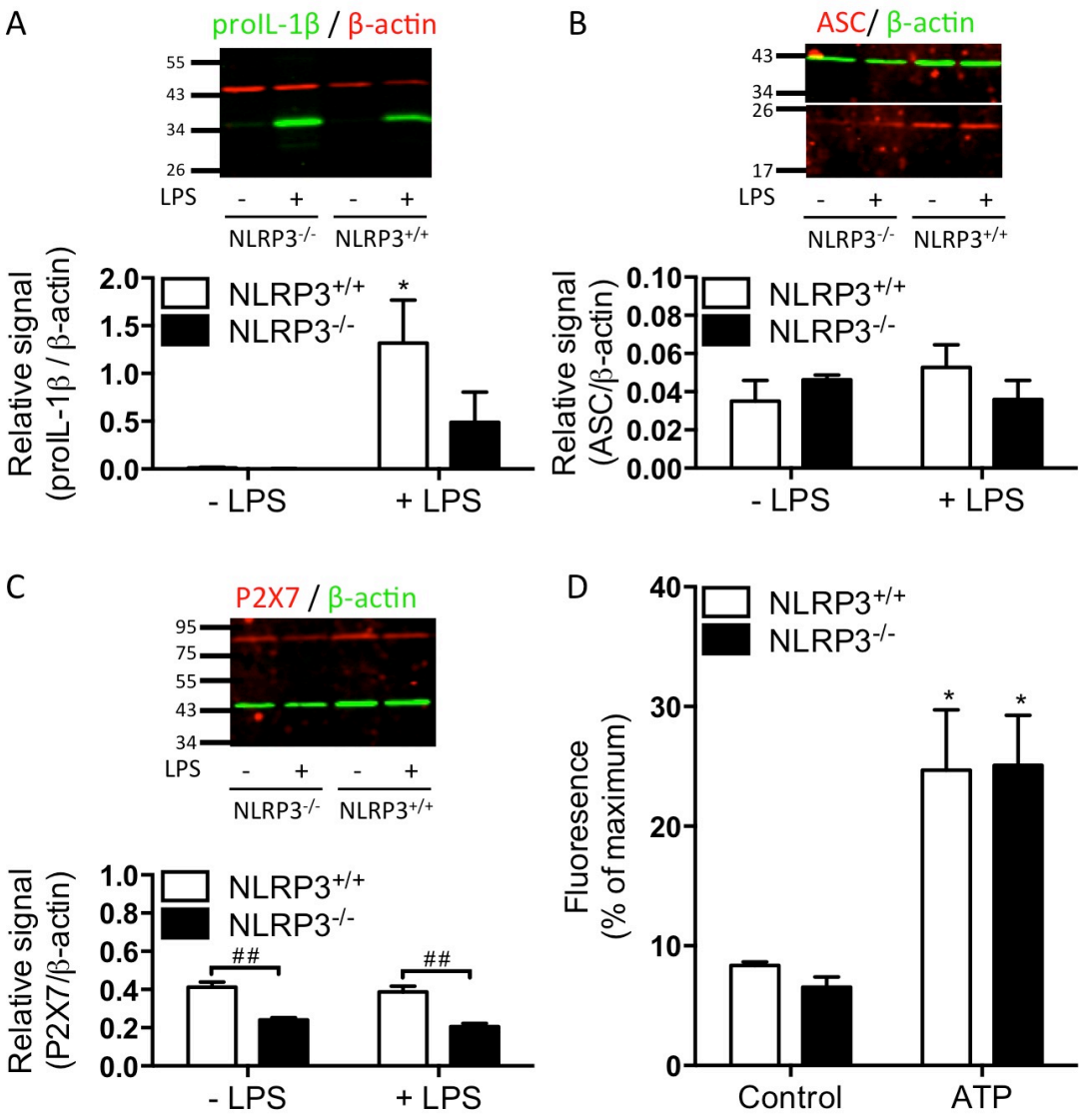

Figure 5.4. Western blot analysis of protein expression and P2X7 receptor function in primary neonatal microglia isolated from NLRP3$^{-/-}$ mice.

ProIL-1β (**A**), ASC (**B**) and P2X7 (**C**) expression with and without LPS stimulation (0.1 µg/ml; 4 hr) in NLRP3$^{+/+}$ and NLRP3$^{-/-}$ microglia cultures (22 DIV). ATP-induced (5 mM; 30 min) uptake of ethidium bromide detected by fluorescence at T+10 min in NLRP3$^{+/+}$ and NLRP3$^{-/-}$ microglia cultures (**D**). Data shown are mean ± SEM (n=3-4) and analysed by two-way ANOVA with Tukey posthoc analysis. *$p < 0.05$ compared to control; $^{\#\#}p < 0.01$.

5.2.1.4 NLRP3$^{-/-}$ neonatal microglia cell death

Cell death of both NLRP3$^{+/+}$ and NLRP3$^{-/-}$ microglia following LPS (0.1 µg/ml; 4 h) and ATP (5 mM; 30 min) stimulation was assessed by the release of LDH (Figure 5.5). A two-way ANOVA revealed a significant effect of treatment ($F_{(1,12)}$ = 43.81, p < 0.001) and genotype ($F_{(1,12)}$ = 12.98, p = 0.0036) on LDH release, but no significant interaction between the two ($F_{(1,12)}$ = 0.4398, p = 0.5198). LPS/ATP stimulation significantly increased LDH release in both NLRP3$^{+/+}$ (172 ± 12 %; n = 4; p < 0.01) and NLRP3$^{-/-}$ microglia (182 ± 9 %; n = 4; p < 0.01). However, the increase observed in NLRP3$^{-/-}$ microglia was significantly attenuated in comparison to NLRP3$^{+/+}$ microglia (76 ± 4 %; p < 0.05). This finding demonstrates reduced cell death in NLRP3$^{-/-}$ microglia, suggesting a resistance to LPS/ATP-induced pyroptosis.

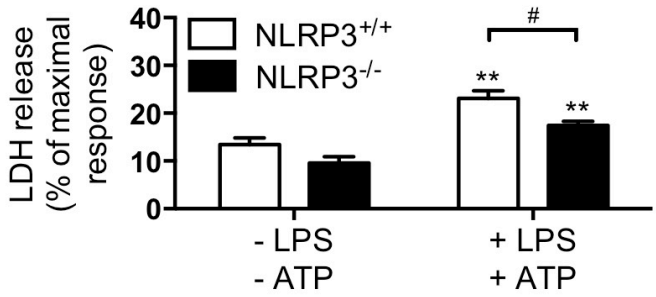

Figure 5.5. Cell death in neonatal primary microglia isolated from NLRP3$^{-/-}$ mice.

The release of lactate dehydrogenase (LDH), an indicator of cell death, in NLRP3$^{+/+}$ and NLRP3$^{-/-}$ microglia cultures (22 DIV) following LPS (0.1 µg/ml; 4 hr) and ATP (5 mM; 30 min) stimulation. Data represent mean ± SEM (n=3) and analysed by two-way ANOVA with Bonferroni's post hoc analysis. **p < 0.01 compared to control; $^{\#}p$ < 0.05.

5.2.2 The role of NLRP3 in repeated LPS-induced sickness and depressive-like behaviour

5.2.2.1 Sickness behaviour

The role of NLRP3 in LPS-induced sickness and depressive-like behaviours was assessed using NLRP3$^{-/-}$ mice and the 3-day ID LPS injection protocol established previously (Section 3.2.5.1). Three treatment groups were included: saline (SAL / SAL / SAL), acute LPS (SAL / SAL / 0.83 mg/kg LPS) and 3-day ID LPS (0.21 / 0.42 / 0.83 mg/kg LPS). A two-way repeated measures ANOVA of body weight over the course of the experiment revealed a significant interaction between treatment group and time ($F_{(20,552)}$ = 130.0, p < 0.001; Figure 5.6A). A two-way ANOVA of body weight at +24 h (Figure 5.6B) revealed a significant effect of treatment ($F_{(2,138)}$ = 658.4, p < 0.001) and genotype ($F_{(1,138)}$ = 8.716, p = 0.0037), though no significant interaction between treatment and genotype ($F_{(2,138)}$ = 2.872, p = 0.06). All LPS treatments resulted in a significant reduction in body weight at +24 h after final injection, regardless of genotype (p < 0.001 for all). Following acute LPS, body weight at +24 h was reduced in comparison in NLRP3$^{+/+}$ (90 ± 0.2 %; n = 24) and NLRP3$^{-/-}$ mice (91 ± 0.2 %; n = 23), respectively, in comparison to saline-treated controls. Following 3-day ID LPS, body weight at +24 h was in NLRP3$^{+/+}$ (87 ± 0.4 %; n = 25) and NLRP3$^{-/-}$ mice (89 ± 0.6 %; n = 24), respectively, in comparison to saline-treated controls. Furthermore, the body weight reduction of 3-day ID LPS-treated mice was significantly greater than acute LPS-treated mice for both NLRP3$^{+/+}$ and NLRP3$^{-/-}$ mice (p < 0.001 for both). However, following 3-day ID LPS, the reduction in body weight of NLRP3$^{-/-}$ mice was significantly attenuated compared to NLRP3$^{+/+}$ mice (p < 0.05). A two-way ANOVA of body weight at +48 h (Figure 5.6C) revealed a significant effect of treatment ($F_{(2,138)}$ = 224.5, p < 0.001), but not of genotype ($F_{(1,138)}$ = 2.518, p = 0.01149). No significant interaction between treatment and genotype was observed ($F_{(2,138)}$ = 0.6639, p = 0.5165). At +48 h after the final injection, all LPS treatment groups still showed a significant reduction in body weight (p < 0.001). Following acute LPS, body weight at +48 h was reduced in NLRP3$^{+/+}$ (93 ± 0.4 %; n = 24) and NLRP3$^{-/-}$ mice (94 ± 0.7 %; n = 23), respectively, in comparison to saline-treated controls. Following 3-day ID LPS, body weight at +48 h was reduced in NLRP3$^{+/+}$ (92 ± 0.4 %; n = 25) and NLRP3$^{-/-}$ mice (93 ± 0.5 %; n = 24), respectively, in comparison to saline-treated controls. There was no significant difference between NLRP3$^{+/+}$ mice and NLRP3$^{-/-}$ mice. These findings suggest the absence of NLRP3 provides some protection against the 3-day ID LPS-induced reduction in body weight in mice.

The distance travelled in the OFT following treatment was assessed at either +6 h or +24 h after the final injection. At +6 h (Figure 5.7A), a two-way ANOVA revealed a significant effect of treatment ($F_{(2,71)}$ = 70.14, p < 0.001) and genotype ($F_{(1,71)}$ = 33.93, p < 0.001) on distance travelled in the OFT. A significant interaction between treatment and genotype was also observed ($F_{(2,71)}$ = 5.536, p = 0.0058). All LPS treatments caused a significant reduction in distance travelled in the OFT at +6 h (p < 0.001 for all). Following acute LPS, distance travelled in the OFT at +6 h was reduced in NLRP3$^{+/+}$ (46 ± 4 %; n = 13) and NLRP3$^{-/-}$ mice (73 ± 4 %; n = 12), respectively, compared to saline-treated controls. Following 3-day ID LPS, distance travelled in the OFT at +6 h was reduced in NLRP3$^{+/+}$ (54 ± 3 %; n = 13) and NLRP3$^{-/-}$ mice (71 ± 4 %; n = 13), respectively, compared to saline-treated controls. However, the reduction in locomotion was significantly greater for NLRP3$^{+/+}$ mice following both acute LPS (p < 0.001) and ID LPS (p < 0.01) in comparison to NLRP3$^{-/-}$ mice. There were no significant differences in distance travelled in the OFT between acute LPS and 3-day ID LPS. At +24 h (Figure 5.7B), a two-way ANOVA revealed a significant effect of treatment ($F_{(2,61)}$ = 11.49, p < 0.001) and genotype ($F_{(1,61)}$ = 6.047, p = 0.0168) on distance travelled in the OFT. A significant interaction between treatment and genotype was also observed ($F_{(2,61)}$ = 8.113, p < 0.001). In NLRP3$^{+/+}$ mice, distance travelled in the OFT at +24 h was reduced following acute LPS (76 ± 2 %; n = 11) and 3-day ID LPS (67 ± 3 %; n = 12) in comparison to saline-treated controls (p < 0.001 for both). However, neither acute LPS nor 3-day ID LPS caused a significant reduction in NLRP3$^{-/-}$ mice at +24 h. Furthermore, following 3-day ID LPS, OFT locomotion was significantly reduced in NLRP3$^{+/+}$ mice compared to NLRP3$^{-/-}$ mice (p < 0.01). These data show that, firstly, LPS-induced sickness behaviour in the OFT is attenuated in NLRP3$^{-/-}$ mice when compared to NLRP3$^{+/+}$ wildtype mice and, secondly, NLRP3$^{+/+}$ wildtype mice still show sickness behaviour in the OFT +24 h after treatment, whilst NLRP3$^{-/-}$ mice do not. This suggests that the lack of NLRP3 provides protection against both acute and 3-day ID LPS-induced sickness behaviours.

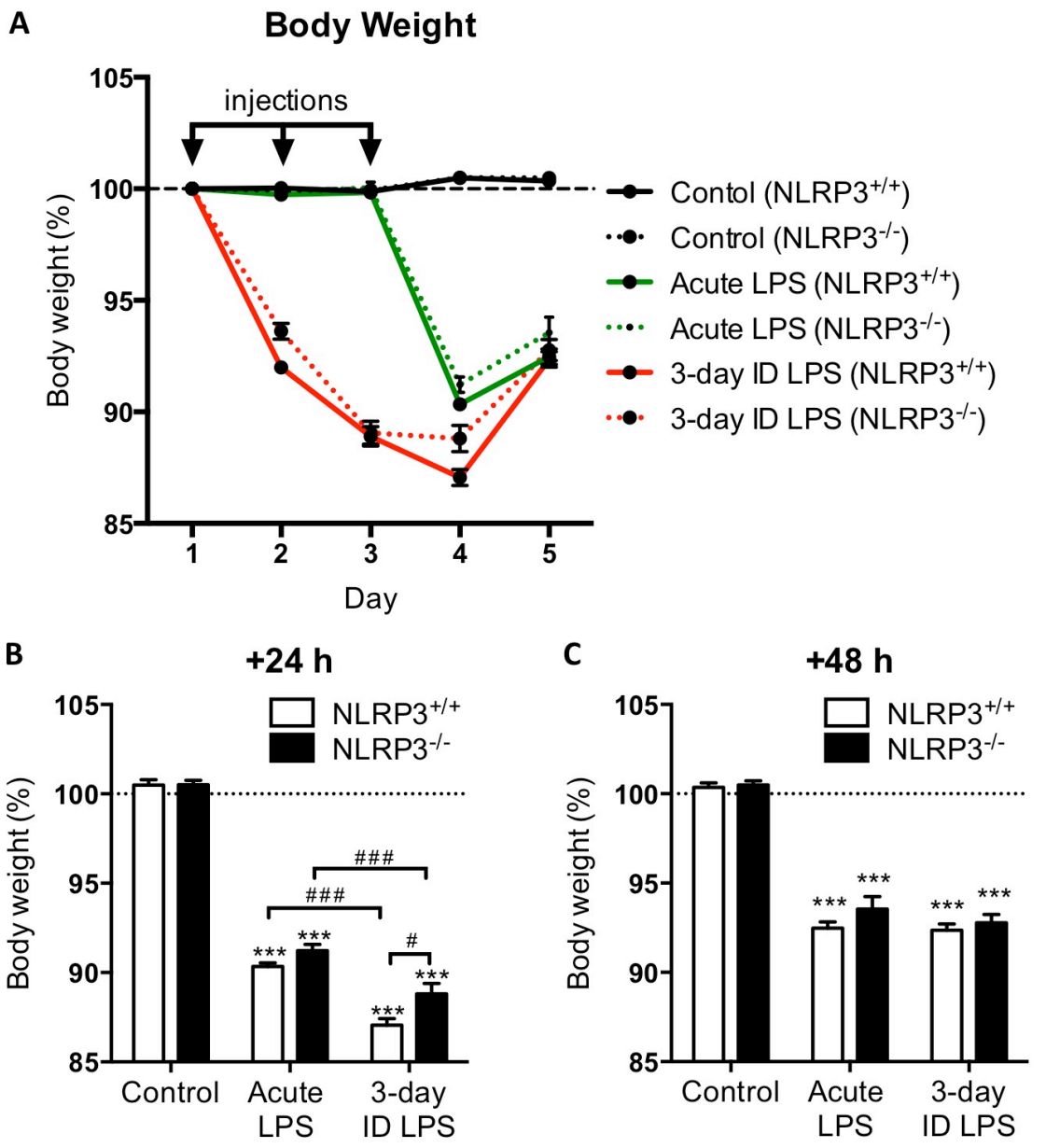

Figure 5.6. The effect of 3-day ID LPS administration on body weight and behaviour in NLRP3$^{-/-}$ mice.

NLRP3$^{+/+}$ and NLRP3$^{-/-}$ mice were treated with saline or LPS for 3 consecutive days. The three groups were: increasing dose (ID) LPS (0.21 / 0.42 / 0.83 mg/kg); acute LPS (0.83 mg/kg); saline controls (**A**). Body weight throughout the 3-day experiment was tracked (**B**). Body weight +24 h (**C**) and +48 h (**D**) after final injection. Values shown are mean ± SEM of n=23-25 per group. $^{***}p < 0.001$ compared to saline injected controls; $^{\#}p < 0.05$, $^{\#\#\#}p < 0.001$.

Time spent in the centre of the OFT at +6 h (Figure 5.7C) and +24 h (Figure 5.7D) was also measured. At +6 h, a two-way ANOVA revealed there was no significant effect of treatment ($F_{(2,71)}$ = 2.511, p = 0.0884) on the time spent in the centre of the OFT, although there was a significant effect of genotype ($F_{(1,71)}$ = 6.737, p = 0.001). Similarly, at +24 h, a two-way ANOVA revealed there was no significant effect of treatment ($F_{(2,61)}$ = 1.73, p = 0.1859) on the time spent in the centre of the OFT, though there was a significant effect of genotype ($F_{(1,61)}$ = 6.627, p = 0.0125). Multiple comparisons revealed no significant differences between groups. These findings indicate no significant effect of acute LPS or 3-day ID LPS treatment on anxiety-like behaviour at +6 h or +24 h in the OFT, although the low level of light used was not optimised to induce anxiety-like behaviours.

5.2.2.2 Depressive-like behaviour

At +24 h after the final injection, FST immobility was assessed (Figure 5.8). A two-way ANOVA revealed a significant effect of treatment on FST immobility ($F_{(2,71)}$ = 11.01, $p < 0.001$), though no significant effect of genotype ($F_{(2,71)}$ = 1.822, p = 0.1813) or interaction ($F_{(2,61)}$ = 0.2544, p = 0.7761) was observed. Post hoc analysis revealed a significant increase in FST immobility following 3-day ID LPS in both NLRP3$^{+/+}$ mice (141 ± 7 %; n = 13; $p < 0.01$) and NLRP3$^{-/-}$ mice (130 ± 8 %; n = 13; $p < 0.05$). This finding indicates that 3-day ID LPS induced a depressive-like behaviour in the FST at +24 h after treatment in both sets of mice and the absence of NLRP3 did not significantly affect this behaviour.

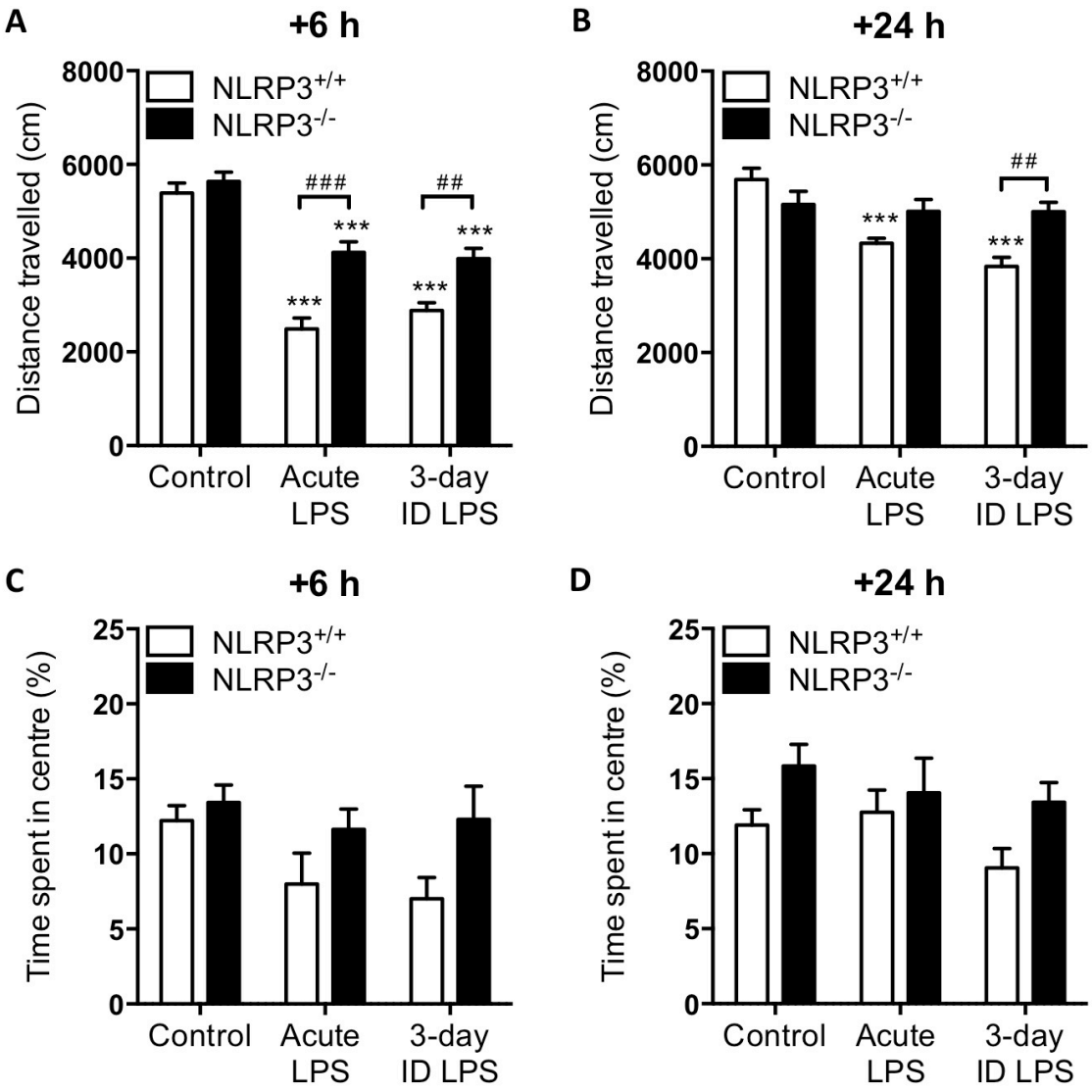

Figure 5.7. The effect of 3-day ID LPS administration on open field test behaviour in NLRP3$^{-/-}$ mice.

NLRP3$^{+/+}$ and NLRP3$^{-/-}$ mice were treated with saline or LPS for 3 consecutive days. The three groups were: increasing dose (ID) LPS (0.21 / 0.42 / 0.83 mg/kg); acute LPS (0.83 mg/kg); saline controls. Distance travelled in the OFT at +6 h (**A**) and +24 h (**B**) after final injection. Time spent in centre (%) of the open field (**C**, **D**). Values shown are mean ± SEM of n=11-13 per group. ***p < 0.001 compared to saline injected controls; $^{\#\#}p$ < 0.01, $^{\#\#\#}p$ < 0.001 within treatment comparisons.

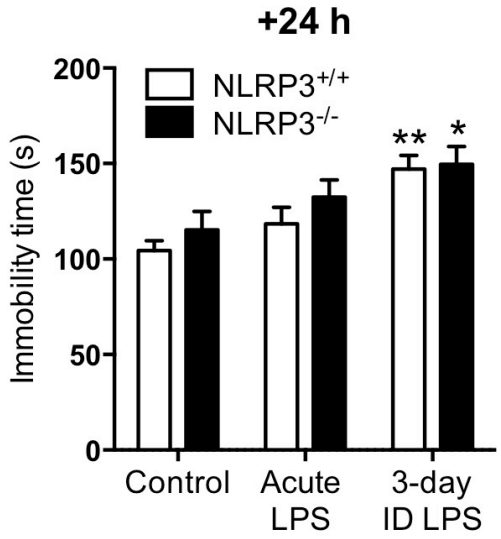

Figure 5.8. The effect of 3-day ID LPS administration on depressive-like behaviour in the forced swim test in NLRP3$^{-/-}$ mice.

NLRP3$^{+/+}$ and NLRP3$^{-/-}$ mice were treated with saline or LPS for 3 consecutive days. The three groups were: increasing dose (ID) LPS (0.21 / 0.42 / 0.83 mg/kg); acute LPS (0.83 mg/kg); saline controls. Time spent immobile in the FST +24 h after final injection. Values shown are mean ± SEM of n=12-13 per group. *p < 0.05, **p < 0.01 compared to saline injected controls.

5.3 Summary of findings

- NLRP3$^{-/-}$ microglia expressed proIL-1β and ASC, but had reduced P2X7 expression in comparison to NLRP3$^{+/+}$ microglia.
- NLRP3$^{-/-}$ microglia did not release IL-1β following LPS (0.1 μg/ml; 4 h) and ATP (5 mM; 30 min) stimulation.
- NLRP3$^{-/-}$ microglia exhibited reduced ATP-induced cell death compared to NLRP3$^{+/+}$ microglia.
- NLRP3$^{-/-}$ mice exhibited reduced sickness behaviour (attenuated reductions in body weight and locomotion) following acute LPS and 3-day ID LPS treatments in comparison to NLRP3$^{+/+}$ mice.
- The absence of NLRP3 in mice had no effect on the depressive-like behaviour in the FST following 3-day ID LPS.

5.4 Discussion

Using NLRP3$^{-/-}$ mice, the role of the NLRP3 inflammasome in the function of microglia and in mediating LPS-induced depressive like behaviour was investigated. It was shown that NLRP3$^{-/-}$ primary microglia (22 DIV), when challenged with LPS (0.1 µg/ml; 4 h), failed to express NLRP3 and did not release IL-1β following ATP stimulation (5 mM; 30 min). Other pro-inflammatory cytokines (TNF-α and IL-6) were produced and ASC protein expression was detected. Interestingly, the expression of P2X7 was reduced and P2X7 receptor-mediated pyroptosis was impaired in comparison to NLRP3$^{+/+}$ primary microglia. *In vivo* experiments with NLRP3$^{-/-}$ mice revealed that sickness behaviour following the 3-day increasing dose LPS paradigm was attenuated but there was no effect on depressive-like behaviours in the FST compared to NLRP3$^{+/+}$ mice.

5.4.1 Proinflammatory signalling and pyroptosis in NLRP3$^{-/-}$ microglia

In this thesis, the absence of NLRP3 did not impair the culture of primary neonatal microglia isolated from NLRP3$^{-/-}$ mice. NLRP3 knockdown in human lymphocytes has been shown to stimulate growth (Salaro et al., 2016), though cell growth has not been reported in other studies using NLRP3$^{-/-}$ macrophage cultures (Harder et al., 2009; Sagulenko et al., 2013) and microglia cultures (Gustin et al., 2015). Consistent with previous findings, NLRP3$^{-/-}$ microglia exhibited impaired IL-1β secretion following ATP-stimulation (Gustin et al., 2015). The small extracellular IL-1β signal seen here in NLRP3$^{-/-}$ microglia is most likely due to the release of proIL-1β following ATP-induced cell death, demonstrated by LDH release. NLRP3$^{-/-}$ microglia exhibited normal proIL-1β and ASC expression and normal ATP-induced expression of IL-6 and TNF-α. Though this is the first demonstration of ATP-induced IL-6 and TNF-α production in NLRP3$^{-/-}$ primary microglia, TNF-α induction by *S. aureus* has also been shown to be unaffected by the absence of NLRP3 (Hanamsagar et al., 2011). A similar finding is observed in primary macrophages, whereby TNF-α production in response to bacterial infection is unchanged in NLRP3$^{-/-}$ macrophages (Harder et al., 2009). These reports support the findings presented here, that the production of TNF-α and IL-6 is independent of NLRP3. In contrast, the partial reduction in IL-1β release in primary microglia following NLRP3 siRNA knockdown paralleled a reduction in TNF-α and IL-6

release, though this was in response to oxygen-glucose deprivation which could alter microglia function in general (Yang et al., 2014).

NLRP3 and P2X7 are strongly linked due to their function in inflammation; P2X7 receptor stimulation is a robust activator of the NLRP3 inflammasome and cell death in response to endogenous ATP (Mariathasan et al., 2006). P2X7 protein expression has not previously been assessed in NLRP3$^{-/-}$ microglia and it was found that P2X7 expression was significantly reduced in comparison to wildtype NLRP3$^{+/+}$ microglia. This finding suggests that the absence of NLRP3 results in a reduced P2X7 expression in microglia. Previously, siRNA knockdown of NLRP3 in THP-1 cells has been shown to enhance P2X7 protein expression, whilst NLRP3 overexpression reduced P2X7 protein expression (Salaro et al., 2016). In NLRP3$^{-/-}$ mice, P2X7 mRNA levels were also increased in macrophages and bone marrow. However, P2X7 protein levels were decreased in embryo fibroblasts but not in lymphocytes (Salaro et al., 2016). These findings demonstrate an influence of cell type on P2X7 expression. Salarao et al. (2016) suggest the upregulation of P2X7 expression in NLRP3$^{-/-}$ mice may be specific to cells of hematopoietic origin. Microglia are thought to originate from hematopoietic stem cells in the yolk sac, so it is unclear why microglia would apparently behave differently to other hematopoietic derived cells. The reduction in P2X7 expression in microglia did not translate into a reduction in ATP-induced uptake of ethidium, as the uptake of ethidium induced by high-dose ATP was not affected by the absence of NLRP3. This finding is supported by ethidium uptake measurements taken from primary macrophages following 5 mM ATP, which show no difference between NLRP3$^{-/-}$ cells and wildtype controls (Muñoz-Planillo et al., 2013). A lower dose of ATP may be more sensitive to the reduction in P2X7 expression, as 5 mM may induce a maximal response (Section 4.2.2.4).

Cell death induced by LPS and ATP stimulation was significantly attenuated in NLRP3$^{-/-}$ microglia. This finding is supported by LPS-primed NLRP3$^{-/-}$ BMDMs that exhibit an inhibited LDH release following ATP stimulation (5 mM) in comparison to wildtype BMDMs (Yu et al., 2014). Furthermore, it has been previously reported that siRNA knockdown of NLRP3 in THP-1 cells increased cell survival and NLRP3 overexpression impaired cell survival (Salaro et al., 2016). Stimulation of NLRP3 inflammasome activity induces caspase-1 activity and IL-1β production. Caspase-1 then cleaves GSDMD, which can rapidly form membrane pores and enable cell lysis (Sborgi et al., 2016). By suppressing NLRP3 signalling, ATP-induced caspase-1 activity and pyroptosis can be attenuated. Caspase-1$^{-/-}$ macrophages also exhibit delayed cell death following stimulation with NLRP3 inflammasome agonist nigericin (Sagulenko et al., 2013). Additionally, nigericin-induced cell death was completely

inhibited in NLRP3$^{-/-}$ macrophages. The study showed that caspase-1 activation induced immediate cell death, whilst the delayed cell death was an apoptotic caspase-8-dependent process. However, the data presented in this thesis show a partial inhibition and not a complete inhibition of ATP-induced necrotic cell death. This finding may be due to differences between the response of macrophages and microglia to brief ATP stimulation. The NLRP3$^{-/-}$ microglia did exhibit reduced P2X7 expression, which would suggest reduced ATP-P2X7 signalling may have contributed to the reduced ATP-induced cell death. However P2X7 receptor-mediated ethidium uptake was unaffected in NLRP3$^{-/-}$ microglia following 5 mM ATP, indicating no difference in ATP-induced P2X7 receptor signalling. In summary, the absence of NLRP3 does not influence the production of other proinflammatory cytokines or LPS-induced priming in microglia, but does attenuate ATP-induced pyroptosis, in support of existing literature.

5.4.2 Attenuated acute and repeated LPS-induced sickness in NLRP3$^{-/-}$ mice

As previously observed in wildtype C57BL/6J mice (Section 3.2.5.1), 3-day ID LPS induced sickness behaviours as seen in body weight reductions and reduced locomotion. Hypolocomotion observed at +6 h was attenuated in NLRP3$^{-/-}$ mice following acute and 3-day ID LPS. There was no indication of LPS tolerance following 3-day ID LPS, as there was no difference in hypolocomotion between acute LPS and 3-day LPS. At +24 h, the body weight reduction and hypolocomotion following 3-day ID LPS, but not acute LPS, was attenuated in NLRP3$^{-/-}$ mice. These findings indicate an impaired sickness response in NLRP3$^{-/-}$ mice, which was more apparent in the sustained inflammation model.

In a repeated stress model of depression, NLRP3$^{-/-}$ mice have also shown normal food consumption whilst wildtype C57BL/6J mice exhibit a reduced food intake, supporting our findings (Alcocer-Gómez et al., 2015). Caspase-1 knockout in C57BL/6 mice does not protect against acute LPS-induced weight loss, both systemically and centrally administered (Lawson et al., 2013a). Consistent with the acute LPS findings presented here, blocking NLRP3 inflammasome signalling does not attenuate acute LPS-induced weight loss. These data suggest the absence of NLRP3 provides significant protection against sustained stress or inflammation, such as the chronic stress model or the 3-day ID LPS model described here. Body weight or food consumption was not reported in previous studies that assessed NLRP3 function via

pharmacological caspase-1 inhibition in the acute LPS model and CMS model of depressive-like behaviour in mice (Zhang et al., 2014; Zhang et al., 2015).

Whilst LPS-induced sickness in the OFT was not completely abolished in NLRP3$^{-/-}$ mice compared to NLRP3$^{+/+}$ mice, it did provide partial protection against acute and sustained inflammation induced by LPS. The hypolocomotion seen in NLRP3$^{+/+}$ mice at +24 h following acute LPS (consistent with earlier findings in Section 3.2.2.2) and 3-day ID LPS indicate the presence of sickness and is a confounding factor in the increased FST immobility. This confounding behaviour is not present in NLRP3$^{-/-}$ mice, indicating an absence of sickness. Locomotion at +24 h after systemic acute LPS has been shown to not be affected by capase-1-knockout, though basal locomotion in those mice were significantly lower than wildtype and may therefore affect LPS-induced changes (Lawson et al., 2013a). Again, sickness behaviour was not assessed during the pharmacological inhibition of caspase-1 in the acute LPS model of depression (Zhang et al., 2014; Zhang et al., 2015). In a repeated stress model, the reduction in social interaction that was observed in wildtype C57BL/6J mice was abolished in NLRP3$^{-/-}$ mice, though this was not an assessment of sickness as it was not assessing an inflammation-based model of depression (Alcocer-Gómez et al., 2015). The data presented here is the first to assess sickness following acute or repeated LPS in NLRP3$^{-/-}$ mice and demonstrates a small protective effect of NLRP3-knockout in the development of sickness following LPS treatment, particularly in a model of sustained inflammation, as assessed by both reduced body weight and hypolocomotion.

5.4.3 NLRP3-knockout failed to attenuate repeated LPS-induced depressive-like behaviour

In NLRP3$^{+/+}$ mice, acute LPS failed to significantly increase FST immobility, whilst the 3-day ID LPS protocol induced a depressive-like behaviour (Section 3.2.5.1, Section 5.2.2.2). However, a similar phenotype was observed in NLRP3$^{-/-}$ mice. This indicates that the absence of NLRP3 attenuated sickness but not depressive-like behaviour induced by sustained inflammation. This contrasts with studies of acute LPS-induced depressive-like behaviours, which are reduced following pharmacological caspase-1 inhibition and in caspase-1-knockout mice (Zhang et al., 2014; Lawson et al., 2013a). In addition, suppressing NLRP3 inflammasome signalling by caspase-1 inhibition and IL-1r knockout has been shown to attenuate stress-induced depressive-like behaviours (Koo and Duman, 2008; Zhang et al., 2015). These findings

demonstrate NLRP3 exerts an important role in the development of depressive-like behaviour in mice following both stress and acute inflammatory insults. However, the data presented here suggests blocking NLRP3 inflammasome signalling does not attenuate sustained inflammation-induced depressive-like behaviour.

Taken together, these findings suggest NLRP3 could be important in the separation of sickness and depressive-like behaviours, as only sickness behaviour was attenuated in NLRP3$^{-/-}$ mice. This may implicate different mechanisms in the origins of these behaviours. The apparent contrast to other models of inflammation-induced depressive-like behaviour may suggest that NLRP3 is not necessary for the development of sustained inflammation-induced depressive-like behaviour, but is important in acute inflammation-induced depressive-like behaviour. As NLRP3-knockout protected against sustained inflammation-induced sickness, it suggests inflammation may have been attenuated. However, this attenuated inflammation did not translate to attenuated depressive-like behaviour in FST immobility. In an opposite fashion, ketamine has been shown to inhibit LPS-induced depressive-like behaviour without affecting LPS-induced reductions in locomotion and food consumption (Walker et al., 2013). This suggests ketamine is capable of targeting inflammation-induced depressive-like behaviour but not general sickness, whilst NLRP3 signalling is critical in sickness but not so in sustained inflammation-induced depressive-like behaviour. NLRP3, like ketamine, may demonstrate a specific signalling pathway that dissociates inflammation-induced sickness from inflammation-induced depressive-like behaviour.

5.4.4 Conclusions

The data presented in this chapter demonstrate a role of NLRP3 in microglial pyroptosis and altered P2X7 expression in NLRP3$^{-/-}$ microglia. NLRP3 was shown to be important in the development of sickness in the LPS models of acute and sustained inflammation, but was not necessary for the development of depressive-like behaviour in the FST, demonstrating a separation between sickness and depressive-like behaviour. Further behavioural assessment is needed to validate the 3-day ID LPS model of depressive-like behaviour and the role of NLRP3 in anhedonic behaviours.

Chapter 6: Discussion

6.1 Validity of LPS models of depressive-like behaviour

Acute LPS enables the dissection of the inflammatory process and the key signalling pathways involved, as well as behavioural changes associated with inflammation. The acute LPS model of depression has been shown, in this thesis and by others, to be unreliable in producing a consistent depressive-like behaviour in mice (Painsipp et al., 2011; Corona et al., 2013; Biesmans et al., 2013; André et al., 2014; Couch et al., 2016). In addition, the acute LPS model exhibits low face validity, as depression in humans is not characterised by a single intense inflammatory event, but a mild elevation in inflammation over an extended period of time (Zalli et al., 2016). Modeling sustained inflammation is necessary to provide a more translatable model of chronic inflammation that better represents inflammation-associated MDD. Repeated LPS administration has recently been used to assess sustained inflammation-induced depressive-like behaviour in a number of studies (Krishna et al., 2016; Kubera et al., 2013; Guo et al., 2016; Guo et al., 2014; Xie et al., 2012). The 3-day ID LPS model developed here still retains many of the negative characteristics of acute LPS due to the relatively short period of time assessed and the relatively high doses of LPS used. However, this model is the first to circumvent repeated LPS-induced behavioural tolerance and induces a depressive-like behaviour. Whilst the sustained inflammation is not the same as MDD, it enables the assessment of a period of sustained inflammation, unlike acute LPS.

The validity of behavioural outputs is another critical aspect of the translatability of this model. Though the FST can exhibit good predictive validity (Lucki et al., 2001), the test has poor construct validity, as the test is based upon the activity of current SSRIs (Hendrie et al., 2013). In addition, the FST assesses a stress-induced behaviour (Gong et al., 2015), which may exhibit stress-inflammation interactions in LPS models that could influence behaviour. The use of a range of behavioural tasks will give LPS-based models of inflammation-induced depressive-like behaviour greater validity. The SPT and FUST could be tested in the 3-day ID LPS model to assess natural behaviours, as well as other measures including social behaviours, such as the social approach task (Yang et al., 2011), and cognition, such as negative cognitive bias (Hales et al., 2014). Furthermore, the time-course of such behaviours, as well as sickness, should be established. $NLRP3^{+/+}$ and $NLRP3^{-/-}$ mouse brains were collected at multiple time points after 3-day ID LPS treatment (+24 h, +1 week and +4 weeks) and biochemical analysis would need to take place to examine the expression pattern of various cytokines and markers of inflammation, as well as the kynurenine pathway. This would enable the assessment of LPS tolerance on a molecular level and how long

residual inflammation can last within the brain, as well as the influence of NLRP3-knockout.

Repeating the 3-day ID LPS protocol after a period of rest, for example, every 4 weeks, could further develop this model of sustained inflammation-induced depressive-like behaviour, similar to a 4-month intermittent LPS model previously demonstrated in mice (Kubera et al., 2013). By doing so, inflammation would be induced over a longer period of time and may induce longer-lasting behavioural changes. Behaviours may not then need to be tested so close to the sickness-depressive border, and could be tested with no confounding influence of sickness.

Alternatively, different inflammatory stimuli could be used to develop novel sustained inflammation models of depressive-like behaviour, such as TNF-α, BCG, poly(I:C) or IFN-α, which have all demonstrated the ability to induce depressive-like behaviour in mice (Kaster et al., 2012; O'Connor et al., 2009b; Gibney et al., 2013; Zheng et al., 2014). Whilst all models of depressive-like behaviour have significant flaws in validity and translatability, the development of such models is critical in understanding the mechanisms that underlie depression and enable drug development for treatments tailored to specific pathology.

6.2 Distinguishing sickness and depressive-like behaviours

In LPS-induced models of depression, the separation of sickness and depressive-like behaviour is considered very important (Dantzer et al., 2008). The presence of overt sickness is a confounding factor on behaviours they rely on movement. As detailed earlier (Table 3.1), there is great variability in the time course of these two categories of behaviour. Many studies assess locomotion at +24 h and have determined there is no sickness, validating depressive-like behaviours at the same time-point (O'Connor et al., 2009a), whilst others have detected sickness and therefore confound the depressive-like behaviour (Biesmans et al., 2013).

An important factor in these findings is the sensitivity of the assessment of sickness. Simply measuring movement between four quadrants in an OFT test is less likely to detect sickness than comprehensively assessing behaviour, such as by accurately tracking mice movement during an OFT, assessing social behaviours, food intake, water intake and even other measures such as cognition. To confidently dissect

the 3-day ID LPS-induced behaviours, depressive-like behaviours would need to be assessed at later time points (weeks or months) to eliminate the variable influence of sickness. Doing so may provide greater face validity as behavioural changes are likely to be a result of residual neuroinflammation as opposed to the transient and intense effect of high dose LPS. This is supported by studies that have shown neuroinflammation following acute LPS can last up to 10 months (Qin et al., 2007).

Alternatively, it could be argued that sickness and inflammation-induced depressive-like behaviour are the same behavioural output and should not be separated. The theory behind the acute LPS model of depressive-like behaviour is that depression in humans is associated with inflammation and that inflammation induces behavioural changes in depression that are similar to sickness (Raison et al., 2006). Therefore, by inducing inflammation and sickness in mice, the sickness behaviours are also the behavioural output that should be targeted for drug development. If a compound can attenuate inflammation-induced sickness, then it could also attenuate inflammation-induced depression, as they are both results of the same process. By this standard, reduced exploratory behaviour and social interaction, commonly used to assessed and separate sickness, could be described as depressive-like behaviours and targeted in a similar way as FST immobility and SPT anhedonia. This approach would focus purely on the inflammation-induced behavioural changes, and not try to differentiate between behaviours.

The findings in this thesis demonstrate the difficulty in attempting to separate sickness and depressive-like behaviour within the short window of testing post-LPS, in both acute and 3-day ID models. By assessing cytokine signalling in the mouse brain at various time-points post-treatment, the longevity of neuroinflammation could be established. Behavioural assessment could subsequently be performed at later time-points in which neuroinflammation, but not sickness, is still present.

6.3 Is NLRP3 a target for antidepressant development?

Previous preclinical studies in acute LPS and chronic stress models of depressive-like behaviour indicate NLRP3 signalling would be a good target for antidepressant intervention in inflammation-associated depression (Alcocer-Gomez et al., 2015; Zhang et al., 2015; Zhang et al., 2014; Iwata et al., 2016). NLRP3$^{-/-}$ mice are protected from chronic stress-induced depressive-like behaviours (Alcocer-Gomez et al., 2015; Iwata et al., 2016), caspase-1 inhibition can reverse acute LPS- and chronic

stress-induced depressive-like behaviours (Zhang et al., 2014; Zhang et al., 2015), and P2X7 receptor inhibition can reduce chronic stress-induced inflammasome activation and depressive-like behaviours (Iwata et al., 2016). Surprisingly, the data presented in this thesis suggest NLRP3 signalling did not mediate the 3-day ID LPS-induced depressive-like behaviour in the FST. However, this finding is not conclusive. Other depressive-like behaviours, such as the SPT and FUST, would need to be tested as well as the time-course of behaviours. Biochemical assessment is also required to establish neuroinflammatory differences and potential compensatory mechanisms in NLRP3$^{-/-}$ mice.

Though NLRP3-knockout did not attenuate depressive-like behaviour, it did reduce to LPS-induced sickness, suggesting targeting NLRP3 may indeed provide protection against the negative effects of sustained inflammation. In addition, *ex vivo* microglia work demonstrated reduced P2X7 expression and signalling in microglia, which may have contributed to the attenuated sickness in NLRP3$^{-/-}$ mice and provide a target for further investigation. A number of stimuli have been shown to stimulate NLRP3 inflammasome activation indirectly via the action of ATP and P2X7, including nigericin and uric acid crystals (Riteau et al., 2012; Muñoz-Planillo et al., 2013). Therefore, changes in P2X7 expression may influence the cellular response to other stimuli. Alternatively, the findings here suggest NLRP3 may be a key protein in separating sickness and depressive-like behaviour, as NLRP3-knockout attenuates one but not the other.

In vitro and *in vivo* findings demonstrate the importance of the NLRP3 inflammasome and IL-1β signalling within the CNS and microglia, and developing drugs to target this pathway may provide significant advances in treating neuroinflammatory and neurodegenerative disorders, though the potential for psychiatric disorders remains unclear.

6.4 Hypoxia or “in situ normoxia”?

The conditions in which microglia are cultured and examined *in vitro* are far removed from the natural conditions within the brain. As detailed earlier, the oxygen availability in the brain has been shown to be far lower than atmospheric levels (Ivanovic, 2009). Recent developments in two-photon microscopy have enabled the measurement of PO_2 within the brain in vivo in awake mice (Lyons et al., 2016). The PO_2 in the somatosensory cortex was recorded to be 23 mmHg, equivalent to 3 % O_2,

demonstrating that under normal conditions, cells within the brain exist in a constant 'hypoxic' environment relative to atmospheric levels. Whilst the O_2 availability for cell culture incubation is rarely deliberately designed, the vast majority of cell culture experiments use "normoxia" set at 20 % O_2. However, the studies presented here indicate that the biological relevance of this for inflammatory signalling in cultured microglia should be considered.

Culturing primary microglia in moderate hypoxia (5 % O_2) can influence cellular function, as NLRP3 signalling was specifically attenuated under moderate hypoxia, with reduced IL-1β and cell death. Whilst the underlying mechanisms responsible were not conclusively examined, it is clear that our understanding of cell signalling is from a hyperoxic state. As microglia priming was not affected, the reduced IL-1β release may be a result of attenuated NLRP3 activation (possibly via reduced ROS generation), or possibly direct attenuation of pyroptosis-mediated pore formation and IL-1β release. A more comprehensive assessment of ROS generation is needed using a more sensitive method of detection, such as electron spin resonance. Obtaining higher density primary microglia cultures may enable greater accuracy in assessing ROS generation. The mechanisms of pyroptosis in microglia has not previously been fully characterised and GSDMD expression and function needs to be investigated. Doing so may elucidate the role of pyroptosis in the reduced IL-1β release seen in low O_2. Finally, assessment of HIF-1α stabilisation has to be carried out at 5 % O_2, as well as a more severe hypoxia for comparison, to understand the role of HIF-1α in moderate hypoxia in microglia.

Eukaryotic cells depend on O_2 for metabolism and the production of ATP as a source of energy for most cellular processes. For this reason, cells are able to sense changes in O_2 availability in order to respond appropriately (Waypa et al., 2016). Understanding the cellular processes that are affected by severe hypoxia is critical in understanding pathological conditions involving ischemia, tumour growth and oxidative stress, though moderate hypoxia can be used to study healthy cellular function. Microglia activation and neuroinflammation has been demonstrated in various neurological disorders, including MDD, AD and others. In order to better understand normal cell function, greater significance must be placed on replicating the microenvironment in which a certain cell type exists in vivo. Only then can a normal cellular response be observed.

6.5 Final conclusions

This thesis details, for the first time, a model of repeated LPS-induced depressive-like behaviour that circumvents the rapid development of LPS tolerance. By doing so, a period of sustained inflammation can be studied. It was also shown that the resulting depressive-like behaviour was not affected by NLRP3-knockout, whilst sickness is attenuated. Furthermore, NLRP3 signalling was characterised in microglia isolated by low concentration trypsin, and NLRP3 inflammasome activity in microglia was assessed for the first time in 5 % O_2 conditions, in an attempt to replicate the *in vivo* environment within the brain. ATP-induced cell death and IL-1β release was shown to be sensitive to O_2 availability and may provide a better model for studying microglia function.

References

Aan Het Rot, M., Collins, K. A., Murrough, J. W., Perez, A. M., Reich, D. L., Charney, D. S., and Mathew, S. J., 2010. Safety and efficacy of repeated-dose intravenous ketamine for treatment-resistant depression. *Biol Psychiat*, 67 (2), 139–145.

Abbott, N. J., Rönnbäck, L., and Hansson, E., 2006. Astrocyte-endothelial interactions at the blood-brain barrier. *Nat Rev Neurosci*, 7 (1), 41–53.

Acarin, L., González, B., Castellano, B., and Castro, A. J., 1996. Microglial response to N-methyl-D-aspartate-mediated excitotoxicity in the immature rat brain. *J Comp Neurol*, 367 (3), 361–374.

Ago, Y., Hasebe, S., Nishiyama, S., Oka, S., Onaka, Y., Hashimoto, H., Takuma, K., and Matsuda, T., 2015. The female encounter test: a novel method for evaluating reward-seeking behavior or motivation in mice. *Int J Neuropsychopharmacol*, 18 (11), pyv062.

Agostini, L., Martinon, F., Burns, K., McDermott, M. F., Hawkins, P. N., and Tschopp, J., 2004. NALP3 forms an IL-1beta-processing inflammasome with increased activity in Muckle-Wells autoinflammatory disorder. *Immun*, 20 (3), 319–325.

Akhondzadeh, S., Jafari, S., Raisi, F., Nasehi, A. A., Ghoreishi, A., Salehi, B., Mohebbi-Rasa, S., Raznahan, M., and Kamalipour, A., 2009. Clinical trial of adjunctive celecoxib treatment in patients with major depression: a double blind and placebo controlled trial. *Depress Anxiety*, 26 (7), 607–611.

Akira, S. and Takeda, K., 2004. Toll-like receptor signalling. *Nat Rev Immunol*, 4 (7), 499–511.

Alcocer-Gómez, E., Ulecia-Morón, C., Marín-Aguilar, F., Rybkina, T., Casas-Barquero, N., Ruiz-Cabello, J., Ryffel, B., Apetoh, L., Ghiringhelli, F., Bullón, P., Sánchez-Alcazar, J. A., Carrión, A. M., and Cordero, M. D., 2015. Stress-induced depressive behaviors require a functional NLRP3 inflammasome. *Mol Neurobiol*. 53 (7), 4874–4882.

Allen, I. C., Scull, M. A., Moore, C. B., Holl, E. K., McElvania-TeKippe, E., Taxman, D. J., Guthrie, E. H., Pickles, R. J., and Ting, J. P. Y., 2009. The NLRP3 inflammasome mediates in vivo innate immunity to influenza A virus through recognition of viral RNA. *Immunity*, 30 (4), 556–565.

Almatroudi, A., Husbands, S. M., Bailey, C. P., and Bailey, S. J., 2015. Combined administration of buprenorphine and naltrexone produces antidepressant-like effects in mice. *J Psychopharmacol*, 29 (7), 812–821.

American Psychiatric Association, 2013. *Diagnostic and Statistical Manual of Mental Disorders (DSM-5®)*. American Psychiatric Pub.

An, L., Li, J., Yu, S.-T., Xue, R., Yu, N.-J., Chen, H.-X., Zhang, L.-M., Zhao, N., Li, Y.-F., and Zhang, Y.-Z., 2015. Effects of the total flavonoid extract of Xiaobuxin-Tang on depression-like behavior induced by lipopolysaccharide and proinflammatory cytokine levels in mice. *J Ethnopharmacol*, 163, 83–87.

Anderson, S. T., Commins, S., Moynagh, P. N., and Coogan, A. N., 2015. Lipopolysaccharide-induced sepsis induces long-lasting affective changes in the mouse. *Brain Behav Immun*, 43, 98–109.

Anderson, S. T., Commins, S., Moynagh, P., and Coogan, A. N., 2016. Chronic fluoxetine treatment attenuates post-septic affective changes in the mouse. *Behav Brain Res*, 297, 112–115.

André, C., Dinel, A. L., Ferreira, G., Layé, S., and Castanon, N., 2014. Diet-induced obesity progressively alters cognition, anxiety-like behavior and lipopolysaccharide-induced depressive-like behavior: focus on brain indoleamine 2,3-dioxygenase

activation. *Brain Behav Immun*, 41, 10–21.
Arndt, S. S., Laarakker, M. C., van Lith, H. A., van der Staay, F. J., Gieling, E., Salomons, A. R., van't Klooster, J., and Ohl, F., 2009. Individual housing of mice--impact on behaviour and stress responses. *Physiol Behav*, 97 (3-4), 385–393.
Autry, A. E., Adachi, M., Nosyreva, E., Na, E. S., Los, M. F., Cheng, P.-F., Kavalali, E. T., and Monteggia, L. M., 2011. NMDA receptor blockade at rest triggers rapid behavioural antidepressant responses. *Nature*, 475 (7354), 91–95.
Avitsur, R., Pollak, Y., and Yirmiya, R., 1997. Different receptor mechanisms mediate the effects of endotoxin and interleukin-1 on female sexual behavior. *Brain Res*. 773 (1-2). 149-161.
Balcombe, J. P., Barnard, N. D., and Sandusky, C., 2004. Laboratory routines cause animal stress. *Contemp Top Lab Anim Sci*, 43 (6), 42–51.
Baldwin, D. S., 2001. Depression and sexual dysfunction. *Brit Med Bull*, 57 (1), 81–99.
Ballabh, P., Braun, A., and Nedergaard, M., 2004. The blood-brain barrier: an overview: structure, regulation, and clinical implications. *Neurobiol Dis*, 16 (1), 1–13.
Bambrick, L. L., Kostov, Y., and Rao, G., 2011. In vitro cell culture pO2 is significantly different from incubator pO2. *Biotechnol Prog*, 27 (4), 1185–1189.
Banasikowski, T. J., Cloutier, C. J., Ossenkopp, K.-P., and Kavaliers, M., 2015. Repeated exposure of male mice to low doses of lipopolysaccharide: dose and time dependent development of behavioral sensitization and tolerance in an automated light-dark anxiety test. *Behav Brain Res*, 286, 241–248.
Banks, W. A. and Robinson, S. M., 2010. Minimal penetration of lipopolysaccharide across the murine blood-brain barrier. *Brain Behav Immun*, 24 (1), 102–109.
Baroja-Mazo, A., Martín-Sánchez, F., Gomez, A. I., Martínez, C. M., Amores-Iniesta, J., Compan, V., Barberà-Cremades, M., Yagüe, J., Ruiz-Ortiz, E., Antón, J., Buján, S., Couillin, I., Brough, D., Arostegui, J. I., and Pelegrin, P., 2014. The NLRP3 inflammasome is released as a particulate danger signal that amplifies the inflammatory response. *Nat Immunol*. 15 (8), 738-748.
Bartlett, R., Yerbury, J. J., and Sluyter, R., 2013. P2X7 receptor activation induces reactive oxygen species formation and cell death in murine EOC13 microglia. *Mediat Inflamm*, 2013, 271813.
Basso, A. M., Bratcher, N. A., Harris, R. R., Jarvis, M. F., Decker, M. W., and Rueter, L. E., 2009. Behavioral profile of P2X7 receptor knockout mice in animal models of depression and anxiety: relevance for neuropsychiatric disorders. *Behav Brain Res*, 198 (1), 83–90.
Bauernfeind, F. G., Horvath, G., Stutz, A., Alnemri, E. S., MacDonald, K., Speert, D., Fernandes-Alnemri, T., Wu, J., Monks, B. G., Fitzgerald, K. A., Hornung, V., and Latz, E., 2009. Cutting edge: NF-kappaB activating pattern recognition and cytokine receptors license NLRP3 inflammasome activation by regulating NLRP3 expression. *J Immunol*, 183 (2), 787–791.
Bauernfeind, F., Bartok, E., Rieger, A., Franchi, L., Nuñez, G., and Hornung, V., 2011. Cutting edge: reactive oxygen species inhibitors block priming, but not activation, of the NLRP3 inflammasome. *J Immunol*, 187 (2), 613–617.
Bay-Richter, C., Janelidze, S., Hallberg, L., and Brundin, L., 2011. Changes in behaviour and cytokine expression upon a peripheral immune challenge. *Behav Brain Res*, 222 (1), 193–199.
Bayer, T. A., Buslei, R., Havas, L., and Falkai, P., 1999. Evidence for activation of microglia in patients with psychiatric illnesses. *Neurosci Lett*. 271 (2), 126-128.
Beasley, C. M., Jr., Koke, S. C., Nilsson, M. E., and Gonzales, J. S., 2000. Adverse

events and treatment discontinuations in clinical trials of fluoxetine in major depressive disorder: an updated meta-analysis. *Clin Ther*, 22 (11), 1319–1330.
Bedard, K. and Krause, K.-H., 2007. The NOX family of ROS-generating NADPH oxidases: physiology and pathophysiology. *Physiol Rev*, 87 (1), 245–313.
Beeson, P. B., 1947. Tolerance to bacterial pyrogens: factors influencing its development. *J Exp Med*, 86 (1), 29–38.
Berger, A., Tran, A. H., Dida, J., Minkin, S., Gerard, N. P., Yeomans, J., and Paige, C. J., 2012. Diminished pheromone-induced sexual behavior in neurokinin-1 receptor deficient (TACR1(-/-)) mice. *Genes Brain Behav*, 11 (5), 568–576.
Bergsbaken, T., Fink, S. L., and Cookson, B. T., 2009. Pyroptosis: host cell death and inflammation. *Nature Rev Microbiol*, 7 (2), 99–109.
Berman, R. M., Cappiello, A., Anand, A., Oren, D. A., Heninger, G. R., Charney, D. S., and Krystal, J. H., 2000. Antidepressant effects of ketamine in depressed patients. *BPS*, 47 (4), 351–354.
Bianco, F., Ceruti, S., Colombo, A., Fumagalli, M., Ferrari, D., Pizzirani, C., Matteoli, M., Di Virgilio, F., Abbracchio, M. P., and Verderio, C., 2006. A role for P2X7 in microglial proliferation. *J Neurochem*, 99 (3), 745–758.
Bierhaus, A., Wolf, J., Andrassy, M., Rohleder, N., Humpert, P. M., Petrov, D., Ferstl, R., Eynatten, von, M., Wendt, T., Rudofsky, G., Joswig, M., Morcos, M., Schwaninger, M., McEwen, B., Kirschbaum, C., and Nawroth, P. P., 2003. A mechanism converting psychosocial stress into mononuclear cell activation. *Proc Natl Acad Sci*, 100 (4), 1920–1925.
Biesmans, S., Meert, T. F., Bouwknecht, J. A., Acton, P. D., Davoodi, N., De Haes, P., Kuijlaars, J., Langlois, X., Matthews, L. J. R., Ver Donck, L., Hellings, N., and Nuydens, R., 2013. Systemic immune activation leads to neuroinflammation and sickness behavior in mice. *Mediat Inflamm*, 2013, 271359.
Black, C. and Miller, B. J., 2015. Meta-analysis of cytokines and chemokines in suicidality: distinguishing suicidal versus nonsuicidal patients. *Biol Psychiat*, 78 (1), 28–37.
Blasi, E., Barluzzi, R., Bocchini, V., Mazzolla, R., and Bistoni, F., 1990. Immortalization of murine microglial cells by a v-raf / v-myc carrying retrovirus. *J Neuroimmunol*, 27 (2-3), 229–237.
Blazer, D. G., 2003. Depression in late life: review and commentary. *J Gerontol A Biol Sci Med Sci*, 58 (3), M249–M265.
Blengio, F., Raggi, F., Pierobon, D., Cappello, P., Eva, A., Giovarelli, M., Varesio, L., and Bosco, M. C., 2013. The hypoxic environment reprograms the cytokine/chemokine expression profile of human mature dendritic cells. *Immunobiol*, 218 (1), 76–89.
Bluthé, R. M., Layé, S., Michaud, B., Combe, C., Dantzer, R., and Parnet, P., 2000. Role of interleukin-1beta and tumour necrosis factor-alpha in lipopolysaccharide-induced sickness behaviour: a study with interleukin-1 type I receptor-deficient mice. *Eur J Neurosci*, 12 (12), 4447–4456.
Bogdanova, O. V., Kanekar, S., D'Anci, K. E., and Renshaw, P. F., 2013. Factors influencing behavior in the forced swim test. *Physiol Behav*, 118, 227–239.
Bonaccorso, S., Marino, V., Puzella, A., Pasquini, M., Biondi, M., Artini, M., Almerighi, C., Verkerk, R., Meltzer, H., and Maes, M., 2002. Increased depressive ratings in patients with hepatitis C receiving interferon-alpha-based immunotherapy are related to interferon-alpha-induced changes in the serotonergic system. *J Clin Psychopharmacol*, 22 (1), 86–90.
Bonello, S., Zähringer, C., BelAiba, R. S., Djordjevic, T., Hess, J., Michiels, C.,

Kietzmann, T., and Görlach, A., 2007. Reactive oxygen species activate the HIF-1alpha promoter via a functional NFkappaB site. *Arterioscler Thromb Vasc Biol*, 27 (4), 755–761.

Boucher, A. A., Arnold, J. C., Hunt, G. E., Spiro, A., Spencer, J., Brown, C., McGregor, I. S., Bennett, M. R., and Kassiou, M., 2011. Resilience and reduced c-fos expression in P2X7 receptor knockout mice exposed to repeated forced swim test. *Neurosci*, 189, 170–177.

Boveris, A. and Chance, B., 1973. The mitochondrial generation of hydrogen peroxide. General properties and effect of hyperbaric oxygen. *Biochem J*, 134 (3), 707–716.

Bradley, J. R., 2008. TNF-mediated inflammatory disease. *J Pathol,* 214 (2), 149–160.

Breder, C. D., Dinarello, C. A., and Saper, C. B., 1988. Interleukin-1 immunoreactive innervation of the human hypothalamus. *Sci*, 240 (4850), 321–324.

Brenes, J. C., Rodríguez, O., and Fornaguera, J., 2008. Differential effect of environment enrichment and social isolation on depressive-like behavior, spontaneous activity and serotonin and norepinephrine concentration in prefrontal cortex and ventral striatum. *Pharmacol Biochem Behav*, 89 (1), 85–93.

Brough, D., Le Feuvre, R. A., Iwakura, Y., and Rothwell, N. J., 2002. Purinergic (P2X7) receptor activation of microglia induces cell death via an interleukin-1-independent mechanism. *Mol Cell Neurosci*, 19 (2), 272–280.

Browne, C. A. and Lucki, I., 2013. Antidepressant effects of ketamine: mechanisms underlying fast-acting novel antidepressants. *Front Pharmacol*, 4, 161.

Brunello, N., Alboni, S., Capone, G., Benatti, C., Blom, J. M. C., Tascedda, F., Kriwin, P., and Mendlewicz, J., 2006. Acetylsalicylic acid accelerates the antidepressant effect of fluoxetine in the chronic escape deficit model of depression. *Int Clin Psychopharmacol*, 21 (4), 219–225.

Butler, P. W. and Besser, G. M., 1968. Pituitary-adrenal function in severe depressive illness. *Lancet*, 1 (7554), 1234–1236.

Campbell, B. M., Charych, E., Lee, A. W., and Möller, T., 2014. Kynurenines in CNS disease: regulation by inflammatory cytokines. *Front Neurosci*, 8, 12.

Capuron, L. and Miller, A. H., 2004. Cytokines and psychopathology: Lessons from interferon-α. *Biol Psychiat*, 56 (11), 819–824.

Capuron, L., Raison, C. L., Musselman, D. L., Lawson, D. H., Nemeroff, C. B., and Miller, A. H., 2003. Association of exaggerated HPA axis response to the initial injection of interferon-alpha with development of depression during interferon-alpha therapy. *Am J Psychiat*, 160 (7), 1342–1345.

Capuron, L., Ravaud, A., Neveu, P. J., Miller, A. H., Maes, M., and Dantzer, R., 2002. Association between decreased serum tryptophan concentrations and depressive symptoms in cancer patients undergoing cytokine therapy. *Mol Psychiat*, 7 (5), 468–473.

Carmeliet, P., Dor, Y., Herbert, J. M., Fukumura, D., Brusselmans, K., Dewerchin, M., Neeman, M., Bono, F., Abramovitch, R., Maxwell, P., Koch, C. J., Ratcliffe, P., Moons, L., Jain, R. K., Collen, D., Keshert, E., and Keshet, E., 1998. Role of HIF-1alpha in hypoxia-mediated apoptosis, cell proliferation and tumour angiogenesis. *Nature*, 394 (6692), 485–490.

Cassel, S. L., Eisenbarth, S. C., Iyer, S. S., Sadler, J. J., Colegio, O. R., Tephly, L. A., Carter, A. B., Rothman, P. B., Flavell, R. A., and Sutterwala, F. S., 2008. The Nalp3 inflammasome is essential for the development of silicosis. *Proc Natl Acad Sci*, 105 (26), 9035–9040.

Cater, D. B., Garattini, S., Marina, F., and Silver, I. A., 1961. Changes of oxygen tension in brain and somatic tissues induced by vasodilator and vasoconstrictor

drugs. *Proc R Soc [Biol]*, 155 (958), 136–158.
Chandel, N. S., McClintock, D. S., Feliciano, C. E., Wood, T. M., Melendez, J. A., Rodriguez, A. M., and Schumacker, P. T., 2000. Reactive oxygen species generated at mitochondrial complex III stabilize hypoxia-inducible factor-1alpha during hypoxia: a mechanism of O2 sensing. *J Biol Chem*, 275 (33), 25130–25138.
Chang, Y., Lee, J.-J., Hsieh, C.-Y., Hsiao, G., Chou, D.-S., and Sheu, J.-R., 2009. Inhibitory effects of ketamine on lipopolysaccharide-induced microglial activation. *Mediat Inflamm*, 2009, 705379.
Chen, K., Zhang, J., Zhang, W., Zhang, J., Yang, J., Li, K., and He, Y., 2013. ATP-P2X4 signaling mediates NLRP3 inflammasome activation: a novel pathway of diabetic nephropathy. *Int J Biochem Cell Biol*, 45 (5), 932–943.
Cherry, J. D., Olschowka, J. A., and O'Banion, M. K., 2014. Neuroinflammation and M2 microglia: the good, the bad, and the inflamed. *J Neuroinflamm*, 11, 98.
Chessell, I. P., Michel, A. D., and Humphrey, P. P., 1998. Effects of antagonists at the human recombinant P2X7 receptor. *Brit J Pharmacol*, 124 (6), 1314–1320.
Chourbaji, S., Zacher, C., Sanchis-Segura, C., Spanagel, R., and Gass, P., 2005. Social and structural housing conditions influence the development of a depressive-like phenotype in the learned helplessness paradigm in male mice. *Behav Brain Res*, 164 (1), 100–106.
Cleare, A., Pariante, C. M., Young, A. H., Anderson, I. M., Christmas, D., Cowen, P. J., Dickens, C., Ferrier, I. N., Geddes, J., Gilbody, S., Haddad, P. M., Katona, C., Lewis, G., Malizia, A., McAllister-Williams, R. H., Ramchandani, P., Scott, J., Taylor, D., Uher, R., Members of the Consensus Meeting, 2015. Evidence-based guidelines for treating depressive disorders with antidepressants: a revision of the 2008 British Association for Psychopharmacology guidelines. *J Psychopharmacol*. 29 (5), 459-525.
Coco, S., Calegari, F., Pravettoni, E., Pozzi, D., Taverna, E., Rosa, P., Matteoli, M., and Verderio, C., 2003. Storage and release of ATP from astrocytes in culture. *J Biol Chem*, 278 (2), 1354–1362.
Cohen, S., Janicki-Deverts, D., Doyle, W. J., Miller, G. E., Frank, E., Rabin, B. S., and Turner, R. B., 2012. Chronic stress, glucocorticoid receptor resistance, inflammation, and disease risk. *Proc Natl Acad Sci*, 109 (16), 5995–5999.
Compan, V., Baroja-Mazo, A., Lopez-Castejon, G., Gomez, A. I., Martínez, C. M., Angosto, D., Montero, M. T., Herranz, A. S., Bazán, E., Reimers, D., Mulero, V., and Pelegrin, P., 2012. Cell volume regulation modulates NLRP3 inflammasome activation. *Immunity*, 37 (3), 487–500.
Copeland, S., Warren, H. S., Lowry, S. F., Calvano, S. E., Remick, D., Inflammation and the Host Response to Injury Investigators, 2005. Acute inflammatory response to endotoxin in mice and humans. *Clin Diagn Lab Immunol*, 12 (1), 60–67.
Corona, A. W., Huang, Y., O'Connor, J. C., Dantzer, R., Kelley, K. W., Popovich, P. G., and Godbout, J. P., 2010. Fractalkine receptor (CX3CR1) deficiency sensitizes mice to the behavioral changes induced by lipopolysaccharide. *J Neuroinflamm*, 7, 93.
Corona, A. W., Norden, D. M., Skendelas, J. P., Huang, Y., O'Connor, J. C., Lawson, M., Dantzer, R., Kelley, K. W., and Godbout, J. P., 2013. Indoleamine 2,3-dioxygenase inhibition attenuates lipopolysaccharide induced persistent microglial activation and depressive-like complications in fractalkine receptor (CX(3)CR1)-deficient mice. *Brain Behav Immun*, 31, 134–142.
Couch, Y., Trofimov, A., Markova, N., Nikolenko, V., Steinbusch, H. W., Chekhonin, V., Schroeter, C., Lesch, K.-P., Anthony, D. C., and Strekalova, T., 2016. Low-dose

lipopolysaccharide (LPS) inhibits aggressive and augments depressive behaviours in a chronic mild stress model in mice. *J Neuroinflamm*, 13 (1), 108.

Couch, Y., Xie, Q., Lundberg, L., Sharp, T., and Anthony, D. C., 2015. A model of post-infection fatigue is associated with increased TNF and 5-HT2A receptor expression in mice. *PLoS ONE*, 10 (7), e0130643.

Couturier, J., Stancu, I.-C., Schakman, O., Pierrot, N., Huaux, F., Kienlen-Campard, P., Dewachter, I., and Octave, J.-N., 2016. Activation of phagocytic activity in astrocytes by reduced expression of the inflammasome component ASC and its implication in a mouse model of Alzheimer disease. *J Neuroinflamm*, 13, 20.

Cruz, C. M., Rinna, A., Forman, H. J., Ventura, A. L. M., Persechini, P. M., and Ojcius, D. M., 2007. ATP activates a reactive oxygen species-dependent oxidative stress response and secretion of proinflammatory cytokines in macrophages. *J Biol Chem*, 282 (5), 2871–2879.

Cummins, E. P., Berra, E., Comerford, K. M., Ginouves, A., Fitzgerald, K. T., Seeballuck, F., Godson, C., Nielsen, J. E., Moynagh, P., Pouysségur, J., and Taylor, C. T., 2006. Prolyl hydroxylase-1 negatively regulates IkappaB kinase-beta, giving insight into hypoxia-induced NFkappaB activity. *Proc Natl Acad Sci*, 103 (48), 18154–18159.

Cunningham, C., Campion, S., Teeling, J., Felton, L., and Perry, V. H., 2007. The sickness behaviour and CNS inflammatory mediator profile induced by systemic challenge of mice with synthetic double-stranded RNA (poly I:C). *Brain Behav Immun*, 21 (4), 490–502.

Custódio, C. S., Mello, B. S. F., Cordeiro, R. C., de Araújo, F. Y. R., Chaves, J. H., Vasconcelos, S. M. M., Nobre Júnior, H. V., de Sousa, F. C. F., Vale, M. L., Carvalho, A. F., and Macêdo, D. S., 2013. Time course of the effects of lipopolysaccharide on prepulse inhibition and brain nitrite content in mice. *Eur J Pharmacol*, 713 (1-3), 31–38.

D'Mello, C., Le, T., and Swain, M. G., 2009. Cerebral microglia recruit monocytes into the brain in response to tumor necrosis factoralpha signaling during peripheral organ inflammation. *J Neurosci*, 29 (7), 2089–2102.

Dantzer, R., 2001. Cytokine-Induced Sickness Behavior: Where Do We Stand? *Brain Behav Immun*, 15 (1), 7–24.

Dantzer, R., O'Connor, J. C., Freund, G. G., Johnson, R. W., and Kelley, K. W., 2008. From inflammation to sickness and depression: when the immune system subjugates the brain. *Nat Rev Neurosci*, 9 (1), 46–56.

Dao-Ung, P., Skarratt, K. K., Fuller, S. J., and Stokes, L., 2015. Paroxetine suppresses recombinant human P2X7 responses. *Purinergic Signal*, 11 (4), 481–490.

David, D. J. P., Renard, C. E., Jolliet, P., Hascoët, M., and Bourin, M., 2003. Antidepressant-like effects in various mice strains in the forced swimming test. *Psychopharmacol*, 166 (4), 373–382.

Davis, B. K., Wen, H., and Ting, J. P. Y., 2011. The Inflammasome NLRs in Immunity, Inflammation, and Associated Diseases. *Ann Rev Immunol*, 29 (1), 707–735.

de Paiva, V. N., Lima, S. N. P., Fernandes, M. M., Soncini, R., Andrade, C. A. F., and Giusti-Paiva, A., 2010. Prostaglandins mediate depressive-like behaviour induced by endotoxin in mice. *Behav Brain Res*, 215 (1), 146–151.

de Rivero Vaccari, J. P., Lotocki, G., Marcillo, A. E., Dietrich, W. D., and Keane, R. W., 2008. A molecular platform in neurons regulates inflammation after spinal cord injury. *J Neurosci*, 28 (13), 3404–3414.

del Rio-Hortega P. 1919. El tercer elemento de los centros nerviosos I La microglia en estado normal II Intervencíon de la microglia en los procesos patológicos III

Naturaleza probable de la microglia. *Bol de la Soc esp de biol* 9: 69–120, 1919.
Delgado, P. L., 2000. Depression: the case for a monoamine deficiency. *The J Clin Psychiat*, 61 Suppl 6, 7–11.
Delgado, P. L., Price, L. H., Miller, H. L., Salomon, R. M., Aghajanian, G. K., Heninger, G. R., and Charney, D. S., 1994. Serotonin and the neurobiology of depression. Effects of tryptophan depletion in drug-free depressed patients. *Arc Gen Psychiat*, 51 (11), 865–874.
Denes, A., Coutts, G., Lénárt, N., Cruickshank, S. M., Pelegrin, P., Skinner, J., Rothwell, N., Allan, S. M., and Brough, D., 2015. AIM2 and NLRC4 inflammasomes contribute with ASC to acute brain injury independently of NLRP3. *Proc Natl Acad Sci,* 112 (13), 4050–4055.
Desbonnet, L., Garrett, L., Clarke, G., Kiely, B., Cryan, J. F., and Dinan, T. G., 2010. Effects of the probiotic Bifidobacterium infantis in the maternal separation model of depression. *Neurosci*, 170 (4), 1179–1188.
Desireddi, J. R., Farrow, K. N., Marks, J. D., Waypa, G. B., and Schumacker, P. T., 2010. Hypoxia increases ROS signaling and cytosolic Ca 2+ in pulmonary artery smooth muscle cells of mouse lungs slices. *Antioxid Redox Signal*, 12 (5), 595–602.
Dick, M. S., Sborgi, L., Rühl, S., Hiller, S., and Broz, P., 2016. ASC filament formation serves as a signal amplification mechanism for inflammasomes. *Nat Commun*, 7, 11929.
Dobos, N., de Vries, E. F. J., Kema, I. P., Patas, K., Prins, M., Nijholt, I. M., Dierckx, R. A., Korf, J., Boer, den, J. A., Luiten, P. G. M., and Eisel, U. L. M., 2012. The role of indoleamine 2,3-dioxygenase in a mouse model of neuroinflammation-induced depression. *J Alzheimers Dis*, 28 (4), 905–915.
Dong, C., Zhang, J.-C., Yao, W., Ren, Q., Yang, C., Ma, M., Han, M., Saito, R., and Hashimoto, K., 2016. Effects of escitalopram, R-citalopram, and reboxetine on serum levels of tumor necrosis factor-α, interleukin-10, and depression-like behavior in mice after lipopolysaccharide administration. *Pharmacol Biochem Behav*, 144, 7–12.
Donnelly-Roberts, D. L., Namovic, M. T., Han, P., and Jarvis, M. F., 2009. Mammalian P2X7 receptor pharmacology: comparison of recombinant mouse, rat and human P2X7 receptors. *Brit J Pharmacol*, 157 (7), 1203–1214.
Dostert, C., Guarda, G., Romero, J. F., Menu, P., Gross, O., Tardivel, A., Suva, M.-L., Stehle, J.-C., Kopf, M., Stamenkovic, I., Corradin, G., and Tschopp, J., 2009. Malarial hemozoin is a Nalp3 inflammasome activating danger signal. *PLoS ONE*, 4 (8), e6510.
Dostert, C., Pétrilli, V., Van Bruggen, R., Steele, C., Mossman, B. T., and Tschopp, J., 2008. Innate immune activation through Nalp3 inflammasome sensing of asbestos and silica. *Science*, 320 (5876), 674–677.
Dowlati, Y., Herrmann, N., Swardfager, W., Liu, H., Sham, L., Reim, E. K., and Lanctôt, K. L., 2010. A meta-analysis of cytokines in major depression. *Biol Psychiat*, 67 (5), 446–457.
Duewell, P., Kono, H., Rayner, K. J., Sirois, C. M., Vladimer, G., Bauernfeind, F. G., Abela, G. S., Franchi, L., Nuñez, G., Schnurr, M., Espevik, T., Lien, E., Fitzgerald, K. A., Rock, K. L., Moore, K. J., Wright, S. D., Hornung, V., and Latz, E., 2010. NLRP3 inflammasomes are required for atherogenesis and activated by cholesterol crystals. *Nature*, 464 (7293), 1357–1361.
Duman, R. S., Li, N., Liu, R.-J., Duric, V., and Aghajanian, G., 2012. Signaling pathways underlying the rapid antidepressant actions of ketamine.

Neuropharmacol, 62 (1), 35–41.

Duncan, J. A., Gao, X., Huang, M. T.-H., O'Connor, B. P., Thomas, C. E., Willingham, S. B., Bergstralh, D. T., Jarvis, G. A., Sparling, P. F., and Ting, J. P. Y., 2009. Neisseria gonorrhoeae activates the proteinase cathepsin B to mediate the signaling activities of the NLRP3 and ASC-containing inflammasome. *J Immunol*, 182 (10), 6460–6469.

Engeland, C. G., Nielsen, D. V., Kavaliers, M., and Ossenkopp, K. P., 2001. Locomotor activity changes following lipopolysaccharide treatment in mice: a multivariate assessment of behavioral tolerance. *Physiol Behav*, 72 (4), 481–491.

Erecińska, M. and Silver, I. A., 2001. Tissue oxygen tension and brain sensitivity to hypoxia. *Respir Physiol*, 128 (3), 263–276.

Erickson, M. A. and Banks, W. A., 2011. Cytokine and chemokine responses in serum and brain after single and repeated injections of lipopolysaccharide: multiplex quantification with path analysis. *Brain Behav Immun*, 25 (8), 1637–1648.

Evans, D. L., Charney, D. S., Lewis, L., Golden, R. N., Gorman, J. M., Krishnan, K. R. R., Nemeroff, C. B., Bremner, J. D., Carney, R. M., Coyne, J. C., Delong, M. R., Frasure-Smith, N., Glassman, A. H., Gold, P. W., Grant, I., Gwyther, L., Ironson, G., Johnson, R. L., Kanner, A. M., Katon, W. J., Kaufmann, P. G., Keefe, F. J., Ketter, T., Laughren, T. P., Leserman, J., Lyketsos, C. G., McDonald, W. M., McEwen, B. S., Miller, A. H., Musselman, D., O'Connor, C., Petitto, J. M., Pollock, B. G., Robinson, R. G., Roose, S. P., Rowland, J., Sheline, Y., Sheps, D. S., Simon, G., Spiegel, D., Stunkard, A., Sunderland, T., Tibbits, P., and Valvo, W. J., 2005. Mood disorders in the medically ill: scientific review and recommendations. *Biol Phsychioat*, 58 (3), 175–189.

Fan, R., Xu, F., Previti, M. L., Davis, J., Grande, A. M., Robinson, J. K., and Van Nostrand, W. E., 2007. Minocycline reduces microglial activation and improves behavioral deficits in a transgenic model of cerebral microvascular amyloid. *J Neurosci*, 27 (12), 3057–3063.

Faustin, B., Lartigue, L., Bruey, J.-M., Luciano, F., Sergienko, E., Bailly-Maitre, B., Volkmann, N., Hanein, D., Rouiller, I., and Reed, J. C., 2007. Reconstituted NALP1 inflammasome reveals two-step mechanism of caspase-1 activation. *Mol Cell*, 25 (5), 713–724.

Fava, M., 2003. Diagnosis and definition of treatment-resistant depression. *Biol Psychiat*. 53 (8), 649-659.

Felger, J. C., Li, L., Marvar, P. J., Woolwine, B. J., Harrison, D. G., Raison, C. L., and Miller, A. H., 2013. Tyrosine metabolism during interferon-alpha administration: association with fatigue and CSF dopamine concentrations. *Brain Behav Immun*, 31, 153–160.

Fernandes-Alnemri, T., Wu, J., Yu, J.-W., Datta, P., Miller, B., Jankowski, W., Rosenberg, S., Zhang, J., and Alnemri, E. S., 2007. The pyroptosome: a supramolecular assembly of ASC dimers mediating inflammatory cell death via caspase-1 activation. *Cell Death Differ*, 14 (9), 1590–1604.

Ferrari, A. J., Charlson, F. J., Norman, R. E., Patten, S. B., Freedman, G., Murray, C. J. L., Vos, T., and Whiteford, H. A., 2013. Burden of depressive disorders by country, sex, age, and year: findings from the global burden of disease study 2010. *PLoS medicine*, 10 (11), e1001547.

Fineberg, N. A., Haddad, P. M., Carpenter, L., Gannon, B., Sharpe, R., Young, A. H., Joyce, E., Rowe, J., Wellsted, D., Nutt, D. J., and Sahakian, B. J., 2013. The size, burden and cost of disorders of the brain in the UK. *J Psychopharmacol*, 27 (9), 761–770.

Fischer, C. W., Liebenberg, N., Elfving, B., Lund, S., and Wegener, G., 2012. Isolation-induced behavioural changes in a genetic animal model of depression. *Behav Brain Res*, 230 (1), 85–91.

Fleury, C., Mignotte, B., and Vayssière, J. L., 2002. Mitochondrial reactive oxygen species in cell death signaling. *Biochimie*. 84 (2-3), 131-141.

Folco, E. J., Sukhova, G. K., Quillard, T., and Libby, P., 2014. Moderate hypoxia potentiates interleukin-1β production in activated human macrophages. *Circul Res*, 115 (10), 875–883.

Fond, G., Loundou, A., Rabu, C., Macgregor, A., Lançon, C., Brittner, M., Micoulaud-Franchi, J.-A., Richieri, R., Courtet, P., Abbar, M., Roger, M., Leboyer, M., and Boyer, L., 2014. Ketamine administration in depressive disorders: a systematic review and meta-analysis. *Psychopharmacol*, 231 (18), 3663–3676.

Fonken, L. K., Finy, M. S., Walton, J. C., Weil, Z. M., Workman, J. L., Ross, J., and Nelson, R. J., 2009. Influence of light at night on murine anxiety- and depressive-like responses. *Behav Brain Res*, 205 (2), 349–354.

Fonken, L. K., Weber, M. D., Daut, R. A., Kitt, M. M., Frank, M. G., Watkins, L. R., and Maier, S. F., 2016. Stress-induced neuroinflammatory priming is time of day dependent. *Psychoneuroendocrinol*, 66, 82–90.

Franchi, L., Eigenbrod, T., and Nuñez, G., 2009. Cutting edge: TNF-alpha mediates sensitization to ATP and silica via the NLRP3 inflammasome in the absence of microbial stimulation. *J Immunol*, 183 (2), 792–796.

Frank, M. G., Baratta, M. V., Sprunger, D. B., Watkins, L. R., and Maier, S. F., 2007. Microglia serve as a neuroimmune substrate for stress-induced potentiation of CNS pro-inflammatory cytokine responses. *Brain Behav Immun*, 21 (1), 47–59.

Frank, M. G., Wieseler-Frank, J. L., Watkins, L. R., and Maier, S. F., 2006. Rapid isolation of highly enriched and quiescent microglia from adult rat hippocampus: immunophenotypic and functional characteristics. *J Neurosci Methods*, 151 (2), 121–130.

Franklin, A. E., Engeland, C. G., Kavaliers, M., and Ossenkopp, K.-P., 2003. Lipopolysaccharide-induced hypoactivity and behavioral tolerance development are modulated by the light-dark cycle in male and female rats. *Psychopharmacol*, 170 (4), 399–408.

Franklin, A. E., Engeland, C. G., Kavaliers, M., and Ossenkopp, K.-P., 2007. The rate of behavioral tolerance development to repeated lipopolysaccharide treatments depends upon the time of injection during the light-dark cycle: a multivariable examination of locomotor activity. *Behav Brain Res*, 180 (2), 161–173.

Frede, S., Stockmann, C., Freitag, P., and Fandrey, J., 2006. Bacterial lipopolysaccharide induces HIF-1 activation in human monocytes via p44/42 MAPK and NF-kappaB. *Biochem J*, 396 (3), 517–527.

Frenois, F., Moreau, M., O'Connor, J., Lawson, M., Micon, C., Lestage, J., Kelley, K. W., Dantzer, R., and Castanon, N., 2007. Lipopolysaccharide induces delayed FosB/DeltaFosB immunostaining within the mouse extended amygdala, hippocampus and hypothalamus, that parallel the expression of depressive-like behavior. *Psychoneuroendocrinol*, 32 (5), 516–531.

Frodl, T., Schaub, A., Banac, S., Charypar, M., Jäger, M., Kümmler, P., Bottlender, R., Zetzsche, T., Born, C., Leinsinger, G., Reiser, M., Möller, H.-J., and Meisenzahl, E. M., 2006. Reduced hippocampal volume correlates with executive dysfunctioning in major depression. *J Psychiat Neurosci.* 31 (5), 316–323.

Fu, X., Zunich, S. M., O'Connor, J. C., Kavelaars, A., Dantzer, R., and Kelley, K. W., 2010. Central administration of lipopolysaccharide induces depressive-like

behavior in vivo and activates brain indoleamine 2,3 dioxygenase in murine organotypic hippocampal slice cultures. *J Neuroinflamm*, 7, 43.
Fujigaki, H., Saito, K., Fujigaki, S., Takemura, M., Sudo, K., Ishiguro, H., and Seishima, M., 2006. The signal transducer and activator of transcription 1alpha and interferon regulatory factor 1 are not essential for the induction of indoleamine 2,3-dioxygenase by lipopolysaccharide: involvement of p38 mitogen-activated protein kinase and nuclear factor-kappaB pathways, and synergistic effect of several proinflammatory cytokines. *J Biochem*, 139 (4), 655–662.
Ganong, W. F., 2000. Circumventricular organs: definition and role in the regulation of endocrine and autonomic function. *Clin Exp Pharmacol Physiol*, 27 (5-6), 422–427.
Gee, J. R. and Keller, J. N., 2005. Astrocytes: regulation of brain homeostasis via apolipoprotein E. *Int J Biochem Cell Biol*, 37 (6), 1145–1150.
Gendron, F. P. and Chalimoniuk, M., 2003. P2X7 nucleotide receptor activation enhances IFNγ-induced type II nitric oxide synthase activity in BV-2 microglial cells. *J Neurochem*, 87 (2), 344-352.
Gibney, S. M., McGuinness, B., Prendergast, C., Harkin, A., and Connor, T. J., 2013. Poly I:C-induced activation of the immune response is accompanied by depression and anxiety-like behaviours, kynurenine pathway activation and reduced BDNF expression. *Brain Behav Immun*, 28, 170–181.
Gilmore, T. D., 2006. Introduction to NF-kappaB: players, pathways, perspectives. *Oncogene*, 25 (51), 6680–6684.
Giulian D, and Baker T. J., 1986. Characterization of ameboid microglia isolated from developing mammalian brain. *J Neurosci*, 6 (8), 2163–2178.
Godbout, J. P., Moreau, M., Lestage, J., Chen, J., Sparkman, N. L., O'Connor, J., Castanon, N., Kelley, K. W., Dantzer, R., and Johnson, R. W., 2008. Aging exacerbates depressive-like behavior in mice in response to activation of the peripheral innate immune system. *Neuropsychopharmacol*, 33 (10), 2341–2351.
Goehler, L. E., Gaykema, R. P., Nguyen, K. T., Lee, J. E., Tilders, F. J., Maier, S. F., and Watkins, L. R., 1999. Interleukin-1beta in immune cells of the abdominal vagus nerve: a link between the immune and nervous systems? *J Neurosci*, 19 (7), 2799–2806.
Goehler, L. E., Relton, J. K., Dripps, D., Kiechle, R., Tartaglia, N., Maier, S. F., and Watkins, L. R., 1997. Vagal paraganglia bind biotinylated interleukin-1 receptor antagonist: a possible mechanism for immune-to-brain communication. *Brain Res Bull*, 43 (3), 357–364.
Gong, S., Miao, Y.-L., Jiao, G.-Z., Sun, M.-J., Li, H., Lin, J., Luo, M.-J., and Tan, J.-H., 2015. Dynamics and correlation of serum cortisol and corticosterone under different physiological or stressful conditions in mice. *PLoS ONE*, 10 (2), e0117503.
Goshen, I., Kreisel, T., Ben-Menachem-Zidon, O., Licht, T., Weidenfeld, J., Ben-Hur, T., and Yirmiya, R., 2008. Brain interleukin-1 mediates chronic stress-induced depression in mice via adrenocortical activation and hippocampal neurogenesis suppression. *Mol Psychiat*, 13 (7), 717–728.
Grady, M. M. and Stahl, S. M., 2012. Practical guide for prescribing MAOIs: debunking myths and removing barriers. *CNS Spectrums*, 17 (1), 2–10.
Greenberg, P. E., Fournier, A.-A., Sisitsky, T., Pike, C. T., and Kessler, R. C., 2015. The economic burden of adults with major depressive disorder in the United States (2005 and 2010). *J Clin Psychiat*, 76 (2), 155–162.
Gregorian, R. S., Golden, K. A., Bahce, A., Goodman, C., Kwong, W. J., and Khan, Z. M., 2002. Antidepressant-induced sexual dysfunction. *Ann Pharmacother*, 36,

1577–1589.
Guo, H., Callaway, J. B., and Ting, J. P. Y., 2015. Inflammasomes: mechanism of action, role in disease, and therapeutics. *Nature Med*, 21 (7), 677–687.
Guo, J., Lin, P., Zhao, X., Zhang, J., Wei, X., Wang, Q., and Wang, C., 2014. Etazolate abrogates the lipopolysaccharide (LPS)-induced downregulation of the cAMP/pCREB/BDNF signaling, neuroinflammatory response and depressive-like behavior in mice. *Neurosci*, 263, 1–14.
Guo, J.-Y., Li, C.-Y., Ruan, Y.-P., Sun, M., Qi, X.-L., Zhao, B.-S., and Luo, F., 2009. Chronic treatment with celecoxib reverses chronic unpredictable stress-induced depressive-like behavior via reducing cyclooxygenase-2 expression in rat brain. *Eur J Pharmacol*, 612 (1-3), 54–60.
Guo, Y., Cai, H., Chen, L., Liang, D., Yang, R., Dang, R., and Jiang, P., 2016. Quantitative profiling of neurotransmitter abnormalities in the hippocampus of rats treated with lipopolysaccharide: Focusing on kynurenine pathway and implications for depression. *J Neuroimmunol*, 295-296, 41–46.
Gustin, A., Kirchmeyer, M., Koncina, E., Felten, P., Losciuto, S., Heurtaux, T., Tardivel, A., Heuschling, P., and Dostert, C., 2015. NLRP3 inflammasome is expressed and functional in mouse brain microglia but not in astrocytes. *PLoS ONE*, 10 (6), e0130624.
Gutierrez, E. G., Banks, W. A., and Kastin, A. J., 1993. Murine tumor necrosis factor alpha is transported from blood to brain in the mouse. *Journal of Neuroimmunol*, 47 (2), 169–176.
Guzy, R. D., Hoyos, B., Robin, E., Chen, H., Liu, L., Mansfield, K. D., Simon, M. C., Hammerling, U., and Schumacker, P. T., 2005. Mitochondrial complex III is required for hypoxia-induced ROS production and cellular oxygen sensing. *Cell Metabol*, 1 (6), 401–408.
Hales, C. A., Stuart, S. A., Anderson, M. H., and Robinson, E. S. J., 2014. Modelling cognitive affective biases in major depressive disorder using rodents. *Brit J Pharmacol*, 171 (20), 4524–4538.
Hall, F. S., Huang, S., Fong, G. F., and Pert, A., 1998. The effects of social isolation on the forced swim test in Fawn hooded and Wistar rats. *J Neurosci Methods*.
Halle, A., Hornung, V., Petzold, G. C., Stewart, C. R., Monks, B. G., Reinheckel, T., Fitzgerald, K. A., Latz, E., Moore, K. J., and Golenbock, D. T., 2008. The NALP3 inflammasome is involved in the innate immune response to amyloid-β. *Nature Immunol,* 9 (8), 857–865.
Hanamsagar, R., Torres, V., and Kielian, T., 2011. Inflammasome activation and IL-1β/IL-18 processing are influenced by distinct pathways in microglia. *J Neurochem*, 119 (4), 736–748.
Hanisch, U.-K., 2002. Microglia as a source and target of cytokines. *Glia*, 40 (2), 140–155.
Hanisch, U.-K. and Kettenmann, H., 2007. Microglia: active sensor and versatile effector cells in the normal and pathologic brain. *Nature Neurosci*, 10 (11), 1387–1394.
Hannestad, J., DellaGioia, N., and Bloch, M., 2011. The effect of antidepressant medication treatment on serum levels of inflammatory cytokines: a meta-analysis. *Neuropsychopharmacol*, 36 (12), 2452–2459.
Hanstein, R., Negoro, H., Patel, N. K., Charollais, A., Meda, P., Spray, D. C., Suadicani, S. O., and Scemes, E., 2013. Promises and pitfalls of a Pannexin1 transgenic mouse line. *Front Pharmacol*, 4, 61.
Harbuz, M. S., Jessop, D. S., Lightman, S. L., and Chowdrey, H. S., 1994. The effects

of restraint or hypertonic saline stress on corticotrophin-releasing factor, arginine vasopressin, and proenkephalin A mRNAs in the CFY, Sprague-Dawley and Wistar strains of rat. *Brain Res*. 667 (1), 6-12.

Harder, J., Franchi, L., Muñoz-Planillo, R., Park, J.-H., Reimer, T., and Nuñez, G., 2009. Activation of the Nlrp3 inflammasome by Streptococcus pyogenes requires streptolysin O and NF-kappa B activation but proceeds independently of TLR signaling and P2X7 receptor. *The Journal of Immunol*, 183 (9), 5823–5829.

Harding, E. J., Paul, E. S., and Mendl, M., 2004. Animal behaviour: cognitive bias and affective state. *Nature*, 427 (6972), 312.

Harijith, A., Ebenezer, D. L., and Natarajan, V., 2014. Reactive oxygen species at the crossroads of inflammasome and inflammation. *Front Physiol*, 5, 352.

Harrigan, R. A. and Brady, W. J., 1999. ECG abnormalities in tricyclic antidepressant ingestion. *Am J Emerg Med*, 17 (4), 387–393.

Hasler, G., 2010. Pathophysiology of depression: do we have any solid evidence of interest to clinicians? *World Psychiat*, 9 (3), 155–161.

He, W.-T., Wan, H., Hu, L., Chen, P., Wang, X., Huang, Z., Yang, Z.-H., Zhong, C.-Q., and Han, J., 2015. Gasdermin D is an executor of pyroptosis and required for interleukin-1β secretion. *Cell Res*, 25 (12), 1285–1298.

Heid, M. E., Keyel, P. A., Kamga, C., Shiva, S., Watkins, S. C., and Salter, R. D., 2013. Mitochondrial reactive oxygen species induces NLRP3-dependent lysosomal damage and inflammasome activation. *J Immunol*, 191 (10), 5230–5238.

Hemphill, J. C., Smith, W. S., Sonne, D. C., Morabito, D., and Manley, G. T., 2005. Relationship between brain tissue oxygen tension and CT perfusion: Feasibility and initial results. *Am J Neuroradiol*, 26 (5), 1095–1100.

Hendrie, C., Pickles, A., Stanford, S. C., and Robinson, E., 2013. The failure of the antidepressant drug discovery process is systemic. *J Psychopharmacol*, 27 (5), 407–16.

Heneka, M. T., Kummer, M. P., Stutz, A., Delekate, A., Schwartz, S., Vieira-Saecker, A., Griep, A., Axt, D., Remus, A., Tzeng, T.-C., Gelpi, E., Halle, A., Korte, M., Latz, E., and Golenbock, D. T., 2014. NLRP3 is activated in Alzheimer's disease andcontributes to pathology in APP/PS1 mice. *Nature*, 493 (7434), 674–678.

Henn, A., Lund, S., Hedtjärn, M., Schrattenholz, A., Pörzgen, P., and Leist, M., 2009. The suitability of BV2 cells as alternative model system for primary microglia cultures or for animal experiments examining brain inflammation. *Altex*, 26 (2), 83.

Henry, C. J., Huang, Y., Wynne, A. M., and Godbout, J. P., 2009. Brain, Behavior, and Immunity. *Brain Behav Immun*, 23 (3), 309–317.

Henry, C. J., Huang, Y., Wynne, A., Hanke, M., Himler, J., Bailey, M. T., Sheridan, J. F., and Godbout, J. P., 2008. Minocycline attenuates lipopolysaccharide (LPS)-induced neuroinflammation, sickness behavior, and anhedonia. *J Neuroinflamm*, 5 (1), 15.

Hernansanz-Agustín, P. and Izquierdo-Álvarez, A., 2014. Acute hypoxia produces a superoxide burst in cells. *Free Radic Biol Med,* 71, 146-156.

Hewinson, J., Moore, S. F., Glover, C., Watts, A. G., and MacKenzie, A. B., 2008. A key role for redox signaling in rapid P2X7 receptor-induced IL-1 beta processing in human monocytes. *J Immunol*, 180 (12), 8410–8420.

Heyes, M. P., Achim, C. L., Wiley, C. A., Major, E. O., Saito, K., and Markey, S. P., 1996. Human microglia convert l-tryptophan into the neurotoxin quinolinic acid. *Biochem J*, 320 (Pt 2), 595–597.

Hiles, S. A., Baker, A. L., de Malmanche, T., and Attia, J., 2012a. Interleukin-6, C-reactive protein and interleukin-10 after antidepressant treatment in people with

depression: a meta-analysis. *Psychol Med*, 42 (10), 2015–2026.
Hiles, S. A., Baker, A. L., de Malmanche, T., and Attia, J., 2012b. A meta-analysis of differences in IL-6 and IL-10 between people with and without depression: Exploring the causes of heterogeneity. *Brain Behavior and Immun*, 26 (7), 1180–1188.
Hines, D. J., Choi, H. B., Hines, R. M., Phillips, A. G., and MacVicar, B. A., 2013. Prevention of LPS-induced microglia activation, cytokine production and sickness behavior with TLR4 receptor interfering peptides. *PLoS ONE*, 8 (3), e60388.
Hinson, R. M., Williams, J. A., and Shacter, E., 1996. Elevated interleukin 6 is induced by prostaglandin E2 in a murine model of inflammation: possible role of cyclooxygenase-2. *Proc Natl Acad Sci*, 93 (10), 4885–4890.
Hodes, G. E., Ménard, C., and Russo, S. J., 2016. Integrating Interleukin-6 into depression diagnosis and treatment. *Neurobiol Stress*. 4, 15-22.
Hoffman, D. L., Salter, J. D., and Brookes, P. S., 2007. Response of mitochondrial reactive oxygen species generation to steady-state oxygen tension: implications for hypoxic cell signaling. *Am J Physiol Heart Circ Physiol*, 292 (1), H101–8.
Honore, P., Donnelly-Roberts, D., Namovic, M. T., Hsieh, G., Zhu, C. Z., Mikusa, J. P., Hernandez, G., Zhong, C., Gauvin, D. M., Chandran, P., Harris, R., Medrano, A. P., Carroll, W., Marsh, K., Sullivan, J. P., Faltynek, C. R., and Jarvis, M. F., 2006. A-740003 [N-(1-{[(cyanoimino)(5-quinolinylamino) methyl]amino}-2,2-dimethylpropyl)-2-(3,4-dimethoxyphenyl)acetamide], a novel and selective P2X7 receptor antagonist, dose-dependently reduces neuropathic pain in the rat. *The J Pharm Exp Ther*, 319 (3), 1376–1385.
Hopkins, S. J., 2003. The pathophysiological role of cytokines. *Leg Med*, 5, S45–S57.
Horak, P., Crawford, A. R., Vadysirisack, D. D., Nash, Z. M., DeYoung, M. P., Sgroi, D., and Ellisen, L. W., 2010. Negative feedback control of HIF-1 through REDD1-regulated ROS suppresses tumorigenesis. *Proc Natl Acad Sci*, 107 (10), 4675–4680.
Hornung, V., Bauernfeind, F., Halle, A., Samstad, E. O., Kono, H., Rock, K. L., Fitzgerald, K. A., and Latz, E., 2008. Silica crystals and aluminum salts activate the NALP3 inflammasome through phagosomal destabilization. *Nature Immunol*, 9 (8), 847–856.
Horvath, R. J., Nutile-McMenemy, N., Alkaitis, M. S., and Deleo, J. A., 2008. Differential migration, LPS-induced cytokine, chemokine, and NO expression in immortalized BV-2 and HAPI cell lines and primary microglial cultures. *J Neurochem*, 107 (2), 557–569.
Howren, M. B., Lamkin, D. M., and Suls, J., 2009. Associations of depression with C-reactive protein, IL-1, and IL-6: a meta-analysis. *Psychosom Med*, 71 (2), 171–186.
Hu, F., Pace, T. W. W., and Miller, A. H., 2009. Interferon-alpha inhibits glucocorticoid receptor-mediated gene transcription via STAT5 activation in mouse HT22 cells. *Brain Behav Immun*, 23 (4), 455–463.
Huang, L. E., Arany, Z., Livingston, D. M., and Bunn, H. F., 1996. Activation of hypoxia-inducible transcription factor depends primarily upon redox-sensitive stabilization of its α subunit. *J Biol Chem,* 271 (50), 32253-9
Huckans, M., Fuller, B., Wheaton, V., Jaehnert, S., Ellis, C., Kolessar, M., Kriz, D., Anderson, J. R., Berggren, K., Olavarria, H., Sasaki, A. W., Chang, M., Flora, K. D., and Loftis, J. M., 2015. A longitudinal study evaluating the effects of interferon-alpha therapy on cognitive and psychiatric function in adults with chronic hepatitis C. *J Psychosom Res*, 78 (2), 184–192.
Humphreys, B. D. and Dubyak, G. R., 1998. Modulation of P2X7 nucleotide receptor

expression by pro- and anti-inflammatory stimuli in THP-1 monocytes. *J Leukoc Biol*, 64 (2), 265–273.

Huynh, T. N., Krigbaum, A. M., Hanna, J. J., and Conrad, C. D., 2011. Sex differences and phase of light cycle modify chronic stress effects on anxiety and depressive-like behavior. *Behav Brain Res*, 222 (1), 212–222.

Ida, T., Hara, M., Nakamura, Y., Kozaki, S., Tsunoda, S., and Ihara, H., 2008. Cytokine-induced enhancement of calcium-dependent glutamate release from astrocytes mediated by nitric oxide. *Neurosci Lett*, 432 (3), 232–236.

Ieraci, A., Mallei, A., and Popoli, M., 2016. Social isolation stress induces anxious-depressive-like behavior and alterations of neuroplasticity-related genes in adult male mice. *Neural Plast*, 2016, 6212983.

Inoue, W., Matsumura, K., Yamagata, K., Takemiya, T., Shiraki, T., and Kobayashi, S., 2002. Brain-specific endothelial induction of prostaglandin E(2) synthesis enzymes and its temporal relation to fever. *Neurosci Res*, 44 (1), 51–61.

Iosif, R. E., 2006. Tumor necrosis factor receptor 1 is a negative regulator of progenitor proliferation in adult hippocampal neurogenesis. *J Neurosci*, 26 (38), 9703–9712.

Ivanovic, Z., 2009. Hypoxia or in situ normoxia: The stem cell paradigm. *J Cell Physiol*, 219 (2), 271–275.

Iwata, M., Ota, K. T., and Duman, R. S., 2013. The inflammasome: Pathways linking psychological stress, depression, and systemic illnesses. *Brain Behav Immun*, 31, 105–114.

Iwata, M., Ota, K. T., Li, X.-Y., Sakaue, F., Li, N., Dutheil, S., Banasr, M., Duric, V., Yamanashi, T., Kaneko, K., Rasmussen, K., Glasebrook, A., Koester, A., Song, D., Jones, K. A., Zorn, S., Smagin, G., and Duman, R. S., 2016. Psychological stress activates the inflammasome via release of adenosine triphosphate and stimulation of the purinergic type 2X7 receptor. *Biol Psychiat*, 80 (1), 12–22.

Jaakkola, P., Mole, D. R., Tian, Y. M., Wilson, M. I., Gielbert, J., Gaskell, S. J., Kriegsheim, von, A., Hebestreit, H. F., Mukherji, M., Schofield, C. J., Maxwell, P. H., Pugh, C. W., and Ratcliffe, P. J., 2001. Targeting of HIF-alpha to the von Hippel-Lindau ubiquitylation complex by O2-regulated prolyl hydroxylation. *Science*, 292 (5516), 468–472.

Jaehne, E. J., Corrigan, F., Toben, C., Jawahar, M. C., and Baune, B. T., 2015. The effect of the antipsychotic drug quetiapine and its metabolite norquetiapine on acute inflammation, memory and anhedonia. *Pharmacol Biochem Behav*, 135, 136–144.

Jangra, A., Kwatra, M., Singh, T., Pant, R., Kushwah, P., Sharma, Y., Saroha, B., Datusalia, A. K., and Bezbaruah, B. K., 2016. Piperine augments the protective effect of curcumin against lipopolysaccharide-induced neurobehavioral and neurochemical deficits in mice. *Inflamm*, 39 (3), 1025–1038.

Jangra, A., Lukhi, M. M., Sulakhiya, K., Baruah, C. C., and Lahkar, M., 2014. Protective effect of mangiferin against lipopolysaccharide-induced depressive and anxiety-like behaviour in mice. *Eur J Pharmacol*, 740, 337–345.

Ji, W.-W., Wang, S.-Y., Ma, Z.-Q., Li, R.-P., Li, S.-S., Xue, J.-S., Li, W., Niu, X.-X., Yan, L., Zhang, X., Fu, Q., Qu, R., and Ma, S.-P., 2014. Effects of perillaldehyde on alternations in serum cytokines and depressive-like behavior in mice after lipopolysaccharide administration. *Pharmacol Biochem Behav*, 116, 1–8.

Jiang, B. H., Semenza, G. L., Bauer, C., and Marti, H. H., 1996. Hypoxia-inducible factor 1 levels vary exponentially over a physiologically relevant range of O2 tension. *Am J Physiol*, 271 (4 Pt 1), C1172–80.

Jick, H., Kaye, J. A., and Jick, S. S., 2004. Antidepressants and the risk of suicidal

behaviors. *JAMA*, 292 (3), 338–343.
Juliana, C., Fernandes-Alnemri, T., Kang, S., Farias, A., Qin, F., and Alnemri, E. S., 2012. Non-transcriptional priming and deubiquitination regulate NLRP3 inflammasome activation. *J Biol Chem*, 287 (43), 36617–36622.
Kahlenberg, J. M. and Dubyak, G. R., 2004. Mechanisms of caspase-1 activation by P2X7 receptor-mediated K+ release. *American journal of physiology. Cell Physiol*, 286 (5), C1100–8.
Kalyanaraman, B., Darley-Usmar, V., Davies, K. J. A., Dennery, P. A., Forman, H. J., Grisham, M. B., Mann, G. E., Moore, K., Roberts, L. J., and Ischiropoulos, H., 2012. Measuring reactive oxygen and nitrogen species with fluorescent probes: challenges and limitations. *Free Radic Biol Med*, 52 (1), 1–6.
Kaneko, N., Kudo, K., Mabuchi, T., Takemoto, K., Fujimaki, K., Wati, H., Iguchi, H., Tezuka, H., and Kanba, S., 2006. Suppression of cell proliferation by interferon-alpha through interleukin-1 production in adult rat dentate gyrus. *Neuropsychopharmacol*, 31 (12), 2619–2626.
Kang, A., Hao, H., Zheng, X., Liang, Y., Xie, Y., Xie, T., Dai, C., Zhao, Q., Wu, X., Xie, L., and Wang, G., 2011. Peripheral anti-inflammatory effects explain the ginsenosides paradox between poor brain distribution and anti-depression efficacy. *J Neuroinflamm*, 8, 100.
Kanneganti, T.-D., Lamkanfi, M., Kim, Y.-G., Chen, G., Park, J.-H., Franchi, L., Vandenabeele, P., and Nuñez, G., 2007. Pannexin-1-mediated recognition of bacterial molecules activates the cryopyrin inflammasome independent of Toll-like receptor signaling. *Immunity*, 26 (4), 433–443.
Karmakar, M., Katsnelson, M. A., Dubyak, G. R., and Pearlman, E., 2016. Neutrophil P2X7 receptors mediate NLRP3 inflammasome-dependent IL-1β secretion in response to ATP. *Nature Comm*, 7, 10555.
Kaster, M. P., Gadotti, V. M., Calixto, J. B., Santos, A. R. S., and Rodrigues, A. L. S., 2012. Depressive-like behavior induced by tumor necrosis factor-a in mice. *Neuropharmacol*, 62 (1), 419–426.
Katsnelson, M. A., Rucker, L. G., Russo, H. M., and Dubyak, G. R., 2015. K+ efflux agonists induce NLRP3 inflammasome activation independently of Ca2+ signaling. *J Immunol*, 194 (8), 3937–3952.
Kaushik, D. K., Gupta, M., Kumawat, K. L., and Basu, A., 2012. NLRP3 inflammasome: key mediator of neuroinflammation in murine Japanese encephalitis. *PLoS ONE*, 7 (2), e32270.
Kawai, T. and Akira, S., 2007. Signaling to NF-kappaB by Toll-like receptors. *Trends Mol Med*, 13 (11), 460–469.
Kayagaki, N., Warming, S., Lamkanfi, M., Vande Walle, L., Louie, S., Dong, J., Newton, K., Qu, Y., Liu, J., Heldens, S., Zhang, J., Lee, W. P., Roose-Girma, M., and Dixit, V. M., 2011. Non-canonical inflammasome activation targets caspase-11. *Nature*, 479 (7371), 117–121.
Kayagaki, N., Wong, M. T., Stowe, I. B., Ramani, S. R., Gonzalez, L. C., Akashi-Takamura, S., Miyake, K., Zhang, J., Lee, W. P., Muszyński, A., Forsberg, L. S., Carlson, R. W., and Dixit, V. M., 2013. Noncanonical inflammasome activation by intracellular LPS independent of TLR4. *Science*, 341 (6151), 1246–1249.
Kessler, R. C., 2003b. Epidemiology of women and depression. *J Affect Disord*, 74 (1), 5–13.
Kessler, R. C., Berglund, P., Demler, O., Jin, R., Koretz, D., Merikangas, K. R., Rush, A. J., Walters, E. E., Wang, P. S., National Comorbidity Survey Replication, 2003a. The epidemiology of major depressive disorder: results from the National

Comorbidity Survey Replication (NCS-R). *JAMA*, 289 (23), 3095–3105.
Kessler, R. C., Chiu, W. T., Demler, O., Merikangas, K. R., and Walters, E. E., 2005. Prevalence, severity, and comorbidity of 12-month DSM-IV disorders in the National Comorbidity Survey Replication. *Arch Gen Psychiat*, 62 (6), 617–627.
Kettenmann, H., Hanisch, U.-K., Noda, M., and Verkhratsky, A., 2011. Physiology of microglia. *Physiol Rev*, 91 (2), 461–553.
Khoury, El, J., Toft, M., Hickman, S. E., Means, T. K., Terada, K., Geula, C., and Luster, A. D., 2007. Ccr2 deficiency impairs microglial accumulation and accelerates progression of Alzheimer-like disease. *Nature Med*, 13 (4), 432–438.
Kilic, M., Kasperczyk, H., Fulda, S., and Debatin, K.-M., 2007. Role of hypoxia inducible factor-1 alpha in modulation of apoptosis resistance. *Oncogene*, 26 (14), 2027–2038.
Kim, S. Y., Choi, Y. J., Joung, S. M., Lee, B. H., Jung, Y.-S., and Lee, J. Y., 2010. Hypoxic stress up-regulates the expression of Toll-like receptor 4 in macrophages via hypoxia-inducible factor. *Immunol*, 129 (4), 516–524.
Kino, T. and Chrousos, G. P., 2003. Tumor necrosis factor alpha receptor- and Fas-associated FLASH inhibit transcriptional activity of the glucocorticoid receptor by binding to and interfering with its interaction with p160 type nuclear receptor coactivators. *J Biol Chem*, 278 (5), 3023–3029.
Kitagami, T., Yamada, K., Miura, H., Hashimoto, R., Nabeshima, T., and Ohta, T., 2003. Mechanism of systemically injected interferon-alpha impeding monoamine biosynthesis in rats: role of nitric oxide as a signal crossing the blood-brain barrier. *Brain Res*, 978 (1-2), 104–114.
Klengel, T., Mehta, D., Anacker, C., Rex-Haffner, M., Pruessner, J. C., Pariante, C. M., Pace, T. W. W., Mercer, K. B., Mayberg, H. S., Bradley, B., Nemeroff, C. B., Holsboer, F., Heim, C. M., Ressler, K. J., Rein, T., and Binder, E. B., 2013. Allele-specific FKBP5 DNA demethylation mediates gene-childhood trauma interactions. *Nature Neurosci*, 16 (1), 33–41.
Kobayashi, K., Imagama, S., Ohgomori, T., Hirano, K., Uchimura, K., Sakamoto, K., Hirakawa, A., Takeuchi, H., Suzumura, A., Ishiguro, N., and Kadomatsu, K., 2013. Minocycline selectively inhibits M1 polarization of microglia. *Cell Death Dis*, 4, e525.
Koenigsknecht-Talboo, J. and Landreth, G. E., 2005. Microglial phagocytosis induced by fibrillar beta-amyloid and IgGs are differentially regulated by proinflammatory cytokines. *J Neurosci*, 25 (36), 8240–8249.
Kohman, R. A., Crowell, B., and Kusnecov, A. W., 2010. Differential sensitivity to endotoxin exposure in young and middle-age mice. *Brain Behav Immun*, 24 (3), 486–492.
Kohno, M., 2010. Applications of electron spin resonance spectrometry for reactive oxygen species and reactive nitrogen species research. *J Clin Biochem Nutr*, 47 (1), 1–11.
Koike, H., Fukumoto, K., Iijima, M., and Chaki, S., 2013. Role of BDNF/TrkB signaling in antidepressant-like effects of a group II metabotropic glutamate receptor antagonist in animal models of depression. *Behav Brain Res*, 238, 48–52.
Kokare, D. M., Dandekar, M. P., Singru, P. S., Gupta, G. L., and Subhedar, N. K., 2010. Involvement of alpha-MSH in the social isolation induced anxiety- and depression-like behaviors in rat. *Neuropharmacol*, 58 (7), 1009–1018.
Koo, J. W. and Duman, R. S., 2008. IL-1 beta is an essential mediator of the antineurogenic and anhedonic effects of stress. *Proc Natl Acad Sci*, 105 (2), 751–756.

Koob, G. F. and Zorrilla, E. P., 2012. Update on corticotropin-releasing factor pharmacotherapy for psychiatric disorders: a revisionist view. *Neuropsychopharmacol*, 37 (1), 308–309.

Kopp, C., Vogel, E., Rettori, M. C., and Delagrange, P., 1998. Effects of a daylight cycle reversal on locomotor activity in several inbred strains of mice. *Physiol Behav*, 63 (4), 577-585.

Kovarova, M., Hesker, P. R., Jania, L., Nguyen, M., Snouwaert, J. N., Xiang, Z., Lommatzsch, S. E., Huang, M. T., Ting, J. P. Y., and Koller, B. H., 2012. NLRP1-dependent pyroptosis leads to acute lung injury and morbidity in mice. *J Immunol*, 189 (4), 2006–2016.

Köhler, O., Benros, M. E., Nordentoft, M., Farkouh, M. E., Iyengar, R. L., Mors, O., and Krogh, J., 2014. Effect of anti-inflammatory treatment on depression, depressive symptoms, and adverse effects: a systematic review and meta-analysis of randomized clinical trials. *JAMA Psychiat*, 71 (12), 1381–1391.

Kraus, M. R., Schäfer, A., Faller, H., Csef, H., and Scheurlen, M., 2002. Paroxetine for the treatment of interferon-α-induced depression in chronic hepatitis C. *Aliment Pharmacol Ther*, 16 (6), 1091–1099.

Krishna, S., Dodd, C. A., and Filipov, N. M., 2016. Behavioral and monoamine perturbations in adult male mice with chronic inflammation induced by repeated peripheral lipopolysaccharide administration. *Behav Brain Res*, 302, 279–290.

Krishnan, V. and Nestler, E. J., 2011. Animal models of depression: molecular perspectives. *Curr Top Behav Neurosci*, 7, 121–147.

Krzyszton, C. P., Sparkman, N. L., Grant, R. W., Buchanan, J. B., Broussard, S. R., Woods, J., and Johnson, R. W., 2008. Exacerbated fatigue and motor deficits in interleukin-10-deficient mice after peripheral immune stimulation. *Am J Physiol Regul Integ Comp Physiol*, 295 (4), R1109–14.

Kubera, M., Curzytek, K., Duda, W., Leskiewicz, M., Basta-Kaim, A., Budziszewska, B., Roman, A., Zajicova, A., Holan, V., Szczesny, E., Lason, W., and Maes, M., 2013. A new animal model of (chronic) depression induced by repeated and intermittent lipopolysaccharide administration for 4 months. *Brain Behav Immun*, 31, 96–104.

Kussmaul, L. and Hirst, J., 2006. The mechanism of superoxide production by NADH:ubiquinone oxidoreductase (complex I) from bovine heart mitochondria. *Proc Natl Acad Sci*, 103 (20), 7607–7612.

Lane, T., Flam, B., Lockey, R., and Kolliputi, N., 2013. TXNIP shuttling: missing link between oxidative stress and inflammasome activation. *Front Physiol*, 4, 50.

Lapidus, K. A. B., Levitch, C. F., Perez, A. M., Brallier, J. W., Parides, M. K., Soleimani, L., Feder, A., Iosifescu, D. V., Charney, D. S., and Murrough, J. W., 2014. A randomized controlled trial of intranasal ketamine in major depressive disorder. *Biol Psychiat*, 76 (12), 970–976.

Larsson, M. K., Faka, A., Bhat, M., Imbeault, S., Goiny, M., Orhan, F., Oliveros, A., Ståhl, S., Liu, X. C., Choi, D. S., Sandberg, K., Engberg, G., Schwieler, L., and Erhardt, S., 2016. Repeated LPS injection induces distinct changes in the kynurenine pathway in mice. *Neurochem Res*, 41 (9), 2243–2255.

Lawrence, T., 2009. The nuclear factor NF-kappaB pathway in inflammation. *Cold Spring Harb Perspect Biol*, 1 (6), a001651.

Lawson, L. J., Perry, V. H., Dri, P., and Gordon, S., 1990. Heterogeneity in the distribution and morphology of microglia in the normal adult mouse brain. *Neurosci*. 39 (1), 151-170.

Lawson, M. A., McCusker, R. H., and Kelley, K. W., 2013a. Interleukin-1 beta converting enzyme is necessary for development of depression-like behavior

following intracerebroventricular administration of lipopolysaccharide to mice. *J Neuroinflamm*, 10, 54.
Lawson, M. A., Parrott, J. M., McCusker, R. H., Dantzer, R., Kelley, K. W., and O Connor, J. C., 2013b. Intracerebroventricular administration of lipopolysaccharide induces indoleamine-2,3-dioxygenase-dependent depression-like behaviors. *J Neuroinflamm*, 10 (1), 87.
Lecoq, J., Tiret, P., Najac, M., Shepherd, G. M., Greer, C. A., and Charpak, S., 2009. Odor-evoked oxygen consumption by action potential and synaptic transmission in the olfactory bulb. *J Neurosci*, 29 (5), 1424–1433.
Lee, H.-J. and Kim, K.-W., 2012. Anti-inflammatory effects of arbutin in lipopolysaccharide-stimulated BV2 microglial cells. *Inflamm Res*, 61 (8), 817–825.
Lee, S. C., Liu, W., Dickson, D. W., Brosnan, C. F., and Berman, J. W., 1993. Cytokine production by human fetal microglia and astrocytes. Differential induction by lipopolysaccharide and IL-1 beta. *J Immunol*, 150 (7), 2659–2667.
Lewis, S. R., Ahmed, S., Dym, C., Khaimova, E., Kest, B., and Bodnar, R. J., 2005. Inbred mouse strain survey of sucrose intake. *Physiol Behav*, 85 (5), 546–556.
Lépine, J.-P. and Briley, M., 2011. The increasing burden of depression. *Neuropsychiatr Dis Treatm*, 7 (Suppl 1), 3–7.
Li, Q. and Verma, I. M., 2002. NF-κB regulation in the immune system. *Nat Rev Immunol,* 2 (10), 725–734.
Li, R., Wang, X., Qin, T., Qu, R., and Ma, S., 2016. Apigenin ameliorates chronic mild stress-induced depressive behavior by inhibiting interleukin-1β production and NLRP3 inflammasome activation in the rat brain. *Behav Brain Res*, 296, 318–325.
Li, R., Zhao, D., Qu, R., Fu, Q., and Ma, S., 2015. The effects of apigenin on lipopolysaccharide-induced depressive-like behavior in mice. *Neurosci Lett,* 594, 17–22.
Li, X., Rong, Y., Zhang, M., Wang, X. L., LeMaire, S. A., Coselli, J. S., Zhang, Y., and Shen, Y. H., 2009. Up-regulation of thioredoxin interacting protein (Txnip) by p38 MAPK and FOXO1 contributes to the impaired thioredoxin activity and increased ROS in glucose-treated endothelial cells. *Biochem Biophysic Res Comm*, 381 (4), 660–665.
Liang, Y., Jing, X., Zeng, Z., Bi, W., Chen, Y., Wu, X., Yang, L., Liu, J., Xiao, S., Liu, S., Lin, D., and Tao, E., 2015. Rifampicin attenuates rotenone-induced inflammation via suppressing NLRP3 inflammasome activation in microglia. *Brain Res*, 1622, 43–50.
Lichtman, J. H., Froelicher, E. S., Blumenthal, J. A., Carney, R. M., Doering, L. V., Frasure-Smith, N., Freedland, K. E., Jaffe, A. S., Leifheit-Limson, E. C., Sheps, D. S., Vaccarino, V., Wulsin, L., American Heart Association Statistics Committee of the Council on Epidemiology and Prevention and the Council on Cardiovascular and Stroke Nursing, 2014. Depression as a risk factor for poor prognosis among patients with acute coronary syndrome: systematic review and recommendations: a scientific statement from the American Heart Association. *Circulation*, 129 (12), 1350–1369.
Lima, H., Jacobson, L. S., Goldberg, M. F., Chandran, K., Diaz-Griffero, F., Lisanti, M. P., and Brojatsch, J., 2013. Role of lysosome rupture in controlling Nlrp3 signaling and necrotic cell death. *Cell Cycle*, 12 (12), 1868–1878.
Liu, B., Wang, K., Gao, H. M., Mandavilli, B., Wang, J. Y., and Hong, J. S., 2001. Molecular consequences of activated microglia in the brain: overactivation induces apoptosis. *J Neurochem*, 77 (1), 182–189.
Liu, J., Narasimhan, P., Lee, Y.-S., Song, Y. S., Endo, H., Yu, F., and Chan, P. H.,

2006. Mild hypoxia promotes survival and proliferation of SOD2-deficient astrocytes via c-Myc activation. *J Neurosci*, 26 (16), 4329–4337.
Liu, S.-L., Lin, X., Shi, D.-Y., Cheng, J., Wu, C.-Q., and Zhang, Y.-D., 2002. Reactive oxygen species stimulated human hepatoma cell proliferation via cross-talk between PI3-K/PKB and JNK signaling pathways. *Arch Biochem Biophysic*, 406 (2), 173–182.
Liu, Y., Ho, R. C.-M., and Mak, A., 2012. Interleukin (IL)-6, tumour necrosis factor alpha (TNF-α) and soluble interleukin-2 receptors (sIL-2R) are elevated in patients with major depressive disorder: A meta-analysis and meta-regression. *J Affect Dis*, 139 (3), 230–239.
Liu, Y.-W., Sakaeda, T., Takara, K., Nakamura, T., Ohmoto, N., Komoto, C., Kobayashi, H., Yagami, T., Okamura, N., and Okumura, K., 2003. Effects of reactive oxygen species on cell proliferation and death in HeLa cells and its MDR1-overexpressing derivative cell line. *Biol Pharmaceut Bull*, 26 (2), 278–281.
Lohoff, F. W., 2010. Overview of the genetics of major depressive disorder. *Curr Psychiat Rep*, 12 (6), 539–546.
Lopez, A. D., Mathers, C. D., Ezzati, M., Jamison, D. T., and Murray, C. J. L., 2006. Global and regional burden of disease and risk factors, 2001: systematic analysis of population health data. *Lancet*, 367 (9524), 1747–1757.
Lu, A., Magupalli, V. G., Ruan, J., Yin, Q., Atianand, M. K., Vos, M. R., Schröder, G. F., Fitzgerald, K. A., Wu, H., and Egelman, E. H., 2014. Unified polymerization mechanism for the assembly of ASC-dependent inflammasomes. *Cell*, 156 (6), 1193–1206.
Lucki, I., Dalvi, A., and Mayorga, A. J., 2001. Sensitivity to the effects of pharmacologically selective antidepressants in different strains of mice. *Psychopharmacol*, 155 (3), 315–322.
Lutz, P.-E. and Kieffer, B. L., 2013. Opioid receptors: distinct roles in mood disorders. *Trends Neurosci*, 36 (3), 195–206.
Lyons, D. G., Parpaleix, A., Roche, M., and Charpak, S., 2016. Mapping oxygen concentration in the awake mouse brain. *eLife*, 5. e12024.
Ma, M., Ren, Q., Zhang, J.-C., and Hashimoto, K., 2014. Effects of brilliant blue G on serum tumor necrosis factor-α levels and depression-like behavior in mice after lipopolysaccharide administration. *Clin Psychopharmacol Neurosci*, 12 (1), 31–36.
Madrigal, J. L. M., Moro, M. A., Lizasoain, I., Lorenzo, P., Fernández, A. P., Rodrigo, J., Boscá, L., and Leza, J. C., 2003. Induction of cyclooxygenase-2 accounts for restraint stress-induced oxidative status in rat brain. *Neuropsychopharmacol*, 28 (9), 1579–1588.
Mague, S. D., 2003. Antidepressant-like effects of kappa-opioid receptor antagonists in the forced swim test in rats. *J Pharmacol Exp Ther*, 305 (1), 323–330.
Majumdar, A., Cruz, D., Asamoah, N., Buxbaum, A., Sohar, I., Lobel, P., and Maxfield, F. R., 2007. Activation of microglia acidifies lysosomes and leads to degradation of Alzheimer amyloid fibrils. *Mol Biol Cell*, 18 (4), 1490–1496.
Malberg, J. E., Eisch, A. J., Nestler, E. J., and Duman, R. S., 2000. Chronic antidepressant treatment increases neurogenesis in adult rat hippocampus. *J Neurosci*, 20 (24), 9104–9110.
Malkesman, O., Scattoni, M. L., Paredes, D., Tragon, T., Pearson, B., Shaltiel, G., Chen, G., Crawley, J. N., and Manji, H. K., 2010. The female urine sniffing test: a novel approach for assessing reward-seeking behavior in rodents. *Biol Psychiat*, 67 (9), 864–871.
Marek, R., Caruso, M., Rostami, A., Grinspan, J. B., and Sarma, Das, J., 2008.

Magnetic cell sorting: a fast and effective method of concurrent isolation of high purity viable astrocytes and microglia from neonatal mouse brain tissue. *J Neurosci Methods*, 175 (1), 108–118.

Mariathasan, S., Weiss, D. S., Newton, K., McBride, J., O'Rourke, K., Roose-Girma, M., Lee, W. P., Weinrauch, Y., Monack, D. M., and Dixit, V. M., 2006. Cryopyrin activates the inflammasome in response to toxins and ATP. *Nature*, 440 (7081), 228–232.

Martin, A. L. and Brown, R. E., 2010. The lonely mouse: verification of a separation-induced model of depression in female mice. *Behav Brain Res*, 207 (1), 196–207.

Martinez, F. O. and Gordon, S., 2014. The M1 and M2 paradigm of macrophage activation: time for reassessment. *F1000prime Rep*, 6, 13.

Martinon, F., Burns, K., and Tschopp, J., 2002. The inflammasome: a molecular platform triggering activation of inflammatory caspases and processing of proIL-beta. *Mol Cell*, 10 (2), 417–426.

Martín-de-Saavedra, M. D., Budni, J., Cunha, M. P., Gómez-Rangel, V., Lorrio, S., Del Barrio, L., Lastres-Becker, I., Parada, E., Tordera, R. M., Rodrigues, A. L. S., Cuadrado, A., and López, M. G., 2013. Nrf2 participates in depressive disorders through an anti-inflammatory mechanism. *Psychoneuroendocrinol*, 38 (10), 2010–2022.

Masamoto, K. and Tanishita, K., 2009. Oxygen transport in brain tissue. *J Biomech Eng*, 131 (7), 074002.

Masson, N., Willam, C., Maxwell, P. H., Pugh, C. W., and Ratcliffe, P. J., 2001. Independent function of two destruction domains in hypoxia-inducible factor-alpha chains activated by prolyl hydroxylation. *Embo J*, 20 (18), 5197–5206.

Masters, S. L., Dunne, A., Subramanian, S. L., Hull, R. L., Tannahill, G. M., Sharp, F. A., Becker, C., Franchi, L., Yoshihara, E., Chen, Z., Mullooly, N., Mielke, L. A., Harris, J., Coll, R. C., Mills, K. H. G., Mok, K. H., Newsholme, P., Nuñez, G., Yodoi, J., Kahn, S. E., Lavelle, E. C., and O'Neill, L. A. J., 2010. Activation of the NLRP3 inflammasome by islet amyloid polypeptide provides a mechanism for enhanced IL-1β in type 2 diabetes. *Nature Immunol*, 11 (10), 897–904.

Mathers, C. D. and Loncar, D., 2006. Projections of global mortality and burden of disease from 2002 to 2030. *PLoS medicine*, 3 (11), e442.

Mazure, N. M. and Pouysségur, J., 2010. Hypoxia-induced autophagy: cell death or cell survival? *Curr Opin Cell Biol*, 22 (2), 177–180.

McEwen, B. S., 1998. Protective and damaging effects of stress mediators. *New Eng J Med,* 338 (3), 171–179.

Medeiros, I. U., Ruzza, C., Asth, L., Guerrini, R., Romão, P. R. T., Gavioli, E. C., and Calo, G., 2015. Blockade of nociceptin/orphanin FQ receptor signaling reverses LPS-induced depressive-like behavior in mice. *Peptides*, 72, 95–103.

Meissner, F., Molawi, K., and Zychlinsky, A., 2008. Superoxide dismutase 1 regulates caspase-1 and endotoxic shock. *Nature Immunol*, 9 (8), 866–872.

Meissner, F., Molawi, K., and Zychlinsky, A., 2010. Mutant superoxide dismutase 1-induced IL-1beta accelerates ALS pathogenesis. *Proc Natl Acad Sci*, 107 (29), 13046–13050.

Mello, B. S. F., Monte, A. S., McIntyre, R. S., Soczynska, J. K., Custódio, C. S., Cordeiro, R. C., Chaves, J. H., Vasconcelos, S. M. M., Nobre, H. V., Florenço de Sousa, F. C., Hyphantis, T. N., Carvalho, A. F., and Macêdo, D. S., 2013. Effects of doxycycline on depressive-like behavior in mice after lipopolysaccharide (LPS) administration. *J Psychiatr Res*, 47 (10), 1521–1529.

Mendelson, S. D. and Pfaus, J. G., 1989. Level searching: A new assay of sexual

motivation in the male rat. *Physiol Behav*, 45 (2), 337–341.
Mendlewicz, J., Kriwin, P., Oswald, P., Souery, D., Alboni, S., and Brunello, N., 2006. Shortened onset of action of antidepressants in major depression using acetylsalicylic acid augmentation: a pilot open-label study. *Int Clin Psychopharmacol*, 21 (4), 227–231.
Miao, E. A., Rajan, J. V., and Aderem, A., 2011. Caspase-1-induced pyroptotic cell death. *Immunol Rev*, 243 (1), 206–214.
Miller, A. H. and Raison, C. L., 2016. The role of inflammation in depression: from evolutionary imperative to modern treatment target. *Nat Rev Immunol,* 16 (1), 22–34.
Miller, G. E., Chen, E., Sze, J., Marin, T., Arevalo, J. M. G., Doll, R., Ma, R., and Cole, S. W., 2008. A functional genomic fingerprint of chronic stress in humans: blunted glucocorticoid and increased NF-kappaB signaling. *Biol Psychiat*, 64 (4), 266–272.
Momeni, M., Ghorban, K., Dadmanesh, M., Khodadadi, H., Bidaki, R., Kazemi Arababadi, M., and Kennedy, D., 2016. ASC provides a potential link between depression and inflammatory disorders: A clinical study of depressed Iranian medical students. *Nord J Psychiat*, 70 (4), 280-284.
Monif, M., Reid, C. A., Powell, K. L., Smart, M. L., and Williams, D. A., 2009. The P2X7 receptor drives microglial activation and proliferation: a trophic role for P2X7R pore. *J Neurosci*, 29 (12), 3781–3791.
Monje, M. L., Toda, H., and Palmer, T. D., 2003. Inflammatory blockade restores adult hippocampal neurogenesis. *Science*, 302 (5651), 1760–1765.
Moussavi, S., Chatterji, S., Verdes, E., Tandon, A., Patel, V., and Ustun, B., 2007. Depression, chronic diseases, and decrements in health: results from the World Health Surveys. *Lancet*, 370 (9590), 851–858.
Mukandala, G., Tynan, R., Lanigan, S., and O'Connor, J. J., 2016. The Effects of Hypoxia and Inflammation on Synaptic Signaling in the CNS. *Brain Sci*, 6 (1).
Muñoz-Planillo, R., Kuffa, P., Martínez-Colón, G., Smith, B. L., Rajendiran, T. M., and Nuñez, G., 2013. K^+ efflux is the common trigger of NLRP3 inflammasome activation by bacterial toxins and particulate matter. *Immunity*, 38 (6), 1142–1153.
Murakami, T., Ockinger, J., Yu, J., Byles, V., McColl, A., Hofer, A. M., and Horng, T., 2012. Critical role for calcium mobilization in activation of the NLRP3 inflammasome. *Proc Natl Acad Sci,* 109 (28), 11282–11287.
Murphy, N., Cowley, T. R., Richardson, J. C., Virley, D., Upton, N., Walter, D., and Lynch, M. A., 2012. The neuroprotective effect of a specific $P2X_7$ receptor antagonist derives from its ability to inhibit assembly of the NLRP3 inflammasome in glial cells. *Brain Pathol*, 22 (3), 295–306.
Murray, C. and Lopez, A. D., 1997. Alternative projections of mortality and disability by cause 1990-2020: Global burden of disease study. *Lancet*, 349 (9064), 1498–1504.
Murrough, J. W., Iosifescu, D. V., Chang, L. C., Jurdi, Al, R. K., Green, C. E., Perez, A. M., Iqbal, S., Pillemer, S., Foulkes, A., Shah, A., Charney, D. S., and Mathew, S. J., 2013. Antidepressant efficacy of ketamine in treatment-resistant major depression: a two-site randomized controlled trial. *American J Psychiat*, 170 (10), 1134–1142.
Muruve, D. A., Pétrilli, V., Zaiss, A. K., White, L. R., Clark, S. A., Ross, P. J., Parks, R. J., and Tschopp, J., 2008. The inflammasome recognizes cytosolic microbial and host DNA and triggers an innate immune response. *Nature*, 452 (7183), 103–107.
Muscat, R., Papp, M., and Willner, P., 1992. Reversal of stress-induced anhedonia by the atypical antidepressants, fluoxetine and maprotiline. *Psychopharmacol*, 109

(4), 433–438.
Musselman, D. L., Lawson, D. H., Gumnick, J. F., Manatunga, A. K., Penna, S., Goodkin, R. S., Greiner, K., Nemeroff, C. B., and Miller, A. H., 2001. Paroxetine for the prevention of depression induced by high-dose interferon alfa. *New Eng J Med*, 344 (13), 961–966.
Müller, L. G., Borsoi, M., Stolz, E. D., Herzfeldt, V., Viana, A. F., Ravazzolo, A. P., and Rates, S. M. K., 2015. Diene valepotriates from Valeriana glechomifolia prevent lipopolysaccharide-induced sickness and depressive-like behavior in mice. 2015. *Evid Based Complementary Altern Med*, 145914.
Müller, N., Schwarz, M. J., Dehning, S., Douhe, A., Cerovecki, A., Goldstein-Müller, B., Spellmann, I., Hetzel, G., Maino, K., Kleindienst, N., Möller, H.-J., Arolt, V., and Riedel, M., 2006. The cyclooxygenase-2 inhibitor celecoxib has therapeutic effects in major depression: results of a double-blind, randomized, placebo controlled, add-on pilot study to reboxetine. *Mol Psychiat*, 11 (7), 680–684.
Na, A. R., Chung, Y. M., Lee, S. B., Park, S. H., Lee, M.-S., and Yoo, Y. D., 2008. A critical role for Romo1-derived ROS in cell proliferation. *Biochem Biophysic Res Comm*, 369 (2), 672–678.
Nagata, K., Imai, T., Yamashita, T., Tsuda, M., Tozaki-Saitoh, H., and Inoue, K., 2009. Antidepressants inhibit P2X4 receptor function: a possible involvement in neuropathic pain relief. *Mol Pain*, 5, 20.
Nakahira, K., Haspel, J. A., Rathinam, V. A. K., Lee, S.-J., Dolinay, T., Lam, H. C., Englert, J. A., Rabinovitch, M., Cernadas, M., Kim, H. P., Fitzgerald, K. A., Ryter, S. W., and Choi, A. M. K., 2011. Autophagy proteins regulate innate immune responses by inhibiting the release of mitochondrial DNA mediated by the NALP3 inflammasome. *Nature Immunol*, 12 (3), 222–230.
Napoli, I. and Neumann, H., 2009. Microglial clearance function in health and disease. *Neurosci*, 158 (3), 1030–1038.
National Collaborating Centre for Mental Health (UK), 2010. Depression in adults with a chronic physical health problem: treatment and management.
Ndubuizu, O. and LaManna, J. C., 2007. Brain tissue oxygen concentration measurements. *Antioxid Redox Signal*, 9 (8), 1207–1219.
Nestler, E. J. and Hyman, S. E., 2010. Animal models of neuropsychiatric disorders. *Nature Neurosci*, 13 (10), 1161–1169.
Nestler, E. J., Barrot, M., DiLeone, R. J., Eisch, A. J., Gold, S. J., and Monteggia, L. M., 2002. Neurobiology of depression. *Neuron*, 34 (1), 13–25.
Nwaigwe, C. I., Roche, M. A., Grinberg, O., and Dunn, J. F., 2000. Effect of hyperventilation on brain tissue oxygenation and cerebrovenous PO2 in rats. *Brain Res*, 868 (1), 150–156.
O'Connor, J. C., Andre, C., Wang, Y., Lawson, M. A., Szegedi, S. S., Lestage, J., Castanon, N., Kelley, K. W., and Dantzer, R., 2009b. Interferon- and Tumor Necrosis Factor- Mediate the upregulation of indoleamine 2,3-dioxygenase and the induction of depressive-like behavior in mice in response to Bacillus Calmette-Guerin. *J Neurosci*, 29 (13), 4200–4209.
O'Connor, J. C., Lawson, M. A., Andre, C., Moreau, M., Lestage, J., Castanon, N., Kelley, K. W., and Dantzer, R., 2009a. Lipopolysaccharide-induced depressive-like behavior is mediated by indoleamine 2,3-dioxygenase activation in mice. *Mol Psychiat*, 14 (5), 511–522.
O'Reilly, K. C., Shumake, J., Gonzalez-Lima, F., Lane, M. A., and Bailey, S. J., 2006. Chronic administration of 13-cis-retinoic acid increases depression-related behavior in mice. *Neuropsychopharmacol*, 31 (9), 1919–1927.

Obermeier, B., Daneman, R., and Ransohoff, R. M., 2013. Development, maintenance and disruption of the blood-brain barrier. *Nature Med*, 19 (12), 1584–1596.
Ock, J., Jeong, J., Choi, W. S., Lee, W.-H., Kim, S.-H., Kim, I. K., and Suk, K., 2007. Regulation of Toll-like receptor 4 expression and its signaling by hypoxia in cultured microglia. *J Neurosci Res*, 85 (9), 1989–1995.
Ohgi, Y., Futamura, T., Kikuchi, T., and Hashimoto, K., 2013. Effects of antidepressants on alternations in serum cytokines and depressive-like behavior in mice after lipopolysaccharide administration. *Pharmacol Biochem Behav*, 103 (4), 853–859.
Ohishi, K., Ueno, R., Nishino, S., Sakai, T., and Hayaishi, O., 1988. Increased level of salivary prostaglandins in patients with major depression. *Biol Psychiatr*, 23 (4), 326–334.
Onaka, Y., Shintani, N., Nakazawa, T., Haba, R., Ago, Y., Wang, H., Kanoh, T., Hayata-Takano, A., Hirai, H., Nagata, K.-Y., Nakamura, M., Hashimoto, R., Matsuda, T., Waschek, J. A., Kasai, A., Nagayasu, K., Baba, A., and Hashimoto, H., 2015. CRTH2, a prostaglandin D2 receptor, mediates depression-related behavior in mice. *Behav Brain Res*, 284, 131–137.
Orihuela, R., McPherson, C. A., and Harry, G. J., 2016. Microglial M1/M2 polarization and metabolic states. *Brit J Pharmacol*, 173 (4), 649–665.
Orr, A. G., Orr, A. L., Li, X. J., Gross, R. E., and Traynelis, S. F., 2009. Adenosine A2A receptor mediates microglial process retraction. *Nature Neurosci*. 12 (7), 872-878.
Pace, T. W. W. and Miller, A. H., 2009. Cytokines and glucocorticoid receptor signaling. Relevance to major depression. *Ann N Y Acad Sci*, 1179, 86–105.
Pace, T. W. W., Mletzko, T. C., Alagbe, O., Musselman, D. L., Nemeroff, C. B., Miller, A. H., and Heim, C. M., 2006. Increased stress-induced inflammatory responses in male patients with major depression and increased early life stress. *Am J Psychiat*, 163 (9), 1630–1633.
Painsipp, E., Köfer, M. J., Sinner, F., and Holzer, P., 2011. Prolonged depression-like behavior caused by immune challenge: influence of mouse strain and social environment. *PLoS ONE*, 6 (6), e20719.
Pan, H. and Wu, X., 2012. Biochemical and Biophysical Research Communications. *Biochem Biophysic Res Comm*, 420 (3), 685–691.
Pan, W. and Kastin, A. J., 2002. TNFalpha transport across the blood-brain barrier is abolished in receptor knockout mice. *Exp Neurol*, 174 (2), 193–200.
Pan, Y., Chen, X.-Y., Zhang, Q.-Y., and Kong, L.-D., 2014. Microglial NLRP3 inflammasome activation mediates IL-1β-related inflammation in prefrontal cortex of depressive rats. *Brain Behav Immun*. 41, 90-100.
Paolicelli, R. C., Bolasco, G., Pagani, F., Maggi, L., Scianni, M., Panzanelli, P., Giustetto, M., Ferreira, T. A., Guiducci, E., Dumas, L., Ragozzino, D., and Gross, C. T., 2011. Synaptic pruning by microglia is necessary for normal brain development. *Science*, 333 (6048), 1456–1458.
Papandreou, I., Krishna, C., Kaper, F., Cai, D., Giaccia, A. J., and Denko, N. C., 2005. Anoxia is necessary for tumor cell toxicity caused by a low-oxygen environment. *Cancer Res*, 65 (8), 3171–3178.
Papp, M., Willner, P., and Muscat, R., 1991. An animal model of anhedonia: attenuation of sucrose consumption and place preference conditioning by chronic unpredictable mild stress. *Psychopharmacology*, 104 (2), 255–259.
Pariante, C. M., 2006. The glucocorticoid receptor: part of the solution or part of the problem? *J Psychopharmacol*, 20 (4 suppl), 79–84.
Pariante, C. M. and Lightman, S. L., 2008. The HPA axis in major depression: classical

theories and new developments. *Trends Neurosci*, 31 (9), 464–468.
Pariante, C. M., Makoff, A., Lovestone, S., Feroli, S., Heyden, A., Miller, A. H., and Kerwin, R. W., 2001. Antidepressants enhance glucocorticoid receptor function in vitro by modulating the membrane steroid transporters. *Brit J Pharmacol*, 134 (6), 1335–1343.
Pariante, C. M., Pearce, B. D., Pisell, T. L., Sanchez, C. I., Po, C., Su, C., and Miller, A. H., 1999. The proinflammatory cytokine, interleukin-1alpha, reduces glucocorticoid receptor translocation and function. *Endocrinol*, 140 (9), 4359–4366.
Park, S. Y., Lee, H., Hur, J., Kim, S. Y., Kim, H., and Park, J. H., 2002. Hypoxia induces nitric oxide production in mouse microglia via p38 mitogen-activated protein kinase pathway. *Brain Res Mol Brain Res,* 107 (1), 9-16.
Park, S.-E., Lawson, M., Dantzer, R., Kelley, K. W., and McCusker, R. H., 2011. Insulin-like growth factor-I peptides act centrally to decrease depression-like behavior of mice treated intraperitoneally with lipopolysaccharide. *J Neuroinflamm*, 8, 179.
Parvathenani, L. K., Tertyshnikova, S., Greco, C. R., Roberts, S. B., Robertson, B., and Posmantur, R., 2003. P2X7 mediates superoxide production in primary microglia and is up-regulated in a transgenic mouse model of Alzheimer's disease. *J Biol Chem*, 278 (15), 13309–13317.
Pelegrin, P. and Surprenant, A., 2006. Pannexin-1 mediates large pore formation and interleukin-1 beta release by the ATP-gated P2X(7) receptor. *Embo J*, 25 (21), 5071–5082.
Perera, T. D., Coplan, J. D., Lisanby, S. H., Lipira, C. M., Arif, M., Carpio, C., Spitzer, G., Santarelli, L., Scharf, B., Hen, R., Rosoklija, G., Sackeim, H. A., and Dwork, A. J., 2007. Antidepressant-induced neurogenesis in the hippocampus of adult nonhuman primates. *J Neurosci*, 27 (18), 4894–4901.
Pétrilli, V., Papin, S., Dostert, C., Mayor, A., Martinon, F., and Tschopp, J., 2007. Activation of the NALP3 inflammasome is triggered by low intracellular potassium concentration. *Cell Death Differ*, 14 (9), 1583–1589.
Piccini, A., Carta, S., Tassi, S., Lasiglié, D., Fossati, G., and Rubartelli, A., 2008. ATP is released by monocytes stimulated with pathogen-sensing receptor ligands and induces IL-1beta and IL-18 secretion in an autocrine way. *Proc Natl Acad Sci*, 105 (23), 8067–8072.
Pittenger, C. and Duman, R. S., 2008. Stress, depression, and neuroplasticity: a convergence of mechanisms. *Neuropsychopharmacol*, 33 (1), 88–109.
Porsolt, R. D., Anton, G., Blavet, N., and Jalfre, M., 1978. Behavioural despair in rats: a new model sensitive to antidepressant treatments. *Eur J Pharmacol*, 47 (4), 379–391.
Praetorius, H. A. and Leipziger, J., 2009. ATP release from non-excitable cells. *Purinergic Signal*, 5 (4), 433–446.
Qin, L., Wu, X., Block, M. L., Liu, Y., Breese, G. R., Hong, J.-S., Knapp, D. J., and Crews, F. T., 2007. Systemic LPS causes chronic neuroinflammation and progressive neurodegeneration. *Glia*, 55 (5), 453–462.
Qu, Y., Misaghi, S., Newton, K., Gilmour, L. L., Louie, S., Cupp, J. E., Dubyak, G. R., Hackos, D., and Dixit, V. M., 2011. Pannexin-1 is required for ATP release during apoptosis but not for inflammasome activation. *J Immunol*, 186 (11), 6553–6561.
Quan, N. and Banks, W. A., 2007. Brain-immune communication pathways. *Brain Behav Immun*, 21 (6), 727–735.
Raison, C. L., Borisov, A. S., Majer, M., Drake, D. F., Pagnoni, G., Woolwine, B. J., Vogt, G. J., Massung, B., and Miller, A. H., 2009. Activation of central nervous

system inflammatory pathways by interferon-alpha: relationship to monoamines and depression. *Biol Psychiat*, 65 (4), 296–303.

Raison, C. L., Dantzer, R., Kelley, K. W., Lawson, M. A., Woolwine, B. J., Vogt, G., Spivey, J. R., Saito, K., and Miller, A. H., 2010. CSF concentrations of brain tryptophan and kynurenines during immune stimulation with IFN-alpha: relationship to CNS immune responses and depression. *Mol Psychiat*, 15 (4), 393–403.

Raison, C. L., Rutherford, R. E., Woolwine, B. J., Shuo, C., Schettler, P., Drake, D. F., Haroon, E., and Miller, A. H., 2013. A randomized controlled trial of the tumor necrosis factor antagonist infliximab for treatment-resistant depression: the role of baseline inflammatory biomarkers. *JAMA Psychiat*, 70 (1), 31–41.

Renault, J. and Aubert, A., 2006. Immunity and emotions: lipopolysaccharide increases defensive behaviours and potentiates despair in mice. *Brain Behav Immun*, 20 (6), 517–526.

Rigato, C., Swinnen, N., Buckinx, R., Couillin, I., Mangin, J.-M., Rigo, J.-M., Legendre, P., and Le Corronc, H., 2012. Microglia proliferation is controlled by P2X7 receptors in a Pannexin-1-independent manner during early embryonic spinal cord invasion. *J Neurosci*, 32 (34), 11559–11573.

Ripoll, N., David, D. J. P., Dailly, E., Hascoët, M., and Bourin, M., 2003. Antidepressant-like effects in various mice strains in the tail suspension test. *Behav Brain Res*, 143 (2), 193–200.

Riteau, N., Baron, L., Villeret, B., Guillou, N., Savigny, F., Ryffel, B., Rassendren, F., Le Bert, M., Gombault, A., and Couillin, I., 2012. ATP release and purinergic signaling: a common pathway for particle-mediated inflammasome activation. *Cell Death Dis*, 3, e403.

Rock, R. B., Gekker, G., Hu, S., Sheng, W. S., Cheeran, M., Lokensgard, J. R., and Peterson, P. K., 2004. Role of microglia in central nervous system infections. *Clin Microbiol Rev*, 17 (4), 942–64– table of contents.

Rodgers, M. A., Bowman, J. W., Fujita, H., Orazio, N., Shi, M., Liang, Q., Amatya, R., Kelly, T. J., Iwai, K., Ting, J., and Jung, J. U., 2014. The linear ubiquitin assembly complex (LUBAC) is essential for NLRP3 inflammasome activation. *J Exp Med*, 211 (7), 1333–1347.

Rosen, R. C., Lane, R. M., and Menza, M., 1999. Effects of SSRIs on sexual function: a critical review. *J Clin Psychopharmacol*, 19 (1), 67–85.

Rossol, M., Pierer, M., Raulien, N., Quandt, D., Meusch, U., Rothe, K., Schubert, K., Schöneberg, T., Schaefer, M., Krügel, U., Smajilovic, S., Bräuner-Osborne, H., Baerwald, C., and Wagner, U., 2012. Extracellular Ca2+ is a danger signal activating the NLRP3 inflammasome through G protein-coupled calcium sensing receptors. *Nature Comm*, 3, 1329.

Roy, A., Fung, Y. K., Liu, X. J., and Pahan, K., 2006. Up-regulation of microglial CD11b expression by nitric oxide. *J Biol Chem*, 281 (21), 14971–14980.

Rush, A. J., Trivedi, M. H., and Wisniewski, S. R., 2006a. Acute and longer-term outcomes in depressed outpatients requiring one or several treatment steps: a STAR* D report. *Am J Pshychiatr,* 163 (11), 1905-1917.

Rushforth, S. L., Steckler, T., and Shoaib, M., 2011. Nicotine improves working memory span capacity in rats following sub-chronic ketamine exposure. *Neuropsychopharmacol*, 36 (13), 2774–2781.

Rygula, R., Abumaria, N., Flügge, G., Hiemke, C., Fuchs, E., Rüther, E., and Havemann-Reinecke, U., 2006. Citalopram counteracts depressive-like symptoms evoked by chronic social stress in rats. *Behav Pharmacol*, 17 (1), 19–29.

Sagulenko, V., Thygesen, S. J., Sester, D. P., Idris, A., Cridland, J. A., Vajjhala, P. R.,

Roberts, T. L., Schroder, K., Vince, J. E., Hill, J. M., Silke, J., and Stacey, K. J., 2013. AIM2 and NLRP3 inflammasomes activate both apoptotic and pyroptotic death pathways via ASC. *Cell Death Diff*, 20 (9), 1149–1160.

Sahay, A. and Hen, R., 2007. Adult hippocampal neurogenesis in depression. *Nature Neurosci*, 10 (9), 1110–1115.

Saijo, K. and Glass, C. K., 2011. Microglial cell origin and phenotypes in health and disease. *Nature Rev Immunol*, 11 (11), 775–787.

Sakadzić, S., Roussakis, E., Yaseen, M. A., Mandeville, E. T., Srinivasan, V. J., Arai, K., Ruvinskaya, S., Devor, A., Lo, E. H., Vinogradov, S. A., and Boas, D. A., 2010. Two-photon high-resolution measurement of partial pressure of oxygen in cerebral vasculature and tissue. *Nature Methods*, 7 (9), 755–759.

Salaro, E., Rambaldi, A., Falzoni, S., Amoroso, F. S., Franceschini, A., Sarti, A. C., Bonora, M., Cavazzini, F., Rigolin, G. M., Ciccone, M., Audrito, V., Deaglio, S., Pelegrin, P., Pinton, P., Cuneo, A., and Di Virgilio, F., 2016. Involvement of the P2X7-NLRP3 axis in leukemic cell proliferation and death. *Sci Rep*, 6, 26280.

Salazar, A., Gonzalez-Rivera, B. L., Redus, L., Parrott, J. M., and O'Connor, J. C., 2012. Indoleamine 2,3-dioxygenase mediates anhedonia and anxiety-like behaviors caused by peripheral lipopolysaccharide immune challenge. *Horm Behav*, 62 (3), 202–209.

Sanberg, P. R., Calderon, S. F., Giordano, M., Tew, J. M., and Norman, A. B., 1989. The quinolinic acid model of Huntington's disease: locomotor abnormalities. *Exp Neurol*, 105 (1), 45–53.

Sanz, J. M., Chiozzi, P., Ferrari, D., Colaianna, M., Idzko, M., Falzoni, S., Fellin, R., Trabace, L., and Di Virgilio, F., 2009. Activation of microglia by amyloid {beta} requires P2X7 receptor expression. *J Immunol*, 182 (7), 4378–4385.

Sapolsky, R. M., 2001. Depression, antidepressants, and the shrinking hippocampus. *Proc Natl Acad Sci*, 98 (22), 12320–12322.

Saura, J., Tusell, J. M., and Serratosa, J., 2003. High-yield isolation of murine microglia by mild trypsinization. *Glia*, 44 (3), 183–189.

Sborgi, L., Rühl, S., Mulvihill, E., Pipercevic, J., Heilig, R., Stahlberg, H., Farady, C. J., Müller, D. J., Broz, P., and Hiller, S., 2016. GSDMD membrane pore formation constitutes the mechanism of pyroptotic cell death. *EMBO Journal*, 35 (16), 1766–1778.

Scheller, J., Chalaris, A., Schmidt-Arras, D., and Rose-John, S., 2011. The pro- and anti-inflammatory properties of the cytokine interleukin-6. *Biochimica et biophysica acta*, 1813 (5), 878–888.

Schilling, W. P., Wasylyna, T., Dubyak, G. R., Humphreys, B. D., and Sinkins, W. G., 1999. Maitotoxin and P2Z/P2X(7) purinergic receptor stimulation activate a common cytolytic pore. *Am J Physiol*, 277 (4 Pt 1), C766–76.

Schofield, C. J. and Ratcliffe, P. J., 2004. Oxygen sensing by HIF hydroxylases. *Nature Rev Mol cell Biol*, 5 (5), 343–354.

Schroder, K. and Tschopp, J., 2010. The inflammasomes. *Cell*, 140 (6), 821–832.

Semenza, G. L., 2007. Oxygen-dependent regulation of mitochondrial respiration by hypoxia-inducible factor 1. *Biochem J*, 405 (1), 1–9.

Sena, L. A. and Chandel, N. S., 2012. Physiological roles of mitochondrial reactive oxygen species. *Mol Cell*, 48 (2), 158–167.

Setiawan, E., Wilson, A. A., Mizrahi, R., Rusjan, P. M., Miler, L., Rajkowska, G., Suridjan, I., Kennedy, J. L., Rekkas, P. V., Houle, S., and Meyer, J. H., 2015. Role of translocator protein density, a marker of neuroinflammation, in the brain during major depressive episodes. *JAMA Psychiat*, 72 (3), 268–275.

Shaikh, A., Dhadde, S. B., Durg, S., Veerapur, V. P., Badami, S., Thippeswamy, B. S., and Patil, J. S., 2016. Effect of Embelin Against Lipopolysaccharide-induced Sickness Behaviour in Mice. *Phytothe Res,* 30 (5), 815–822.

Sheng, W., Zong, Y., Mohammad, A., Ajit, D., Cui, J., Han, D., Hamilton, J. L., Simonyi, A., Sun, A. Y., Gu, Z., Hong, J.-S., Weisman, G. A., and Sun, G. Y., 2011. Pro-inflammatory cytokines and lipopolysaccharide induce changes in cell morphology, and upregulation of ERK1/2, iNOS and sPLA. *J Neuroinflamm*, 8 (1), 121.

Shi, F., Yang, L., Kouadir, M., Yang, Y., Wang, J., Zhou, X., Yin, X., and Zhao, D., 2012. The NALP3 inflammasome is involved inneurotoxic prion peptide-inducedmicroglial activation. *J Neuroinflamm*, 9 (1), 1–1.

Shi, J., Zhao, Y., Wang, K., Shi, X., Wang, Y., Huang, H., Zhuang, Y., Cai, T., Wang, F., and Shao, F., 2015. Cleavage of GSDMD by inflammatory caspases determines pyroptotic cell death. *Nature*, 526 (7575), 660–665.

Shi, J., Zhao, Y., Wang, Y., Gao, W., Ding, J., Li, P., Hu, L., and Shao, F., 2014. Inflammatory caspases are innate immune receptors for intracellular LPS. *Nature*, 514 (7521), 187–192.

Shibakawa, Y. S., Sasaki, Y., Goshima, Y., Echigo, N., Kamiya, Y., Kurahashi, K., Yamada, Y., and Andoh, T., 2005. Effects of ketamine and propofol on inflammatory responses of primary glial cell cultures stimulated with lipopolysaccharide. *Brit J Anaesth*, 95 (6), 803–810.

Shimada, K., Crother, T. R., Karlin, J., Dagvadorj, J., Chiba, N., Chen, S., Ramanujan, V. K., Wolf, A. J., Vergnes, L., Ojcius, D. M., Rentsendorj, A., Vargas, M., Guerrero, C., Wang, Y., Fitzgerald, K. A., Underhill, D. M., Town, T., and Arditi, M., 2012. Oxidized mitochondrial DNA activates the NLRP3 inflammasome during apoptosis. *Immunity*, 36 (3), 401–414.

Shimizu, S., Eguchi, Y., Kamiike, W., Itoh, Y., Hasegawa, J., Yamabe, K., Otsuki, Y., Matsuda, H., and Tsujimoto, Y., 1996. Induction of apoptosis as well as necrosis by hypoxia and predominant prevention of apoptosis by Bcl-2 and Bcl-XL. *Cancer Res*, 56 (9), 2161–2166.

Shirasuna, K., Shimamura, N., Seno, K., Ohtsu, A., Shiratsuki, S., Ohkuchi, A., Suzuki, H., Matsubara, S., Nagayama, S., Iwata, H., and Kuwayama, T., 2015. Moderate hypoxia down-regulates interleukin-6 secretion and TLR4 expression in human Sw.71 placental cells. *Cell Physiol Biochem*, 36 (6), 2149–2160.

Skelly, D. T., Hennessy, E., Dansereau, M.-A., and Cunningham, C., 2013. A systematic analysis of the peripheral and CNS effects of systemic LPS, IL-1β, TNF-α and IL-6 challenges in C57BL/6 mice. *PLoS ONE*, 8 (7), e69123.

Slattery, D. A. and Cryan, J. F., 2014. The ups and downs of modelling mood disorders in rodents. *ILAR J*, 55 (2), 297–309.

Song, C. and Wang, H., 2011. Cytokines mediated inflammation and decreased neurogenesis in animal models of depression. *Prog Neuropsychopharmacol Biol Psychiat*, 35 (3), 760–768.

Spencer, N. G., Schilling, T., Miralles, F., and Eder, C., 2016. Mechanisms underlying interferon-γ-induced priming of microglial reactive oxygen species production. *PLoS ONE*, 11 (9), e0162497.

Sperlágh, B., Haskó, G., Németh, Z., and Vizi, E. S., 1998. ATP released by LPS increases nitric oxide production in raw 264.7 macrophage cell line via P2Z/P2X7 receptors. *Neurochem Int*, 33 (3), 209–215.

Sriram, C. S., Jangra, A., Gurjar, S. S., Hussain, M. I., Borah, P., Lahkar, M., Mohan, P., and Bezbaruah, B. K., 2015. Poly (ADP-ribose) polymerase-1 inhibitor, 3-aminobenzamide pretreatment ameliorates lipopolysaccharide-induced

neurobehavioral and neurochemical anomalies in mice. *Pharmacol Biochem Behav*, 133, 83–91.

Sriram, C. S., Jangra, A., Gurjar, S. S., Mohan, P., and Bezbaruah, B. K., 2016. Edaravone abrogates LPS-induced behavioral anomalies, neuroinflammation and PARP-1. *Physiol Behav*, 154, 135–144.

Steiner, J., Bielau, H., Brisch, R., Danos, P., Ullrich, O., Mawrin, C., Bernstein, H.-G., and Bogerts, B., 2008. Immunological aspects in the neurobiology of suicide: elevated microglial density in schizophrenia and depression is associated with suicide. *J Psychiat Res*, 42 (2), 151–157.

Steiner, J., Walter, M., Gos, T., Guillemin, G. J., Bernstein, H.-G., Sarnyai, Z., Mawrin, C., Brisch, R., Bielau, H., Meyer zu Schwabedissen, L., Bogerts, B., and Myint, A.-M., 2011. Severe depression is associated with increased microglial quinolinic acid in subregions of the anterior cingulate gyrus: evidence for an immune-modulated glutamatergic neurotransmission? *J Neuroinflamm*, 8, 94.

Stence, N., Waite, M., and Dailey, M. E., 2001. Dynamics of microglial activation: a confocal time-lapse analysis in hippocampal slices. *Glia*, 33 (3), 256–266.

Stone, J. R. and Collins, T., 2002. The role of hydrogen peroxide in endothelial proliferative responses. *Endothelium*, 9 (4), 231–238.

Su, Q., Tao, W., Huang, H., Du, Y., Chu, X., and Chen, G., 2016. Protective effect of liquiritigenin on depressive-like behavior in mice after lipopolysaccharide administration. *Psychiat Res*, 240, 131–136.

Suarez, E. C., Lewis, J. G., Krishnan, R. R., and Young, K. H., 2004. Enhanced expression of cytokines and chemokines by blood monocytes to in vitro lipopolysaccharide stimulation are associated with hostility and severity of depressive symptoms in healthy women. *Psychoneuroendocrinol*, 29 (9), 1119–1128.

Sugama, S., Fujita, M., Hashimoto, M., and Conti, B., 2007. Stress induced morphological microglial activation in the rodent brain: involvement of interleukin-18. *Neurosci*, 146 (3), 1388–1399.

Sugama, S., Takenouchi, T., Fujita, M., Conti, B., and Hashimoto, M., 2009. Differential microglial activation between acute stress and lipopolysaccharide treatment. *J Neuroimmunol*, 207 (1-2), 24–31.

Sugimoto, Y. and Narumiya, S., 2006. Prostaglandin E receptors. *J Biol Chem*, 282 (16), 11613–11617.

Suk, K., 2004. Minocycline suppresses hypoxic activation of rodent microglia in culture. *Neurosci Lett*, 366 (2), 167–171.

Sulakhiya, K., Keshavlal, G. P., Bezbaruah, B. B., Dwivedi, S., Gurjar, S. S., Munde, N., Jangra, A., Lahkar, M., and Gogoi, R., 2016. Lipopolysaccharide induced anxiety- and depressive-like behaviour in mice are prevented by chronic pre-treatment of esculetin. *Neurosci Lett*, 611, 106–111.

Sulakhiya, K., Kumar, P., Jangra, A., Dwivedi, S., Hazarika, N. K., Baruah, C. C., and Lahkar, M., 2014. Honokiol abrogates lipopolysaccharide-induced depressive like behavior by impeding neuroinflammation and oxido-nitrosative stress in mice. *Eur J Pharmacol*, 744, 124–131.

Sun, J., Wang, X.-D., Liu, H., and Xu, J.-G., 2004. Ketamine suppresses intestinal NF-kappa B activation and proinflammatory cytokine in endotoxic rats. *World J Gastroenterol*, 10 (7), 1028–1031.

Surprenant, A., Rassendren, F., Kawashima, E., North, R. A., and Buell, G., 1996. The cytolytic P2Z receptor for extracellular ATP identified as a P2X receptor (P2X7). *Science*, 272 (5262), 735–738.

Takata, K., Kitamura, Y., Yanagisawa, D., Morikawa, S., Morita, M., Inubushi, T., Tsuchiya, D., Chishiro, S., Saeki, M., Taniguchi, T., Shimohama, S., and Tooyama, I., 2007. Microglial transplantation increases amyloid-beta clearance in Alzheimer model rats. *FEBS Lett*, 581 (3), 475–478.

Tamura, M., Tanaka, S., Fujii, T., Aoki, A., Komiyama, H., Ezawa, K., Sumiyama, K., Sagai, T., and Shiroishi, T., 2007. Members of a novel gene family, Gsdm, are expressed exclusively in the epithelium of the skin and gastrointestinal tract in a highly tissue-specific manner. *Genomics*, 89 (5), 618–629.

Tanaka, T., Kai, S., Matsuyama, T., Adachi, T., Fukuda, K., and Hirota, K., 2013. General anesthetics inhibit LPS-induced IL-1β expression in glial cells. *PLoS ONE*, 8 (12), e82930.

Tanimoto, K., 2000. Mechanism of regulation of the hypoxia-inducible factor-1alpha by the von Hippel-Lindau tumor suppressor protein. *EMBO J*, 19 (16), 4298–4309.

Tao, W., Wang, H., Su, Q., Chen, Y., Xue, W., Xia, B., Duan, J., and Chen, G., 2016. Paeonol attenuates lipopolysaccharide-induced depressive-like behavior in mice. *Psychiat Res*, 238, 116–121.

Tarr, A. J., Chen, Q., Wang, Y., Sheridan, J. F., and Quan, N., 2012. Neural and behavioral responses to low-grade inflammation. *Behav Brain Res*, 235 (2), 334–341.

Tartter, M., Hammen, C., Bower, J. E., Brennan, P. A., and Cole, S., 2015. Effects of chronic interpersonal stress exposure on depressive symptoms are moderated by genetic variation at IL6 and IL1β in youth. *Brain Behav Immun*, 46, 104–111.

Thomas, D. M. and Kuhn, D. M., 2005. MK-801 and dextromethorphan block microglial activation and protect against methamphetamine-induced neurotoxicity. *Brain Res*, 1050 (1-2), 190–198.

Ting, J. P. Y., Lovering, R. C., Alnemri, E. S., Bertin, J., Boss, J. M., Davis, B. K., Flavell, R. A., Girardin, S. E., Godzik, A., Harton, J. A., Hoffman, H. M., Hugot, J.-P., Inohara, N., Mackenzie, A., Maltais, L. J., Nuñez, G., Ogura, Y., Otten, L. A., Philpott, D., Reed, J. C., Reith, W., Schreiber, S., Steimle, V., and Ward, P. A., 2008. The NLR gene family: a standard nomenclature. *Immunity*, 28 (3), 285–287.

Torres-Platas, S. G., Cruceanu, C., Chen, G. G., Turecki, G., and Mechawar, N., 2014. Evidence for increased microglial priming and macrophage recruitment in the dorsal anterior cingulate white matter of depressed suicides. *Brain Behav Immun*, 42, 50–59.

Toulme, E., Garcia, A., Samways, D., Egan, T. M., Carson, M. J., and Khakh, B. S., 2010. P2X4 receptors in activated C8-B4 cells of cerebellar microglial origin. *J Gen Physiol*, 135 (4), 333–353.

Trivedi, M. H., Rush, A. J., Wisniewski, S. R., Nierenberg, A. A., Warden, D., Ritz, L., Norquist, G., Howland, R. H., Lebowitz, B., McGrath, P. J., Shores-Wilson, K., Biggs, M. M., Balasubramani, G. K., Fava, M., STAR*D Study Team, 2006. Evaluation of outcomes with citalopram for depression using measurement-based care in STAR*D: implications for clinical practice. *Am J Psychiat*, 163 (1), 28–40.

Trueblood, K. E., Mohr, S., and Dubyak, G. R., 2011. Purinergic regulation of high-glucose-induced caspase-1 activation in the rat retinal Müller cell line rMC-1. *American journal of physiology. Cell Physiol*, 301 (5), C1213–23.

Truett, G. E., Heeger, P., Mynatt, R. L., Truett, A. A., Walker, J. A., and Warman, M. L., 2000. Preparation of PCR-quality mouse genomic DNA with hot sodium hydroxide and tris (HotSHOT). *BioTechniques*, 29 (1), 52–54.

Tschopp, J. and Schroder, K., 2010. NLRP3 inflammasome activation: the convergence of multiple signalling pathways on ROS production? *Nat Rev*

Immunol, 10 (3), 210–215.
Tschopp, J., Martinon, F., and Burns, K., 2003. NALPs: a novel protein family involved in inflammation. *Nature Rev Mol Cell Biol*, 4 (2), 95–104.
Turrens, J. F., 2003. Mitochondrial formation of reactive oxygen species. *J Physiology*, 552 (Pt 2), 335–344.
Turrens, J. F., Freeman, B. A., Levitt, J. G., and Crapo, J. D., 1982. The effect of hyperoxia on superoxide production by lung submitochondrial particles. *Arch Biochem Biophysic*, 217 (2), 401–410.
van Buel, E. M., Bosker, F. J., van Drunen, J., Strijker, J., Douwenga, W., Klein, H. C., and Eisel, U. L. M., 2015. Electroconvulsive seizures (ECS) do not prevent LPS-induced behavioral alterations and microglial activation. *J Neuroinflamm*, 12, 232.
Vázquez, G. H., Holtzman, J. N., Tondo, L., and Baldessarini, R. J., 2015. Efficacy and tolerability of treatments for bipolar depression. *J Affect Dis*, 183, 258–262.
Verma, P., Hellemans, K. G. C., Choi, F. Y., Yu, W., and Weinberg, J., 2010. Circadian phase and sex effects on depressive/anxiety-like behaviors and HPA axis responses to acute stress. *Physiol Behav*, 99 (3), 276–285.
Verstrepen, L., Bekaert, T., Chau, T.-L., Tavernier, J., Chariot, A., and Beyaert, R., 2008. TLR-4, IL-1R and TNF-R signaling to NF-kappaB: variations on a common theme. *Cell Mol Life Sci*, 65 (19), 2964–2978.
Viana, A. F., Maciel, I. S., Dornelles, F. N., Figueiredo, C. P., Siqueira, J. M., Campos, M. M., and Calixto, J. B., 2010. Kinin B1 receptors mediate depression-like behavior response in stressed mice treated with systemic E. coli lipopolysaccharide. *J Neuroinflamm*, 7, 98.
Videbech, P. and Ravnkilde, B., 2004. Hippocampal volume and depression: a meta-analysis of MRI studies. *Am J Psychiat*, 161 (11), 1957–1966.
Vitiello, L., Gorini, S., Rosano, G., and la Sala, A., 2012. Immunoregulation through extracellular nucleotides. *Blood*, 120 (3), 511–518.
Walev, I., Reske, K., Palmer, M., Valeva, A., and Bhakdi, S., 1995. Potassium-inhibited processing of IL-1 beta in human monocytes. *Embo J*, 14 (8), 1607–1614.
Walker, A. K., Budac, D. P., Bisulco, S., Lee, A. W., Smith, R. A., Beenders, B., Kelley, K. W., and Dantzer, R., 2013. NMDA receptor blockade by ketamine abrogates lipopolysaccharide-induced depressive-like behavior in C57BL/6J mice. *Neuropsychopharmacol*, 38 (9), 1609–1616.
Walsh, J. G., Muruve, D. A., and Power, C., 2014a. Inflammasomes in the CNS. *Nat Rev Neurosci*, 15 (2), 84–97.
Walsh, J. G., Reinke, S. N., Mamik, M. K., McKenzie, B. A., Maingat, F., Branton, W. G., Broadhurst, D. I., and Power, C., 2014b. Rapid inflammasome activation in microglia contributes to brain disease in HIV/AIDS. *Retrovirol*, 11, 35.
Wang, X., Wu, H., and Miller, A. H., 2004. Interleukin 1alpha (IL-1alpha) induced activation of p38 mitogen-activated protein kinase inhibits glucocorticoid receptor function. *Molecular Psychiatry*, 9 (1), 65–75.
Wang, Z., Zhang, Q., Yuan, L., Wang, S., Liu, L., Yang, X., Li, G., and Liu, D., 2014. The effects of curcumin on depressive-like behavior in mice after lipopolysaccharide administration. *Behav Brain Res*, 274, 282–290.
Waypa, G. B., Smith, K. A., and Schumacker, P. T., 2016. O2 sensing, mitochondria and ROS signaling: the fog is lifting. *Mol Aspects Med*, 47-48, 76–89.
Weinmann, M., Jendrossek, V., Handrick, R., Güner, D., Goecke, B., and Belka, C., 2004. Molecular ordering of hypoxia-induced apoptosis: critical involvement of the mitochondrial death pathway in a FADD/caspase-8 independent manner. *Oncogene*, 23 (21), 3757–3769.

Willner, P. and Mitchell, P. J., 2002. The validity of animal models of predisposition to depression. *Behav Pharmacol*, 13 (3), 169–188.

Willner, P., Towell, A., Sampson, D., Sophokleous, S., and Muscat, R., 1987. Reduction of sucrose preference by chronic unpredictable mild stress, and its restoration by a tricyclic antidepressant. *Psychopharmacol*, 93 (3), 358–364.

Woehrle, T., Yip, L., Elkhal, A., Sumi, Y., Chen, Y., Yao, Y., Insel, P. A., and Junger, W. G., 2010. Pannexin-1 hemichannel-mediated ATP release together with P2X1 and P2X4 receptors regulate T-cell activation at the immune synapse. *Blood*, 116 (18), 3475–3484.

Woodward, H. N., Anwar, A., Riddle, S., Taraseviciene-Stewart, L., Fragoso, M., Stenmark, K. R., and Gerasimovskaya, E. V., 2009. PI3K, Rho, and ROCK play a key role in hypoxia-induced ATP release and ATP-stimulated angiogenic responses in pulmonary artery vasa vasorum endothelial cells. *Lung Cell Mol Physiol*, 297 (5), L954–L964.

Wu, T.-Y., Liu, L., Zhang, W., Zhang, Y., Liu, Y.-Z., Shen, X.-L., Gong, H., Yang, Y.-Y., Bi, X.-Y., Jiang, C.-L., and Wang, Y.-X., 2015. High-mobility group box-1 was released actively and involved in LPS induced depressive-like behavior. *J Psychiat Res*, 64, 99–106.

Wu, Y., Fu, Y., Rao, C., Li, W., Liang, Z., Zhou, C., Shen, P., Cheng, P., Zeng, L., Zhu, D., Zhao, L., and Xie, P., 2016. Metabolomic analysis reveals metabolic disturbances in the prefrontal cortex of the lipopolysaccharide-induced mouse model of depression. *Behav Brain Res*, 308, 115–127.

Xie, Y., Wang, Y., Zhang, T., Ren, G., and Yang, Z., 2012. Effects of nanoparticle zinc oxide on spatial cognition and synaptic plasticity in mice with depressive-like behaviors. *J Biomed Sci*, 19, 14.

Yamamoto, M., Yaginuma, K., Tsutsui, H., Sagara, J., Guan, X., Seki, E., Yasuda, K., Yamamoto, M., Akira, S., Nakanishi, K., Noda, T., and Taniguchi, S., 2004. ASC is essential for LPS-induced activation of procaspase-1 independently of TLR-associated signal adaptor molecules. *Genes Cell*, 9 (11), 1055–1067.

Yang, F., Wang, Z., Wei, X., Han, H., Meng, X., Zhang, Y., Shi, W., Li, F., Xin, T., Pang, Q., and Yi, F., 2014. NLRP3 deficiency ameliorates neurovascular damage in experimental ischemic stroke. *J Cereb Blood Flow Metab,* 34 (4), 660–667.

Yang, J., Qi, F., and Yao, Z., 2016. Neonatal Bacillus Calmette-Guérin vaccination alleviates lipopolysaccharide-induced neurobehavioral impairments and neuroinflammation in adult mice. *Mol Med Rep*, 14 (2), 1574–1586.

Yang, M., Silverman, J. L., and Crawley, J. N., 2011. Automated three-chambered social approach task for mice. *Curr Protoc Neurosci*, Chapter 8, Unit 8.26.

Yao, L., Kan, E. M., Lu, J., Hao, A., Dheen, S. T., Kaur, C., and Ling, E.-A., 2013. Toll-like receptor 4 mediates microglial activation and production of inflammatory mediators in neonatal rat brain following hypoxia: role of TLR4 in hypoxic microglia. *J Neuroinflamm*, 10, 23.

Yao, W., Zhang, J.-C., Dong, C., Zhuang, C., Hirota, S., Inanaga, K., and Hashimoto, K., 2015. Effects of amycenone on serum levels of tumor necrosis factor-α, interleukin-10, and depression-like behavior in mice after lipopolysaccharide administration. *Pharmacol Biochem Behav*, 136, 7–12.

Yirmiya, R., Rimmerman, N., and Reshef, R., 2015. Depression as a microglial disease. *Trends Neurosci*, 38 (10), 637–658.

Yu, J., Nagasu, H., Murakami, T., Hoang, H., Broderick, L., Hoffman, H. M., and Horng, T., 2014. Inflammasome activation leads to Caspase-1-dependent mitochondrial damage and block of mitophagy. *Proc Natl Acad Sci*, 111 (43), 15514–15519.

Zalli, A., Jovanova, O., Hoogendijk, W. J. G., Tiemeier, H., and Carvalho, L. A., 2016. Low-grade inflammation predicts persistence of depressive symptoms. *Psychopharmacol*, 233 (9), 1669–1678.

Zarate, C. A., Singh, J. B., Carlson, P. J., Brutsche, N. E., Ameli, R., Luckenbaugh, D. A., Charney, D. S., and Manji, H. K., 2006. A randomized trial of an N-methyl-D-aspartate antagonist in treatment-resistant major depression. *Arch Gen Psychiat*, 63 (8), 856–864.

Zeisberger, E. and Roth, J., 1998. Tolerance to pyrogens. *Ann N Y Acad Sci*, 856, 116–131.

Zhang, K., Liu, J., You, X., Kong, P., Song, Y., Cao, L., Yang, S., Wang, W., Fu, Q., and Ma, Z., 2016. P2X7 as a new target for chrysophanol to treat lipopolysaccharide-induced depression in mice. *Neurosci Lett*, 613, 60–65.

Zhang, X., Feng, J., Zhu, P., and Zhao, Z., 2013. Ketamine inhibits calcium elevation and hydroxyl radical and nitric oxide production in lipopolysaccharide-stimulated NR8383 alveolar macrophages. *Inflamm*, 36 (5), 1094–1100.

Zhang, Y., Liu, L., Liu, Y.-Z., Shen, X.-L., Wu, T.-Y., Zhang, T., Wang, W., Wang, Y.-X., and Jiang, C.-L., 2015. NLRP3 inflammasome mediates chronic mild stress-induced depression in mice via neuroinflammation. *Int J Neuropsychopharmacol*, 18 (8). pyv006.

Zhang, Y., Liu, L., Peng, Y.-L., Liu, Y.-Z., Wu, T.-Y., Shen, X.-L., Zhou, J.-R., Sun, D.-Y., Huang, A.-J., Wang, X., Wang, Y.-X., and Jiang, C.-L., 2014. Involvement of inflammasome activation in lipopolysaccharide-induced mice depressive-like behaviors. *CNS Neurosci Therap*, 20 (2), 119–124.

Zhou, L., Luo, L., Qi, X., Li, X., and Gorodeski, G. I., 2009. Regulation of P2X(7) gene transcription. *Purinergic Signal*, 5 (3), 409–426.

Zhou, R., Tardivel, A., Thorens, B., Choi, I., and Tschopp, J., 2010. Thioredoxin-interacting protein links oxidative stress to inflammasome activation. *Nature Immunol*, 11 (2), 136–140.

Zhou, R., Yazdi, A. S., Menu, P., and Tschopp, J., 2011. A role for mitochondria in NLRP3 inflammasome activation. *Nature*, 469 (7329), 221–225.

Zhou, Y., Lu, M., Du, R.-H., Qiao, C., Jiang, C.-Y., Zhang, K.-Z., Ding, J.-H., and Hu, G., 2016. MicroRNA-7 targets Nod-like receptor protein 3 inflammasome to modulate neuroinflammation in the pathogenesis of Parkinson's disease. *Mol Neurodegen*, 11, 28.

Zhu, C.-B., Blakely, R. D., and Hewlett, W. A., 2006. The proinflammatory cytokines interleukin-1beta and tumor necrosis factor-alpha activate serotonin transporters. *Neuropsychopharmacol*, 31 (10), 2121–2131.

Zhu, C.-B., Lindler, K. M., Owens, A. W., Daws, L. C., Blakely, R. D., and Hewlett, W. A., 2010. Interleukin-1 receptor activation by systemic lipopolysaccharide induces behavioral despair linked to MAPK regulation of CNS serotonin transporters. *Neuropsychopharmacol*, 35 (13), 2510–2520.

Zhu, L., Wei, T., Gao, J., Chang, X., He, H., Miao, M., and Yan, T., 2015. Salidroside attenuates lipopolysaccharide (LPS) induced serum cytokines and depressive-like behavior in mice. *Neurosci Lett*, 606, 1–6.

Zorrilla, E. P. and Koob, G. F., 2010. Progress in corticotropin-releasing factor-1 antagonist development. *Drug Discov Today*, 15 (9-10), 371–383.

Zunszain, P. A., Anacker, C., Cattaneo, A., Choudhury, S., Musaelyan, K., Myint, A.-M., Thuret, S., Price, J., and Pariante, C. M., 2012. Interleukin-1β: a new regulator of the kynurenine pathway affecting human hippocampal neurogenesis. *Neuropsychopharmacol*, 37 (4), 939–949.

Published abstracts

Wickens, R. A., Ver Donck, L., Bailey, S. J. and Mackenzie, A. B., 2013. Lipopolysaccharide regulation of the NLRP3 inflammasome and proIL-1β under normoxic versus hypoxic conditions in cultured (BV-2) mouse microglia. *Proc Brit Pharmacol Soc,* 11 (3), 058P.

Wickens, R., Ver Donck, L., Mackenzie, A. and Bailey, S. J., 2014. Acute And Chronic Lipopolysaccharide Induces Sickness But Fails To Produce A Depressive-Like Behaviour In Mice. *J Psychopharmacol*, 28 (8), A107.

Wickens, R., Ver Donck, L., Mackenzie, A. and Bailey, S., 2015. The effect of housing conditions on lipopolysaccharide-induced depressive-like behaviour in mice. *J Psychopharmacol*, 29 (8), A08.

Wickens, R., Ver Donck, L., Bailey, S. and Mackenzie, A., 2015. Primary microglia isolated from neonatal mice provide a model for the study of NLRP3 inflammasome and the effect of long-term hypoxia. *Soc Neurosci.* 809.29 (W42).

Conferences

British Pharmacological Society. *London 2013*. Lipopolysaccharide regulation of the NLRP3 inflammasome and proIL-1β under normoxic versus hypoxic conditions in cultured (BV-2) mouse microglia. *Poster – Winner of poster prize.*

European Behavioural Pharmacological Society. *Brighton 2014*. The female urine sniffing test: assessing inflammation-mediated changes in depression-related behaviour. *Poster.*

British Association for Psychopharmacology. *Cambridge 2014*. Acute And Chronic Lipopolysaccharide Induces Sickness But Fails To Produce A Depressive-Like Behaviour In Mice. *Poster – selected for oral presentation.*

British Neuroscience Association. *Edinburgh 2015*. Inflammation-induced changes in depressive-like behaviour in the mouse female urine sniffing test. *Poster.*

British Association for Psychopharmacology. *Brighton 2015*. The effect of housing conditions on lipopolysaccharide-induced depressive-like behaviour in mice. *Poster.*

Society for Neuroscience. *Chicago 2015*. Primary microglia isolated from neonatal mice provide a model for the study of NLRP3 inflammasome and the effect of long-term hypoxia. *Poster.*